



U.S. Department of Transportation
Federal Highway Administration

FOREWORD

Intersection crashes account for approximately 22 percent of fatal crashes and 40 percent of all crashes in the United States. When designing new roadways or retrofitting existing roadways, careful consideration should be given to mitigation measures for skewed intersections. This research sought to obtain quantitative relationships between intersection angle and safety, where intersection crashes define safety. The relationships were used to determine appropriate crash modification factors for reducing or eliminating the skew angle of an intersection.

The study was conducted with data from Minnesota and Ohio. Models were derived separately for rural and urban three- and four-leg intersections. The relationships between intersection angle and safety in the Minnesota and Ohio data were used to determine the critical minimum angle at which safety is substantially diminished (75 degrees, 60 degrees, or other). The study developed new crash modification functions for intersection angles and new considerations for critical minimum angles commonly applied by roadway designers. The results and insights will be useful for highway engineers, safety engineers, and associations and nongovernmental organizations that develop nationally recognized guidelines.

Brian P. Cronin, P.E.
Director, Office of Safety and Operations
Research and Development

Notice

This document is disseminated under the sponsorship of the U.S. Department of Transportation (USDOT) in the interest of information exchange. The U.S. Government assumes no liability for the use of the information contained in this document.

The U.S. Government does not endorse products or manufacturers. Trademarks or manufacturers' names appear in this report only because they are considered essential to the objective of the document.

Quality Assurance Statement

The Federal Highway Administration (FHWA) provides high-quality information to serve Government, industry, and the public in a manner that promotes public understanding. Standards and policies are used to ensure and maximize the quality, objectivity, utility, and integrity of its information. FHWA periodically reviews quality issues and adjusts its programs and processes to ensure continuous quality improvement.

Cover photos source: FHWA.

TECHNICAL REPORT DOCUMENTATION PAGE

1. Report No. FHWA-HRT-20-067	2. Government Accession No.	3. Recipient's Catalog No.	
4. Title and Subtitle Impact of Intersection Angle on Highway Safety		5. Report Date January 2021	
		6. Performing Organization Code	
7. Author(s) David Harkey, Bo Lan (ORCID: 0000-0002-7998-7252), Raghavan Srinivasan (ORCID: 0000-0002-3097-5154), Wesley Kumfer (ORCID:0000-0002-6705-5298), Daniel Carter (ORCID: 0000-0001-6572-6548), and Anusha Patel Nujjetty (ORCID: 0000-0002-1148-718X)		8. Performing Organization Report No.	
9. Performing Organization Name and Address Highway Safety Research Center University of North Carolina Chapel Hill, NC 27599		10. Work Unit No.	
		11. Contract or Grant No. DTFH61-11-C-00050	
12. Sponsoring Agency Name and Address Office of Safety Research and Development Federal Highway Administration 6300 Georgetown Pike McLean, VA 22101		13. Type of Report and Period Covered Final Report; January 2011–April 2014; June 2017–September 2020	
		14. Sponsoring Agency Code HRDS-20	
15. Supplementary Notes This report was produced as a research product of the Highway Safety Information System (HSIS) under the direction of HSIS Program Managers Carol Tan, Ph.D. (HRDS-20; ORCID 0000-0002-0549-9782) and Ana Maria Eigen, Ph.D. (HRDS-20; ORCID 0000-0003-4056-361X).			
16. Abstract The preferred design for conventional intersections includes adjacent legs that intersect at 90 degrees. However, there are occasions when physical constraints result in intersection angles less than 90 degrees and thus produce skewed intersections. Skewed intersections may create potential safety and operational problems for both motorists and nonmotorists. To date, the research on problems related to skewed intersections has been limited, which may explain the lack of consensus among the policies and guidance that now exists in practice. The objective of this study was to derive quantitative relationships between intersection angle and safety for which intersection crashes define safety. The relationships were used to determine appropriate crash modification functions (CMFunction) for reducing or eliminating the skew angle of an intersection, determine if there is a critical minimum angle at which safety is substantially diminished, and assess the need for revising current geometric design policies and practices. Data-mining and -regression techniques were used to identify the most important predictor variables from many independent variables. Data from minor road stop-controlled intersections in Minnesota and Ohio were used to estimate negative binomial regression models using the identified variables. These models were used to derive CMFunctions for rural and urban three- and four-leg intersections. The relationship between the crash modification factor and intersection angle (represented by the CMFunctions) differs from previous studies. Agencies should consider modifying the minimum critical angle for intersections in roadway design policies to be revised to reflect the results of this research.			
17. Key Words Intersection angle, intersection safety, crash modification factor, crash modification function, skew angle, negative binomial regression, stop controlled		18. Distribution Statement No restrictions. This document is available to the public through the National Technical Information Service, Springfield, VA 22161. http://www.ntis.gov	
19. Security Classif. (of this report) Unclassified	20. Security Classif. (of this page) Unclassified	21. No. of Pages 207	22. Price N/A

SI* (MODERN METRIC) CONVERSION FACTORS

APPROXIMATE CONVERSIONS TO SI UNITS

Symbol	When You Know	Multiply By	To Find	Symbol
LENGTH				
in	inches	25.4	millimeters	mm
ft	feet	0.305	meters	m
yd	yards	0.914	meters	m
mi	miles	1.61	kilometers	km
AREA				
in ²	square inches	645.2	square millimeters	mm ²
ft ²	square feet	0.093	square meters	m ²
yd ²	square yard	0.836	square meters	m ²
ac	acres	0.405	hectares	ha
mi ²	square miles	2.59	square kilometers	km ²
VOLUME				
fl oz	fluid ounces	29.57	milliliters	mL
gal	gallons	3.785	liters	L
ft ³	cubic feet	0.028	cubic meters	m ³
yd ³	cubic yards	0.765	cubic meters	m ³
NOTE: volumes greater than 1,000 L shall be shown in m ³				
MASS				
oz	ounces	28.35	grams	g
lb	pounds	0.454	kilograms	kg
T	short tons (2,000 lb)	0.907	megagrams (or "metric ton")	Mg (or "t")
TEMPERATURE (exact degrees)				
°F	Fahrenheit	5 (F-32)/9 or (F-32)/1.8	Celsius	°C
ILLUMINATION				
fc	foot-candles	10.76	lux	lx
fl	foot-Lamberts	3.426	candela/m ²	cd/m ²
FORCE and PRESSURE or STRESS				
lbf	poundforce	4.45	newtons	N
lbf/in ²	poundforce per square inch	6.89	kilopascals	kPa

APPROXIMATE CONVERSIONS FROM SI UNITS

Symbol	When You Know	Multiply By	To Find	Symbol
LENGTH				
mm	millimeters	0.039	inches	in
m	meters	3.28	feet	ft
m	meters	1.09	yards	yd
km	kilometers	0.621	miles	mi
AREA				
mm ²	square millimeters	0.0016	square inches	in ²
m ²	square meters	10.764	square feet	ft ²
m ²	square meters	1.195	square yards	yd ²
ha	hectares	2.47	acres	ac
km ²	square kilometers	0.386	square miles	mi ²
VOLUME				
mL	milliliters	0.034	fluid ounces	fl oz
L	liters	0.264	gallons	gal
m ³	cubic meters	35.314	cubic feet	ft ³
m ³	cubic meters	1.307	cubic yards	yd ³
MASS				
g	grams	0.035	ounces	oz
kg	kilograms	2.202	pounds	lb
Mg (or "t")	megagrams (or "metric ton")	1.103	short tons (2,000 lb)	T
TEMPERATURE (exact degrees)				
°C	Celsius	1.8C+32	Fahrenheit	°F
ILLUMINATION				
lx	lux	0.0929	foot-candles	fc
cd/m ²	candela/m ²	0.2919	foot-Lamberts	fl
FORCE and PRESSURE or STRESS				
N	newtons	2.225	poundforce	lbf
kPa	kilopascals	0.145	poundforce per square inch	lbf/in ²

*SI is the symbol for International System of Units. Appropriate rounding should be made to comply with Section 4 of ASTM E380. (Revised March 2003)

TABLE OF CONTENTS

CHAPTER 1. INTRODUCTION	1
Background	1
Magnitude of the Problem.....	2
Objectives and Scope	5
Organization of the Report	6
CHAPTER 2. LITERATURE REVIEW	7
Current Design Guidance.....	7
Safety Research	9
Crash Research.....	9
Visibility Research.....	12
Physiology Research.....	13
Summary.....	14
CHAPTER 3. METHODOLOGY AND APPROACH.....	17
Analysis Approach	17
Variable Selection	17
Safety-Prediction Model Development and CMFunction Derivation.....	18
Summary.....	20
CHAPTER 4. DATA ACQUISITION AND PREPARATION	21
Data Source and Assessment.....	21
MN Data.....	21
OH Data	23
Data Acquisition.....	23
Supplemental Geometric Data Collection	26
Data Preparation.....	30
Data Description.....	31
MN Data.....	31
OH Data	40
Data Comparison	50
CHAPTER 5. ANALYSIS AND INTERPRETATION OF RESULTS.....	53
Data Mining.....	54
Safety-Prediction Models	59
Total Crashes for Four-Leg Intersections	62
Total Crashes for Three-Leg Intersections	68
Development of CMFs and Functions.....	72
All Rural Four-Leg CMFunctions	74
Rural Four-Leg Two-Lane CMFunctions.....	74
Rural Four-Leg Multilane CMFunctions	76
All Rural Three-Leg CMFunctions.....	76
Rural Three-Leg Two-Lane CMFunctions	77
Total Urban Four-Leg CMFunctions	78
Urban Four-Leg Two-Lane CMFunctions.....	79
All Urban Three-Leg CMFunctions.....	80

Urban Three-Leg Two-Lane CMFunctions	81
Critical Angle Assessment	82
Comparison of Results to Prior CMFs	85
CHAPTER 6. SUMMARY AND CONCLUSIONS	93
Summary	93
Research Conclusions	95
Methodology Conclusions	98
CHAPTER 7. FUTURE RESEARCH	99
APPENDIX A. HSIS DATA VARIABLES	101
APPENDIX B. SUPPLEMENTAL DATA-COLLECTION PROCEDURE AND ISSUES	107
MN Data-Collection Procedure	107
Issue 1—Corrected Skewed Intersection	109
Issue 2—Missing Approach Legs	110
Issue 3—Misclassification	111
Issue 4—Grade Separation	112
Issue 5—Incorrect Classification.....	113
APPENDIX C. DATA TABLES	115
APPENDIX D. DATA DESCRIPTORS AND DATA-MINING RESULTS	125
Data Mining: Background and Application	125
Data Mining: Procedure and Analysis	126
Data Descriptors for Minnesota	129
Data Descriptors for Ohio	145
APPENDIX E. SUPPLEMENTAL SAFETY-PREDICTION MODELS	149
MN Supplemental Safety-Prediction Models	150
All Four-Leg Intersections—Base Models for Total Crashes	150
All Four-Leg Intersections—Interaction Model for Total Crashes	153
Three-Leg Intersections—Base Models for Total Crashes.....	155
Three-Leg Intersections—Interaction Model for Total Crashes.....	159
Four-Leg Intersections—Additional Models.....	160
OH Supplemental Safety-Prediction Models	169
APPENDIX F. CMFUNCTION DEVELOPMENT AND ADDITIONAL MODELS	173
MN CMFunctions	173
Four-Leg Intersections—Total Crashes at All Intersections	173
Four-Leg Intersections—Total Crashes at Rural Intersections.....	175
Four-Leg Intersections—Total Crashes at Two-Lane Rural Intersections	177
Four-Leg Intersections—Total Crashes at Multilane Rural Intersections	179
ACKNOWLEDGMENTS	183
REFERENCES	185

LIST OF FIGURES

Figure 1. Chart. Percentage of fatal crashes in the United States by location (data from NHTSA). ⁽⁷⁾	2
Figure 2. Chart. Percentage of total crashes in the United States by location (data from NHTSA). ⁽⁷⁾	3
Figure 3. Chart. Percentage of MN intersections by number of legs and angle classification (2008 data).....	4
Figure 4. Chart. Percentage of MN intersection crashes by number of legs and angle classification (2008 data). ¹	4
Figure 5. Equation. CMF for skew angle at a three-leg intersection of rural two-lane two-way roads. ⁽²⁴⁾	9
Figure 6. Equation. CMF for skew angle at a four-leg intersection of rural two-lane two-way roads. ⁽²⁴⁾	10
Figure 7. Equation. Number of predicted crashes at a three-leg intersection. ⁽²⁵⁾	10
Figure 8. Equation. Number of predicted crashes at a four-leg intersection. ⁽²⁵⁾	10
Figure 9. Equation. Total crash CMF for skew angle at a three-leg intersection of rural multilane and minor-leg stop-controlled roads. ⁽²⁴⁾	11
Figure 10. Equation. Total crash CMF for skew angle at a four-leg intersection of rural multilane and minor-leg stop-controlled roads. ⁽²⁴⁾	11
Figure 11. Equation. Fatal and injury crash CMF for skew angle at a three-leg intersection of rural multilane and minor-leg stop-controlled roads. ⁽²⁴⁾	11
Figure 12. Equation. Fatal and injury crash CMF for skew angle at a four-leg intersection of rural multilane and minor-leg stop-controlled roads. ⁽²⁴⁾	11
Figure 13. Equation. Number of predicted crashes for three- and four-leg rural two-lane intersections. ⁽²⁸⁾	12
Figure 14. Map. Skewed and nonskewed four-leg intersections in MN.....	29
Figure 15. Map. Density of skewed and nonskewed three-leg intersections in MN.	29
Figure 16. Graph. Annual average total crash rate by intersection angle category, number of legs, and rural/urban classification in MN.....	39
Figure 17. Graph. Annual average total crash rate for rural four-leg intersections by intersection angle category and number of approach lanes on the major road in MN.....	40
Figure 18. Graph. Annual average total crash rate by intersection angle category, number of legs, and rural/urban classification in OH.....	49
Figure 19. Graph. Annual average total crash rate for rural four-leg intersections by intersection angle category and number of approach lanes on the major road in OH.	49
Figure 20. Plot. Results of regression tree (ctree) analysis for total crashes at four-leg intersections.....	58
Figure 21. Equation. AIC.....	60
Figure 22. Equation. BIC.....	60
Figure 23. Graph. Average total crashes per intersection for all four-leg intersections in MN and functional form of $[(1 + \cos(\text{angle})) \times \text{intersection AADT}]$ as distributed across the range of intersection angles.....	63
Figure 24. Graph. Average total crashes per intersection for all four-leg intersections in MN and functional form of $[(1 + \cos(\text{angle})) \times \text{minor road AADT}]$ as distributed across the range of intersection angles.....	64

Figure 25. Equation. Derived variable that incorporates intersection AADT and cosine of the intersection angle.....	64
Figure 26. Equation. Derived variable that incorporates minor road AADT and cosine of the intersection angle.....	64
Figure 27. Equation. Derivation of partial crash prediction term using intersection AADT, minor road AADT, and cosine of the intersection angle.....	65
Figure 28. Graph. Average total crashes per intersection for all three-leg intersections in MN and functional form of $[(1 + \cos(\text{angle})) \times \text{intersection AADT}]$ as distributed across the range of intersection angles.....	69
Figure 29. Graph. Average total crashes per intersection for all three-leg intersections in MN and functional form of $[(1 + \cos(\text{angle})) \times \text{minor road AADT}]$ as distributed across the range of intersection angles.....	69
Figure 30. Equation. CMFunction calculation.....	72
Figure 31. Equation. CMFunction flexible form model 1 calculation for total crashes at all four-leg intersections.....	73
Figure 32. Equation. General form of Hoerl Curve.....	73
Figure 33. Graph. CMF for all rural four-leg intersections.....	74
Figure 34. Graph. CMFunctions for rural four-leg two-lane intersections.....	75
Figure 35. Graph. CMFunctions for rural four-leg two-lane intersections with NC data.....	75
Figure 36. Graph. CMFunctions for rural four-leg multilane intersections.....	76
Figure 37. Graph. CMFunctions for rural three-leg total intersections.....	77
Figure 38. Graph. CMFunction for rural three-leg two-lane intersections.....	78
Figure 39. Graph. CMFunction for urban four-leg total intersections.....	79
Figure 40. Graph. CMFunction for urban four-leg two-lane intersections.....	80
Figure 41. Graph. CMFunction for urban three-leg total intersections.....	81
Figure 42. Graph. CMFunction for urban three-leg two-lane intersections.....	82
Figure 43. Graph. MN CMFs derived from the flexible form models for four-leg intersections, considering different severities.....	84
Figure 44. Graph. CMFunctions derived from the MN flexible form models for rural four-leg intersections with different severities.....	85
Figure 45. Graph. CMFs from the HSM for total crashes at rural two-lane roadway intersections. ⁽²⁴⁾	86
Figure 46. Graph. CMFs from the HSM for total crashes at rural multilane roadway intersections. ⁽²⁴⁾	87
Figure 47. Graph. CMFs from the current study and the HSM for total crashes at rural four-leg two-lane intersections.....	89
Figure 48. Graph. CMFs from the current study and the HSM for total crashes at rural three-leg two-lane intersections.....	89
Figure 49. Graph. CMFs from the current study and the HSM for total crashes at rural four-leg multilane intersections.....	90
Figure 50. Graph. Crash-reduction potential based on CMFs for rural two-lane and multilane intersections.....	91
Figure 51. Equation. Recommended CMFunction for all four-leg intersections, fatal-and-injury crashes.....	96
Figure 52. Equation. Recommended CMFunction for all four-leg intersections, PDO crashes.....	96

Figure 53. Equation. Recommended CMFunction for rural four-leg intersections, total crashes.	96
Figure 54. Equation. Recommended CMFunction for rural four-leg intersections, injury-and-fatal crashes.	96
Figure 55. Equation. Recommended CMFunction for rural four-leg intersections, PDO crashes.	96
Figure 56. Equation. Recommended CMFunction for rural four-leg two-lane intersections, total crashes.	96
Figure 57. Equation. Recommended CMFunction for rural four-leg two-lane intersections, fatal-and-injury crashes.	96
Figure 58. Equation. Recommended CMFunction for rural four-leg two-lane intersections, PDO crashes.	96
Figure 59. Equation. Recommended CMFunction for rural four-leg multilane intersections, total crashes.	97
Figure 60. Equation. Recommended CMFunction for rural four-leg multilane intersections, fatal-and-injury crashes.	97
Figure 61. Equation. Recommended CMFunction for rural four-leg multilane intersections, PDO crashes.	97
Figure 62. Equation. Recommended CMFunction for urban four-leg intersections total crashes.	97
Figure 63. Equation. Recommended CMFunction for urban four-leg two-lane intersections, total crashes.	97
Figure 64. Equation. Recommended CMFunction for rural three-leg intersections, total crashes.	97
Figure 65. Equation. Recommended CMFunction for rural three-leg two-lane intersections, total crashes.	97
Figure 66. Equation. Recommended CMFunction for urban three-leg intersections, total crashes.	97
Figure 67. Equation. Recommended CMFunction for urban three-leg two-lane intersections, total crashes.	97
Figure 68. Illustration. Measured intersection angle with the ArcGIS COGO tool and a 50-foot radius (67 degrees). ⁽⁵⁹⁾	108
Figure 69. Illustration. Measured intersection angle with the ArcGIS™ COGO tool and a 100-foot radius (62 degrees). ⁽⁵⁹⁾	108
Figure 70. Illustration. Intersection shown as skewed four-leg location in the GIS roadway network and as two three-leg intersections in the aerial image. ⁽⁷⁵⁾	110
Figure 71. Illustration. Intersection shown with a single minor leg approach in the GIS roadway network but with two minor leg approaches and a median connector in the aerial image. ⁽⁷⁶⁾	111
Figure 72. Illustration. Intersection shown as a full access four-leg location in the GIS roadway network but as two three-leg intersections (no median connector) in the aerial image. ⁽⁷⁷⁾	112
Figure 73. Illustration. Grade-separated intersection that should not have been included in the original HSIS data received. ⁽⁷⁸⁾	113

Figure 74. Illustration. Intersection that was classified as skewed in the HSIS database but is a right-angle intersection in both the GIS roadway network and the aerial imagery. ⁽⁷⁹⁾	114
Figure 75. Plot. Results of conditional RF (cforest) analysis for total crashes at four-leg intersections.	128
Figure 76. Plot. Conditional RF (cforest) results for total crashes at four-leg intersections.	133
Figure 77. Plot. Conditional RF (cforest) results for fatal-and-injury crashes at four-leg intersections.	134
Figure 78. Plot. Conditional RF (cforest) results for PDO crashes at four-leg intersections.	135
Figure 79. Plot. Conditional RF (cforest) results for total crashes at three-leg intersections.	136
Figure 80. Plot. Conditional RF (cforest) results for fatal-and-injury crashes at three-leg intersections.	137
Figure 81. Plot. Conditional RF (cforest) results for PDO crashes at three-leg intersections. ...	138
Figure 82. Plot. Regression tree for total crashes at four-leg intersections (results from ctree analysis).	139
Figure 83. Plot. Regression tree for fatal-and-injury crashes at four-leg intersections (results from ctree analysis).	140
Figure 84. Plot. Regression tree for PDO crashes at four-leg intersections (results from ctree analysis).	141
Figure 85. Plot. Regression tree for total crashes at three-leg intersections (results from ctree analysis).	142
Figure 86. Plot. Regression tree for injury crashes at three-leg intersections (results from ctree analysis).	143
Figure 87. Plot. Regression tree for PDO crashes at three-leg intersections (results from ctree analysis).	144
Figure 88. Graph. Scatterplot of intersection AADT versus major road AADT for all four-leg intersections in MN.	151
Figure 89. Graph. Scatterplot of intersection AADT versus minor road AADT for all four-leg intersections in MN.	151
Figure 90. Equation. Interaction term of intersection AADT and cosine of the intersection angle.	153
Figure 91. Equation. Interaction term of minor road to intersection AADT ratio and cosine of the intersection angle.	154
Figure 92. Equation. Interaction term of intersection AADT and skew angle expressed in radians.	154
Figure 93. Graph. Scatterplot of intersection AADT versus major road AADT for all three-leg intersections in MN.	156
Figure 94. Graph. Scatterplot of intersection AADT versus minor road AADT for all three-leg intersections in MN.	156
Figure 95. Equation. CMF base model calculation for total crashes at all four-leg intersections.	173
Figure 96. Graph. CMFs derived from the flexible form model 1 and alternative base model for total crashes at all four-leg intersections in MN.	173
Figure 97. Equation. CMF flexible form model 2 calculation for total crashes at all four-leg intersections.	174

Figure 98. Graph. CMFs derived from the flexible form models 1 and 2 and alternative base model for total crashes at all four-leg intersections in MN.....	174
Figure 99. Graph. CMF derived from the alternative base model for total crashes at all four-leg intersections in MN.	175
Figure 100. Equation. CMF base model calculation for total crashes at rural four-leg intersections.....	175
Figure 101. Graph. CMF derived from the alternative base model for total crashes at rural four-leg intersections in MN.	176
Figure 102. Graph. CMFs derived from the flexible form model 1 and alternative base model for total crashes at rural four-leg intersections in MN.	177
Figure 103. Equation. CMF base-model calculation for total crashes at rural four-leg two-lane intersections.	177
Figure 104. Graph. CMF derived from the alternative base model for total crashes at rural four-leg two-lane intersections in MN.	178
Figure 105. Graph. CMFs derived from the flexible form model 1 and alternative base model for total crashes at rural four-leg two-lane intersections in MN.	179
Figure 106. Equation. CMF base model calculation for total crashes at rural four-leg multilane intersections.....	179
Figure 107. Graph. CMFs derived from the alternative base model for total crashes at rural four-leg multilane intersections in MN.	180
Figure 108. Graph. CMFs derived from the flexible form model 1 and alternative base model for total crashes at rural four-leg multilane intersections.....	181

LIST OF TABLES

Table 1. Number of MN intersections by traffic control type and skew classification (2008 data).....	22
Table 2. Number of crashes by intersection type for the first and last years (1999 and 2008) of the potential analysis period. ²	22
Table 3. Number of crashes per intersection by intersection type for the first and last years (1999 and 2008) of the potential analysis period.	23
Table 4. Number of minor leg stop-controlled intersections without changes in the skew/nonskew attributes over time (1999–2008). ³	23
Table 5. Distribution of four-leg intersections by angle classification and area type in MN.	31
Table 6. Distribution of three-leg intersections by angle classification and area type in MN.	32
Table 7. Distribution of four-leg intersections by intersection angle category and area type in MN. ⁶	32
Table 8. Distribution of three-leg intersections by intersection angle category and area type in MN.	33
Table 9. Distribution of rural four-leg intersections by intersection angle category and number of lanes on the major road in MN.	34
Table 10. Distribution of skewed intersections by intersection angle for four-leg and three-leg intersections in MN.	34
Table 11. Distribution of total crashes and total crashes/intersection at four-leg intersections by intersection angle category and area type in MN.	35
Table 12. Distribution of total crashes and total crashes/intersection at three-leg intersections by intersection angle category and area type in MN. ¹⁰	35
Table 13. Range of intersection AADT for four-leg intersections by intersection angle and area type in MN.	36
Table 14. Range of intersection AADT for three-leg intersections by intersection angle and area type in MN. ¹¹	37
Table 15. Range of intersection AADT for four-leg intersections by intersection angle category and the number of lanes on the major road in MN.	38
Table 16. Distribution of four-leg intersections by angle classification and area type in OH.	40
Table 17. Distribution of three-leg intersections by angle classification and area type in OH.	41
Table 18. Distribution of four-leg intersections by intersection angle category and area type in OH.	41
Table 19. Distribution of three-leg intersections by intersection angle category and area type in OH.	42
Table 20. Distribution of rural four-leg intersections by intersection-angle category and number of lanes on the major road in OH.	43
Table 21. Distribution of skewed intersections by intersection angle for four-leg and three-leg intersections in OH.	43
Table 22. Distribution of total crashes and total crashes per intersection at four-leg intersections by intersection-angle category and area type in OH.	44
Table 23. Distribution of total crashes and total crashes per intersection at three-leg intersections by intersection-angle category and area type in OH.	45

Table 24. Distribution of total crashes and total crashes per intersection at rural four-leg intersections by intersection angle category and the number of lanes on the major road in OH.	45
Table 25. Range of intersection AADT for four-leg intersections by intersection angle and area type in OH.	46
Table 26. Range of intersection AADT for three-leg intersections by intersection angle and area type in OH.	47
Table 27. Range of intersection AADT for four-leg intersections by intersection angle category and the number of lanes on the major road in OH.	48
Table 28. Quantity of total intersections by number of legs in each dataset.	50
Table 29. Quantity of skewed intersections by number of legs in each dataset.	50
Table 30. Weighted intersection volumes by roadway type, number of legs, and number of lanes in each State’s dataset.	51
Table 31. Total crashes by number of legs in each dataset.	51
Table 32. Analysis framework for MN—summary of crashes by collision severity and intersection classification in the final database.	53
Table 33. Analysis framework for OH—summary of crashes by collision severity and intersection classification in the final database.	54
Table 34. Most important predictor variables for MN four-leg intersections (results from cforest analysis).	56
Table 35. Most important predictor variables for MN three-leg intersections (results from cforest analysis).	57
Table 36. General guidance for interpretation of models using AIC and BIC criteria.	60
Table 37. Different roadways with sufficient data for total crash CMFunction development.	62
Table 38. Flexible form model 1 results for total crashes at all four-leg intersections for MN.	66
Table 39. Model fit statistics for OH for total rural four-leg intersections.	67
Table 40. Model fit statistics for OH for urban four-leg total intersections.	67
Table 41. Flexible form model 1 results for total crashes at all three-leg intersections for MN.	70
Table 42. Model fit statistics for OH for rural three-leg all intersections.	71
Table 43. Model fit statistics for OH for urban three-leg, all intersections.	71
Table 44. Peak CMFunction values and corresponding angles for total crashes for all intersection types.	83
Table 45. CMFunction values derived from all models for total crashes at all intersections.	84
Table 46. List of variables available from the HSIS MN crash file.	101
Table 47. List of variables available from the HSIS MN roadlog file.	102
Table 48. List of variables available from the HSIS MN intersection file.	103
Table 49. Four-leg intersections by angle classification and area type in MN.	115
Table 50. Total crashes (2003–2009) at four-leg intersections by angle classification and area type in MN.	115
Table 51. Four-leg intersections by intersection angle and area type in MN.	115
Table 52. Total crashes (2003–2009) at four-leg intersections by intersection angle and area type in MN.	116
Table 53. Fatal-and-injury crashes (2003–2009) at four-leg intersections by intersection angle and area type in MN.	116

Table 54. PDO crashes (2003–2009) at four-leg intersections by intersection angle and area type in MN.	117
Table 55. Intersection AADT for four-leg intersections by intersection angle and area type in MN.	117
Table 56. Minor road AADT for four-leg intersections by intersection angle and area type in MN.	118
Table 57. Major road AADT for four-leg intersections by intersection angle and area type in MN.	118
Table 58. Total crash rates (per 100 M entering vehicles) for four-leg intersections by intersection angle and area type in MN.	119
Table 59. Fatal-and-Injury crash rates (per 100 M entering vehicles) for four-leg intersections by intersection angle and area type in MN.	119
Table 60. PDO crash rates (per 100 M entering vehicles) for four-leg intersections by intersection angle and area type in MN.	120
Table 61. Three-leg intersections by angle classification and area type in MN.	120
Table 62. Total crashes (2003–2009) at three-leg intersections by angle classification and area type in MN.	120
Table 63. Three-leg intersections by intersection angle and area type in MN.	120
Table 64. Total crashes (2003–2009) at three-leg intersections by intersection angle and area type in MN.	121
Table 65. Fatal-and-injury crashes (2003–2009) at three-leg intersections by intersection angle and area type in MN.	121
Table 66. PDO crashes (2003–2009) at three-leg intersections by intersection angle and area type in MN.	121
Table 67. Intersection AADT for three-leg intersections by intersection angle and area type in MN.	122
Table 68. Minor road AADT for three-leg intersections by intersection angle and area type in MN.	122
Table 69. Major road AADT for three-leg intersections by intersection angle and area type in MN.	123
Table 70. Total crash rates (per 100 M entering vehicles) for three-leg intersections by intersection angle and area type in MN.	123
Table 71. Fatal-and-injury crash rates (per 100 M entering vehicles) for three-leg intersections by intersection angle and area type in MN.	123
Table 72. PDO crash rates (per 100 M entering vehicles) for three-leg intersections by intersection angle and area type in MN.	124
Table 73. Variable names, descriptors, definitions, and attributes for MN.	130
Table 74. Variable names, descriptors, definitions, and attributes for OH.	145
Table 75. Number of sites in each angle bin for all rural, four-leg intersections in OH.	145
Table 76. Number of sites in each angle bin for rural four-leg two-lane intersections in OH. ..	146
Table 77. Number of sites in each angle bin for rural four-leg multilane intersections in OH.	146
Table 78. Number of sites in each angle bin for rural three-leg total intersections in OH.	146
Table 79. Number of sites in each angle bin for rural three-leg two-lane intersections in OH.	146
Table 80. Number of sites in each angle bin for urban four-leg total intersections in OH.	147

Table 81. Number of sites in each angle bin for urban four-leg two-lane intersections in OH.	147
Table 82. Number of sites in each angle bin for urban three-leg total intersections in OH.	147
Table 83. Number of sites in each angle bin for urban three-leg two-lane intersections in OH.	147
Table 84. Summary of severity models included in appendix E.	149
Table 85. Initial base model results for total crashes at all four-leg intersections in MN.	152
Table 86. Alternative base model results for total crashes at all four-leg intersections in MN.	153
Table 87. Interaction model results for total crashes at all four-leg intersections in MN.	155
Table 88. Initial base model results for total crashes at all three-leg intersections in MN.	157
Table 89. Alternative base model results for total crashes at all three-leg intersections in MN.	158
Table 90. Flexible form model 2 results for total crashes at all three-leg intersections in MN.	158
Table 91. Interaction model results for total crashes at all three-leg intersections in MN.	159
Table 92. Flexible form model 1 results for fatal-and-injury crashes at all four-leg intersections in MN.	160
Table 93. Alternative base model results for PDO crashes at all four-leg intersections in MN.	161
Table 94. Flexible form model 1 results for PDO crashes at all four-leg intersections in MN.	161
Table 95. Alternative base model results for total crashes at all rural four-leg intersections in MN.	162
Table 96. Flexible form model 1 results for total crashes at all rural four-leg intersections in MN.	162
Table 97. Alternative base model results for fatal-and-injury crashes at all rural four-leg intersections in MN.	163
Table 98. Flexible form model 1 results for fatal-and-injury crashes at all rural four-leg intersections in MN.	163
Table 99. Alternative base model results for PDO crashes at all rural four-leg intersections in MN.	164
Table 100. Flexible form 1 model results for PDO crashes at all rural four-leg intersections in MN.	164
Table 101. Alternative base model results for total crashes at rural two-lane, four-leg intersections in MN.	165
Table 102. Flexible form model 1 results for total crashes at rural two-lane, four-leg intersections in MN.	165
Table 103. Flexible form model 1 results for fatal-and-injury crashes at rural two-lane, four-leg intersections in MN.	166
Table 104. Alternative base model results for PDO crashes at rural two-lane, four-leg intersections in MN.	166
Table 105. Flexible form model 1 results for PDO crashes at rural two-lane, four-leg intersections in MN.	167
Table 106. Alternative base model results for total crashes at rural multilane four-leg intersections in MN.	167

Table 107. Flexible form model 1 results for total crashes at rural multilane four-leg intersections in MN.	167
Table 108. Flexible form model 2 results for fatal-and-injury crashes at rural multilane four-leg intersections in MN.	168
Table 109. Alternative base model results for PDO crashes at rural multilane four-leg intersections in MN.	168
Table 110. Model fit statistics for OH for rural four-leg two-lane intersections in OH.	169
Table 111. Model fit statistics for OH for rural four-leg multilane intersections in OH.	170
Table 112. Model fit statistics for OH for rural three-leg two-lane intersections in OH.	170
Table 113. Model fit statistics for OH for urban four-leg two-lane intersections in OH.	171
Table 114. Model fit statistics for OH for urban three-leg two-lane intersections in OH.	171
Table 115. CMF functions derived by NB model form for MN.	182
Table 116. CMF values derived from the flexible form models for four-leg rural intersections.	182

LIST OF ACRONYMS AND ABBREVIATIONS

AADT	annual average daily traffic
AASHTO	American Association of State Highway and Transportation Officials
AIC	Akaike information criterion
APS	accessible pedestrian signal
BIC	Bayesian information criterion
CA	California
CART	classification and regression tree
CMFunction	crash modification function
CMF	crash modification factor
CRF	conditional random forest
DOT	department of transportation
F&I	fatal and injury
FARS	Fatality Analysis Reporting System
FHWA	Federal Highway Administration
GA	Georgia
GIS	geographic information system
HSIS	Highway Safety Information System
HSM	<i>Highway Safety Manual</i>
IHSDM	Interactive Highway Safety Design Model
ITE	Institute of Transportation Engineers
MARS	multivariate adaptive regression splines
MDT	Montana Department of Transportation
MI	Michigan
MN	Minnesota
MNDOT	Minnesota Department of Transportation
NB	negative binomial
NC	North Carolina
NCHRP	National Cooperative Highway Research Program
NHTSA	National Highway Traffic Safety Administration
NM	negative multinomial
ODOT	Ohio Department of Transportation
OH	Ohio
PDO	property damage only
RAM	random access memory
RF	random forest
ROW	right-of-way
SPF	safety performance function
vpd	vehicles per day

CHAPTER 1. INTRODUCTION

BACKGROUND

The preferred design for conventional intersections in which all movements are accommodated includes adjacent legs that intersect at 90 degrees. However, there are occasions where physical constraints result in intersection angles less than 90 degrees, which produce skewed intersections. Such intersections may create potential safety and operational problems for both motorists and nonmotorists.

Skewed intersections generally result in larger intersections. The additional space needed for skewed intersections introduces a couple of potential problems for drivers. First, drivers have a longer distance to travel when crossing the intersection or making certain turning maneuvers, which results in increased exposure within the intersection. Second, the increased surface area may result in driver confusion regarding alignment on the approach to the intersection or while turning or crossing. Both potential problems may also apply to bicyclists on the roadway.

The angles introduced at skewed intersections create additional problems. First, the orientation of crossing traffic to the waiting driver, bicyclist, or pedestrian may make it more difficult to detect and judge the speed of approaching vehicles on conflicting paths. Second, intersecting legs with acute angles between them can adversely affect the turning radius of the intersection, making it more difficult to accommodate large trucks. Third, acute angles may introduce additional sight obstructions, including possible obstructions from the body of the driver's vehicle. For older drivers, acute angles introduce the problem of not being able to physically turn their heads, necks, or upper bodies to create the necessary sight lines for seeing crossing traffic.

Skewed intersections present several problems to pedestrians. First, the distances that must be crossed by a pedestrian are greater at skewed intersections than at right-angle intersections. This problem increases the exposure time for a crossing pedestrian and is exacerbated for pedestrians, such as older persons, who may be traveling at a slower pace. Second, the sight lines between the pedestrian and driver are altered from a typical right-angle intersection, which creates an environment in which the two parties may not be looking at the correct places for potential conflicts. Third, skewed intersections are problematic for visually impaired pedestrians. Skewed intersections create an environment in which it is difficult for visually impaired pedestrians to align themselves for the crossing, ascertain the direction of traffic from sounds, and maintain alignment when crossing the street.

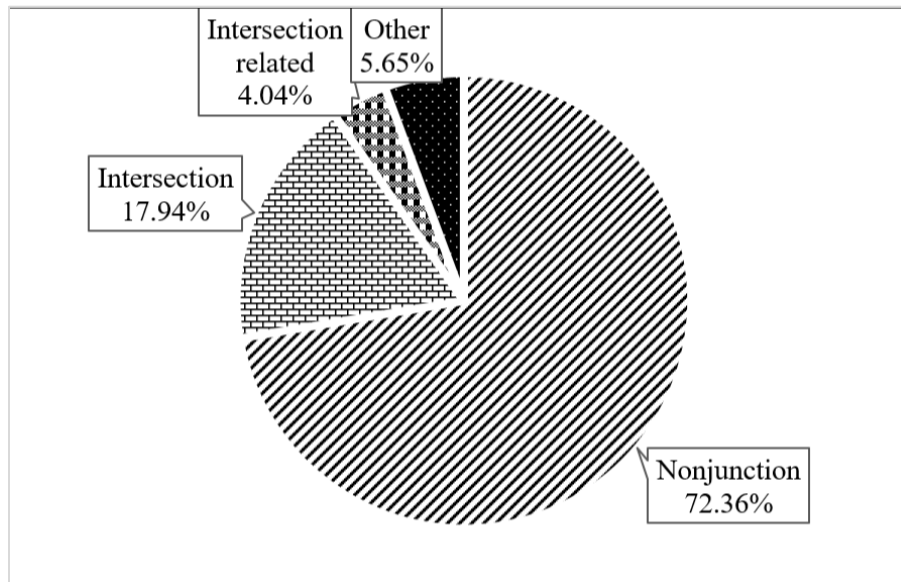
Properly addressing the operational and safety problems that result from skewed intersections requires sound design policies and practices. In *A Policy on Geometric Design of Highways and Streets*, the American Association of State Highway and Transportation Officials (AASHTO) recommends that "intersecting roads should generally meet at or nearly at right angles."⁽¹⁾ The Green Book also indicates that some deviation from a 90-degree angle is permissible but that an angle of at least 60 degrees provides most of the same benefits.⁽¹⁾ The Institute of Transportation Engineers' (ITE's) *Traffic Engineering Handbook* provides similar guidance.⁽²⁾ However, prior ITE guidance recommended a minimum intersection angle of 70–75 degrees.^(3–5)

The Federal Highway Administration's (FHWA's) *Highway Design Handbook for Older Drivers and Pedestrians* also recommends right-angle intersections where right-of-way (ROW) is not restricted and a minimum intersection angle of 75 degrees where ROW is restricted.⁽⁶⁾ There are also differences among State departments of transportation (DOTs) regarding the desired minimum intersection angle.

To date, crash-based research on safety and operational implications of intersection angles has been limited. The limited research might explain the lack of consensus among existing policies and guidance. Researchers, practitioners, and agencies need to better understand the effects of intersection angles on crashes and enhance the current design guidance.

MAGNITUDE OF THE PROBLEM

Intersections account for a large portion of road-safety problems in the United States. Per data from the National Highway Traffic Safety Administration (NHTSA), almost 22 percent of fatal crashes (figure 1) and more than 40 percent of total crashes (figure 2) occur at or are related to intersections.⁽⁷⁾ These facts are not unexpected because intersections are the locations on the Nation's roadway system that have the most conflicts. The number of potential conflicts is also a function of traffic volume; therefore, urban intersections are likely to have more collisions than rural intersections. Kuciemba and Cirillo found that intersections account for more than 50 percent of total crashes in urban areas while intersections account for just over 30 percent of total crashes in rural areas.⁽⁸⁾ A study of California (CA) crashes found similar results. The CA study showed that, on average, 1.5 crashes per year occur at rural unsignalized intersections and 2.5 crashes per year occur at urban unsignalized intersections.⁽⁹⁾

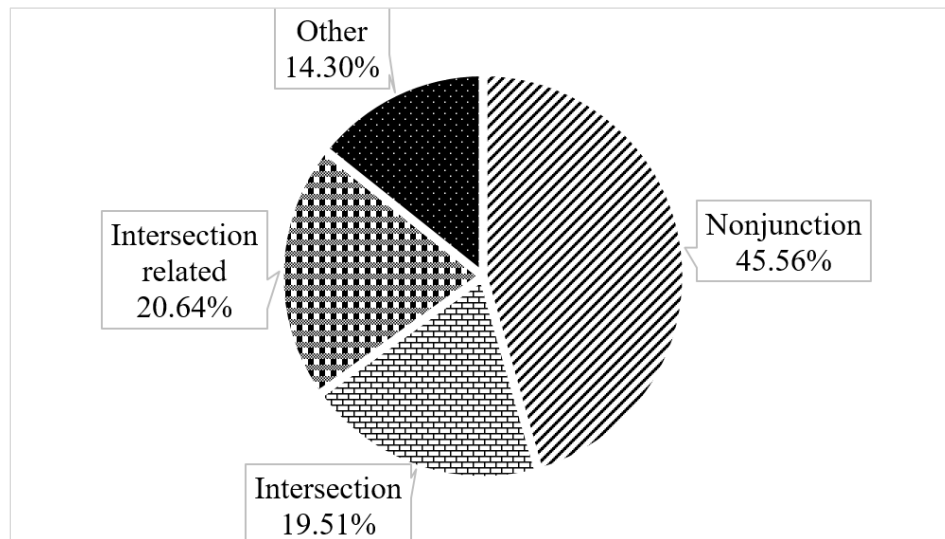


Source: FHWA.

Figure 1. Chart. Percentage of fatal crashes in the United States by location (data from NHTSA).⁽⁷⁾

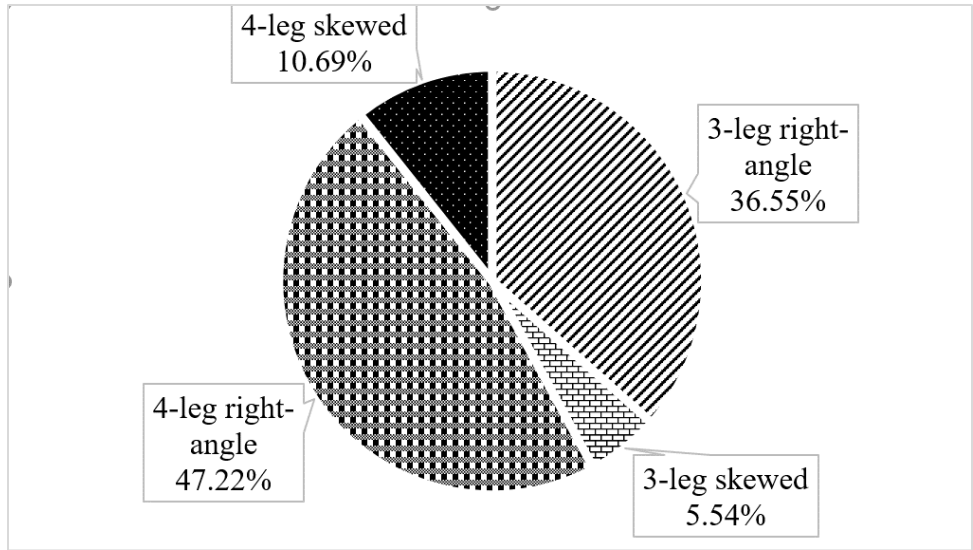
The number of these fatal crashes that occur at skewed intersections is more difficult to determine. There is no national database that includes geometric data on intersections.

Similarly, there are few States that have this information readily available. The Minnesota (MN) Department of Transportation (MNDOT) has this information available for most of its State-maintained intersections, as does the Ohio Department of Transportation (ODOT). An analysis of MNDOT's 2008 intersection inventory data revealed that more than 16 percent of the intersections are skewed (figure 3). This percentage includes signalized and unsignalized locations. A review of MNDOT crash data indicates that almost 18 percent of intersection crashes occurred at these skewed locations (figure 4), which indicates that such locations may be slightly overrepresented.⁽¹⁰⁾ However, these statistics do not account for traffic volume, area type, or other factors that may contribute to the crash problem.



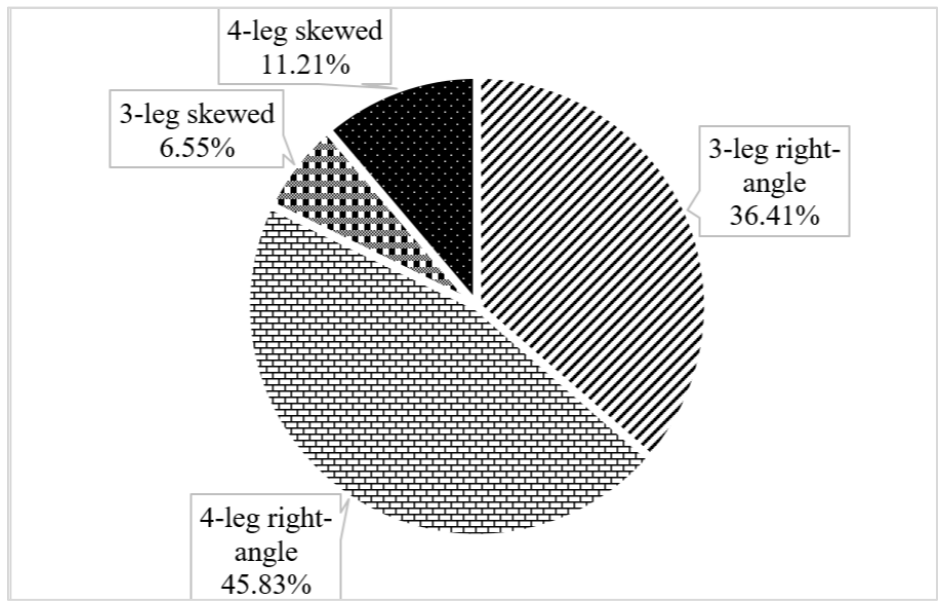
Source: FHWA.

Figure 2. Chart. Percentage of total crashes in the United States by location (data from NHTSA).⁽⁷⁾



Source: FHWA.

Figure 3. Chart. Percentage of MN intersections by number of legs and angle classification (2008 data).¹



Source: FHWA.

Figure 4. Chart. Percentage of MN intersection crashes by number of legs and angle classification (2008 data).¹

Intersections account for approximately 40 percent of the locations of crashes on U.S. roads. From the limited data available from MN, more than 16 percent of intersections in the State may be classified as skewed, and these locations may be overrepresented in terms of total crash occurrence.⁽¹⁰⁾

¹Data available from HSIS.

This conclusion was supported by Fatality Analysis Reporting System (FARS) data for Ohio from 2016, which showed that roughly 26 percent of fatal crashes occurred at intersections in Ohio (OH).⁽¹²⁾

Given the facts obtained from MN and OH data, careful consideration should be given to mitigate skewed intersections when designing new roadways or retrofitting existing roadways. Guidance from the Green Book, State highway design manuals, and other resources range in terms of complexity.⁽¹⁾ Examples of mitigations include realignment of an intersection to generate a right-angle location, addition of traffic signals or signs to prohibit or more closely control certain movements, addition of auxiliary turning and acceleration lanes to lessen the severity of the angles and allow drivers to use their mirrors to detect conflicting traffic, addition of channelization to provide better guidance through the intersection and accommodate pedestrians, and installation of accessible pedestrian signals to meet the needs of visually impaired pedestrians.^(1,13–16)

OBJECTIVES AND SCOPE

The objective of this study was to derive quantitative relationships between intersection angles and safety where intersection crashes define safety. The relationships were used as follows:

- Determine appropriate crash modification factors (CMFs) for reducing or eliminating the skew angle of an intersection.
- Determine if there is a critical minimum angle at which safety is substantially diminished (75 degrees, 60 degrees, or other).
- Assess the need for revision of current geometric design policies and practices.

This study was restricted to the analysis and interpretation of intersection crash data. Other observational studies examined specific aspects of skewed intersections, such as sight distance or pedestrian-crossing behaviors, which are described in chapter 2. Resources are available that discuss other aspects of the problem of skewed intersections and subsequent countermeasure possibilities and costs.^(13,15) The greatest need related to the topic of intersection angles and safety at this time is a sound crash-based evaluation.

The statistics in the section that examines the magnitude of the problem did not fully differentiate among characteristics—such as type of area (rural versus urban), number of legs, type of traffic control present, and other features—used to further define and scope the problem. Many of these characteristics were used to limit the scope of this study for both practical reasons related to supplemental data-collection efforts and methodological reasons related to adequate sample size. Chapter 4 of this report examines the scope of this research effort in more detail.

One of the anticipated outcomes of this study is possible new guidance for design policies and practices. This new guidance may include recommended changes to the Green Book.⁽¹⁾ The current policy, which includes the critical minimum angle of 60 degrees, has been in place for decades. The 1965 AASHTO policy on geometric design notes that angles greater than 60 degrees produce only a small reduction in visibility; therefore, realignment may not be warranted.⁽¹⁷⁾

Other agencies and organizations, including FHWA and ITE, have recommended critical minimum angles of 70–75 degrees in recent years based on behavioral and observational research. AASHTO policymakers have reviewed these recommendations but have not yet revised the contents of the Green Book,⁽¹⁾ which may partly be a function of desiring definitive safety results on this issue. This study aims to fill this void.

ORGANIZATION OF THE REPORT

Chapter 1 presented an overview of intersection angles and skewed intersections. Chapter 2 reviews literature related to the topic of intersection angles. This chapter includes studies that have attempted to quantify the crash effects of intersection angles as well as studies that have addressed visibility (sight distance) and physiological issues of drivers and pedestrians. Chapter 3 describes the methodology and analysis approach. Chapter 4 discusses the data acquired for this project. Chapter 5 includes the results of the MN data analysis, and chapter 6 presents the OH analysis results. Chapter 7 includes a summary of the study and conclusions. Chapter 8 presents ideas for additional research related to intersection angles. There are also six appendices that include additional information related to the data and analysis results.

CHAPTER 2. LITERATURE REVIEW

As noted in the introduction, addressing the potential safety and operational problems of skewed intersections requires sound design policies and practices. The first part of this chapter describes the design policies and guidance that currently exist in the United States. These policies should be informed by or based on research that has been conducted on the topic. The second part of this chapter discusses the limited research that has addressed intersection angles and their effect on safety.

CURRENT DESIGN GUIDANCE

The Green Book addresses the issue of intersection alignment and skew angle in several chapters. In chapter 9, which focuses on intersections, the recommendation is that “intersecting roads should generally meet at or nearly at right angles” (p. 9-25).⁽¹⁾ This chapter also includes recommendations related to the realignment of a skewed intersection, noting that “the angle of the realigned intersection should be as close to 90 degrees as practical.”⁽¹⁾ However, the policy includes a section indicating that some deviation from a right angle is permissible and that providing “an angle of at least 60 degrees provides most of the benefits of a 90-degree intersection angle while reducing the right-of-way takings and construction costs often associated with providing a right-angle intersection” (p. 9-27).⁽¹⁾ The foundation for the statement on deviations and their benefits is unclear.

The Green Book chapter on intersections also addresses the effect of skew angle on intersection sight distance. The chapter notes that the sight triangles at a skewed intersection will be larger or smaller, depending on the quadrant, than what is present at a right-angle intersection.⁽¹⁾ The policy examines the issues associated with longer crossing distances within the intersection and the effect longer crossing distances might have on sight-distance computations. Line-of-sight issues for the approaching driver are also discussed, and recommendations are provided for adjusting the sight-distance computation. The effect of skew angles on turning radius is addressed later in the chapter on intersections, with recommendations for defining the control radius and point of tangency that should be used when developing design alternatives for channelization at skewed intersections.⁽¹⁾

In chapter 5 of the Green Book, which focuses on designing intersections of local roads and streets, the recommended policy is for intersecting streets to “meet at approximately a 90-degree angle” and for the alignment design to “avoid an angle of intersection of less than 60 degrees.”⁽¹⁾ For collector roads and streets, the recommendation specifically addresses stop-controlled intersections. The policy indicates that the intersecting legs “should intersect at right angles, wherever practical, and should not intersect at an angle less than 60 degrees.”⁽¹⁾

The Green Book is a product of State transportation engineers, designers, and policymakers.⁽¹⁾ State DOTs, therefore, use the Green Book as the starting point for their own internal design policies.⁽¹⁾ The policies of several States were examined regarding intersection design and skew angle. Iowa’s design manual addresses the intersection of crossroads with rural two-lane or multilane primary highways. The policy establishes an intersecting angle of 90 degrees as “ideal,” between 90 and 75 degrees as “desirable,” and between 75 and 60 degrees as

“acceptable.” Any intersections with angles less than 60 degrees “will be realigned to provide a desirable intersection angle.”⁽¹⁸⁾

The Montana Department of Transportation (MDT) policy indicates that “roadways should intersect at or as close to 90 degrees as practical” and provides several reasons why skewed intersections are undesirable. The policy notes that the intersection angle should not exceed 30 degrees from perpendicular. Regarding realignment, the MDT policy notes that it will rarely be warranted to realign “the intersection so that its skew is within 30 degrees of perpendicular.” If the skew angle is greater than 30 degrees, the policy notes that “the intersection may require geometric improvements (realignment, auxiliary lanes, greater corner sight distance).”⁽¹⁹⁾

The policy for the Illinois Department of Transportation states that “highways should intersect at right angles” (p. 34-1(1)) and provides several reasons why acute angles are undesirable. However, the policy also notes that the angle should be within 15 degrees of perpendicular and “this amount of skew can often be tolerated because the impact on sight lines and turning movements is not significant” (p. 34-1(2)). The policy further notes that an intersection angle up to 30 degrees from perpendicular may be used under restricted conditions. For a skew angle greater than 30 degrees, geometric improvements or more positive traffic control (e.g., all stop, traffic signals) may be warranted.⁽²⁰⁾

The California Department of Transportation (Caltrans) also recommends intersection angles of 90 degrees, and when a 90-degree angle cannot be achieved, it recommends a minimum angle of 75 degrees. The justification includes the following statement: “A 75 degree angle does not unreasonably increase the crossing distance or generally decrease visibility” (p. 400-5). For intersection angles less than 75 degrees, Caltrans recommends that a series of retrofit improvement strategies be considered, including realignment, provision of acceleration lanes, and turning movement restrictions.⁽²¹⁾

The Iowa DOT design manual cites the *Intersection Channelization Design Guide*. This National Cooperative Highway Research Program (NCHRP) publication includes recommended guidance regarding intersection angles for both new construction and reconstruction/rehabilitation. The recommendation for new construction is to maintain angles between 75 and 90 degrees unless there are “costly or severe constraints.” If such constraints exist, angles as low as 60 degrees are acceptable. For reconstruction/rehabilitation projects, the *Intersection Channelization Design Guide* recommends examining crash rates and patterns that may be attributable to the skew of the intersection.⁽¹⁶⁾

The *Traffic Engineering Handbook* provides similar guidance to the guidance in the Green Book and other resources regarding the desire for right-angle intersections.^(1,2) This handbook also acknowledges the safety and operational problems that exist at intersecting angles less than 60 degrees. The document does not recommend a minimum desirable angle, but prior ITE guidance documents have recommended minimum intersection angles. The 1999 edition of the *Traffic Engineering Handbook* recommends a minimum angle of 75 degrees.⁽⁴⁾ The *Neighborhood Street Design Guidelines* recommends a minimum angle of 70 degrees.⁽³⁾ A recommended practice for subdivision streets indicates that “in no case should the angle be less than 75 degrees.”⁽⁵⁾

FHWA has published two guidance documents that include recommendations related to skewed intersections. The *Highway Design Handbook for Older Drivers and Pedestrians* recommends right-angle intersections in which ROW is not constrained.⁽⁶⁾ For intersections in which ROW is restricted, the recommendation is for a minimum intersection angle of 75 degrees.⁽⁶⁾ This handbook also recommends the prohibition of right turns on red in approach legs where the intersecting angle to the driver's left is less than 75 degrees. In *Signalized Intersections: Informational Guide*, the authors discuss several operational and safety issues associated with skewed intersections. A brief synopsis is provided of the range of minimum intersection angles from 60 to 75 degrees recommended in different sources.⁽²²⁾ This guide does not make a recommendation on a minimum angle value.

AASHTO's *Guide for the Planning, Design, and Operation of Pedestrian Facilities* discusses the implications of skewed intersections on pedestrians.⁽²³⁾ Concerns include longer crossing distances, increased exposure to traffic and possible conflicts, and proper location of the crosswalks. The authors also discuss navigational issues for the visually impaired pedestrian, including the pedestrian's ability to properly align themselves for crossing the intersection and maintaining alignment while crossing. This guide, however, does not make any recommendations regarding desirable or minimum intersection angles. The difficulties that visually impaired pedestrians have at skewed intersections are addressed in a best practices guide on accessible pedestrian signals (APS).⁽¹⁴⁾ This APS best practices guide includes a prioritization tool for rating intersections regarding the need for APS to help pedestrians cross the street. A skewed crossing received the second highest number of points (more points equates to greater crossing difficulty) of any operational or geometric characteristic at a crosswalk.

SAFETY RESEARCH

The research available on the safety effects of intersection angles is limited and not definitive. The work that has been conducted can be divided into three types of studies: crash, visibility, and physiology. The crash-based research explored the relationships between the intersection skew angle and crash frequencies or rates. The visibility-based research focused on the sight lines and sight-distance requirements using observational inputs from drivers. The physiology-based research primarily addressed the diminished physical skills of older persons and how these diminished skills impacted the drivers' abilities to negotiate skewed intersections. A summary of the studies discovered in each of these areas follows.

Crash Research

The *Highway Safety Manual* (HSM) includes CMFs for skew angles at three- (figure 5) and four-leg (figure 6) intersections as part of the predictive method for rural two-lane two-way roads.⁽²⁴⁾

$$CMF (3\text{-leg intersection}) = \text{EXP}(0.0040 \times skew)$$

Figure 5. Equation. CMF for skew angle at a three-leg intersection of rural two-lane two-way roads.⁽²⁴⁾

$$CMF \text{ (4-leg intersection)} = \text{EXP} (0.0054 \times skew)$$

Figure 6. Equation. CMF for skew angle at a four-leg intersection of rural two-lane two-way roads.⁽²⁴⁾

Where:

CMF = crash modification factor for total crashes.

skew = intersection skew angle in degrees; the absolute value of the difference between 90 degrees and the actual intersection angle.

For example, consider an intersection (either a three- or four-leg intersection) in which the smallest angle between any two legs is 70 degrees. The skew angle is 20 degrees, calculated as the difference between 90 and 70 degrees. Inserting 20 degrees into the equations shown in figure 5 and figure 6, the CMFs would be calculated as 1.08 and 1.11 for three- and four-leg intersections, respectively. Thus, a three-leg rural stop-controlled intersection with a 70-degree intersection angle is expected to have 8 percent more total crashes than a right-angle intersection. Similarly, a four-leg rural stop-controlled intersection is expected to experience 11 percent more total crashes.

These CMFs were developed as part of an FHWA study to develop an algorithm for predicting the safety performance of a rural two-lane highway.⁽²⁵⁾ This algorithm became the initial crash prediction module within FHWA's Interactive Highway Safety Design Model (IHSDM). The CMFs were derived from negative binomial (NB) regression models, which were developed using data from 382 three-leg and 324 four-leg stop-controlled intersections in MN. The distribution of these locations by the angle of intersection at each site was not provided. The models took the forms shown in figure 7 and figure 8.

$$N_{3-leg} = \text{EXP}(-12.82 + 1.01\ln ADT_{maj} + 0.406\ln ADT_{min} + RHRI + 0.33RT + 0.0040SKEW_3)$$

Figure 7. Equation. Number of predicted crashes at a three-leg intersection.⁽²⁵⁾

$$N_{4-leg} = \text{EXP}(-9.34 + 0.60\ln ADT_{maj} + 0.61\ln ADT_{min} + 0.13ND_{maj} + 0.0054SKEW_4)$$

Figure 8. Equation. Number of predicted crashes at a four-leg intersection.⁽²⁵⁾

Where:

N_{3-leg} = predicted number of total crashes per year at a particular three-leg intersection and within 250 ft in either direction along the major road.

N_{4-leg} = predicted number of total crashes per year at a particular four-leg intersection and within 250 ft in either direction along the major road.

ADT_{maj} = average daily traffic volume vehicles per day (vpd) on the major road.

ADT_{min} = average daily traffic volume (vpd) on the minor road.

ND_{maj} = number of driveways on the major road within 250 ft of the intersection.

$RHRI$ = roadside hazard rating within 250 ft of the intersection on the major road.

RT = presence of right-turn lane on the major road (0 = no turn lane present; 1 = turn lane present).

$SKEW_3$ = intersection angle (degrees) minus 90 for the angle between the major-road leg in the direction of increasing stations and a leg to the right; 90 minus intersection angle (degrees) for the angle between the major-road leg in the direction of increasing stations and a leg to the left.

$SKEW_4$ = intersection angle (degrees) expressed as one-half of the angle to the right minus one-half of the angle to the left for the angles between the major-road leg in the direction of increasing stations and the right and left legs, respectively.

The four-leg model included all crash types and only variables that were significant at a significance level of 0.15 or less; skew angle was significant at a significance level (p -value) equal to 0.108. The three-leg model included only those crash types generally related to intersection operations; the p -value for skew angle in this model was 0.17. As part of this same study, a panel of road-safety research experts evaluated these models and determined that the coefficients for skew angles were appropriate to use for CMFs to ascertain the safety effect of intersection angles. However, the panel also recommended further research on this geometric characteristic.

The HSM also includes CMFs shown in figure 9 through figure 12 for intersection angles in which rural multilane highways intersect with minor roads under stop-control.⁽²⁴⁾ In figure 9 through figure 12, $CMF(X)$ is the crash modification factor for the specified number of legs and crash type.

$$CMF(3\text{-leg, total crashes}) = [(0.016 \times skew)/(0.98 + 0.016 \times skew)] + 1$$

Figure 9. Equation. Total crash CMF for skew angle at a three-leg intersection of rural multilane and minor-leg stop-controlled roads.⁽²⁴⁾

$$CMF(4\text{-leg, total crashes}) = [(0.053 \times skew)/(1.43 + 0.053 \times skew)] + 1$$

Figure 10. Equation. Total crash CMF for skew angle at a four-leg intersection of rural multilane and minor-leg stop-controlled roads.⁽²⁴⁾

$$CMF(3\text{-leg, injury crashes}) = [(0.017 \times skew)/(0.52 + 0.017 \times skew)] + 1$$

Figure 11. Equation. Fatal and injury crash CMF for skew angle at a three-leg intersection of rural multilane and minor-leg stop-controlled roads.⁽²⁴⁾

$$CMF(4\text{-leg, injury crashes}) = [(0.048 \times skew)/(0.72 + 0.048 \times skew)] + 1$$

Figure 12. Equation. Fatal and injury crash CMF for skew angle at a four-leg intersection of rural multilane and minor-leg stop-controlled roads.⁽²⁴⁾

These CMFs were developed as part of an FHWA study to validate and calibrate the crash prediction statistical models for rural intersections within IHSDM.⁽²⁶⁾ The original models were developed using 3 yr of crash data (1993–1995) for a set of intersections in CA and Michigan (MI).⁽²⁷⁾ The validation study added 2 yr of crash data (1996–1997) for the same set of intersections and 2 yr of data (1996–1997) for a set of intersections in Georgia (GA). The CMFs were derived from the recalibrated NB regression models for three- and four-leg stop-controlled

intersections. The intersections included in the analysis had two lanes on the minor road and four lanes on the major road. The three-leg analysis included data from 218, 24, and 52 intersections in CA, MI, and GA, respectively. The four-leg analysis included data from 152, 18, and 52 intersections in CA, MI, and GA, respectively. As with the two-lane study previously noted, the distribution of these locations by the angle of intersection at each site was not provided.

A study designed to develop guidelines for the realignment of intersections in Nebraska used crash data from three- and four-leg rural two-lane roadway intersections.⁽²⁸⁾ Three years of crash data for 29 skewed intersections and 39 comparable nonskewed intersections were used to develop the Poisson regression model shown in figure 13.

$$N = 0.050 \left(\frac{ADT_{maj}}{100} \right)^{0.545} \left(\frac{ADT_{min}}{100} \right)^{\beta} e^{0.011\alpha}$$

Figure 13. Equation. Number of predicted crashes for three- and four-leg rural two-lane intersections.⁽²⁸⁾

Where:

N = number of crashes per year.

ADT_{maj} = annual average daily traffic (vpd) on major roadway.

ADT_{min} = annual average daily traffic (vpd) on minor roadway.

β = intersection-type factor = $0.129 + 0.260F$.

$F = 0$ for three-leg intersection; 1 for four-leg intersection.

α = skew angle (degrees).

e = natural exponent.

The model produces an increase in crashes as the traffic volume and skew angle increases, with four-leg intersections having more crashes than three-leg intersections for the same volumes and skew angle.

Another study of three-leg intersections found that wye (skewed) intersections had crash rates approximately 50 percent higher than tee (right-angle) intersections, suggesting an effect of intersection angle.⁽²⁹⁾ A study of intersections in Finland found that acute and obtuse skew angles affected safety differently.⁽³⁰⁾ This phenomenon was discussed by the expert panel convened for the FHWA study on rural two-lane roads, but it was decided that this study alone “did not provide a sufficient basis for challenging the widely accepted view that any intersection skew that departs from a 90-degree angle, whether positive or negative, is detrimental to safety.”⁽²⁵⁾

Visibility Research

Gattis and Low conducted a field study and measured the angles at which drivers’ lines of sight were obstructed by the body of their vehicles when looking to the right.^(31,32) Two driver positions (sit back and lean forward) were used. A 13.5-degree vision angle (with respect to a line perpendicular to the vehicle path) was selected to represent an intermediate posture, between the sit-back and the lean-forward positions. The authors concluded that a 60-degree left-skewed intersection may result in an obstructed line of sight to the right for a driver for certain types of vehicles. Thus, the minimum angle present in the Green Book may not be appropriate.⁽¹⁾ Instead,

a minimum intersection angle of 70 to 75 degrees is recommended to offer an improved line of sight.

Son, Kim, and Lee also analyzed the right lateral visibility of drivers in both passenger cars and heavy trucks at left-skewed intersections.⁽³³⁾ Available sight distances were calculated using driver positions similar to what Gattis and Low used.⁽³¹⁾ Son, Kim, and Lee concluded that intersection angles less than 70 degrees should not be used when the design vehicle is a large vehicle or semitrailer.

Two studies from Spain examined visibility at skewed intersections and merging areas.^(34,35) Driver behaviors were observed in the field and through microsimulation. The authors concluded that an intersection angle of no less than 70 degrees should be used at intersections and no less than 7 degrees for merging areas.

Physiology Research

Angles between the legs of an intersection can impact one's ability to make decisions at and maneuver through intersections. These impacts are most negative for those who have diminished physical capabilities. Older persons are a demographic that might experience problems at skewed intersections. The following section examines a synthesis from an FHWA report that discusses the reasons for some of the problems older persons might experience as well as the supporting evidence from observations.⁽³⁶⁾

Older persons often experience reduced head and neck mobility. One study showed that joint flexibility was estimated to decline as much as 25 percent due to a variety of age-related factors.⁽³⁷⁾ Other research showed older persons (age 70 and older) have approximately one-third the range of movement when turning their heads compared to younger counterparts (age 30 and younger).⁽³⁸⁾ Loss of flexibility can lead to a restricted range of motion that affects a driver's ability to turn and scan for conflicting vehicles and pedestrians at intersections.⁽³⁹⁾ One survey showed that many older drivers were aware of this problem: 21 percent reported difficulties turning their heads to scan behind them while driving.⁽⁴⁰⁾ Skewed intersections exacerbated this problem when older persons had to turn their heads farther than would be required at right-angle intersections.

A 1997 study was conducted to specifically explore the problems that older drivers may experience at skewed or channelized intersections where an exaggerated turn of the head was required to scan for oncoming traffic.⁽⁴¹⁾ The comments received from participants indicated that they more often relied on their external mirrors when negotiating highly skewed intersections.

At the same time, they reported the most difficulty with the middle range of angles (40 to 55 degrees). In the middle range, drivers had difficulty turning their heads to scan for traffic and mirrors were of marginal benefit.

A 2007 observational field study was conducted to explore performance differences in younger and older drivers at skewed and right-angle intersections.⁽⁴²⁾ More than 70 participants, accompanied by a front-seat evaluator, drove an instrumented vehicle through five right-angle intersections and five skewed intersections (75 degrees or less). The results showed no significant differences in the performance of the two age groups (25 to 45 and 65 to 85).

However, results showed that right-angle intersections were associated with fewer behavioral errors (e.g., vehicle positioning, signaling, visual scanning, and gap acceptance) when compared to skewed intersections. The right-angle intersections also resulted in better driver performance as measured by the kinematics of lateral and longitudinal acceleration and yaw.

Diminished capabilities related to age may also impact the ability of older pedestrians to safely cross intersections. Research has shown that older pedestrians are more likely to delay before crossing, spend more time at the curb, take longer to cross the road, and make more head movements before and during crossing.⁽⁴³⁾ Skewed intersections typically require pedestrians to walk a longer distance to cross the intersection. The pace of crossing, therefore, becomes critical to minimize the exposure time in the vehicular travel lanes.

Older pedestrian Walking speeds of older pedestrians have been studied by numerous researchers. Most recently, ITE and the American Automobile Association's Foundation for Traffic Safety published *Pedestrian Signal Safety for Older Persons*, a study on pedestrian-walking rates of older persons and the effects of slower rates on signal timing operations.⁽⁴⁴⁾ The study included a review of past studies and the collection of additional observational data in six cities throughout the United States. The results showed the 15th percentile walking rates of older pedestrians range between 3.4 and 3.8 feet per second (ft/s). The ITE and American Automobile's Foundation for Traffic Safety study recommended a walking speed of 3.5 ft/s. However, additional guidance used a walking speed of 3.0 ft/s at locations where pedestrians are routinely crossing at a slower pace. Under those conditions, it is also recommended that the crossing distance used in the calculation of the walk and pedestrian clearance interval be measured from 6 ft back from the edge of the curb (starting location assumption) to the far side of the travel way being crossed.

The ITE/AAA study formed the basis of the recommendation in the FHWA *Handbook for Designing Roadways for the Older Population* to use a walking speed of 3.0 ft/s.⁽³⁶⁾ This recommendation is less than the 3.5 ft/s currently recommended in the *Manual on Uniform Traffic Control Devices*.⁽⁴⁵⁾

SUMMARY

A consensus exists among the policy and design guidance in the highway-design field that intersecting roadways should be aligned to meet at 90 degrees. There is also a common recognition of the safety and operational problems introduced for different modes of travel once an intersection becomes skewed. However, differences exist among these documents regarding the critical minimum angle, which currently ranges from 60 to 75 degrees depending on the reference. Consideration should be given to realigning the intersection or implementing additional traffic-control measures.

Few studies have attempted to define the safety implications of intersection angles using crash data. An expert panel of road-safety researchers reviewed several of these studies as part of an effort for FHWA to quantify crash effects of specific design elements that could be used in the IHSDM. The panel decided that the results from the Harwood et al. analysis were the most credible at the time.⁽²⁵⁾ However, the panel also noted that more work was needed to better quantify the effects of intersection angles.

There is evidence that intersection angles can impact drivers and pedestrians whose physical capabilities have diminished. Older persons who have reduced flexibility may have difficulty turning their heads and necks to judge gaps in traffic at skewed intersections. Older or disabled pedestrians who walk at slower speeds will be exposed to traffic for a longer time at crossings that are lengthened because of the intersection angle. These research findings led to the 75-degree critical-minimum-angle recommendation in the FHWA *Handbook for Designing Roadways for the Older Population* to accommodate age-related performance deficits.⁽³⁶⁾

The lack of consistency among current design policies and practices regarding critical minimum intersection angles, the potential negative safety implications of skew angles on drivers and pedestrians with diminished capabilities, and the limited crash-based research to date justify the need for the research conducted in this study.

CHAPTER 3. METHODOLOGY AND APPROACH

ANALYSIS APPROACH

The analytical approach for this evaluation was twofold. First, variables were selected for each of Ohio's and Minnesota's models using slightly different methods for each State. These methods are briefly introduced in this chapter, and the data are further explored in chapter 4. Prior to model development, random forest (RF) and classification and regression tree analyses were used on the MN data to help identify the most appropriate variables for the models.⁽⁴⁶⁻⁵⁰⁾ This data-mining approach offers some unique advantages over the traditional iterative approach to variable selection when building predictive models. OH data were less detailed but contained more samples; therefore, this data-mining procedure was not used for that State. Instead, a backward regression procedure was used to eliminate nonsignificant variables from the models.

Second, the analytical approach included developing a series of cross-sectional models using the latest state-of-the-practice statistical method for developing crash-prediction models in the road-safety field. Currently, the favored modeling choice is NB regression, and models from both States were developed using this method. Finally, crash modification functions (CMFunctions) for intersection angle were derived from the NB models. The CMFunctions developed were then used to make recommendations for policy and design guidance documents, such as the Green Book.⁽¹⁾

This analytical approach required a large sample of intersections that are skewed and not skewed. To determine if there was a minimum critical safety angle, it was desirable that the sample of intersections range in terms of skew severity. The next chapter on data acquisition and preparation discusses the data collected, including key data elements acquired through a supplemental data-collection effort.

The remainder of this chapter discusses of CMFunction development and the different safety performance function (SPF) functional forms attempted. The Safety Prediction Model Development and CMFunction Derivation section provide the justification for and discussion of the NB regression models chosen for this research and the derivation of CMFunctions for intersection angles.

VARIABLE SELECTION

Traditionally, selecting variables for inclusion in a regression model is accomplished through an iterative process in which variables are added or deleted in a sequential, one-at-a-time manner. Backward elimination is the process of including all independent variables under consideration in the model and deleting those not significant. Forward selection uses the opposite approach, adding one variable at a time and testing for a significant contribution to the predictive ability. Stepwise regression is a modification of forward selection in which nonsignificant variables are removed as new variables are added. This regression can be a time-consuming process with many variables. Selecting the order of entry or removing variables in the model can also affect the final set of independent variables, and the analyst must define the interactions among the independent variables. Alternatively, other approaches to variable selection focus on the relationships among the variables available for the model. One approach promoted by Hauer

explores the functional form of the possible explanatory variables and requires careful consideration of how the variables are introduced. This approach involves the methodical examination of the relationships among all independent variables before choosing those for inclusion in the model and the appropriate functional form for each.^(50,51) Both approaches offer advantages over the traditional techniques previously noted for variable selection and more deliberate model development. However, both techniques require a substantial investment of time, particularly if the number of variables under consideration is large, as is the case in the current study.

As part of this effort, researchers used a data-mining approach for variable selection of MN data because this approach is believed to be a more efficient method for identifying the most relevant variables from a large list. A data-mining approach also allowed for the identification of interactions between variables in a systematic way prior to the development of the NB regression models. Both RFs and regression trees were used in the analysis to identify the independent variables believed to be the best predictors for the NB regression models. Tree analysis was also used to determine the interactions that exist among these variables. These techniques and past applications are further described in appendix D.

This data-mining process was not used for the OH data because this dataset did not include the same level of site characteristics detail as the MN dataset, and the project team felt that the data-mining approach would not provide any value. Instead, a more traditional NB regression process was used. Specifically, a backward elimination procedure was used to systematically eliminate variables with nonsignificant p-variables one at a time. Periodically, alternative models with different sets of eliminated variables were tested to ensure potentially significant explanatory variables were not being removed.

Data and variables are further explained in chapter 4. As described in that chapter, the final MN dataset consisted of 2,778 stop-controlled intersections with a range of variables, including traffic volumes for each approach, lane configurations, shoulder characteristics, speed limits, roadway classification, curb design, area type, access points, and more. By comparison, the OH dataset included 12,888 stop-controlled intersections with variables for traffic volume for each approach, lighting, roadway classification, number of lanes, trafficway description, and minimum angle.

SAFETY-PREDICTION MODEL DEVELOPMENT AND CMFUNCTION DERIVATION

Much of the research exploring relationships between crashes and roadway characteristics has relied on the development and interpretation of cross-sectional or regression models. The current state of the practice for road-safety models attempting to define relationships between crashes and geometric/roadside characteristics is using NB regression. Thus, NB regression was selected as the modeling approach for this research. This approach has been used to develop many of the predictive models included in the *Highway Safety Manual*.⁽²⁴⁾

NB models were developed using the most important predictor variables identified from the data-mining analysis. The models were estimated using maximum likelihood methods. While NB modeling is the current state of the practice, the models have the following limitations:

- Requires a large sample size of data, which can sometimes be costly or otherwise impractical for certain crash types and categories.
- Assumes that crashes fit the NB regression distribution. Recent studies have argued for the use of other distributions (e.g., Lord and Mannering).⁽⁵²⁾
- Involves difficult to handle multivariate correlation distributions, which can be problematic when crash data with different levels of severity and/or different types are available for safety evaluation. Intuitively, there should be some correlation between crashes of different severity levels, and disregarding this correlation may lead to biased results.

The range of models produced in the current study was highly dependent upon each State's available data due to differences in the range and depth of each final dataset. The goal at the start of the analysis was to produce separate total crash-prediction models for three- and four-leg intersections. Further model development based on factors, such as injury severity and rural/urban designation, was a function of sample size and range of data for some of the variables (e.g., intersection angle) in the final database.

Another outcome from the developed models was the identification of other potential contributing factors, other than intersection angles, that impact safety at intersections. These results provide insight into the geometric and operational characteristics of intersections as well as nonroadway factors that might contribute to safety problems at both skewed and nonskewed intersections.

The regression coefficients of the independent variable—the intersection angle—in the NB safety-prediction models were used to derive CMFunctions. The approach to this derivation of CMFunctions was similar to what was described in the literature review for the Harwood et al. study.⁽²⁵⁾ This same approach to CMFunction development has been applied to numerous studies in recent years. Many of the CMFunctions contained in the CMF Clearinghouse, an online repository of CMFs, were derived in this manner from cross-sectional models.⁽⁵³⁾ The number of models developed during the analysis dictated the number of CMFunctions produced.

The methodology used in this study for CMFunction development is not without limitations. There is some concern about whether cross-sectional analyses, such as those used for this study, can truly account for crash causality and mitigation as can be done with a well-designed before–after study. For an effective before–after study, researchers needed to collect a large sample size of entities with similar properties aside from that treatment/improvement under investigation.⁽⁵⁴⁾ If the treatment/improvement is very expensive (e.g., change in intersection or skew angle), there are often insufficient numbers of cases for an effective before–after analysis. The cross-sectional analysis approach was used in this study because of a lack of sound before–after data. As shown in the next chapter, skewed, stop-controlled intersections comprise a small proportion of total intersections, so a before–after evaluation would have been practically impossible. To compensate for the limitations of cross-sectional analysis when developing CMFs, the researchers paid careful attention to the functional forms of the variables in the model. Multiple functional forms were investigated for annual average daily traffic (AADT) and intersection angle. Cumulative residual plots were checked (as discussed in appendix D) as the predictive models were developed to ensure some consistency of data between intersection sites. In addition to paying careful attention to the functional form of the variables, researchers used data from two

States—MN and OH. If the resulting CMFunctions for intersections from the two States are similar, then this result provides further credence to the reliability of the CMFunctions that have been developed in this study.

SUMMARY

The approach chosen to evaluate the effect of intersection angles on safety consisted of data-mining tools, such as RF and classification and regression techniques, used to identify the most important predictors of intersection crashes from the relatively long list of independent variables. These techniques were also used to identify potential interactions among these same variables. NB regression models were developed separately for three- and four-leg intersections. The most important predictors identified with data-mining techniques served as the initial set of variables for the MN models, and only statistically significant variables that fit the desired functional forms were retained for the OH models. The regression coefficients for the variables associated with intersection angles were used to develop CMFunctions. An assessment of the critical minimum angle was made based on the derived CMFunction values.

CHAPTER 4. DATA ACQUISITION AND PREPARATION

DATA SOURCE AND ASSESSMENT

Data required for this study included crash data, intersection geometric data, and traffic volume data that can be linked by location. The Highway Safety Information System (HSIS) is a roadway-based system that was developed in 1990 and provides quality data from seven States and one urban center on several crash, roadway, and traffic variables.⁽¹⁰⁾ Data are acquired annually, processed into a common format, documented, and prepared for analysis. Data from HSIS can be used to analyze many safety problems, including the development of models that attempt to predict future crashes from roadway characteristics and traffic factors. HSIS data were used for MN, but HSIS intersection inventory data were not yet available for OH. The research team subsequently acquired data directly from ODOT, including intersection, roadway, and crash data, and was able to use these data to validate the findings from MN.

MN Data

A review of the HSIS Guidebooks revealed that the MN intersection data include a unique data element to indicate if an intersection is skewed. Specifically, the element “TYPEDESC,” or intersection description, includes the following attributes:

- 31 = Tee Intersection (tee).
- 32 = Wye Intersection (wye).
- 33 = Crossing at Right Angles Intersection (CROSS).
- 34 = Crossing Skewed Intersection (SKEW).

These attributes were used to distinguish skewed and nonskewed intersections. The first two attributes were used to separate skewed and nonskewed three-leg intersections. The last two attributes were used to make this separation for four-leg intersections. This variable allowed for a quick assessment of the number of intersections in each of these four categories.

The researchers used the HSIS website to request the last 10 yr of MN data, including crash, roadway, and intersection data.⁽⁵⁵⁾ At the time of the request, this period was 1999 to 2008.

Upon receipt of the data, the research team determined the number of intersections with the Intersection Description attributes. Using data from 2008, skew category and traffic control type determined the number of three- and four-leg intersections available for analysis. As shown in table 1, the majority of intersections are locations with minor-leg stop controls. The number and diversity of intersections available for the analysis within the other categories of intersection traffic control are limited. Thus, the scope of this research was limited to minor-leg stop-controlled intersections.

Table 1. Number of MN intersections by traffic control type and skew classification (2008 data).²

Traffic Control	Three-Leg Right-Angle Intersection	Three-Leg Skewed Intersection	Four-Leg Right-Angle Intersection	Four-Leg Skewed Intersection	Total
Yield control intersection	12	4	0	0	16
Minor-leg stop-control intersection	2,573	387	2,642	599	6,201
All-way stop-control intersection	4	0	39	4	47
Amber/red flashers	3	2	32	14	51
Red/red flashers	0	0	19	6	25
Signalized intersection	72	9	709	156	946
Other	3	2	4	1	10
Total	2,667	404	3,445	780	7,296

The research team then made sure that the primary characteristic of interest (i.e., skew) had not changed over the analysis period of interest. At the time of this assessment, the analysis period had not been determined. Based on experience with similar studies, it was likely to require between 5 and 10 yr of data to accumulate enough crashes for the analysis. Table 2 shows a count of crashes across the four classes of intersections for the first and last year of the 10-yr period (1999 to 2008). The number of crashes per intersection during these 2 yr for each of the intersection classifications is shown in table 3. The researchers realized that the sample of sites may be further reduced for a variety of reasons once the analysis was conducted, so they chose a 10-yr period (1998 to 2008) to check for consistency across all possible years.

Table 2. Number of crashes by intersection type for the first and last years (1999 and 2008) of the potential analysis period.²

Year	Three-Leg Right-Angle Intersection	Three-Leg Skewed Intersection	Four-Leg Right-Angle Intersection	Four-Leg Skewed Intersection	Total
1999	4,349	724	5,509	1,230	11,812
2008	4,073	733	5,128	1,254	11,188

Researchers conducted the consistency check by examining the classification indication each year for each site over the 10-yr period. If the indication remained consistent through the entire period (e.g., “CROSS” for all 10 yr), the site was retained as a “consistent” intersection. If the indication changed at all (e.g., wye to tee), researchers understood this as an indication that something about the intersection geometry may have changed during the 10-yr period, and the site was deemed “inconsistent.” The results of this analysis are shown in table 4. Between 75 and 80 percent of the intersections in each of the four classification categories remained consistent in terms of traffic control (minor-leg stop-control) and skewed or nonskewed. This set of

²This table was produced by the authors using data from HSIS.

4,780 consistent intersections served as the starting point for the supplemental data-collection effort discussed later in this chapter.

Table 3. Number of crashes per intersection by intersection type for the first and last years (1999 and 2008) of the potential analysis period.³

Year	Three-Leg Right-Angle Intersection	Three-Leg Skewed Intersection	Four-Leg Right-Angle Intersection	Four-Leg Skewed Intersection	Total
1999	1.69	1.87	2.09	2.05	1.90
2008	1.58	1.89	1.94	2.09	1.80

Table 4. Number of minor leg stop-controlled intersections without changes in the skew/nonskew attributes over time (1999–2008).³

Traffic Control	Three-Leg Right-Angle Intersection	Three-Leg Skewed Intersection	Four-Leg Right-Angle Intersection	Four-Leg Skewed Intersection	Total
Minor-leg stop-control	1,930	305	2,095	450	4,780
% of original total*	75	80	80	76	78

*As shown in table 1.

OH Data

MN data were limited to only stop-controlled intersections, so only intersections with this type of traffic control were needed for the OH analysis to provide an accurate comparison for validation of the MN results. HSIS did not contain intersection inventory files for OH, so intersection data were acquired directly from ODOT. The intersection inventory provided from OH contained approximately 39,000 intersections stored as spatial data with attributes specific to the intersection in addition to the individual intersection approaches. One attribute of particular benefit to this study was that the approach-level information contained the angle between each approach leg. The research team examined this angle information as part of the initial investigation of the data. Intersections that had minimum angles of 5 degrees or less were deemed inaccurate and eliminated from the data (this was observed to be an artifact of the structure of the spatial linework). Data were further split by urban/rural distinction, number of legs (three or four), and number of lanes on the major approach (two or more). After these filters were applied, 12,981 intersections remained. Crash data were then requested directly from ODOT.

DATA ACQUISITION

The data available within HSIS are documented in guidebooks and are available on the HSIS website.⁽⁵⁵⁾ The Minnesota Guidebook was used to determine which data elements to request for the proposed analysis.⁽⁵⁶⁾ The available data of interest to the MN study were in three separate files: crash, roadlog, and intersection/interchange. The list of possible elements from these files is included in appendix A of this report. Crash data elements were selected to allow

³This table was produced by the authors using data from HSIS.

models to be developed for total crashes, injury crashes, and specific collision-type crashes (e.g., rear-end crashes). Additional data elements needed for further model disaggregation or that could be important safety predictors within the models were selected from all files. The final variables selected are highlighted in the appendix tables. The tables include those variables required to link information from the various files for each intersection. HSIS data elements acquired for analysis consideration, excluding the linkage variables, are included in the following lists:

- HSIS MN crash file:
 - Date, year, hour, and day of week.
 - Collision type (e.g., rear end, sideswipe).
 - Roadway type.
 - Location type.
 - First-harmful-event location.
 - Light conditions.
 - Number of vehicles involved.
 - Urban/rural designation.
 - Alignment characteristics (e.g., curve and grade).
 - Road-surface conditions.
 - Roadway classification.
 - Road-work characteristics (e.g., work zones).
 - Route-system classification.
 - Severity.
 - Posted speed limit.
 - Traffic control devices.
 - Travel direction.
 - Weather conditions.
- HSIS MN roadlog file:
 - AADT.
 - Commercial AADT.
 - AADT year.
 - Curb presence.
 - Functional classification.
 - Number of lanes.
 - Lane width.
 - Shoulder type and width.
 - Median type and width.
 - Parking presence and type.
 - Number of vehicles involved.
 - Urban/municipal code.
- HSIS MN intersection file:
 - Intersection type.
 - Intersection description (used for skew indication).
 - Number of legs.
 - Leg direction (e.g., north, northeast, south).
 - Type of traffic control.

- Lighting.
- Number of through lanes.
- Travel description (one way versus two way).
- Surrounding land use.
- Intersection AADT.
- Major road AADT.
- Minor road AADT.
- AADT year.

Data were requested from HSIS for years 2003 to 2009 to gather more recent crash history for these entities encompassed by the 10 yr of data used to validate no change in intersection geometry. Based on experience with prior cross-sectional studies and the large sample of intersections noted in table 4, researchers concluded that 7 yr of data were enough to produce reliable and meaningful results without introducing concerns about the age of the data (e.g., effects of an older vehicle fleet on crash experience at intersections). The requested HSIS data were received in four Microsoft Excel™ files: four-leg skew, two-leg cross, three-leg wye, and three-leg tee. The number of intersections in each file matched the numbers shown in table 4. Each file included a separate record for each leg of each intersection and the attributes for all data elements previously listed. The roadlog data elements were appended to each intersection leg using the appropriate linkage variables in each file. Similarly, the number of crashes on each leg (within 250 ft of the intersection) for each of the 7 yr requested (2003–2009) were added to each intersection. Crash totals were provided for fatal, injury, and property-damage-only (PDO) crashes.

Crash and intersection data for OH were unavailable within the HSIS system at the time of analysis. However, the research team acquired data from ODOT in three separate files: crash, roadlog, and intersection. The data are detailed in the following list:

- ODOT OH crash file:
 - Date, year, hour, and day of week.
 - Roadway type.
 - Urban/rural designation.
 - Alignment characteristics (e.g., curve and grade).
 - Roadway classification.
 - Route system classification.
 - Severity.
 - Traffic control devices.
- ODOT OH roadlog file:
 - AADT.
 - AADT year.
 - Functional classification.
 - Number of lanes.
 - Lane width.
 - Roadway division.

- ODOT OH intersection file:
 - Number of legs.
 - Leg direction (e.g., north, northeast, south).
 - Type of traffic control.
 - Stop control.
 - Lighting.
 - Number of through lanes.
 - Travel description (one way versus two way).
 - Intersection AADT.
 - Major road AADT.
 - Minor road AADT.
 - AADT year.
 - Minimum angle.

Data were requested from ODOT for years 2011 through 2015. Although fewer years were available for analysis than for the MN dataset, data were sufficiently recent to ensure no major changes in vehicle fleet type or intersection control. Using only 5 yr of data also ensured no significant but unknown changes were made to intersection design. Unlike the MN data, the OH data contained sufficient information to determine minimum angle, so classifications such as wye or tee and manual measurement of angles were not needed. Crashes were carefully linked to specific intersections rather than individual legs by ODOT staff. Crash totals were provided for fatal, injury, and PDO crashes.

SUPPLEMENTAL GEOMETRIC DATA COLLECTION

For the MN data, the critical missing element from the list of MN variables is the actual intersection angle. Without this piece of information, it is not feasible to determine if there is a critical minimum angle at which safety is compromised nor is it possible to develop a CMF for a change in the angle of the intersection. Both needs are key objectives of the research. Thus, a supplemental data-collection effort was required to obtain this particular data element.

The full supplemental data-collection process for the MN data is beyond the scope of this report, but the process is described in detail in appendix B. While the intersecting angle between legs was deemed the most critical element to be collected in the supplemental data-acquisition effort, it was not the only element believed to be important for this analysis. Additional data elements were acquired for each approach leg of each intersection as part of this supplemental effort (some for confirmation of the HSIS data). The additional data elements are provided in the following list:

- Number of intersections within 250 ft.
- Sight obstructions on corner clockwise from approach leg (e.g., yes, no, maybe, not applicable).
- Curve on approach within 250 ft of intersection (e.g., none, slight, sharp).
- Terrain on approach (e.g., level, crest, sag).
- Number of through lanes.
- Number of exclusive left-turn lanes.
- Number of exclusive right-turn lanes.

- Type of channelized right-turn lanes (e.g., none, raised, painted, depressed, present but unknown type).
- Median presence/type (e.g., none, two-way left-turn lane, raised, painted, depressed, present but unknown type).
- Right-turning traffic from this leg has acceleration lane (e.g., yes/no).
- Ramp or street.
- Traffic flow (e.g., two way, one-way in, one-way out).
- Crosswalk on approach? (e.g., yes/no)
- Sidewalk along approach (e.g., yes, no, unknown).
- Number of major commercial/industrial driveway(s) on approach within 250 ft of intersection.
- Number of minor commercial/industrial driveway(s) on approach within 250 ft of intersection.
- Number of multifamily residential driveways on approach within 250 ft of intersection.
- Number of single-family residential driveways on approach within 250 ft of intersection.
- Onstreet parking presence (painted spaces visible or parked cars) (e.g., yes/no).

The approach selected to acquire these data made use of two sources of information—geographic information system (GIS) data and aerial images. Two GIS data components were required. The necessary base layer was the roadway network for MN. The GIS basemap is available for download from the MNDOT website for each county.⁽⁵⁷⁾ The research team downloaded the individual county files and then merged the files into a single shapefile that included the State roadway network. The second layer required was a point file of the intersections. This information was also acquired from MNDOT; it is part of their GIS point file that includes intersections, interchanges, bridges, and ramps. The aerial images were acquired from Google® Maps™.⁽⁵⁸⁾

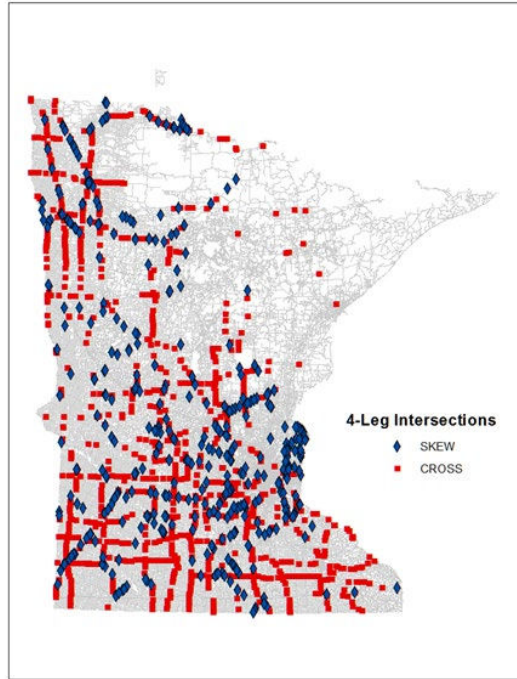
A Microsoft Excel workbook was developed for recording the supplemental data elements. The workbook was initially populated with the intersection identification numbers and approach leg cardinal directions from the HSIS data received. Fields were then added for the supplemental data elements. The data-collection protocol included the following steps for all skewed intersections:

1. Copy the intersection ID number from the Excel file and locate the intersection in the MN GIS layer. Use the info tool in ArcGIS™ to find the intersection coordinates (latitude and longitude).⁽⁵⁹⁾ Record the coordinates in the Excel file.
2. Copy the intersection coordinates from Excel to Google Maps.
3. Check to make sure the visual information between the spatial file and the aerial image match in terms of the number and direction of the intersecting legs. If they do not match, flag the intersection, make a note in the Excel file about the inconsistency, and continue to the next intersection.
4. Determine which legs in the Excel file correlate to legs in ArcGIS. Use the cardinal attribute within the “Direction” data element in the Excel file to match the intersecting legs.

5. Access the COGO (name derived from coordinate geometry) tool for measuring angles. The following discussion examines how this tool was applied.⁽⁷¹⁾ Beginning with the leg with the cardinal direction of north or to the right of north, measure each angle between adjacent legs. Record the values in the Excel workbook.
6. Collect the information about nearby intersections using the 250-foot buffer in ArcGIS. Record the information in the Excel workbook.
7. Collect the remaining supplemental data using Google Maps.⁽⁵⁸⁾ As necessary, use StreetView™ to ensure that the information is accurate. Record the information in the Excel workbook.

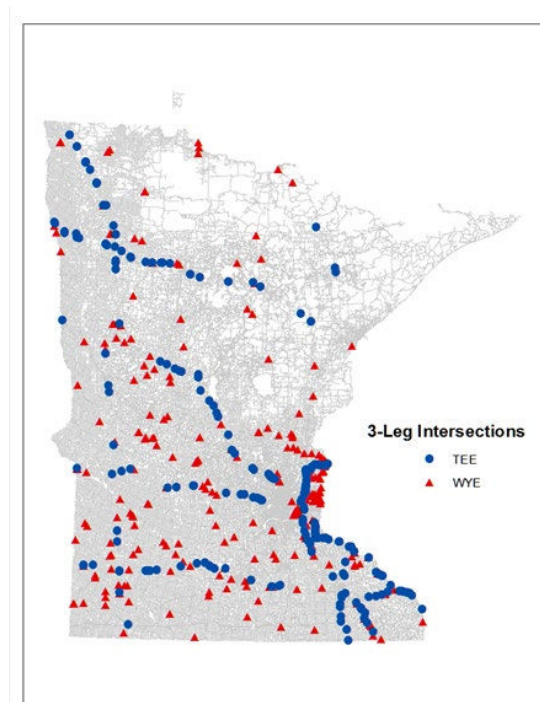
At the conclusion of the data-collection effort, data were acquired for 2,960 intersections: 1,185 three-leg and 1,775 four-leg locations. While the supplemental data intersections were randomly selected from the original pool of locations, care was taken to ensure that the skewed and nonskewed intersections had similar geographic distributions across MN. As shown in figure 14 and figure 15, the goal of similar distributions for skewed and nonskewed locations was obtained for both three- and four-leg intersections. The MN data within HSIS only include the roadways and intersections that are part of the State-owned highway network. Thus, the intersections included in the analysis are typically more rural and located along routes classified as collector and higher in the roadway functional classification scheme.

The primary reason for the supplemental data-collection effort was acquisition of the measured intersection angle. The analysis would otherwise have been limited to an assessment of safety based only on the attributes of skewed or nonskewed in the HSIS MN database. The collection of the measured angles provided additional insight into the value of data verification. The reliability and accuracy of the skewed versus nonskewed attributes were unknown to MNDOT and HSIS staff because they had not been verified for an extended period of time. The results of the supplemental data-collection effort clarified that approximately 24 percent of the four-leg intersections and 30 percent of the the three-leg intersections classified as right-angle intersections in the HSIS database had measured angles of 85 degrees or less. Misclassification in the other direction was also present. Approximately 3 percent of four-leg intersections and 15 percent of three-leg intersections classified as skewed in the HSIS database had measured angles of 86 to 94 degrees. The reasons for these misclassifications are not known but have been sent to HSIS database administrators and MNDOT staff for further investigation. The analysis conducted in this study relied only on the measured results.



Source: FHWA.

Figure 14. Map. Skewed and nonskewed four-leg intersections in MN.



Source: FHWA.

Figure 15. Map. Density of skewed and nonskewed three-leg intersections in MN.

A stringent supplemental data-collection process was unnecessary for the OH dataset. The data from OH contained the measurement of angles between any two approach legs, which eliminated the need for manual measurement. This made it feasible to include a much larger dataset in OH. More skewed intersections were included in the OH dataset than in the MN dataset.

DATA PREPARATION

The supplemental data collected for MN were merged with the HSIS data acquired for the 2,960 intersections. A series of quality-control checks were then used to produce a clean quality dataset for the analysis. The series of quality-control checks included the following steps:

1. Check the sum of the measured angles at each intersection, which should be 360 degrees. Intersections with summations less than 350 degrees or greater than 370 degrees were dropped. (Seven intersections were deleted.)
2. Check to make sure the number of stop-controlled legs is correct: one at three-leg intersections and two at four-leg intersections. (Sixty-nine intersections were deleted.)
3. Eliminate intersections where the traffic control includes anything other than minor street stop-control. (Ten intersections were deleted.)
4. Check the comments field in the supplemental data-collection Excel workbook for any issues that may warrant deletion of the intersection. (Nineteen intersections were deleted.)
5. Eliminate intersections that are on a ramp. (One intersection was deleted.)
6. Eliminate intersections that have one-way traffic flow. (Six intersections were deleted.)
7. Eliminate intersections with a right-turn acceleration lane. (Fifteen intersections were deleted.)
8. Check to make sure there were no changes in the intersection description data element from 2008 to 2009; years 1999–2008 were used to initially categorize the intersections with respect to being skewed. (One intersection was deleted.)
9. Eliminate three-leg intersections with multiple acute-adjacent angles and intersections in which the minimum angle exceeded 95 degrees. (Seven intersections were deleted.)
10. Check for missing values for key variables known to be significant safety predictors (e.g., AADT). (Forty-five intersections were deleted.)
11. Eliminate intersections with outlier crash frequencies across the 7-yr period and intersections with abnormally high frequencies in any of the 7 yr. (Two sites were deleted.)

At the conclusion of this series of quality-control checks, the final MN dataset included 2,778 intersections. The quality-control checks resulted in 6 percent of the initial locations being eliminated. The Data Description section provides a more complete description of this final set of intersections.

Similarly, OH data were prepared to produce a clean dataset for development of prediction models and CMFunctions. The data preparation steps include:

1. Stop-controlled intersections in the State System intersections database⁴ were identified, totaling approximately 39,000 intersections.
2. Approach leg files were joined to the intersection file to eliminate any legs that may not have met the stop-controlled intersection criteria.
3. Intersections with double leg lines in GIS that resulted in very small in-between angles (5 degrees or less) were eliminated from the dataset.
4. Lanes were then added to the intersection file using the roadway inventory.
5. Intersections without a clean set of lanes consistent through the intersection area (either two, four, or six) on each leg were removed.

The result for the OH dataset was a file with 12,981 intersections. These sites were additionally narrowed to 12,888 because sites without the required data characteristics were removed. Crash data were linked to these intersections, and the intersections were further grouped based on area type (rural/urban) and number of legs. This sorting process removed over half the possible starting intersections, but the final sample is of significant size and far larger than the MN dataset.

DATA DESCRIPTION

MN Data

The data files produced for the MN analysis included 1,109 three-leg intersections and 1,669 four-leg intersections. Provided in this section of the report is a limited number of tables intended to provide an overview of the data characteristics for the final database for MN. Additional tables are provided in appendix C. Table 5 and table 6 show the distribution of the study intersections by angle classification (skewed versus right angle measured through the supplemental data-collection effort) and area type (rural versus urban) for four-leg and three-leg intersections, respectively. The protocol for the supplemental data-collection effort classified any intersection with an angle of 85 degrees or greater as a right-angle intersection. The descriptive tables that follow reflect this fact. Approximately 39 percent of the four-leg intersections in rural areas are skewed compared to 38 percent of the intersections in urban areas. For three-leg intersections, 39 percent of the rural intersections are skewed compared to 54 percent of the urban sites. For three-leg intersections, almost 20 percent of the sites are in urban environments compared to only 12 percent of the four-leg intersections.

Table 5. Distribution of four-leg intersections by angle classification and area type in MN.⁵

Area Type	Number of Rural Intersections	Rural (%)	Number of Urban Intersections	Urban (%)	Total
Right angle	892	60.6	123	62.4	1,015
Skewed	580	39.4	74	37.6	654
Total	1,472	100.0	197	100.0	1,669

⁴This database contains locations of intersections in OH. Ohio DOT provided the information to the authors for this report.

⁵This table was produced by the authors using data from HSIS.

Table 6. Distribution of three-leg intersections by angle classification and area type in MN.⁶

Area Type	Number of Rural Intersections	Rural (%)	Number of Urban Intersections	Urban (%)	Total
Right angle	538	60.6	101	45.7	639
Skewed	350	39.4	120	54.3	470
Total	888	100.0	221	100.0	1,109

Table 7 and table 8 show the distributions of the study intersections among 10 categories of intersection angle for four-leg and three-leg intersections, respectively. As shown in table 7, the skewed rural intersections are fairly evenly distributed across the angle categories, ranging from a low of 2.9 percent of the intersections in the less-than-40-degree category to 5.4 percent in the 70-to-74-degree category. In the urban area, the skewed intersections tend to be less concentrated in the smaller-angle categories. Of the 74 urban skewed intersections in the database, only 23 of those intersections had angles less than 60 degrees.

For three-leg intersections (table 8), the distribution of the skewed rural intersections is evenly distributed among the angle categories, ranging from 2.7 percent in the 40-to-49-degree category to 6.0 percent in the 80-to-84-degree category. The range is wider for the skewed urban sites, from 2.3 percent in the 55-to-59-degree category to 9.0 percent in the 70-to-74-degree category.

Table 7. Distribution of four-leg intersections by intersection angle category and area type in MN.⁶

Intersection Angle (Degrees)	Number of Rural Intersections	Rural (%)	Number of Urban Intersections	Urban (%)	Total
<40	42	2.9	2	1.0	44
40–49	67	4.6	10	5.1	77
50–54	50	3.4	6	3.0	56
55–59	67	4.6	5	2.5	72
60–64	63	4.3	6	3.0	69
65–69	75	5.1	10	5.1	85
70–74	79	5.4	13	6.6	92
75–79	70	4.8	12	6.1	82
80–84	67	4.6	10	5.1	77
≥85 (right angle)	892	60.6	123	62.4	1,015
Total	1,472	100.0	197	100.0	1,669

⁶This table was produced by the authors using data from HSIS.

Table 8. Distribution of three-leg intersections by intersection angle category and area type in MN.⁷

Intersection Angle (Degrees)	Number of Rural Intersections	Rural (%)	Number of Urban Intersections	Urban (%)	Total
<40	53	5.9	17	7.7	70
40–49	24	2.7	9	4.1	33
50–54	30	3.4	10	4.5	40
55–59	32	3.6	5	2.3	37
60–64	30	3.4	9	4.1	39
65–69	39	4.4	17	7.7	56
70–74	41	4.6	16	7.2	57
75–79	48	5.4	20	9.0	68
80–84	53	6.0	17	7.7	70
≥85 (right angle)	538	60.6	101	45.7	645
Total	888	100.0	221	100.0	1,109

Further breakdown of the rural four-leg intersections is provided in table 9, which shows the distributions of the study intersections among 10 categories of intersection angles by the number of lanes present on the major road approaches to the intersection. A two-lane intersection is defined as having two lanes (both travel directions) on the minor road and two lanes (both travel directions) on the major road. A multilane intersection is defined as having two lanes (both travel directions) on the minor road and four lanes (both travel directions) on the major road. For the 1,348 two-lane locations, more than 62 percent are categorized as right-angle intersections. The remaining skewed two-lane sites are fairly evenly distributed across the other angle categories. For the 103 multilane locations, less than half are right-angle intersections, and there is only one intersection with an angle less than 40 degrees.

Table 10 provides a more detailed breakdown of the skewed intersections in the database for each 5-degree category of intersection angle between 5 and 84 degrees. There are no intersections in the database with angles less than 20 degrees for four-leg intersections. Only 9 intersections (1.38 percent of the total number of skewed four-leg intersections) have angles between 20 and 29 degrees, while 35 intersections (5.36 percent) have angles between 30 and 39 degrees. More than 93 percent of the four-leg skewed intersections have angles between 40 and 84 degrees. The three-leg intersections have a different distribution. There are sites with extremely acute angles, including 10 intersections (2.13 percent of the total number of skewed three-leg intersections) with angles less than 15 degrees. An additional 25 sites (5.32 percent) have angles between 15 and 29 degrees. More than 85 percent of the three-leg skewed intersections have angles between 40 and 84 degrees.

⁷This table was produced by the authors using data from HSIS.

Table 9. Distribution of rural four-leg intersections by intersection angle category and number of lanes on the major road in MN.⁸

Intersection Angle (Degrees)	Number of Two-Lane Intersections	Two-Lane (%)	Number of Multilane Intersections	Multilane (%)
<40	41	3.0	1	1.0
40–49	57	4.2	9	8.7
50–54	44	3.3	5	4.9
55–59	64	4.7	3	2.9
60–64	59	4.4	3	2.9
65–69	63	4.7	8	7.8
70–74	65	4.8	10	9.7
75–79	62	4.6	7	6.8
80–84	56	4.2	9	8.7
≥85 (right angle)	837	62.1	48	46.6
Total	1,348	100.0	103	100.0

Table 10. Distribution of skewed intersections by intersection angle for four-leg and three-leg intersections in MN.⁹

Intersection Angle (Degrees)	Number of Four-Leg Intersections	Four-Leg (%)	Number of Three-Leg Intersections	Three-Leg (%)
>10	—	—	4	0.85
10–14	—	—	6	1.28
15–19	—	—	11	2.34
20–24	2	0.31	4	0.85
25–29	7	1.07	10	2.13
30–34	16	2.45	15	3.19
35–39	19	2.91	20	4.26
40–44	29	4.43	18	3.83
45–49	48	7.34	15	3.19
50–54	56	8.56	40	8.51
55–59	72	11.01	37	7.87
60–64	69	10.55	39	8.30
65–69	85	13.00	56	11.91
70–74	92	14.07	57	12.13
75–79	82	12.54	68	14.47
80–84	77	11.77	70	14.89
Total	654	100.00	470	100.00

—No data available.

The number of total crashes and crashes per intersection for the 7-yr study period (2003 through 2009) are provided in table 11 and table 12, respectively, as distributed across the intersection-angle categories. Rural right-angle four-leg intersections experienced 3.28 crashes per intersection. The number of crashes per intersection at rural skewed four-leg intersections ranged from 2.71 crashes for intersections in the less-than-40-degree category to 7.76 crashes for intersections in the 65-to-69-degree category. Urban four-leg intersections experienced a much greater rate of crashes per site when compared to their comparable rural intersections.

⁸This table was produced by the authors using data from HSIS.

⁹This table was produced by the authors using data from HSIS.

Urban right-angle four-leg intersections experienced 13.9 crashes per intersection. The rates varied between 9.30 and 17.50 crashes for urban skewed four-leg intersections.

Rural right-angle three-leg intersections experienced 3.24 crashes per intersection. The number of crashes per intersection at rural skewed three-leg intersections ranged from 2.07 crashes for intersections in the 60-to-64-degree category to 3.73 crashes for intersections in the 70-to-74-degree category. Urban three-leg intersections, like four-leg urban intersections, experienced a much higher rate of crashes per site when compared to their comparable rural intersections. Urban right-angle three-leg intersections experienced 10.06 crashes per intersection. The rates varied between 2.40 and 12.00 crashes for urban skewed three-leg intersections.

Table 11. Distribution of total crashes and total crashes/intersection at four-leg intersections by intersection angle category and area type in MN.¹⁰

Intersection Angle (Degrees)	Rural Crashes	Rural Crashes per Intersection	Urban Crashes	Urban Crashes per Intersection
—	114	2.71	35	17.50
40–49	259	3.87	93	9.30
50–54	328	6.56	82	13.67
55–59	250	3.73	79	15.80
60–64	330	5.24	57	9.50
65–69	582	7.76	122	12.20
70–74	378	4.78	186	14.31
75–79	404	5.77	123	10.25
80–84	295	4.40	129	12.90
≥85 (right angle)	2,928	3.28	1,708	13.89
Total	5,868	3.99	2,614	13.27

—No data available.

Table 12. Distribution of total crashes and total crashes/intersection at three-leg intersections by intersection angle category and area type in MN.¹⁰

Intersection Angle (Degrees)	Rural Crashes	Rural Crashes per Intersection	Urban Crashes	Urban Crashes per Intersection
—	191	3.60	129	7.59
40–49	51	2.13	108	12.00
50–54	81	2.70	24	2.40
55–59	90	2.81	53	10.60
60–64	62	2.07	63	7.00
65–69	123	3.15	95	5.59
70–74	153	3.73	113	7.06
75–79	156	3.25	158	7.90
80–84	180	3.39	141	8.29
≥85 (right angle)	1,742	3.24	1,017	10.06
Total	2,829	3.19	1,901	8.60

—No data available.

A further breakdown of the crashes at rural four-leg intersections is provided in table 12, which shows the distributions of crashes and crashes per intersection among 10 categories of

¹⁰This table was produced by the authors using data from HSIS.

intersection angle by the number of lanes present on the major road. Two-lane right-angle intersections experienced 2.98 crashes per intersection. The number of crashes per intersection at two-lane skewed intersections ranged from 2.61 crashes for intersections in the less-than-40-degree category to 5.34 crashes for intersections in the 50-to-54-degree category. Multilane intersections experienced a much greater rate of crashes per site when compared to their comparable two-lane intersections. Multilane right-angle intersections experienced 7.83 crashes per intersection. The rates varied between 6.90 and 24.38 crashes for multilane skewed four-leg intersections. Note that the number of multilane intersections in each of the skew-angle categories in table 9 is relatively small.

The traffic volume characteristics at the study intersections are shown in table 13 and table 14. Intersection AADTs for four-leg intersections ranged from a low of 163 vpd to 53,108 vpd (table 13). Average AADT for rural and urban right-angle intersections was 3,847 and 15,022 vpd, respectively. Average AADT values for skewed rural intersections ranged from 3,875 vpd for the less-than-40-degree category to 6,221 vpd for the 65-to-69-degree category. For skewed urban intersections, average AADT values ranged from 9,395 vpd for the 40-to-49-degree category to 22,943 vpd for the less-than-40-degree category.

Table 13. Range of intersection AADT for four-leg intersections by intersection angle and area type in MN.¹¹

Intersection Angle (Degrees)	Rural Min	Rural Avg	Rural Max	Urban Min	Urban Avg	Urban Max
<40	622	3,875	26,514	18,772	22,943	27,114
40–49	163	4,911	25,985	5,113	9,395	19,839
50–54	640	5,678	26,462	4,586	13,737	36,710
55–59	805	4,258	25,467	6,369	11,369	21,563
60–64	787	4,675	22,204	4,642	13,903	37,000
65–69	643	6,221	30,172	5,821	13,225	29,631
70–74	995	4,984	28,146	10,632	21,785	52,827
75–79	527	4,987	19,683	5,491	11,753	32,625
80–84	767	4,812	17,869	2,474	18,215	36,781
≥85 (right angle)	178	3,847	31,056	3,440	15,022	53,108
Weighted average	—	4,293	—	—	14,969	—

—No data available.

Min = minimum; Avg = average; Max = maximum.

¹¹This table was produced by the authors using data from HSIS.

Table 14. Range of intersection AADT for three-leg intersections by intersection angle and area type in MN.¹¹

Intersection Angle (Degrees)	Rural Min	Rural Avg	Rural Max	Urban Min	Urban Avg	Urban Max
<40	531	4,606	22,026	1,735	12,903	27,057
40–49	658	4,999	25,755	4,817	14,772	40,475
50–54	549	5,193	25,849	6,210	10,854	20,770
55–59	1,055	4,042	20,593	8,179	19,052	35,955
60–64	710	4,399	19,196	5,689	10,736	27,724
65–69	674	3,937	17,110	5,821	15,232	36,971
70–74	380	6,200	24,998	4,066	14,268	43,288
75–79	400	6,547	31,433	4,836	17,418	40,718
80–84	1,005	5,591	25,643	6,228	16,352	36,857
≥85 (right angle)	322	5,393	31,520	3,480	20,255	57,975
Weighted average	—	5,275	—	—	18,274	—

—No data available.

Min = minimum; Avg = average; Max = maximum.

For the three-leg intersections, intersection AADTs ranged from 322 to 57,975 vpd. The average AADTs for rural and urban right-angle intersections were 5,393 and 20,255 vpd, respectively. The average AADT for rural skewed intersections ranged from 3,937 vpd for the 65-to-69-degree category to 6,547 vpd for the 75-to-79-degree category. For urban skewed intersections, the average AADT ranged from 10,736 vpd for the 60-to-64-degree category to 19,052 vpd for the 55-to-59-degree category.

A further breakdown of the AADTs at rural four-leg intersections is provided in table 15, which the distributions of traffic volumes among 10 categories of intersection angle by the number of lanes present on the major road. The two-lane intersections in the study averaged 3,570 vpd, while the multilane intersections averaged almost three times that volume at 12,677 vpd. The distribution of AADTs for the right-angle intersections and the skewed intersections were comparable for both two-lane and multilane intersections.

Table 15. Range of intersection AADT for four-leg intersections by intersection angle category and the number of lanes on the major road in MN.¹²

Intersection Angle (Degrees)	Two-Lane Min	Two-Lane Avg	Two-Lane Max	Multilane Min	Multilane Avg	Multilane Max
<40	622	3,324	10,589	26,514	26,514	26,514
40–49	163	3,317	16,965	3,978	14,974	25,985
50–54	640	4,531	16,048	3,567	16,220	26,462
55–59	805	3,954	25,467	4,690	10,748	20,308
60–64	787	4,244	19,951	7,358	12,596	22,204
65–69	643	3,863	11,832	7,569	20,120	30,172
70–74	995	3,637	11,429	6,013	11,846	28,146
75–79	527	4,399	19,683	4,512	10,089	19,306
80–84	767	4,163	13,607	4,752	8,548	17,869
≥85 (right angle)	178	3,330	15,922	2,812	12,245	31,056
Weighted average	—	3,570	—	—	12,677	—

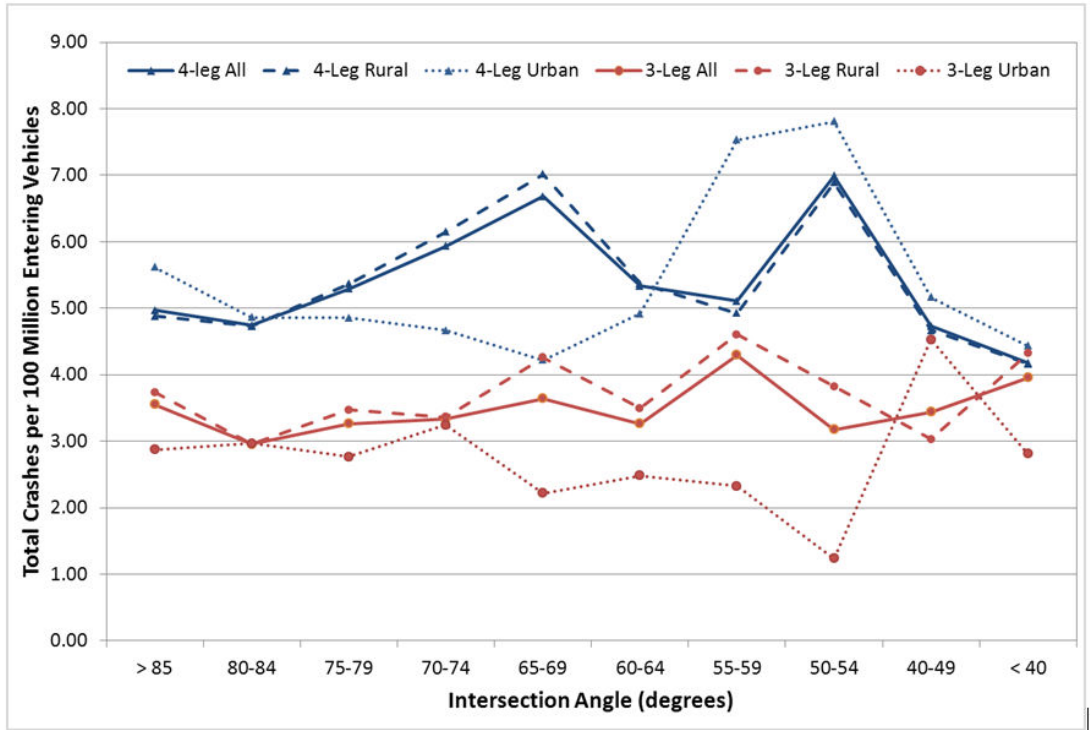
—No data available.

Min = minimum; Avg = average; Max = maximum.

Crash frequencies and traffic volumes were combined to develop intersection crash rates. Figure 16 shows the annual average total crash rates per 100 million entering vehicles for each intersection-angle category. Separate crash rates were included for three-leg rural and urban intersections and four-leg rural and urban intersections. The four-leg intersections consistently exhibited higher crash rates than the three-leg intersections. The rural crash-rate patterns followed total crash patterns very closely because the sample of intersections in the database was predominately rural (88 percent for four-leg intersections and 80 percent for three-leg intersections). The highest crash rates for four-leg all and rural four-leg locations were present in the 50-to-54-degrees and 65-to-69-degrees categories. Urban four-leg intersections had the highest rates in the 50-to-54-degrees and 55-to-59-degrees categories. The highest crash rates for all and rural three-leg intersections occurred in the 55-to-59-degrees category and the less-than-40-degree category. Urban three-leg intersections experienced the highest rate in the 40-to-49-degree category.

Figure 16 depicts six plotted lines showing the number of crashes per 100 million entering vehicles (y-axis) at different intersection angles (x-axis) for six different intersection types. The line for all four-leg intersections peaks at approximately 6.9 and 7.0 million vehicles at 65–69 degrees and 50–54 degrees, respectively. The line for four-leg rural intersections depicts the same two peaks, except the rate is 7.0 million. The line for four-leg urban intersection shows is mostly below four-leg all intersections line and the four-leg rural intersections line until approximately 60–64 degrees. The rate then rises rapidly until peaking at almost 8.00 at 50–54 degrees. The line for all three-leg intersections oscillates until peaking at about 4.5 million vehicles at 55–59 degrees. The line for rural three-leg roadways follows roughly the same trend as the line for all three-leg intersections, except its peak at 55–59 degrees is almost 4.75 million vehicles. Another line plots the rate for urban three-leg intersections; this line stays below the three-leg all intersections line and the three-leg rural intersections line except at 40–49 degrees, where it peaks at approximately 4.75. These crash rates are for Minnesota.

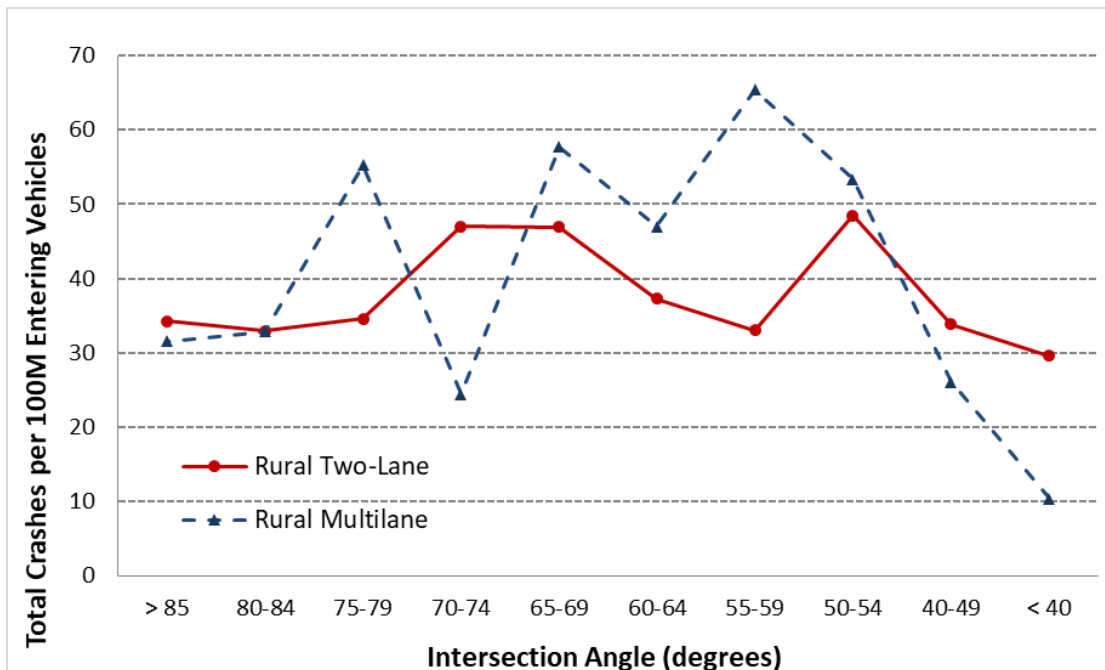
¹²This table was produced by the authors using data from HSIS.



Source: FHWA.

Figure 16. Graph. Annual average total crash rate by intersection angle category, number of legs, and rural/urban classification in MN.

Additional crash rates for the four-leg rural intersections are shown in figure 17. The crash rates for the intersections with two-lanes on major approach legs followed a similar pattern to the four-leg rural crash rates shown in figure 16. This was not unexpected because 93 percent of the four-leg rural intersections included two-lanes on the major approaches. The highest crash rates for these two-lane intersections occurred at locations with intersection angles of 50–54 degrees and 65–74 degrees. For the rural four-leg multilane intersections, the highest crash rates were present in the 55-to-59-, 65-to-69-, and 75-to-79-degrees categories.



Source: FHWA.

Figure 17. Graph. Annual average total crash rate for rural four-leg intersections by intersection angle category and number of approach lanes on the major road in MN.

OH Data

A key difference between the OH and MN datasets is the wider range of available sites for analysis within the OH set. Although there were only 5 yr of crash data available (2011–2015), there were 3,766 four-leg intersections in this set compared to the 1,669 four-leg intersection sites in the MN dataset. Additionally, there were 9,122 three-leg intersections in the OH dataset compared to 1,109 three-leg intersection sites in the MN dataset. This wider scope of available intersections allowed for more crash models to be developed, but there were tradeoffs for the available variables, which are addressed in chapter 5.

Table 16 shows there were significantly more rural four-leg intersections than urban four-leg intersections. Of 3,338 rural four-leg intersections, over half were skewed; this is true also for urban four-leg intersections, although the percent skewed was even higher at 62.1 percent. These distributions are a key difference from the MN dataset where the majority of four-leg intersections were right-angle intersections. The smaller proportion of urban intersections potentially explains the lack of urban models developed in the analysis of these data.

Table 16. Distribution of four-leg intersections by angle classification and area type in OH.

Angle Classification	Number of Rural	Rural (%)	Number of Urban	Urban (%)	Total
Right angle	1,569	47.0	162	37.9	1,731
Skewed	1,769	53.0	266	62.1	2,035
Total	3,338	100.0	428	100.0	3,766

This discrepancy between right-angle sites and skewed sites in the OH dataset remains true for three-leg intersections. More than half (62.4 percent) of the rural three-leg intersections and 51.4 percent of the urban three-leg intersections were skewed. Only urban three-leg intersections in MN had more sites skewed than right-angle intersections. Table 17 shows that there were still more rural three-leg intersections than urban three-leg intersections, although the number of sites in the three-leg categories was significantly higher than in the four-leg categories.

Table 17. Distribution of three-leg intersections by angle classification and area type in OH.

Angle Classification	Number of Rural	Rural (%)	Number of Urban	Urban (%)	Total
Right angle	2,760	37.6	863	48.6	3,623
Skewed	4,587	62.4	912	51.4	5,499
Total	7,347	100.0	1,775	100.0	9,122

Table 18 presents a closer examination of the angle categories for OH four-leg intersections for both rural and urban intersections. Table 18 shows that for both rural and urban four-leg intersections, 97 percent of the sites in the dataset had intersection angles greater than 40 degrees. The angle category with the largest percentage of the total number of intersections for both rural and urban sites was ≥ 85 degrees. For rural four-leg intersections, the angle category with the second largest number of sites was 80–84 degrees and for urban four-leg intersections, the angle category was 75–79 degrees. For both area types, the number of sites skewed toward larger intersection angles.

Table 18. Distribution of four-leg intersections by intersection angle category and area type in OH.

Intersection Angle (Degrees)	Number of Rural	Rural (%)	Number of Urban	Urban (%)	Total
<40	89	2.67	13	3.04	102
40–49	154	4.61	23	5.37	177
50–54	134	4.01	22	5.14	156
55–59	153	4.58	18	4.21	171
60–64	148	4.43	21	4.91	169
65–69	236	7.07	34	7.94	270
70–74	224	6.71	32	7.48	256
75–79	305	9.14	58	13.55	363
80–84	326	9.77	45	10.51	371
≥ 85 (right angle)	1,569	47.00	162	37.85	1,731
Total	3,338	100.00	428	100.00	3,766

The distribution of sites in different angle categories for three-leg intersections in OH is shown in table 19. Compared to four-leg intersections, there are more three-leg intersections with intersection angles less than 40 degrees in both rural and urban areas. As with four-leg intersections, the highest number of sites are within the right-angle categories for both rural and urban intersections. However, three-leg intersections differ from four-leg intersections in that three-leg intersections have a higher concentration of right-angle sites in urban areas than in rural areas.

Table 19. Distribution of three-leg intersections by intersection angle category and area type in OH.

Intersection Angle (Degrees)	Number of Rural	Rural (%)	Number of Urban	Urban (%)	Total
<40	519	7.06	75	4.23	594
40–49	402	5.47	39	2.20	441
50–54	237	3.23	37	2.08	274
55–59	295	4.02	56	3.15	351
60–64	371	5.05	82	4.62	453
65–69	480	6.53	112	6.31	592
70–74	633	8.62	122	6.87	755
75–79	749	10.19	172	9.69	921
80–84	901	12.26	217	12.23	1,118
≥85 (right angle)	2,760	37.57	863	48.62	3,623
Total	7,347	100.00	1,775	100.00	9,122

The four-leg intersections are further broken down in table 20. The majority of rural four-leg intersections (3,230) were on roadways with two lanes on the major approach. A much smaller number, 108, were on multilane roadways. Due to the low number of four-leg multilane sites, there were few intersections in several angle categories. This distribution informed the model development and results discussed in the next sections because such low numbers may provide unreliable results.

Table 21 presents a more-detailed distribution of OH sites in both leg categories. There were no sites in the category of 5–10 degree in either leg division. This may be because the sites with very small skew angles were initially eliminated from the dataset. Only three-leg intersections had any sites in the range of 10–14 degrees. The highest concentration of both four-leg intersections and three-leg intersections were for sites with an intersection angle greater than 65 degrees.

Table 20. Distribution of rural four-leg intersections by intersection-angle category and number of lanes on the major road in OH.

Intersection Angle (Degrees)	Number of Two-Lane	Two-Lane (%)	Number of Multilane	Multilane (%)
<40	88	2.72	1	0.93
40–49	150	4.64	4	3.70
50–54	133	4.12	1	0.93
55–59	150	4.64	3	2.78
60–64	144	4.46	4	3.70
65–69	214	6.63	22	20.37
70–74	214	6.63	10	9.26
75–79	295	9.13	10	9.26
80–84	315	9.75	11	10.19
≥85 (right angle)	1,527	47.28	42	38.89
Total	3,230	100.00	108	100.00

Table 21. Distribution of skewed intersections by intersection angle for four-leg and three-leg intersections in OH.

Intersection Angle (Degrees)	Number of Four-Leg	Four-Leg (%)	Number of Three-Leg	Three-Leg (%)
5–10	—	—	—	—
10–14	—	—	18	0.33
15–19	3	0.15	57	1.04
20–24	9	0.44	119	2.16
25–29	12	0.59	117	2.13
30–34	32	1.57	129	2.35
35–39	46	2.26	154	2.80
40–44	78	3.83	192	3.49
45–49	99	4.86	249	4.53
50–54	156	7.67	274	4.98
55–59	171	8.40	351	6.38
60–64	169	8.30	453	8.24
65–69	270	13.27	592	10.77
70–74	256	12.58	755	13.73
75–79	363	17.84	921	16.75
80–84	371	18.23	1,118	20.33
Total	2,035	100.00	5,499	100.00

—No data available.

Crash rates per intersection were also calculated for four-leg and three-leg intersections for the OH dataset. Table 22 shows the four-leg rural and urban intersection total crash counts and crashes per intersection. These were not annualized rates but represent all crashes in the 5-yr dataset. The intersection angle category with the largest number of total crashes in the four-leg rural category was the right-angle set, but the crash per intersection rate for this angle category was the lowest of any angle category. The highest crash per intersection rate for four-leg rural intersections in OH was 4.89 for intersections in the 60-to-64-degree category. In contrast, the intersection-angle category with the highest crash rate per intersection for urban four-leg sites were the range of 50–54 degrees. This rate was 11.27 crashes per intersection, and every rate per angle category was higher for four-leg urban intersections than for four-leg rural intersections.

Table 22. Distribution of total crashes and total crashes per intersection at four-leg intersections by intersection-angle category and area type in OH.

Intersection Angle (Degrees)	Rural Crashes	Rural Crashes per Intersection	Urban Crashes	Urban Crashes per Intersection
<40	292	3.28	100	7.69
40–49	612	3.97	184	8.00
50–54	590	4.40	248	11.27
55–59	615	4.02	107	5.94
60–64	724	4.89	207	9.86
65–69	1,092	4.63	263	7.74
70–74	1,023	4.57	263	8.22
75–79	1,309	4.29	482	8.31
80–84	1,349	4.14	408	9.07
≥85 (right angle)	4,735	3.02	1,448	8.94
Total	12,341	3.70	3,710	8.67

A similar, albeit less pronounced relationship, can be seen for the three-leg intersections in the OH dataset. The crashes per intersection were greater for every angle category for urban intersections than for rural intersections, though the difference was smaller. The rural three-leg intersection-angle category with the highest sum of total crashes was right-angle sites (4,873 total crashes), and the highest rate corresponded to the range of 65–69 degrees (2.03 crashes per intersection). For urban three-leg intersections, the highest total sum of crashes was for right-angle intersections, but the highest crash per intersection rate corresponded to the range of 55–59 degrees.

The four-leg and three-leg intersections in OH showed crash rates per intersection peaked in the angle range between 50 and 70 degrees. This finding questions the general guidance regarding critical angle suggestions discussed in chapters 1 and 2. If crashes per intersection do peak in the range of 50–70-degrees, a 60-degree minimum angle may be insufficient.⁽¹⁾

Table 23. Distribution of total crashes and total crashes per intersection at three-leg intersections by intersection-angle category and area type in OH.

Intersection Angle (Degrees)	Rural Crashes	Rural Crashes per Intersection	Urban Crashes	Urban Crashes per Intersection
<40	1,004	1.93	411	5.48
40–49	764	1.90	221	5.67
50–54	420	1.77	201	5.43
55–59	516	1.75	387	6.91
60–64	681	1.84	359	4.38
65–69	972	2.03	561	5.01
70–74	1,254	1.98	611	5.01
75–79	1,306	1.74	752	4.37
80–84	1,749	1.94	1,109	5.11
≥85 (right angle)	4,873	1.77	4,744	5.50
Total	13,539	1.84	9,356	5.27

This high crash-per-intersection rate in the range of 50–70 degrees can also be observed for the more specific breakdown of rural four-leg two-lane intersections, as shown in table 24. For the four-leg two-lane intersection facility type, the crash rate per intersection peaks at 60–64 degrees with 4.74 crashes per intersection, and the lowest crash per intersection rate, 2.97, corresponds to right-angle intersections. This behavior, however, does not pertain to rural four-leg multilane intersections. For the rural four-leg multilane intersection facility type, the highest crash per intersection rate corresponds to the range of 80–84 degrees with 11.09 crashes per intersection; the second largest rate corresponds to the range of 60–64 degrees with 9.00 crashes per intersection.

For each facility type, three-leg or four-leg, the right-angle category has the highest number of total crashes. This finding indicates that there are more of these facilities in the dataset so more crashes in total occur at these intersections. The higher rates that occur at skewed intersections concern researchers most.

Table 24. Distribution of total crashes and total crashes per intersection at rural four-leg intersections by intersection angle category and the number of lanes on the major road in OH.

Intersection Angle (Degrees)	Two-Lane Crashes	Two-Lane Crashes per Intersection	Multilane Crashes	Multilane Crashes per Intersection
<40	291	3.31	0	0.00
40–49	596	3.97	0	0.00
50–54	576	4.33	7	7.00
55–59	605	4.03	8	2.67
60–64	683	4.74	36	9.00
65–69	957	4.47	36	1.64
70–74	969	4.53	85	8.50
75–79	1,253	4.25	82	8.20
80–84	1,266	4.02	122	11.09
≥85 (right angle)	4,534	2.97	319	7.60
Total	11,730	3.63	695	6.44

Table 25 through table 27 presents the AADT ranges for four-leg, three-leg, and rural four-leg intersections, respectively. For the four-leg intersections, shown in table 25, there was no clear trend regarding minimum and maximum AADT ranges as the intersection angle increases. For rural four-leg intersections, the lowest AADT count was observed at a right-angle intersection, and the highest count was observed at an intersection in the range of 65–69 degrees. The weighted average AADT (i.e., the average AADT weighted by the number of sites in each angle category for all four-leg rural intersections) is 3,627 vehicles per day, which is expectedly lower than the weighted average of 8,868 vpd at urban four-leg intersections. The highest maximum AADT occurred at right-angle intersections for urban four-leg sites, and the lowest AADT count occurred at intersections in the range of 50–54 degrees. The lack of uniformity in minima and maxima made it difficult to determine to what degree traffic volume interacts with intersection angle across the different angle categories.

Table 25. Range of intersection AADT for four-leg intersections by intersection angle and area type in OH.

Intersection Angle (Degrees)	Rural Min	Rural Avg	Rural Max	Urban Min	Urban Avg	Urban Max
<40	348	3,600	10,487	1,414	7,480	12,906
40–49	494	3,927	19,852	1,819	8,262	17,807
50–54	618	3,476	15,082	544	7,672	28,397
55–59	307	3,883	11,555	1,203	6,978	22,999
60–64	151	3,963	23,928	1,536	7,364	13,658
65–69	393	4,416	26,120	2,231	8,484	32,052
70–74	413	3,914	22,830	2,486	8,150	23,664
75–79	217	3,917	24,441	2,123	8,840	31,764
80–84	287	3,777	22,837	792	9,246	42,705
≥85 (right angle)	205	3,309	25,751	734	9,761	63,541
Weighted average	—	3,627	—	—	8,868	—

—No data available.

Min = minimum; Avg = average; Max = maximum.

Similar patterns were also observable for three-leg intersections in the OH dataset. The lowest AADT for rural three-leg intersections was observed at both 75-to-79-degree intersections and intersections with an angle less than 40 degrees, and the highest AADT count was observed at intersections in the range of 70–74 degrees. The weighted average for rural three-leg intersections is 3,356 vpd, and the weighted average for urban three-leg intersections is 9,369 vpd. A similar lack of scaling traffic volumes can be observed for the three-leg urban intersections as for the rural intersections because the lowest AADT count is observed at a right-angle intersection while the highest AADT count is observed at intersections in the range of 70–74 degrees. For these reasons, the relationship between traffic volume and intersection angle bears consideration in the cross-sectional models. In fact, the research team accounted for traffic volume’s interaction with minimum angle through the functional form of the predictive models developed, which is discussed in chapter 5.

Table 26. Range of intersection AADT for three-leg intersections by intersection angle and area type in OH.

Intersection Angle (Degrees)	Rural Min	Rural Avg	Rural Max	Urban Min	Urban Avg	Urban Max
<40	172	2,905	13,704	1,346	7,852	37,238
40–49	300	2,958	15,204	991	8,192	20,827
50–54	295	3,078	11,928	1,261	8,030	22,154
55–59	248	3,050	10,898	1,954	8,161	19,898
60–64	208	3,279	18,421	1,947	7,717	30,859
65–69	191	3,333	22,842	2,122	9,161	32,052
70–74	309	3,601	22,830	1,220	8,925	43,419
75–79	172	3,324	16,527	1,042	8,701	34,140
80–84	309	3,423	22,755	1,015	9,085	32,647
≥85 (right angle)	183	3,524	28,638	826	10,235	34,976
Weighted average	—	3,356	—	—	9,369	—

—No data available.

Min = minimum; Avg = average; Max = maximum.

The four-leg rural intersection set was further broken into intersections with two lanes or multiple lanes on the major approach to identify whether rural intersections have some unique volume characteristics. For rural four-leg intersections with major two-lane roads, the lowest observed AADT is in the range of 60–64 degrees. The highest observed AADT is in the right-angle range. For rural four-leg intersections with multilane major approaches, the lowest observed AADT is in the range of 40–49 degrees and the highest observed AADT is in the range of 60–64 degrees. The weighted average AADT for rural four-leg intersections with two-lane major roads was 3,386 vpd, and the weighted average AADT for rural four-leg intersections with multilane major roads is 10,858 vpd. This difference is understandable given that multilane roadways are designed to carry more traffic. Of interest, though, is that in the OH dataset, the highest minimum volume for rural four-leg intersections with multilane major roads is in the range of 60–64 degrees, and this minimum AADT is larger than many of the maximum AADT values observed for intersections with two-lane roads. However, the largest maximum AADT observed for intersections with two-lane roads, 25,751 vehicles per day, is greater than any observed AADT for rural four-leg intersections with major multilane approaches. These results may simply be outliers, but they certainly warrant a consideration of the interaction between traffic volume and intersection angle in the predictive model development.

Table 27. Range of intersection AADT for four-leg intersections by intersection angle category and the number of lanes on the major road in OH.

Intersection Angle (Degrees)	Two-Lane Min	Two-Lane Avg	Two-Lane Max	Multilane Min	Multilane Avg	Multilane Max
<40	348	3,599	10,487	3,712	3,712	3,712
40–49	494	3,805	13,686	2,686	8,476	19,852
50–54	618	3,468	15,082	4,527	4,527	4,527
55–59	307	3,785	11,555	3,904	8,766	11,285
60–64	151	3,667	15,400	11,031	14,620	23,928
65–69	393	3,527	14,274	4,462	13,058	26,120
70–74	413	3,568	18,409	3,659	11,334	22,830
75–79	217	3,722	24,441	4,124	9,684	18,305
80–84	287	3,543	14,721	3,840	10,494	22,837
≥85 (right angle)	205	3,117	25,751	4,193	10,307	19,769
Weighted average	—	3,386	—	—	10,858	—

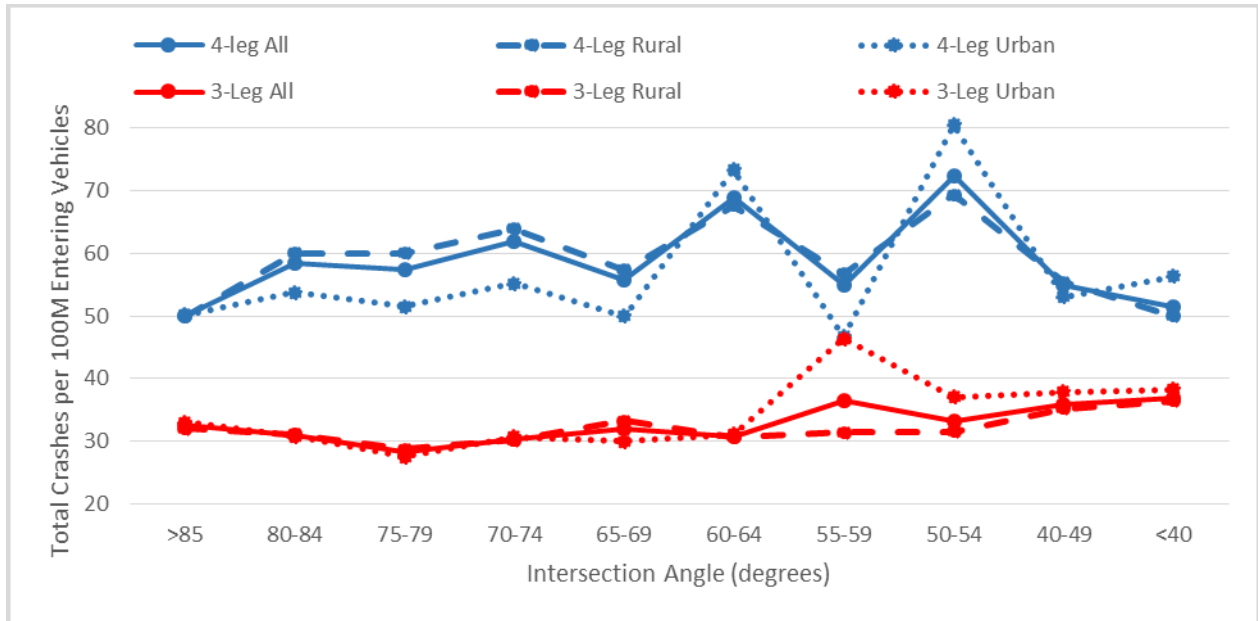
—No data available.

Min = minimum; Avg = average; Max = maximum.

Figure 18 and figure 19 compare crashes per 100-million-entering vehicles for the major intersection types in the OH database. Figure 18 shows the crash rates for all four-leg intersections, four-leg rural intersections, four-leg urban intersections, all three-leg intersections, three-leg rural intersections, and three-leg urban intersections, respectively. As shown in figure 18, the crash rates for four-leg intersections were higher than the crash rates for three-leg intersections. For four-leg intersections, crashes peaked in two ranges: 60–64 degrees and 50–54 degrees. For the larger angle measures (65 degrees to greater than or equal to 85 degrees), the rural crash rate was higher than the other two, but the urban crash rate becomes higher for most angle categories at lower angle measures. For three-leg intersections, the three roadway types show consistent trends of crash rates peaking in the range of 55–59 degrees. The three-leg urban-intersection type emerged with the highest trends for three-leg intersections with angles 60 degrees or less.

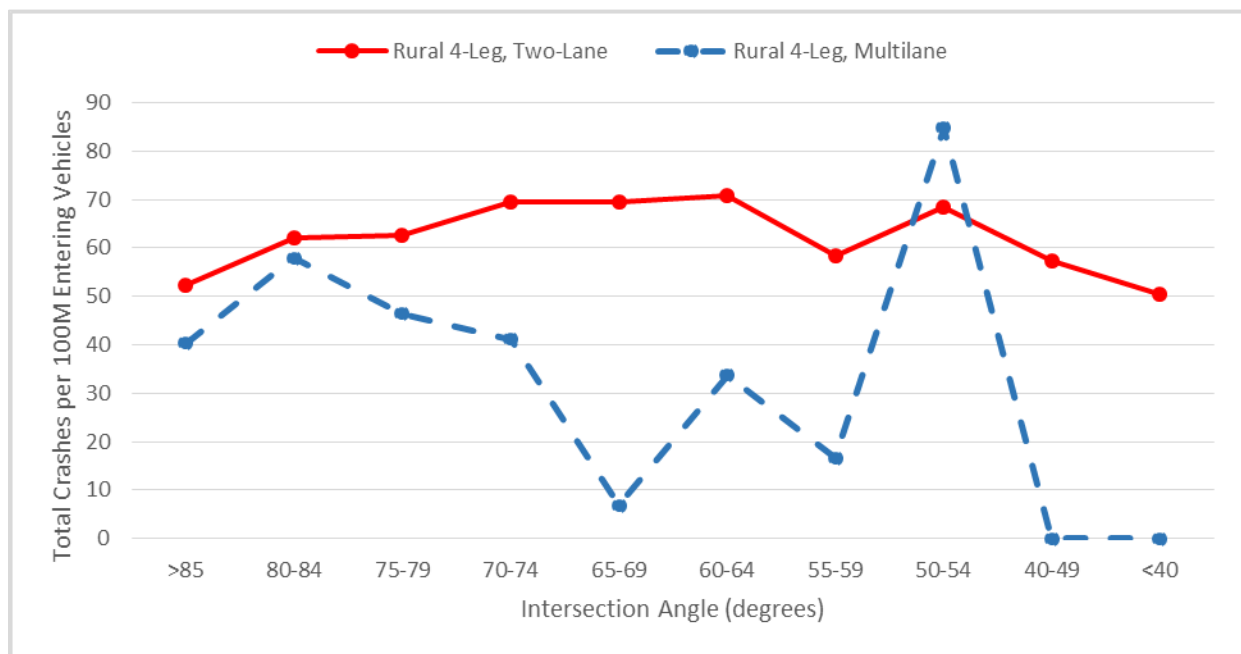
Figure 19 explores the crash trends for rural four-leg intersections more specifically. Rural four-leg two-lane intersections are compared to rural four-leg multilane intersections. Aside from the category of 50–54 degree, the rural four-leg two-lane roadways displayed higher crashes per 100-million-entering vehicles. This result is unexpected given the lower volumes but similar crash counts on this facility type, but researchers found it interesting that crashes on these facilities spike in the lower-angle categories: 60–64 degrees for rural two-lane intersections, and 50–54 degrees for rural intersections with multilane major approaches.

None of the crash trends peak below 40 degrees. While this could be because of a low sample of sites or lower traffic volumes at these uncommon intersections, these curves could also be indicative of problems with the general guidance for minimum angles.⁽¹⁾ Crash rates for four-leg intersections reached one of their peaks in the range of 60–64 degrees and rates were their highest between 70 and 50 degrees for all intersection types. These crash rates suggested that the guidance of 60-degree-minimum angles affording most of the safety benefits of right angles should be challenged, although more specific model development and verification is needed.



Source: FHWA.

Figure 18. Graph. Annual average total crash rate by intersection angle category, number of legs, and rural/urban classification in OH.



Source: FHWA.

Figure 19. Graph. Annual average total crash rate for rural four-leg intersections by intersection angle category and number of approach lanes on the major road in OH.

DATA COMPARISON

Although the results from MN and OH suggested a need for a more careful analysis of the CMFs and treatment guidance for intersection angles, there are key differences between the data available for the two States. The major discrepancy between the two States is the scope and breadth of the intersection data. MN data were retrieved from the HSIS and supplemented through further data collection; therefore, several additional variables existed for building models for MN than for OH. Including the full list of available site characteristics was beyond the scope of this section because these variables were tested and analyzed in a process described in chapter 5 in this report, but the difference in available data indicate that the MN dataset contained more specific information regarding the roadways in the dataset, intersection treatments, speed, and other design characteristics. The OH dataset contained only those variables necessary to divide the data into the requisite categories plus a few extra site descriptors, such as division of roadway, functional classification, and lighting.

The difference in data breadth was also characterized by the number of sites in each sample. These differences are summarized in table 28. The table shows that there were almost five times as many available intersections in the OH dataset as in the MN dataset despite fewer years of crash data gathered for OH. The OH dataset included more three-leg intersections than four-leg intersections; the opposite was true for the MN dataset. For MN, crash data were gathered from 2003 to 2009. For OH, crash data were gathered from 2011 to 2015. The number of skewed intersections per intersection type per State are shown in table 29.

Table 28. Quantity of total intersections by number of legs in each dataset.

Intersection Type	MN	OH
Three leg	1,109	9,122
Four leg	1,669	3,766
Total	2,778	12,981

The table shows that there were more skewed intersections in the OH dataset than in the MN dataset. These results enabled a wider range of models to be developed for the OH dataset.

Table 29. Quantity of skewed intersections by number of legs in each dataset.

Intersection Type	MN Rural	MN Urban	MN Total	OH Rural	OH Urban	OH Total
Three leg	350	120	470	4,587	912	5,499
Four leg	580	74	654	1,769	266	2,035
Total	930	194	1,124	6,356	1,178	7,534

Average AADT values were higher for every intersection type for MN than for OH. Despite the higher traffic volumes on the sample sites in MN, observed crashes in OH were larger for every facility type. This is likely explained by the sheer number of sites in the OH datasets. Comparing table 13 through table 16 reveals no bias toward high-crash intersections for OH, although the rate per million entering vehicles considered in addition to the crash sums and AADT values might explain why the rates in figure 18 are higher than the companion frequencies for MN.

As seen in the CMF Clearinghouse’s guidance on calibration and on documentation of crash rates for MN and OH, MN’s crash rates are lower than many other States in the Nation.⁽⁶⁰⁻⁶³⁾ The weighted intersection AADTs also differed for MN and OH (table 30).

Table 30. Weighted intersection volumes by roadway type, number of legs, and number of lanes in each State’s dataset.

Roadway Type Intersection Type	MN AADT Average	OH AADT Average
Rural two-lane four-leg	3,570	3,386
Multilane rural four-leg	12,677	10,858
Total rural four-leg	4,293	3,627
Total urban four-leg	14,969	8,868
Total rural three-leg	5,275	3,356
Total urban three-leg	18,274	9,369

Table 31. Total crashes by number of legs in each dataset.

Intersection Type	MN Rural	MN Urban	MN Total	OH Rural	OH Urban	OH Total
Three-leg	2,829	1,901	4,730	13,539	9,356	22,895
Four-leg	5,868	2,614	8,482	12,341	3,710	16,051
Total	8,697	4,515	13,212	25,880	13,066	38,946

CHAPTER 5. ANALYSIS AND INTERPRETATION OF RESULTS

The application of the methodology and the results of the analysis of both State datasets are presented in this chapter. The chapter starts with a brief discussion of data-mining efforts for MN that identified the most important independent variables and interactions among the variables. The Development of CMFs and Functions discusses the NB regression models developed for both States and presents the two finalized model forms tested for both MN and OH. The development of CMFs or CMFunctions for intersection angles in both States is described in Critical Angle Assessment and Comparison of Results to Prior CMFs includes the interpretation of results related to critical minimum intersection angles. The framework for the analysis is shown in table 32 and table 33. The objective of the analysis was to produce results for three- and four-leg intersections separately for total crashes. Additional efforts were explored to further separate the data based on area type (rural versus urban) and collision severity. Collision-severity levels for the analysis are defined as follows:

- Total includes all crashes.
- Fatal and Injury (F&I) includes only those crashes in which a vehicle occupant, pedestrian, or bicyclist was killed or injured.
- PDO includes only those crashes in which there were no injuries or fatalities.

The primary focus of this analysis is total crashes. The main reason for this focus is the inherent need to establish clear guidelines for intersection minimum angle, which will help agencies design intersections to meet a specific guideline rather than accounting for the potential variations in CMFunctions that may result from developing different models for different severities. Another reason for this focus is that identifying the true crash type is difficult without delineating the specific leg of the intersection to which the crash belongs, and assigning crashes to specific legs is a time-consuming process beyond the scope of this report. Further disaggregating results by severity may only dilute the sample sizes for analysis. The focus of this study, therefore, is on total crashes. Findings for other crash severities were included when necessary to verify the main conclusions drawn from total crash CMFunctions.

Table 32. Analysis framework for MN—summary of crashes by collision severity and intersection classification in the final database.

Collision Severity	Four Legs All (1,669 sites)	Four Legs Rural (1,472 sites)	Four Legs Urban (197 sites)	Three Legs All (1,109 sites)	Three Legs Rural (888 sites)	Three Legs Urban (221 sites)
Total 7-yr total	8,482	5,868	2,614	4,730	2,829	1,901
Total 7-yr avg	5.08	3.99	13.27	4.27	3.19	8.60
Total ann avg	0.73	0.57	1.90	0.61	0.46	1.23
F&I 7-yr total	3,202	2,335	867	1,682	1,029	653
F&I 7-yr avg	1.92	1.59	4.40	1.52	1.16	2.95
F&I ann avg	0.27	0.23	0.63	0.22	0.17	0.42
PDO 7-yr total	5,204	3,484	1,720	3,007	1,784	1,223
PDO 7-yr avg	3.12	2.37	8.73	2.71	2.01	5.53
PDO ann avg	0.45	0.34	1.25	0.39	0.29	0.79

Ann = annual; Avg = average; F&I = fatal and injury; PDO = property damage only.

Table 33. Analysis framework for OH—summary of crashes by collision severity and intersection classification in the final database.

Total Crashes	Four Legs All (3,766 sites)	Four Legs Rural (3,338 sites)	Four Legs Urban (428 sites)	Three Legs All (9,122 sites)	Three Legs Rural (7,347 sites)	Three Legs Urban (1,775 sites)
5-yr total	16,051	12,341	3,710	22,895	13,539	9,356
5-yr avg	4.26	3.70	8.67	2.51	1.84	5.27
Ann avg	0.85	0.74	1.73	0.50	0.37	1.05

Ann = annual; Avg = average.

DATA MINING

The data-mining efforts for the MN dataset were used for two purposes: to determine the most important predictor variables from the large number of available independent variables in the final database and determine the interactions among the important predictor variables. The results of the data-mining analysis were then used to develop the safety prediction models.

The final raw database for MN included more than 60 possible predictor variables from HSIS and the supplemental data-collection effort. Each variable was examined to determine if it should be included in the analysis as a continuous or categorical variable or eliminated from further consideration. For some variables, such as intersection angle, the continuous data variable was retained. Categorical variables were obtained for further exploration in the data-mining analysis. Some variables were very unbalanced, where attributes in a variable are disproportionate and almost all of observations have only one of the attributed (i.e., more than 90 percent of the intersections were associated with one attribute of the data element). For example, the number of intersections in the database with sight obstructions was 43 out of 2,778, indicating 97 percent of the intersection do not have sign obstructions. These unbalanced variables would not likely contribute to safety-prediction models and were eliminated from the analysis database. Other variables were eliminated because they had missing values, which cannot be supported in the development of the NB regression models. The final modified database used in the data-mining analysis included 39 and 34 potential predictor variables for four-leg and three-leg intersections, respectively. Table 74 in appendix D includes the complete list of variable names, descriptors, definitions, and attributes. The variable names are included in the tabular and graphical results from the data-mining analysis and the NB regression models in the remainder of this report.

RF methods were applied for determining the most important predictor variables. Two different statistical packages were explored for this analysis: Package randomForest, version 4.6-7 and cforest within Package party in R, version 1.0-6.^(46,64-68) The two packages are similar because they both use random subsets of the input data to do recursive partitioning of the data and develop multiple classification or regression trees. The aggregated result of these multiple trees is then used to estimate the importance of each predictor variable in modeling the dependent variable. There are, however, key differences in these packages that relate to determining predictor variable importance. First, randomForest is best suited to predictor variables of the same type (e.g., continuous or categorical). When variables of different types are included, the randomForest algorithm tends to be biased toward the continuous variables and variables with many categories.⁽⁶⁷⁾ Second, randomForest does not accurately account for correlation among predictor variables. The result is an overestimation of the importance of highly correlated predictors.⁽⁶⁸⁾ The cforest algorithm overcomes these shortcomings by using a conditional

permutation-importance measure.⁽⁴⁹⁾ Third, randomForest requires that the continuous dependent variables be normally distributed. Crashes are commonly known to have an NB distribution. In brief, the cforest algorithm can better handle predictor variables of different types and does not tend to introduce the biases previously described. The algorithm also considers the marginal measure of importance of each predictor variable based on the intercorrelation with other predictors.

Given that the database for this study includes both continuous and categorical variables, the fact that some of the variables are likely correlated, and the fact that the dependent variable (number of crashes) is not normally distributed, cforest within Package party in R was selected for the RF analysis to determine the most important predictor variables. Using the analysis framework previously described, conditional random forest (CRF) results were produced separately for the following six conditions:

- Four-leg total crashes.
- Four-leg fatal-and-injury crashes.
- Four-leg PDO crashes.
- Three-leg total crashes.
- Three-leg fatal-and-injury crashes.
- Three-leg PDO crashes.

All cforest plots for the six scenarios (three leg and four leg; total, injury and fatal, and PDO crashes) are provided in appendix D. Each plot shows the chosen cutoff point. Table 34 and table 35 provide lists of the top predictor variables selected for each of these six scenarios. A total of 16, 15, and 15 predictor variables (table 36) were selected for total, injury and fatal, and PDO crashes, respectively, for four-leg intersections. For three-leg intersections, a total of 10, 12, and 10 predictor variables were selected for total, injury and fatal, and PDO crashes, respectively.

Table 34. Most important predictor variables for MN four-leg intersections (results from cforest analysis).

Total Crashes	Fatal-and-Injury Crashes	PDO Crashes
Intersection AADT	Intersection AADT	Intersection AADT
Major road AADT	Minor road AADT	Major road AADT
Minor road AADT	Major road AADT	Minor road AADT
Roadway class (major road)	Intersection angle (categorical)	Roadway class (major road)
Intersection angle (categorical)	Speed limit (minor road)	Area type (urban/rural)
Land use	Roadway class (major road)	Speed limit (major road)
Area type (urban/rural)	Land use	Commercial driveways (major road)
Speed limit (major road)	Speed limit (major road)	Crosswalk presence (major road)
Commercial driveways (major road)	Curb presence (major road)	Land use
Number of thru lanes (intersection)	Right-turn lane presence (major road)	Right-shoulder width (major road)
Left-turn lane presence (major road)	Number of thru lanes (intersection)	Number of thru lanes (intersection)
Crosswalk presence (major road)	Sidewalk presence (major road)	Crosswalk presence (major road)
Right-shoulder width (major road)	Left-turn lane presence (major road)	Commercial driveways (major/minor)
Left-shoulder width (major road)	Area type (urban/rural)	Adjacent intersections (major road)
Speed limit (minor road)	Onstreet parking (minor road)	Intersection angle (categorical)
Right-turn lane presence (major road)	—	—

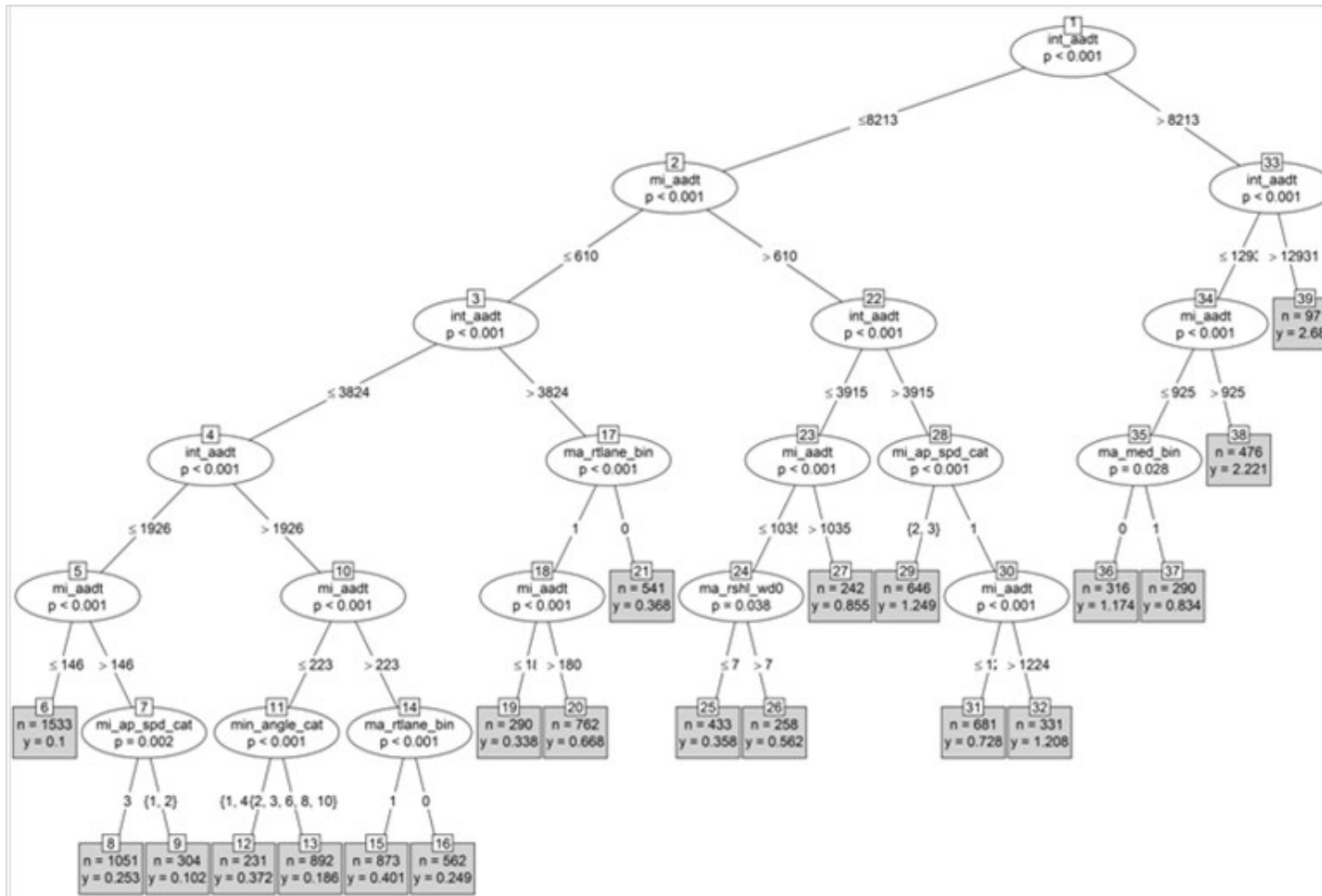
—No data available.

The proceeding results are from the ctree output for total crashes at four-leg intersections. Figure 20 shows the tree produced for this scenario. The first node in the tree is intersection AADT, which shows that it is the most important predictor for total crashes at four-leg intersections. The tree splits at an intersection AADT value of 8,213 vpd. For those intersections with an AADT greater than 8,213, intersection AADT enters the tree again as the most important predictor for this subset of intersections and branches at a value of 12,391 vpd. For those locations with an intersection AADT greater than 12,391, the tree then terminates. Termination of a branch occurs when any of the previously described stopping criteria are met. For those intersections with an intersection AADT less than or equal to 12,391 vpd, the tree splits again based on minor road AADT. This is followed by a split for intersections with a minor road AADT equal to or less than 925 vpd on the variable indicating presence of a median on the major road. That side of the tree terminates at that branch. The other side of the tree can be traced with a similar interpretation of the results.

Table 35. Most important predictor variables for MN three-leg intersections (results from cforest analysis).

Total Crashes	Fatal-and-Injury Crashes	PDO Crashes
Intersection AADT	Intersection AADT	Intersection AADT
Minor road AADT	Minor road AADT	Minor road AADT
Major road AADT	Major road AADT	Major road AADT
Speed limit (major road)	Roadway class (major road)	Speed limit (major road)
Roadway class (major road)	Land use	Roadway class (major road)
Intersection angle (categorical)	Speed limit (minor road)	Lane width (major road)
Land use	Speed limit (major road)	Land use
Curb presence (major road)	Left-turn lane presence (major road)	Intersection angle (categorical)
Lane width (major road)	Intersection angle (categorical)	Curb presence (major road)
Speed limit (minor road)	Residential single-family driveways (minor road)	Right-shoulder width (major road)
—	Curb presence (major road)	—
—	Driveways (major road)	—

—No data available.



Source: FHWA.

Figure 20. Plot. Results of regression tree (ctree) analysis for total crashes at four-leg intersections.

There are three reasons for the value from this analysis. First, the results confirm what was previously found from the CRF analysis: the AADT values are the most important predictor variables. The first three levels of the tree split on intersection AADT or minor road AADT. Six of the 10 nodes in the next two levels are the intersection AADT or minor road AADT variables. Second, a strong association exists between these two variables within the tree. Five branches within the trees that extend between levels are between intersection AADT and minor road AADT, which might indicate the need for an interaction variable within the negative binomial model that will be subsequently developed. Finally, the intersection-angle variable enters the tree as a significant variable for total crashes and fatal-and-injury crashes for both four-leg and three-leg intersections and for PDO crashes for three-leg intersections. The variable does not enter the PDO tree for four-leg intersections. These results confirm what was previously found from the CRF analysis regarding this last result: intersection angle for PDO crashes at four-leg intersections was the last variable selected before the cutoff point. Less-significant variables entering a single tree at the lower levels can be sensitive to small changes in the input variables. For this reason, CRF results, which combine the predictions of many different trees to produce an aggregated prediction, are more stable and robust and provide better indicators of variable importance.

Additional regression trees were produced for fatal-and-injury crashes and PDO crashes at four-leg intersections and total, fatal-and-injury, and PDO crashes at three-leg intersections. The results for all regression trees are provided in appendix D. All trees replicate the key findings previously noted, which are that AADT variables are important and there is a strong association between intersection AADT and minor road AADT.

SAFETY-PREDICTION MODELS

The NB regression models were developed using the GENMOD procedure (Release 9.3) developed by SAS.⁽⁶⁹⁾ The goal of the analysis was to develop models for each of the cells in the analysis framework presented in table 35 and table 36. Small sample sizes and limited data ranges for some variables prevented the development of models for some of the scenarios. The most important predictor variables from the MN data-mining analysis, as previously shown in table 35 and table 36, provided the candidate variables considered for each developed model for the MN dataset. Data mining was not conducted for OH data to identify potential explanatory variables within the dataset because of the limited number of descriptive parameters available. Instead, SPF models were tested in a backward regression format where all available parameters, including derived model parameters, were tested in an NB model using the GENMOD procedure. Statistically nonsignificant variables (at the $p < 0.05$ level), or variables not entered into the model, were removed until only a set of statistically significant explanatory variables that provided the best fit remained. The remainder of this section of the report describes the models developed for each scenario. The models developed for four-leg intersections are presented first, followed by the three-leg intersection models.

The focus of the discussion is on the models developed for predicting total crashes; however, the CMFunctions described later in this chapter are also for total crashes. Models were also developed for fatal-and-injury and PDO crashes when sample sizes permitted their development. Additional tables describing these supplemental models are provided in appendix E. All models were independently derived and the results from models for PDO crashes cannot be combined

with results from fatal-and-injury models to produce an estimate that would be equivalent to the estimate produced from the model for total crashes.

Two criteria were used to assess the goodness of fit for each model developed: Akaike information criterion (AIC) and Bayesian information criterion (BIC) or the Schwarz criterion.^(70,71) The criteria are expressed as shown in figure 21 and figure 22.

$$AIC = 2k - 2\ln(L)$$

Figure 21. Equation. AIC.

$$BIC = k\ln(n) - 2\ln(L)$$

Figure 22. Equation. BIC.

Where:

k = number of free parameters in the model.

n = sample size.

L = maximized value of the likelihood function.

A smaller value for either criterion indicates a better model fit to the data. A larger L produced a smaller value for both metrics. Likewise, fewer k also produced a smaller value for both criteria. The difference in the two criteria is the magnitude of the penalty assigned for the number of parameters in the model. The AIC used a multiplier of 2.0 and did not account for sample size. The BIC accounted for the size of the sample with the multiplier $\ln(n)$. For example, a sample size of 10,000 had a \log_e value of 9.2. In this example, the BIC added 9.2 to the value for each additional parameter, while the AIC added 2.0. The goal was to select the model with the best fit and the fewest parameters. Thus, the BIC was chosen as the preferred criterion for comparison of models. However, the AIC was also used when there was no or little change in the BIC. The magnitude of the change in these criteria when choosing among models was also considered. The values in table 36 provide general guidance on interpreting the change in value for the two criteria.

Table 36. General guidance for interpretation of models using AIC and BIC criteria.

Change in AIC	Model Difference Interpretation ⁽⁷²⁾	Change in BIC	Model Difference Interpretation ⁽⁷³⁾
0–2	Indistinguishable	0–2	Negligible
4–7	Substantial	2–6	Positive
>10	Very strong	6–10	Strong
—	—	>10	Very strong

—No data available.

For the OH dataset, regression models were developed in SAS twice for each intersection type to test two slightly different variable sets related to two potential functional forms used for CMFunction predictions. The first form, flexible form model 1, was initially developed using the MN data and is described in the next section. The second form, the Hoerl Curve suggested by Ezra Hauer, was suitable for capturing data with a parabolic shape.⁽⁷⁴⁾ Although the roadway variables were consistent in both the flexible form model 1 and Hoerl Curve models, the angle

and volume parameters were slightly different; therefore, two separate models were prepared for each intersection type to find the best fit, and the model that retained its fundamental variables for CMFunction development and had the lower AIC and BIC values was selected.

The variable set for the OH SPF development includes the following:

- *Minimum Angle.*
- *Lighting.*
- *Roadway Division of Major Approach.*
- *Functional Classification of Major Approach.*
- *AADT of Major Approach.*
- *AADT of Minor Approach.*
- *Total Intersection AADT (derived variable).*
- *Minor Road/Intersection AADT Ratio (derived variable).*
- *Natural Log of Major Approach AADT (derived variable).*
- *Natural Log of Minor Approach AADT (derived variable).*
- *Natural Log of Total Intersection AADT (derived variable).*
- *Natural Log of Minor Road/Intersection AADT Ratio (derived variable).*
- *Log Cos(intersection AADT) (derived for flexible form model 1).*
- *Log Cos(minor road AADT) (derived for flexible form model 1).*
- *Natural Log of Minimum Angle (derived for Hoerl curve).*

A full variable list, as well as their abbreviations, is included in appendix D.

The scope of the OH dataset allowed for even more SPFs to be developed than for the MN dataset (table 37). However, models were only tested for total crashes. Separate models were not developed for different crash severities using OH data.

Table 37. Different roadways with sufficient data for total crash CMFunction development.

Roadway Type	MN Dataset	OH Dataset
Rural four-leg two-lane	X	X
Rural four-leg multilane	X	X
Rural three-leg two-lane	—	X
Rural three-leg multilane	—	X
Urban four-leg all roads	—	X
Urban three-leg all roads	—	X
Urban four-leg two-lane	—	X
Urban four-leg multilane	—	X
Urban two lane	—	X
Urban three-leg multilane	—	X
Rural three-leg all roads	X	X
Rural four-leg all roads	X	X
Rural and urban three-leg	X	X

— Sufficient data not present.

X = sufficient data present.

Although data were available for each of the roadway types listed in table 38, the final list of prediction models was narrowed down to a smaller set because of unreliable results. The results were considered unreliable if the functional form provided poor fit (i.e., if the shape of the CMFunction produced by the prediction model was irregular and did not corroborate the observed shape of the other model curves) or if the variables necessary for either functional form were not statistically significant (i.e., if neither *lgcos_int* or *lgcos_mi* were significant for flexible form model 1 or if the log minimum angle term was not significant for the Hoerl Curve). After narrowing down the models, the following prediction results remained for total crashes:

- Rural four-leg all roads.
- Rural four-leg two-lane.
- Rural four-leg multilane.
- Rural three-leg all roads.
- Rural three-leg two-lane.
- Urban four-leg total.
- Urban four-leg two-lane.
- Urban three-leg all roads.
- Urban three-leg two-lane.

The next sections show the model parameters and fit statistics for total predicted crashes on each of three- and four-leg facilities. The specific model fit statistics for the further disaggregated facility types are included in appendix E.

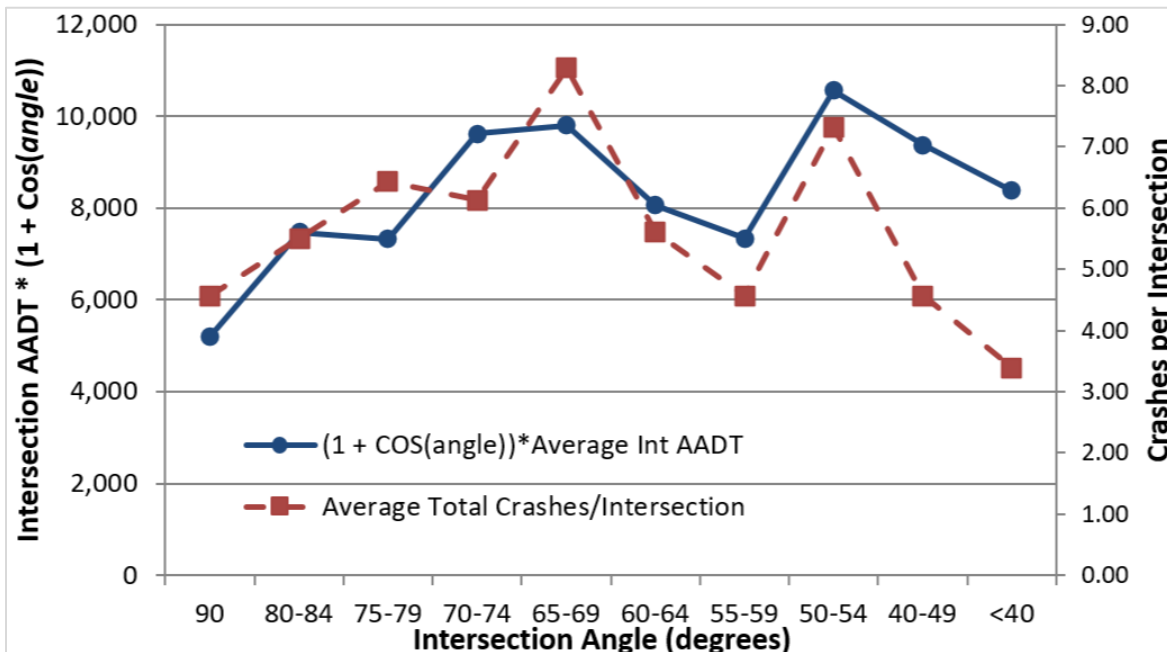
Total Crashes for Four-Leg Intersections

Multiple models were developed and tested to find the best-fitting functional form. Initially, a standard NB model was developed to predict total crashes using MN data; this model was referred to as the base model and is shown in appendix E. The model assumed a monotonic relationship between crashes and intersection angles. From the plot of crash rate (per 100 million entering vehicles) versus the intersection-angle category in figure 16 and figure 18, it is apparent

that this is not a monotonic relationship. For all four-leg intersections (rural and urban combined), the highest crash rates occurred in the categories of 65–69 degrees and 50–54 degrees. Crash rates for intersections with angles lower than 40 degrees are less than the crash rates for right-angle intersections. Given this nonmonotonic relationship, the researchers desired a more flexible form model 1 that better replicated the raw data. The alternating peaks and valleys in the data as one moves from a right angle to angles less than 40 degrees required a functional form that accounts for these changes in the data. Several variations of the angle parameter were tried to determine which form most closely matches the shape of the raw data.

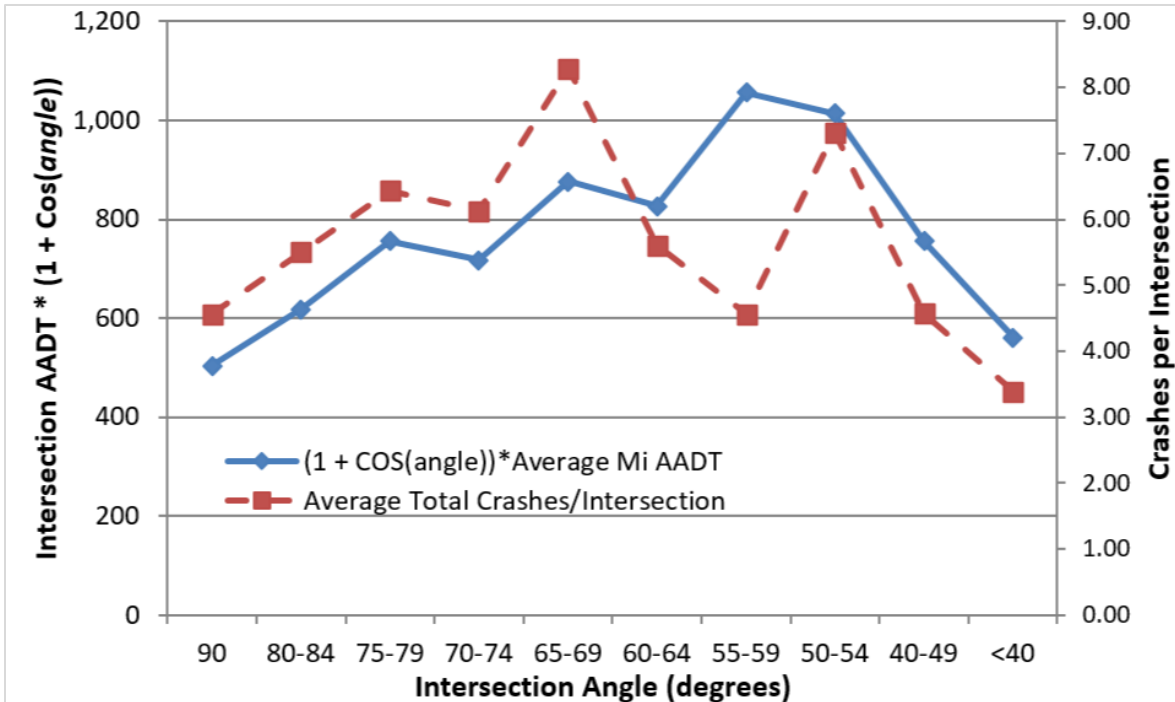
The final form chosen was $1 + \cos(\text{angle})$. For right-angle intersections, the value of the function becomes 1.0 as the $\cos(90 \text{ degrees})$ equals 0.0. As the intersection angle decreased, the value of the function increased. Figure 23 shows the plot of this functional form when multiplied by the average intersection AADT values from the angle categories and the plot of the average number of total crashes per intersection for four-leg intersections in these same categories. The patterns of peaks and valleys in the two lines across the range of intersection angles were very similar. The correlation coefficient ($r = 0.519$) indicated a strong association.

Figure 24 shows the plot of $1 + \cos(\text{angle})$ multiplied by the average minor road AADT values from the angle categories and the plot of the average number of total crashes per intersection for four-leg intersections in these same categories. Again, the patterns exhibited for the two lines across the range of intersection angles were very similar. The strength of association between these two variables was also strong ($r = 0.476$). Based on these strong associations, the variable $1 + \cos(\text{angle})$ was included in the flexible form model 1.



Source: FHWA.

Figure 23. Graph. Average total crashes per intersection for all four-leg intersections in MN and functional form of $[(1 + \cos(\text{angle})) \times \text{intersection AADT}]$ as distributed across the range of intersection angles.



Source: FHWA.

Figure 24. Graph. Average total crashes per intersection for all four-leg intersections in MN and functional form of $[(1 + \cos(\text{angle})) \times \text{minor road AADT}]$ as distributed across the range of intersection angles.

Two models were developed using the $1 + \cos(\text{angle})$ term. The first model, referred to hereafter as flexible form model 1, incorporated the term as shown in figure 23 and figure 24 because this was the association drawn with the raw data. The term was added to the AADT variables previously used in the base model. The new variables were structured as shown in figure 25 and figure 26.

$$l\text{gcos_int} = \ln [(\text{intersection_aadt}) \times (1 + \cos(\text{angle}))]$$

Figure 25. Equation. Derived variable that incorporates intersection AADT and cosine of the intersection angle.

$$l\text{gcos_mi} = \ln [(\text{minor road_aadt}) \times (1 + \cos(\text{angle}))]$$

Figure 26. Equation. Derived variable that incorporates minor road AADT and cosine of the intersection angle.

The form of the variable structure allows the parameter estimates for these two variables to be summed and applied to the angle term $1 + \cos(\text{angle})$. Figure 27 shows the derivation that allows for the separation of the terms within the variables in figure 25 and figure 26 and the application of the sum of the parameter estimates to produce the estimated crash predictive effect of this component within the model.

$$\begin{aligned}
N_p &= \text{EXP} \{ \ln[\text{int_aadt} \times (1 + \cos(\alpha))] | \beta_1 \} \times \text{EXP} \{ | \ln[(\text{mi_aadt}) \times (1 + \cos(\alpha))] | \beta_2 \} \\
&= [(\text{int_aadt}) \times (1 + \cos(\alpha))]^{\beta_1} \times [(\text{mi_aadt}) \times (1 + \cos(\alpha))]^{\beta_2} \\
&= (\text{int_aadt})^{\beta_1} \times [1 + \cos(\alpha)]^{\beta_1} \times (\text{mi_aadt})^{\beta_2} \times [(1 + \cos(\alpha))]^{\beta_2} \\
&= (\text{int_aadt})^{\beta_1} \times (\text{mi_aadt})^{\beta_2} \times [1 + \cos(\alpha)]^{(\beta_1 + \beta_2)} \\
&= (\text{int_aadt})^{\beta_1} \times (\text{mi_aadt})^{\beta_2} \times [1 + \cos(\alpha)]^{\beta_3}
\end{aligned}$$

Figure 27. Equation. Derivation of partial crash prediction term using intersection AADT, minor road AADT, and cosine of the intersection angle.

Where:

- N_p = partial crash prediction using the parameters shown.
- int_aadt = intersection AADT (vpd).
- mi_aadt = minor road AADT (vpd).
- α = intersection angle, degrees.
- $\beta_1, \beta_2, \beta_3$ = parameter estimates from the regression model.
- $\beta_3 = \beta_1 + \beta_2$.

A second model, hereafter referred to as flexible form model 2, incorporated the term $1 + \cos(\text{angle})$ as a unique variable ($\text{lgcos}_1 = \ln[1 + \cos(\text{angle})]$). The original AADT variables (lgint_aadt and lgmi_aadt) used in the base models were retained.

The results from flexible form model 1 for the MN data are shown in table 38. The same variables that were significant in the base models remained significant in this model. Intersection angle (min_angle) was included in the model as before and is significant with a p -value of <0.0001 . The estimate for this variable was 0.0124. The additional variables incorporating the $1 + \cos(\text{angle})$ terms and AADT were both significant with p -values of <0.0001 . The sum of the estimates for these two parameters was 1.1816.

The BIC and AIC for flexible form model 1 are 23,073 and 22,963, respectively. For flexible form model 2, the BIC and AIC are 23,078 and 22,960, respectively. The goodness-of-fit parameters were in opposing directions. The BIC showed a positive improvement in model 1 over model 2, while the AIC showed the two models to be close to indistinguishable. Considering both criteria, flexible form model 1 was the better of the two. The BIC and AIC values for the alternative base model, shown in appendix E, were 23,087 and 22,977, respectively. The fit metrics for the flexible form model 1 were much lower, indicating a very strong improvement in the model fit.

Table 38. Flexible form model 1 results for total crashes at all four-leg intersections for MN.

Parameter Description	Estimate	Standard Error	Lower 95% CL	Upper 95% CL	Chi-Square	Statistical Significance
Intercept	-10.6485	0.2614	-11.1607	-10.1363	1660.09	<0.0001
<i>lgcos int</i>	0.8454	0.0325	0.7818	0.909	678.11	<0.0001
<i>lgcos mi</i>	0.3362	0.0282	0.281	0.3915	142.44	<0.0001
<i>min angle</i>	0.0124	0.001	0.0104	0.0143	158.92	<0.0001
<i>mi int</i>	0.7427	0.2284	0.295	1.1904	10.57	0.0011
<i>ma rodwycls cat (1)</i>	0.2258	0.0576	0.1129	0.3386	15.38	<0.0001
<i>ma rodwycls cat (2)</i>	0.1068	0.0617	-0.0142	0.2278	2.99	0.0836
<i>ma rodwycls cat (3)</i>	-0.0403	0.0476	-0.1336	0.053	0.72	0.397
<i>ma rodwycls cat (4)</i>	0	0	0	0	—	—
<i>spec env cat (0)</i>	-0.1225	0.0549	-0.2301	-0.0149	4.98	0.0257
<i>spec env cat (1)</i>	-0.1233	0.0539	-0.229	-0.0177	5.24	0.0221
<i>spec env cat (2)</i>	-0.4814	0.0575	-0.5941	-0.3687	70.11	<0.0001
<i>spec env cat (3)</i>	0	0	0	0	—	—
<i>ma ap spd cat (1)</i>	-0.2349	0.0583	-0.3492	-0.1207	16.23	<0.0001
<i>ma ap spd cat (2)</i>	-0.0899	0.0526	-0.193	0.0133	2.92	0.0877
<i>ma ap spd cat (3)</i>	0	0	0	0	—	—
<i>ma rshl wd0</i>	-0.0218	0.0049	-0.0313	-0.0123	20.13	<0.0001
Dispersion	0.4294	0.0245	0.3839	0.4802	—	—
Goodness-of-fit parameters: AIC (smaller is better)	—	22,963	—	—	—	—
Goodness-of-fit parameters: BIC (smaller is better)	—	23,073	—	—	—	—

—No data available.

Table 38 is a representative example of a four-leg intersection SPF developed using data from MN. SPFs were also developed for each entity in the OH database, and two model fit statistics tables are included here (table 39 and table 42) to demonstrate the disaggregation of four-leg sites in OH.

For the rural four-leg intersection model for all roads, flexible form model 1 provided a better fit than the Hoerl Curve (discussed in greater detail in the Crash-Prediction Model section) based on the AIC and BIC values. In addition to the *lgcos_int* and *lgcos_mi* variables, this model included logarithmic variables for both major approach AADT and total intersection AADT. Minimum angle was critical for prediction, and roadway characteristics like major road division and major road functional classification were statistically significant. Minimum-angle categories were further discretized down to 20 degrees because of the wider range of intersections available in the dataset. The highest concentrations of intersections were in the upper three brackets.

Table 39. Model fit statistics for OH for total rural four-leg intersections.

Parameter Description	Category	Estimate	Standard Error	Statistical Significance
Intercept	N/A	-40.3087	6.1746	<0.0001
<i>lgcos int</i>	N/A	3.8250	0.5997	<0.0001
<i>lgcos mi</i>	N/A	0.2055	0.0385	<0.0001
<i>min angle</i>	N/A	0.0432	0.0072	<0.0001
<i>lgma aadt</i>	N/A	-0.7958	0.1902	<0.0001
<i>lgint aadt</i>	N/A	-2.2125	0.6325	0.0005
<i>ma division</i>	Divided	-0.3448	0.0988	0.0005
<i>ma division</i>	Undivided	Base category	—	—
<i>ma rodwycls cat</i>	Local	0.2030	0.1354	0.1338
<i>ma rodwycls cat</i>	Major collector	0.2071	0.0598	0.0005
<i>ma rodwycls cat</i>	Minor arterial	0.1336	0.0594	0.0245
<i>ma rodwycls cat</i>	Minor collector	0.3290	0.0998	0.0010
<i>ma rodwycls cat</i>	Principal arterial	Base category	—	—
Dispersion	N/A	0.4584	0.0202	—
Goodness-of-fit parameters: AIC (smaller is better)	14,799.8243	—	—	—
Goodness-of-fit parameters: BIC (smaller is better)	14,873.1711	—	—	—

—No data available.

N/A = not applicable.

Unlike the MN dataset, the OH dataset was sufficiently robust to allow multiple prediction models to be developed for urban intersections. The first of these presented is the urban four-leg total intersection-prediction model. Flexible form model 1 provided the best fit for this intersection type based on the AIC and BIC and statistically significant variables. However, this fit was provided by a partial flexible form model 1 that excluded the *lgcos_mi* variable. The statistically significant predictor variables included *lgcos_int*, *lgma_aadt*, and *min_angle*.

Unlike several of the other models, the total urban four-leg model had a truncated angle set because of a low quantity of sample counts less than 30 degrees.

Table 40. Model fit statistics for OH for urban four-leg total intersections.

Parameter Description	Category	Estimate	Standard Error	Statistical Significance
Intercept	N/A	-12.9443	2.6861	<0.0001
<i>lgcos int</i>	N/A	1.3249	0.2551	<0.0001
<i>lgma aadt</i>	N/A	-0.6556	0.2288	0.0042
<i>lin Angle</i>	N/A	0.0133	0.0041	0.0014
Dispersion	N/A	0.5150	0.0457	—
Goodness-of-fit parameters: AIC (smaller is better)	2,614.5293	—	—	—
Goodness-of-fit parameters: BIC (smaller is better)	2,634.7780	—	—	—

—No data available.

N/A = not applicable.

Additional crash-prediction models were developed for four-leg intersections using the OH dataset. The model fit statistics for these models are included in appendix E. In total, five different four-leg models were developed using the OH data.

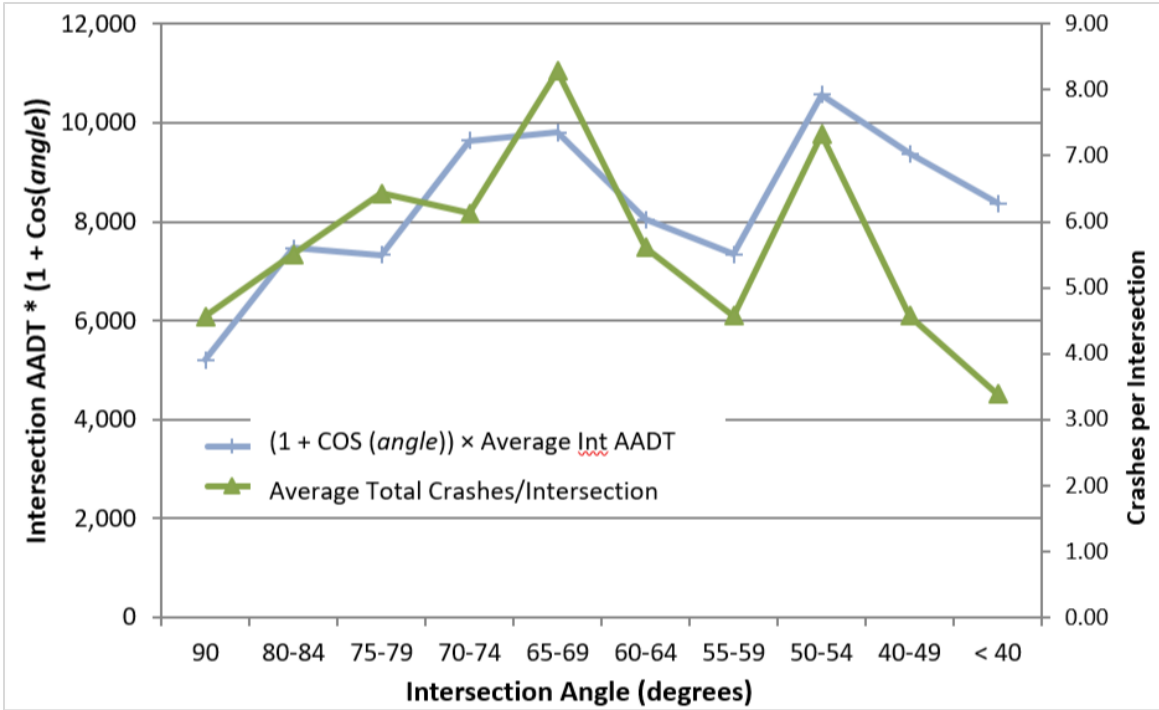
Total Crashes for Three-Leg Intersections

For the MN dataset, the base models revealed that the variable for intersection angles was not significant. From the plot of crash rate (per 100 million entering vehicles) versus intersection angle category in figure 16 and figure 18, it is apparent that this is not a monotonic relationship. For all three-leg intersections (rural and urban combined), the highest crash rates occurred in the categories of 55–59 degrees and less than 40 degrees. Crash rates for intersections with angles between 70–84 degrees were less than the crash rates for right-angle intersections. Similar to what was done for four-leg intersections, a more flexible form model 1 was desired that better replicated raw data. Recall that the final term chosen for the four-leg intersections was $1 + \cos(\text{angle})$. For right-angle intersections, the value of the function becomes 1.0 as the $\cos(90 \text{ degrees})$ equals 0.0. As the intersection angle decreases, the value of the function increases.

One plot (figure 28) shows the functional form when multiplied by the average intersection AADT values for three-leg intersections within the angle categories, while the other plot, figure 29, shows the average number of total crashes per intersection for three-leg intersections across the same categories. The patterns of peaks and valleys in the two lines across the range of intersection angles are very similar. The correlation coefficient ($r = 0.385$) indicates a moderate association.

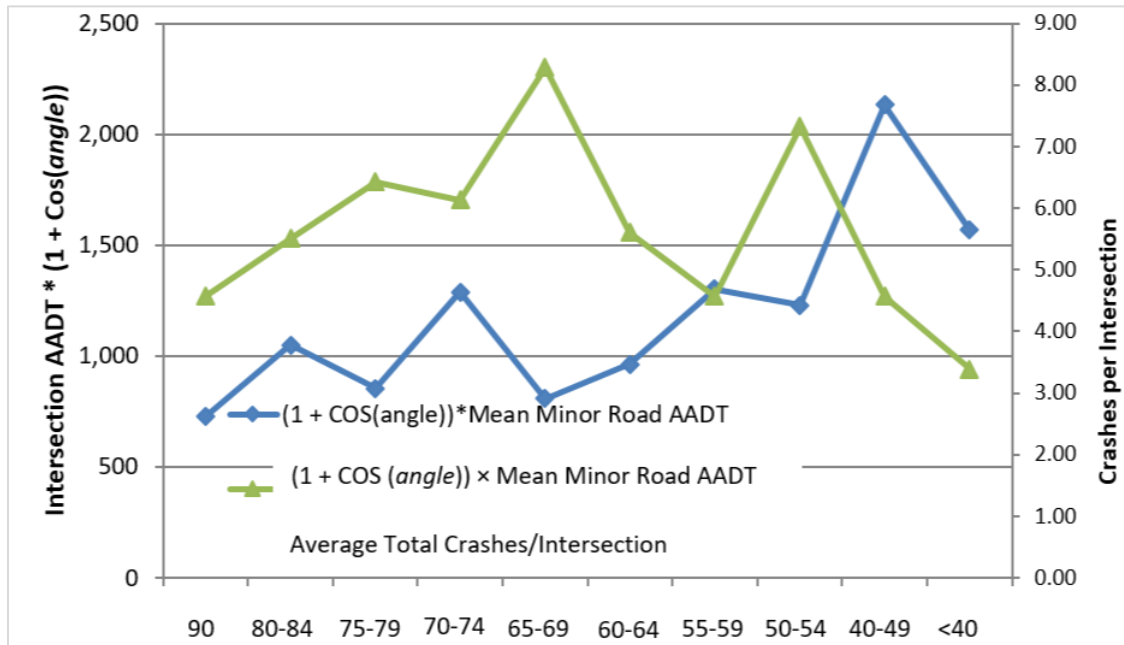
Figure 29 shows two lines. One line is the plot of $1 + \cos(\text{angle})$ multiplied by the average minor road AADT values from the angle categories. The other line is the plot of the average number of total crashes per intersection for three-leg intersections. The patterns exhibited for the two lines across the range of intersection angles are less similar for minor road AADT than for intersection AADT. The strength of association ($r = 0.281$) between this variable and crashes is much smaller when compared to the same variable comparison for four-leg intersections ($r = 0.478$).

However, the strength of the association between intersection AADT and crashes was strong enough to justify inclusion of the variable $1 + \cos(\text{angle})$ into the model.



Source: FHWA.

Figure 28. Graph. Average total crashes per intersection for all three-leg intersections in MN and functional form of $[(1 + \cos(\text{angle})) \times \text{intersection AADT}]$ as distributed across the range of intersection angles.



Source: FHWA.

Figure 29. Graph. Average total crashes per intersection for all three-leg intersections in MN and functional form of $[(1 + \cos(\text{angle})) \times \text{minor road AADT}]$ as distributed across the range of intersection angles.

The results from flexible form model 1 are shown in table 41. Intersection angle (*min_angle*) is now included in this model and is significant with a *p*-value of <0.0001. The estimate for this variable is 0.011. The additional variables incorporating the $1 + \cos(\text{angle})$ terms and AADT are both significant with a *p*-value of <0.0001. The sum of the estimates for these two parameters is 1.0707.

Table 41. Flexible form model 1 results for total crashes at all three-leg intersections for MN.

Parameter Description	Estimate	Standard Error	Lower 95% CL	Upper 95% CL	Chi-Square	Statistical Significance
Intercept	-10.4104	0.2515	-10.9034	-9.9175	1,713.46	<0.0001
<i>lgcos_int</i>	0.8717	0.0297	0.8135	0.9299	862.72	<0.0001
<i>lgcos_mi</i>	0.199	0.0265	0.1471	0.2509	56.47	<0.0001
<i>mi_int</i>	1.187	0.4819	0.2425	2.1314	6.07	0.0138
<i>ma_lane_wd0</i>	0.0087	0.0019	0.005	0.0124	21.16	<0.0001
<i>spec_env_cat</i> (0)	-0.2377	0.0601	-0.3555	-0.1199	15.63	<0.0001
<i>spec_env_cat</i> (1)	-0.3307	0.0514	-0.4315	-0.2299	41.34	<0.0001
<i>spec_env_cat</i> (2)	-0.5184	0.0542	-0.6246	-0.4121	91.46	<0.0001
<i>spec_env_cat</i> (3)	0	0	0	0	—	—
<i>min_angle</i>	0.011	0.001	0.009	0.0131	113.73	<0.0001
Dispersion	0.6031	0.041	0.5279	0.689	—	—
Goodness-of-fit parameters: AIC (smaller is better)	14,289	—	—	—	—	—
Goodness-of-fit parameters: BIC (smaller is better)	14,358	—	—	—	—	—

—No data available.

As with the four-leg intersections, disaggregated three-leg intersection SPFs were developed using OH data. Total rural three-leg model specifications are shown in table 42. Flexible form model 1 was used for this dataset because the AIC value for that model (23,489.2110) was slightly smaller than that of the Hoerl Curve (23,492.2450). Several variables were retained in this model because of the large sample size. In addition to the *lgcos_int*, *lgcos_mi*, and *min_angle* terms required for flexible form model 1, *lgma_aadt*, *ma_division*, and *ma_rodwycls_cat* were retained in the model as explanatory variables. The large sample size also benefitted the angle categories, allowing the model not to be truncated for smaller-angle measures.

Table 42. Model fit statistics for OH for rural three-leg all intersections.

Parameter Description	Category	Estimate	Standard Error	Statistical Significance
Intercept	N/A	-16.0384	1.5532	<0.0001
<i>lgcos int</i>	N/A	1.5072	0.1675	<0.0001
<i>llgcos mi</i>	N/A	0.0941	0.0286	0.0010
<i>lgma aadt</i>	N/A	-0.6397	0.1440	<0.0001
<i>min angle</i>	N/A	0.0139	0.0017	<0.0001
<i>ma division</i>	Divided	-0.4365	0.1339	0.0011
<i>ma division</i>	Undivided	Base category	—	—
<i>ma rodwycls cat</i>	Local	-0.1220	0.1223	0.3182
<i>ma rodwycls cat</i>	Major Collector	0.1476	0.0462	0.0014
<i>ma rodwycls cat</i>	Minor Arterial	0.0561	0.0459	0.2217
<i>ma rodwycls cat</i>	Minor Collector	0.0843	0.0809	0.2973
<i>ma rodwycls cat</i>	Principal Arterial	Base category	—	—
Dispersion	N/A	0.4426	0.0188	—
Goodness-of-fit parameters: AIC (smaller is better)	23,489.2110	—	—	—
Goodness-of-fit parameters: BIC (smaller is better)	23,564.5241	—	—	—

—No data available.

N/A = not applicable.

A model was also developed for the total urban three-leg intersection subset. A partial flexible form model 1 that excluded the *lgcos mi* variable provided the best fit; the Hoerl Curve was unable to fit the data. The statistically significant variables in the model included *lgcos int*, *min angle*, and *ma division*. All angle categories greater than 10 degrees were sufficiently populated for this dataset.

Table 43. Model fit statistics for OH for urban three-leg, all intersections.

Parameter Description	Category	Estimate	Standard Error	Statistical Significance
Intercept	N/A	-10.0343	0.3837	<0.0001
<i>lgcos int</i>	N/A	1.0339	0.0382	<0.0001
<i>min angle</i>	N/A	0.0059	0.0014	<0.0001
<i>ma division</i>	Divided	-0.4967	0.1450	0.0006
<i>ma division</i>	Undivided	Base category	—	—
Dispersion	N/A	0.5668	0.0286	—
Goodness-of-fit parameter: AIC (smaller is better)	8,625.2848	—	—	—
Goodness-of-fit parameter: BIC (smaller is better)	8,652.4205	—	—	—

—No data available.

N/A = not applicable.

Several other model forms were attempted, including an interaction term and the base term, but the research team found for most models that flexible form model 1 provided the best functional form fit, so that model, or a partial form of it, was used to develop most of the CMFunctions to be shown. One other functional form was attempted while comparing the MN results to those in

OH: the Hoerl Curve. The derivation of this model is presented in greater detail in the next section. Further model derivations for specific intersection types are shown in appendix E.

DEVELOPMENT OF CMFs AND FUNCTIONS

One of the principal goals of this study was to develop CMFs or CMFunctions that could be used by road-safety professionals to assess the change in crashes associated with changes in intersection angles. The coefficients from the NB models were used to derive the CMFunctions and show the relationship between crashes and intersection angles. The CMFunctions derived from the base models include a single regression coefficient applied to the intersection angle variable and is, therefore, a simple CMFunction. The CMFunctions from the flexible form and interaction models include multiple regression coefficients applied to different forms of the variable intersection angle as well as AADT variables. Many of the comparative plots simply use CMFunction value on the vertical axis, which is consistent with the presentation of the CMFs in the HSM.⁽²⁴⁾

The remainder of the discussion in this section of the report focuses on intersection angle CMFunctions developed for total crashes for four-leg and three-leg intersections. Intersection angles in all CMFunctions were defined as the smallest angle between any two adjacent legs at an intersection. This angle (in degrees) was denoted as α in the CMFunction equations in figure 30 and figure 31. Additional CMFunctions were developed for injury crashes and PDO crashes at four-leg intersections. All CMFunctions derived are shown in table 45.

Each CMFunction developed had a nominal value of 1.0 for the base condition of intersection angle equal to 90 degrees. A CMFunction with a value greater than 1.0 indicated more crashes would be expected when compared to the base condition. A CMFunction with a value less than 1.0 indicated fewer crashes would be expected when compared to the base condition. Each CMFunction was calculated using the equation shown in figure 30.

$$CMF(\text{model form}) = F(\alpha)/F(90)$$

Figure 30. Equation. CMFunction calculation.

Where:

CMF = crash modification factor or function for a specific model form.

$F(\alpha)$ = effectiveness factor for intersection angle α , expressed in degrees.

$F(90)$ = effectiveness factor for intersection angle of 90 degrees.

This equation in figure 30 provides the CMF associated with changing the intersection angle from 90 degrees to angle α , which is less than 90 degrees. This was mainly done for convenience. However, agencies would be interested in doing the opposite (i.e., converting from an intersection angle α to 90 degrees), and the safety effect associated with this change would be the inverse of the value from this equation.

The calculations in the remainder of the report are expressed as a CMFunction for each model form, with an understanding that the CMFunction values produced are normed to the nominal base condition of intersection angles equal to 90 degrees. The conditions under which each

developed CMFunction is applicable are clearly indicated in the appropriate figures and tables in the remainder of this report. These conditions include crash level (i.e., total, injury, PDO), intersection level (i.e., all, rural, urban), and number of lanes (i.e., two-lane, multilane).

Two different functional forms derived from figure 23, figure 24, figure 28, and figure 29 and the SPFs presented in Safety-Prediction Models were used to develop each of the CMFunctions presented in the next section. The first functional form, flexible form model 1, was previously introduced to account for the non-log-linear relationship between traffic volume and intersection angle. Its functional form is shown in figure 31.

$$CMF(\text{flex1}) = \frac{\{EXP(\beta_1 \alpha) \times [(1 + \cos(\alpha))^{(\beta_2 + \beta_3)}]\}}{\{EXP(\beta_1 90) \times [1 + \cos(90)]^{(\beta_2 + \beta_3)}\}} \\ = EXP[(\beta_1(\alpha - 90))] \times [(1 + \cos(\alpha))^{(\beta_2 + \beta_3)}]$$

Figure 31. Equation. CMFunction flexible form model 1 calculation for total crashes at all four-leg intersections.

Where:

- α = intersection angle, expressed in degrees.
- β_1 = coefficient estimate for intersection angle.
- β_2 = coefficient estimate for *lgcos_int*.
- β_3 = coefficient estimate for *lgcos_mi*.

The only noteworthy difference between the use of flexible form model 1 for the MN data and the OH data is that certain OH intersection types required a partial form of the equation that excluded the *lgcos_mi* term to fit the data. In these cases, the estimate of the *lgcos_int* term typically compensated for the lack of a *lgcos_mi* term and was sufficient for capturing the curved shape of the data. The key difference between the Hoerl Curve functional form and the flexible form models is the use of both a minimum angle and log minimum angle to capture a curve shape. The Hoerl curve equation is shown in figure 32.

$$CMF(\text{Hoerl}) = EXP[\beta_1 \times \alpha + \beta_2 \times \ln(\alpha)]$$

Figure 32. Equation. General form of Hoerl Curve.

Where:

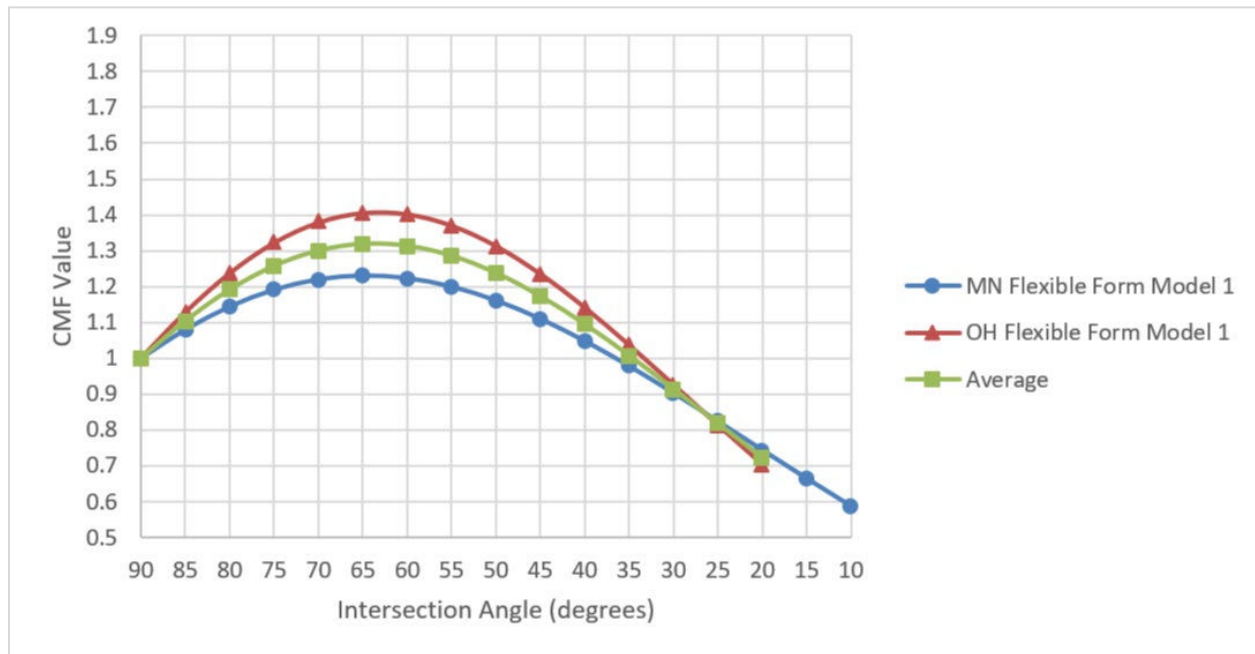
- β_1 = NB estimate for minimum angle variable.
- β_2 = NB estimate for natural log of minimum angle.

This section shows the predicted CMFunction for each of the OH intersection types compared to the final model selected for each of the MN intersection types. All CMFunctions shown are for total crashes. Where applicable, average curves were developed for the OH and MN data. These average curves account for the occasionally conflicting minimum angle identifications of the two States. It is encouraging that, in most cases, the shapes of the CMFunctions from the two States are very similar. Hence, the research team thought that taking the average of the curves was a reasonable option.

In each figure, the intersection angle axis refers to the minimum angle of each intersection used to identify that intersection's skew. For example, an intersection with a minimum angle equal to 50 degrees would be considered to have an intersection angle of 50 degrees.

All Rural Four-Leg CMFunctions

Figure 33 shows a comparison between the MN and OH total rural four-leg CMFunction for total crashes. The MN curve predicts slightly lower CMFunction values for nearly all angle categories than the OH curve, but both peak at the same minimum angle. The minimum angle at which the CMFunction values peak for both the OH dataset and the MN dataset is 65 degrees. This peak is also reflected in the average CMFunction. The OH CMFunction inclines and declines more rapidly than the MN curve, eventually predicting a lower CMFunction value than the MN curve between 30 degrees and 10 degrees. Both OH and average curves are truncated at 20 degrees because of a small sample size below this point. Both the MN and OH curves were developed using flexible form model 1.

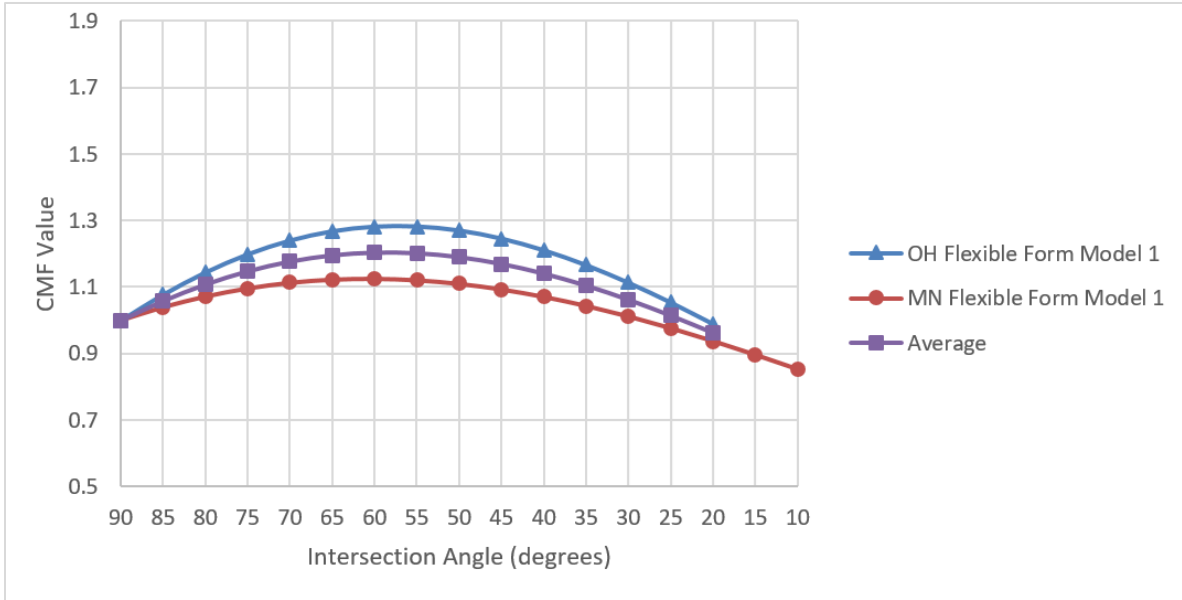


Source: FHWA.

Figure 33. Graph. CMF for all rural four-leg intersections.

Rural Four-Leg Two-Lane CMFunctions

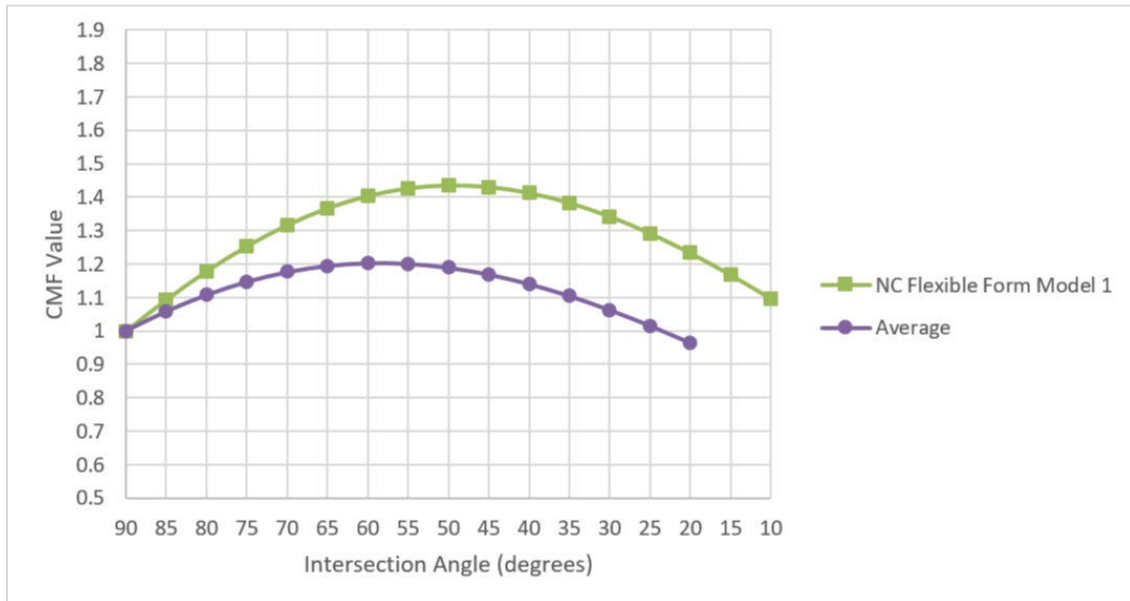
The CMFunctions for total crashes on rural four-leg intersections with two-lane major roadways are shown in figure 34. As with the CMFunctions for total rural four-leg intersections, the OH curve predicts more crashes than the MN curve, with nearly 20 percent difference between the two at their peak values. The OH curve peaks at 55 degrees, and the MN curve peaks at 60 degrees. The OH dataset was truncated at 20 degrees; therefore, the average curve does not show predictions for angles below this measure. Although the OH curve only dips below a CMFunction value of 1 at approximately 20 degrees, the MN curve shows a potential crash-reduction effect for minimum angles below 30 degrees.



Source: FHWA.

Figure 34. Graph. CMFunctions for rural four-leg two-lane intersections.

During this analysis, a small sample of intersection data were acquired from facilities in North Carolina (NC). Although this dataset was too small to provide an adequate comparison for all roadway types, a flexible form model 1 equation was derived for rural four-leg two-lane intersections. This CMFunction peaked at 50 degrees and predicted higher CMFunction values than either of the other two State datasets or the average curve (which does not include data from NC); however, it does verify the shape of the CMFunction.

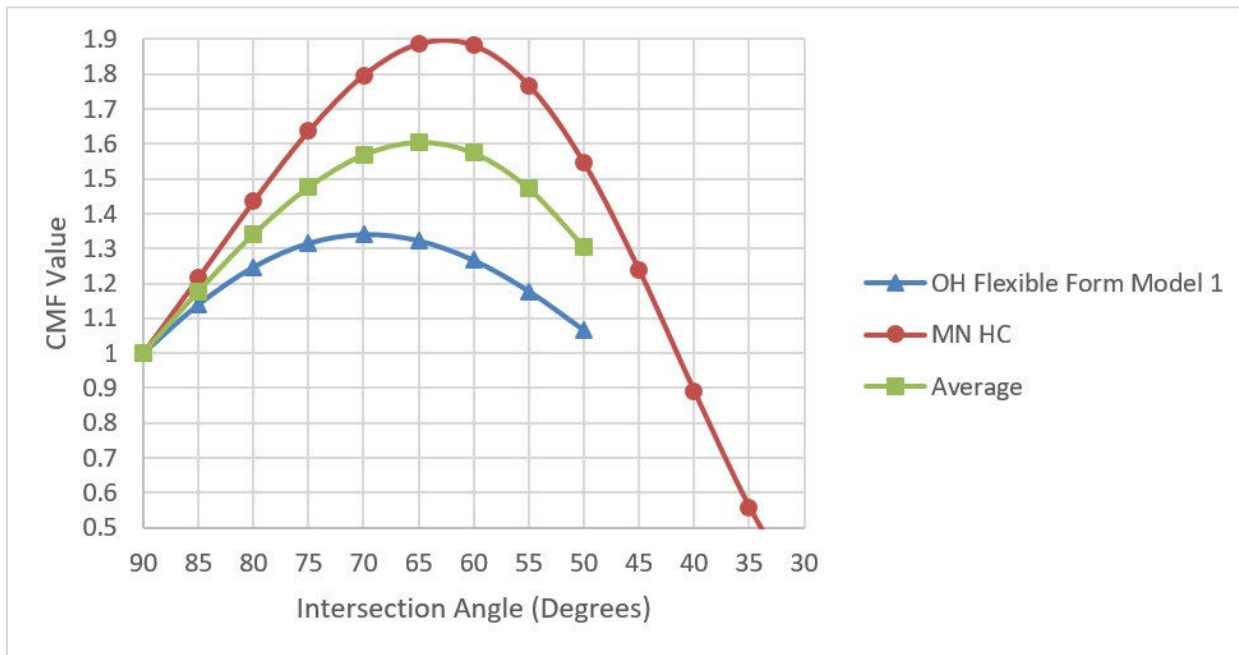


Source: FHWA.

Figure 35. Graph. CMFunctions for rural four-leg two-lane intersections with NC data.

Rural Four-Leg Multilane CMFunctions

For comparison, a Hoerl Curve model was developed for MN data for rural four-leg intersections with multilane major-road approaches. This model had comparably low AIC and BIC values and allowed for comparison between the OH data and the MN data. This MN CMFunction developed using the Hoerl Curve predicts more crashes at each intersection-angle category than the OH CMFunction, which was developed using flexible form model 1. The MN CMFunction, which peaks at 65 degrees, predicts an increase in total crashes at this facility type by 88 percent. Comparatively, the OH CMFunction, which peaks at 70 degrees, predicts only a 34 percent increase in crashes at this minimum angle. The OH function and the average function, which follows the shape of the OH function, are both truncated at 50 degrees due to a small number of sample sites below this. The inclines and declines of the MN function are sharper than those of the OH function; the percentage of predicted crashes changed by approximately 20 percent with each 5-degree change in minimum angle. The MN function also shows a protective effect on crashes below 40 degrees. Although this MN function predicts higher CMFunction values than the OH function predicts, this result is not consistent with the other intersection types. The high MN values may be due to either some inherent population differences between the two States or some other bias introduced into the data-selection process. Still, the functions for both States follow roughly the same shape.



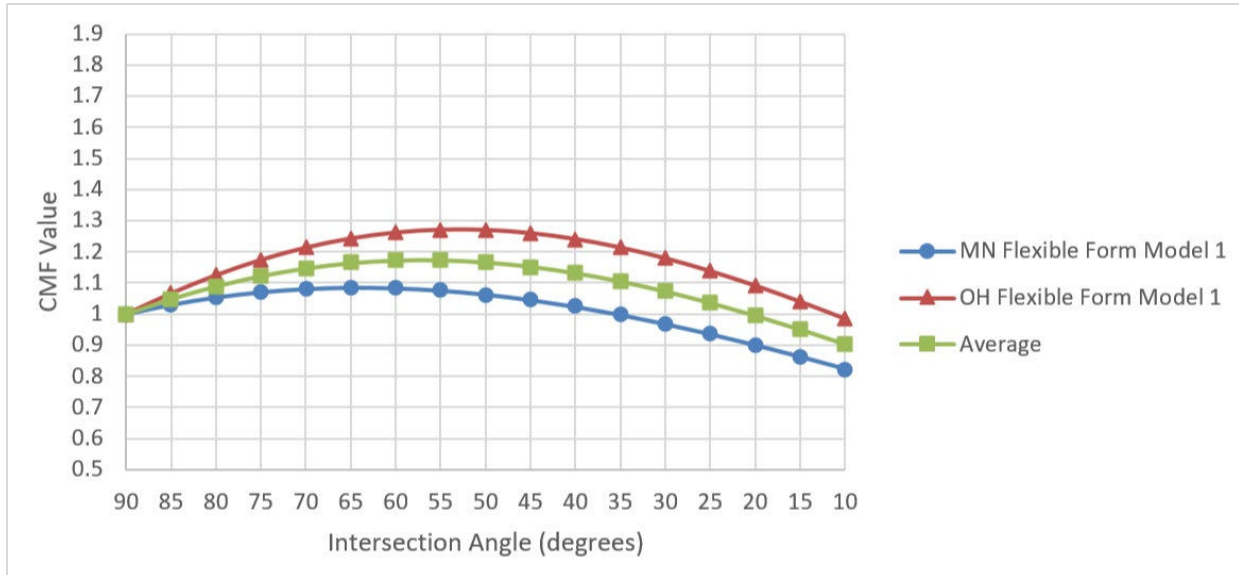
Source: FHWA.

Figure 36. Graph. CMFunctions for rural four-leg multilane intersections.

All Rural Three-Leg CMFunctions

The CMFunctions for total crashes at all rural three-leg intersections are shown in figure 37. As shown in the figure, the OH CMFunction predicts more crashes per intersection angle than the MN curve predicted; the OH CMFunction shows an increase or decrease in crashes of roughly five percent per five degrees. The MN CMFunction is flatter and shows a reduction in crashes

for minimum angles below 35 degrees. Both CMF curves were developed using flexible form model 1, but the curves peak at slightly different angles. The OH curve peaks at 55 degrees, and the MN curve peaks at 65 degrees. CMFunction values peak at 1.27 and 1.09 percent at these angle measures, respectively. The average curve peaks at 55 degrees like the OH curve with a CMFunction value equal to 1.17.

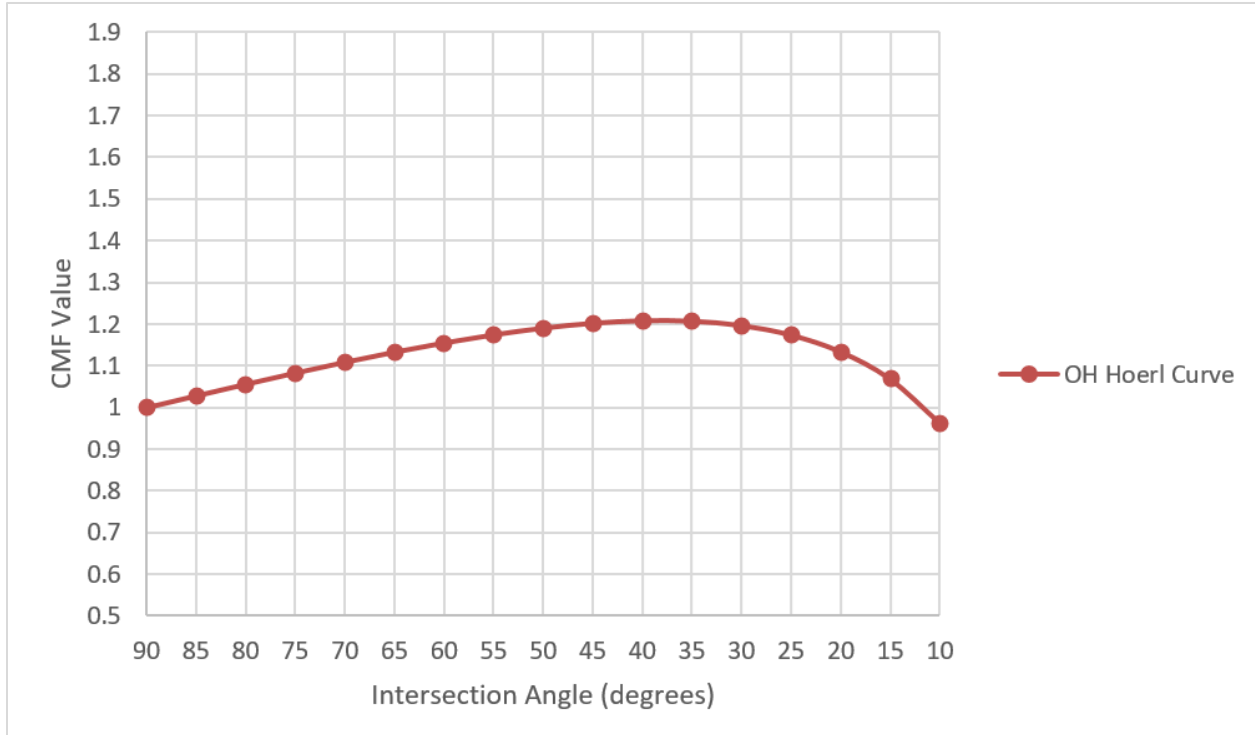


Source: FHWA.

Figure 37. Graph. CMFunctions for rural three-leg total intersections.

Rural Three-Leg Two-Lane CMFunctions

The CMFunction for rural three-leg intersections with two-lane major approaches is shown in figure 38. Due to a lack of data, only a single curve for the OH data could be derived. This curve differs from many of the other CMFunctions because it was derived using the Hoerl Curve equation. The curve also shows lower variation in CMFunction value than many of the other CMFunctions developed for other intersection types. The CMFunction value only changes approximately 10 percent between 90 degrees and 70 degrees. The curve peaks at 40 degrees at a CMFunction value of 1.21. It then declines quickly, as the CMFunction value decreases by almost 10 percent over 10 degrees. There is a protective effect for a minimum angle of 10 degrees, and no angle measures are truncated from the model.

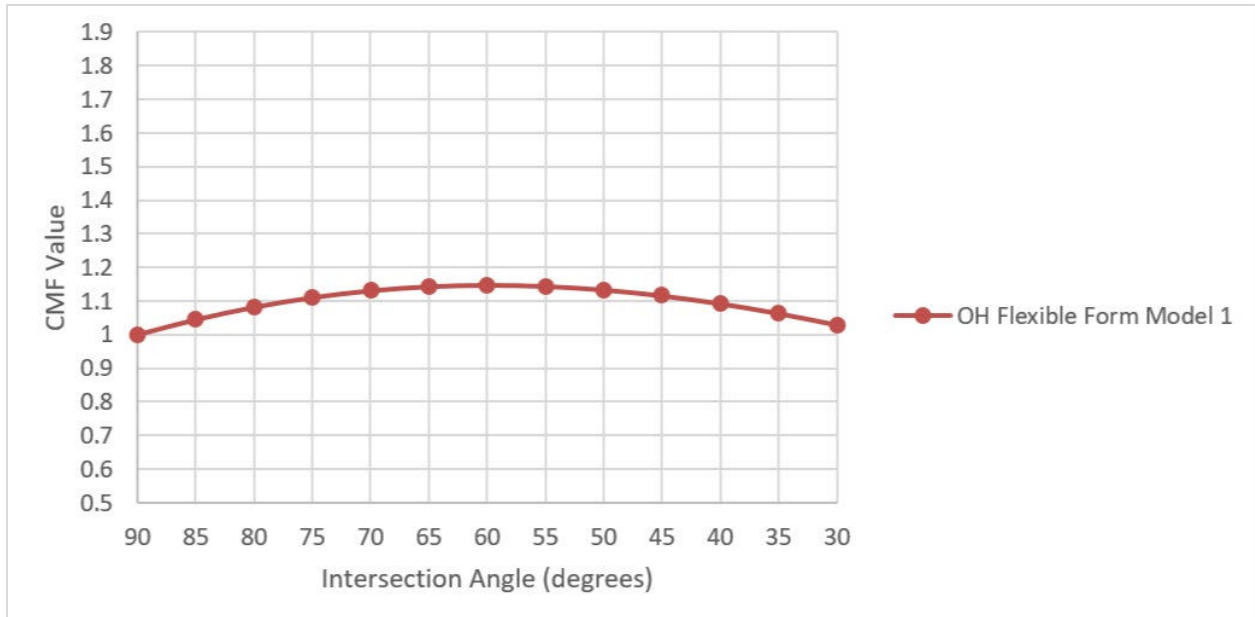


Source: FHWA.

Figure 38. Graph. CMFunction for rural three-leg two-lane intersections.

Total Urban Four-Leg CMFunctions

Only the OH data could be used to produce a CMFunction for all urban four-leg intersections. The CMFunction was developed using estimates from the flexible form model 1 for this facility type for OH data. The function is shown in figure 39. The curve is relatively symmetrical around the 60-degree peak and shows only minimal changes in CMFunction values between angle measurements. A 5-degree increase or decrease in minimum angle resulted in only a 2- or 3-percent change in the CMFunction value. The peak CMFunction value was approximately 1.15. The results were truncated at 30 degrees, but with the 3-percent decrease in CMFunction value on the declining tail of the curve, a protective effect may have been observed at low-angle measurements.

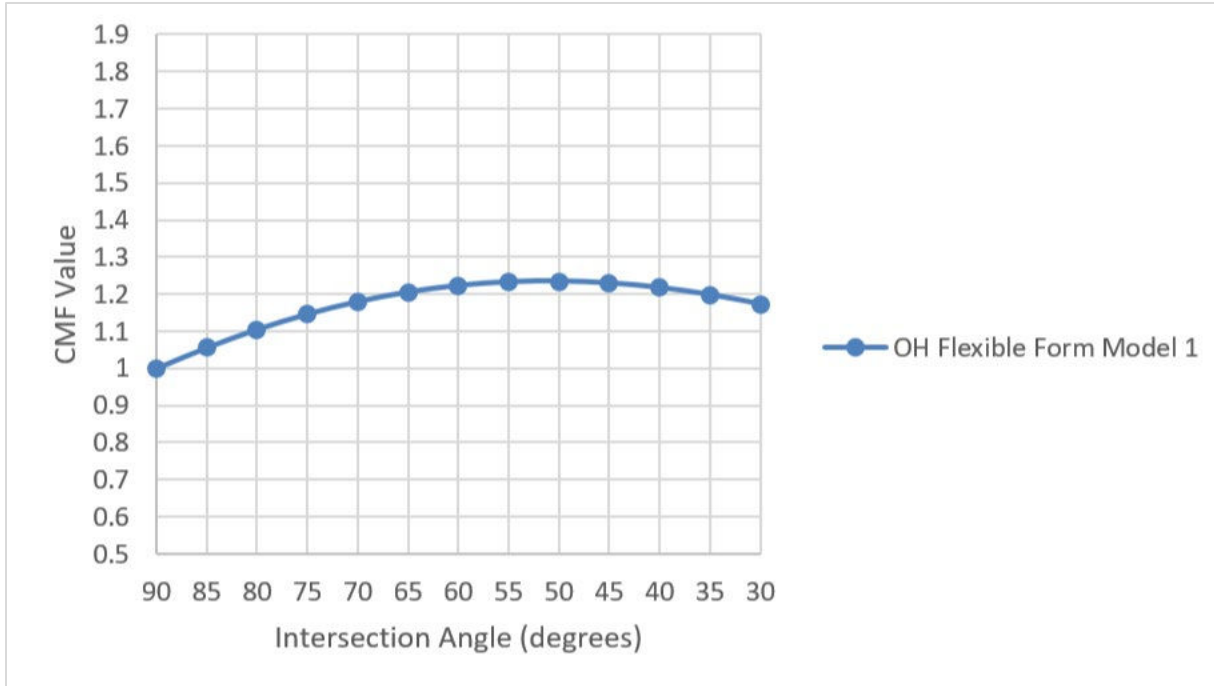


Source: FHWA.

Figure 39. Graph. CMFunction for urban four-leg total intersections.

Urban Four-Leg Two-Lane CMFunctions

The CMFunction for urban four-leg intersections with two-lane major approaches developed using data from OH is shown in figure 40. This curve was developed using the flexible form model 1. No CMFunction was developed using MN data; therefore, no average curve could be graphed. This curve's lowest CMFunction value corresponds to a minimum angle of 90 degrees, and the curve peaks at a minimum angle of 50 degrees with a CMFunction value equal to 1.23. The initial increase in CMFunction value per five-degree decrease in minimum angle is approximately 5 percent, but the curve slightly flattens at the top, which results in one-percent or two-percent changes in CMFunction value per 5-degree change in minimum angle. The curve is truncated at 30 degrees because of small sample size, and at this cutoff point, the CMFunction value is still roughly 17 percent greater than the value at 90 degrees.

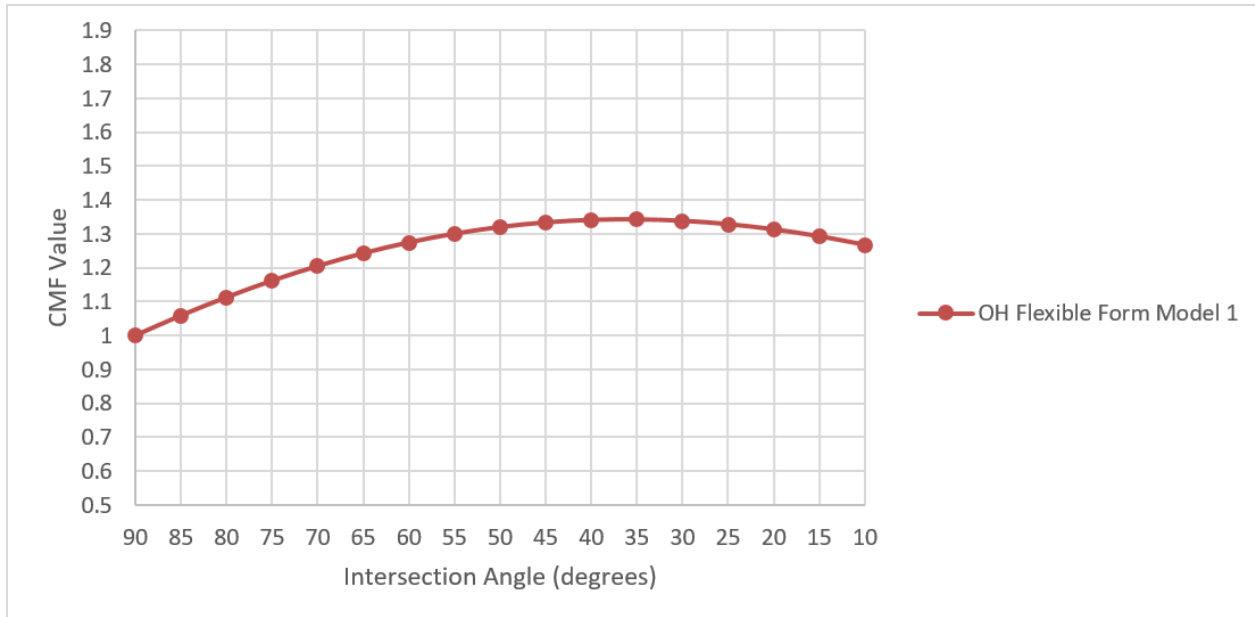


Source: FHWA.

Figure 40. Graph. CMFunction for urban four-leg two-lane intersections.

All Urban Three-Leg CMFunctions

The CMFunction for total crashes at all urban three-leg intersections is shown in figure 41. This curve was developed using the OH dataset and the flexible form model 1. This curve shows a consistent change of three percent to four percent in the CMFunction value per change in five degrees of the minimum angle. The lowest CMFunction value occurs at 90 degrees; the highest CMFunction value occurs at 35 degrees. This peak CMFunction value is 1.34, signifying a 34-percent increase in total crashes at this minimum angle. At 60 degrees, the CMFunction value is 27-percent higher than the base value at 90 degrees. There is no truncation in this dataset.

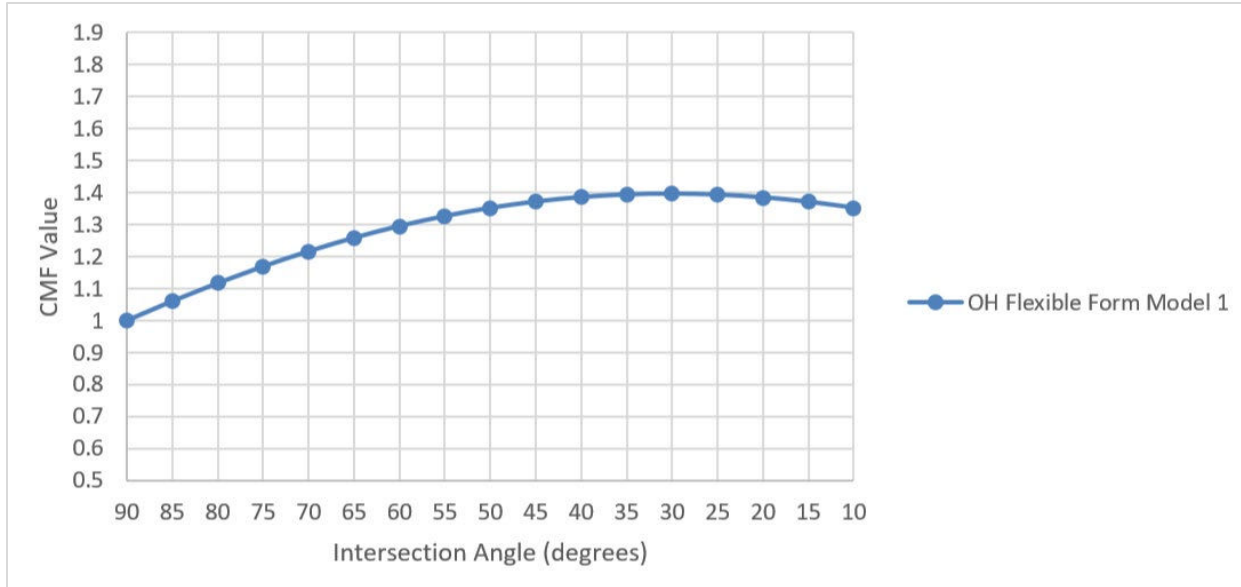


Source: FHWA.

Figure 41. Graph. CMFunction for urban three-leg total intersections.

Urban Three-Leg Two-Lane CMFunctions

The CMFunction for total crashes at urban three-leg intersections with two lanes on the major approach, as shown in figure 42, is similar to that of all urban three-leg intersections. This CMFunction was developed using only data from OH sites, and the model form used to derive the estimates was flexible form model 1. The lowest CMFunction value predicted by the curve occurs at 90 degrees, and the highest occurs at 30 degrees; the peak CMFunction value is approximately 1.40. The CMFunction value at 60 degrees is approximately 1.29. There is no truncation in this dataset.



Source: FHWA.

Figure 42. Graph. CMFunction for urban three-leg two-lane intersections.

CRITICAL ANGLE ASSESSMENT

In addition to the development of CMFunctions, the other objective of this research was to determine if there is a critical minimum angle at which safety is substantially diminished. Recall that the Green Book (page 9-27) currently recommends a minimum angle of 60 degrees: “...an angle of at least 60 degrees provides most of the benefits of a 90-degree intersection while reducing the right-of-way takings and construction costs often associated with providing a right-angle intersection.”⁽¹⁾ The purpose of this assessment was to determine if the policy requiring a minimum angle of 60 degrees is appropriate.

Table 44 shows intersection angles at which CMFunction values peaked for OH curves and MN curves and average curves, where applicable. It also shows the CMFunction value for these peak intersection angles. All CMFunction values shown are solely for total crashes. As seen in the table, the results of this analysis question the conventional wisdom of a minimum intersection angle of 60 degrees providing most of the benefits of a 90-degree intersection.⁽¹⁾ In fact, two of the CMFunctions developed showed crashes peaking at 60 degrees, namely for rural four-leg intersections with two lanes on the major approach and for all urban four-leg intersections. The CMFunction values at these two peaks were 1.20 and 1.15, respectively. Several other CMFunctions, specifically those for all rural four-leg intersections, rural four-leg intersections with more than two lanes on the major approach, all rural three-leg intersections, and urban four-leg intersections with two lanes on the major approach, peaked within five or ten degrees of this prescribed minimum CMFunction value. Based on these curves for total crashes, the design recommendation of a minimum angle of 60 degrees should be reconsidered.

Table 44. Peak CMFunction values and corresponding angles for total crashes for all intersection types.

Intersection Type	Peak Intersection Angle (OH, MN, Avg)	Peak CMF Value (OH, MN, Avg)
Rural four-leg total	65, 65, 65	1.40, 1.23, 1.32
Rural four-leg two-lane	55, 60, 60	1.13, 1.28, 1.20
Rural four-leg multilane	70, 65, 65	1.34, 1.89, 1.61
Rural three-leg total	55, 65, 55	1.27, 1.09, 1.17
Rural three-leg two-lane	40, —, —	1.21, —, —
Urban four-leg total	60, —, —	1.15, —, —
Urban four-leg two-lane	50, —, —	1.23
Urban three-leg total	35, —, —	1.34
Urban three-leg two-lane	30, —, —	1.40

—No data available.

Avg = average.

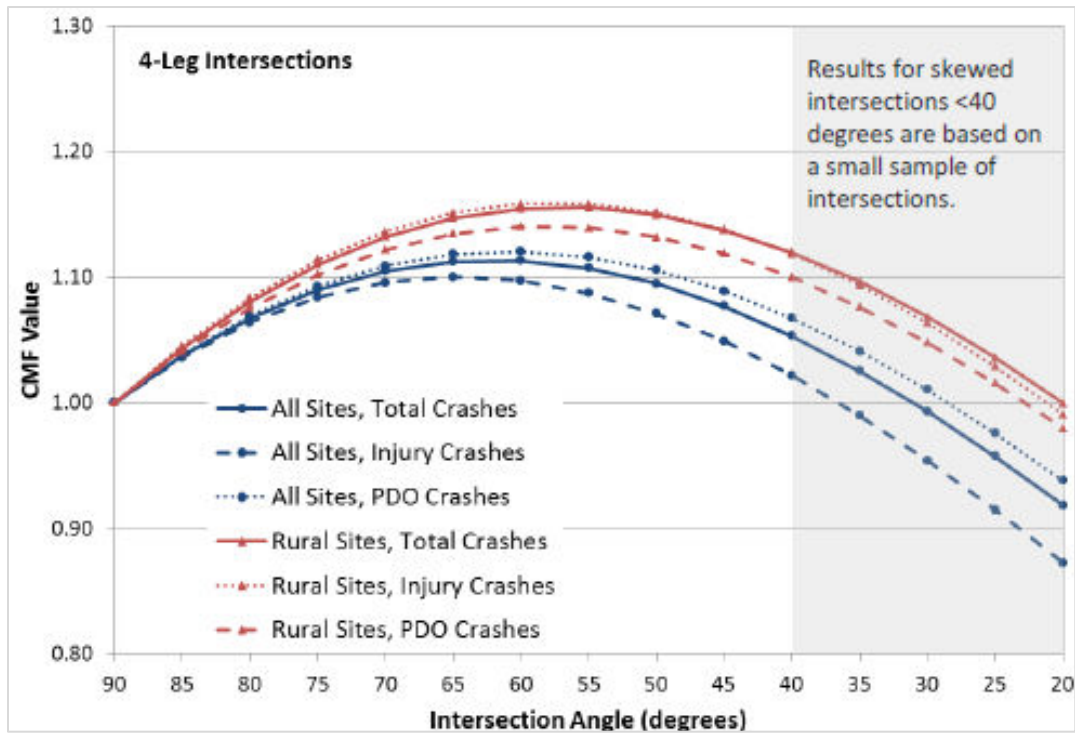
The CMFunction values for total crashes at different angle categories, as identified either by an average CMFunction or an OH function when other data were unavailable, are shown in table 45. Aside from rural three-leg intersections with two lanes on the major approach, total urban three-leg intersections, and urban three-leg intersections with two-lanes on the major approach, all intersection types for which CMFunction were developed for total crashes showed crashes peaking between 65 degrees and 50 degrees. These results question design recommendations that intersections with minimum angles equal to 60 degrees are suitable and have minimal impacts on safety. In fact, for at least one intersection type (rural four-leg multilane), the crashes at a 60-degree intersection angle were 57 percent higher than they were at a 90-degree angle. Although the intersection types with unshaded columns have CMFunctions that peaked at much lower intersection-angle values, most of these curves show fewer crashes at severe-angle skews or even protective effects for severe skews. These results confirm that remedial efforts may show the greatest safety benefits if targeted at intersections with minimum angles in the range of 65–50 degrees.

These results are also confirmed by the CMFunction analysis specifically conducted using MN data for crashes of different severities at four-leg rural intersections as reported in appendix F in table 117. As shown in figure 43 and figure 44, the largest crash reductions occur between the intersection angles of 80 and 55 degrees. Depending on the scenario, the maximum value occurs between 65 degrees and 55 degrees.

Table 45. CMFunction values derived from all models for total crashes at all intersections.

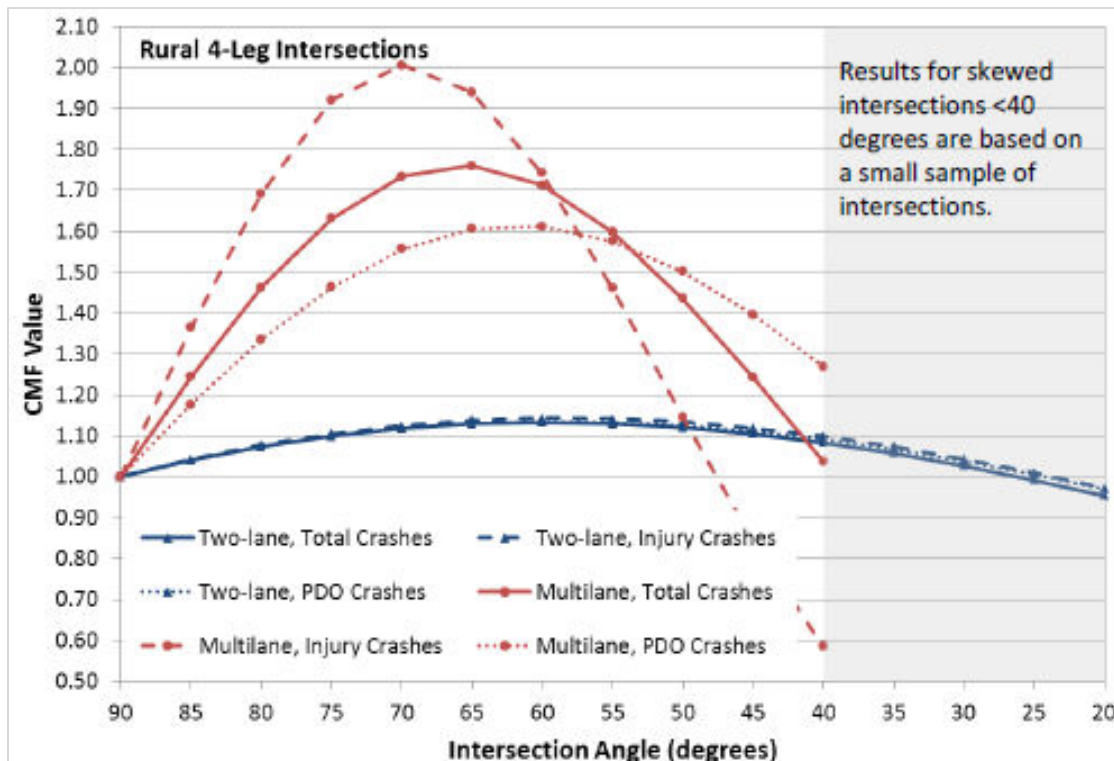
Intersection Scenario	80 Degrees	75 Degrees	70 Degrees	65 Degrees	60 Degrees	55 Degrees	50 Degrees
Rural four-leg total (avg)	1.19	1.26	1.30	1.32*	1.31	1.29	1.24
Rural four-leg two-lane (avg)	1.11	1.15	1.18	1.20*	1.20*	1.20*	1.19
Rural four-leg multilane (avg)	1.34	1.48	1.57	1.61*	1.57	1.47	1.31
Rural three-leg total (avg)	1.09	1.12	1.15	1.16	1.17*	1.17*	1.17*
Rural three-leg two-lane (OH)	1.06	1.08	1.11	1.13	1.15	1.17	1.19
Urban four-leg total (OH)	1.08	1.11	1.13	1.14	1.15*	1.14	1.13
Urban four-leg two lane (OH)	1.10	1.15	1.18	1.20	1.22	1.23*	1.23*
Urban three-leg total (OH)	1.11	1.16	1.20	1.214	1.27	1.30	1.32
Urban three-leg two-lane (OH)	1.12	1.17	1.22	1.26	1.29	1.33	1.35

*Peak CMFunction values for each facility type.
Avg = average.



Source: FHWA.

Figure 43. Graph. MN CMFs derived from the flexible form models for four-leg intersections, considering different severities.



Source: FHWA.

Figure 44. Graph. CMFunctions derived from the MN flexible form models for rural four-leg intersections with different severities.

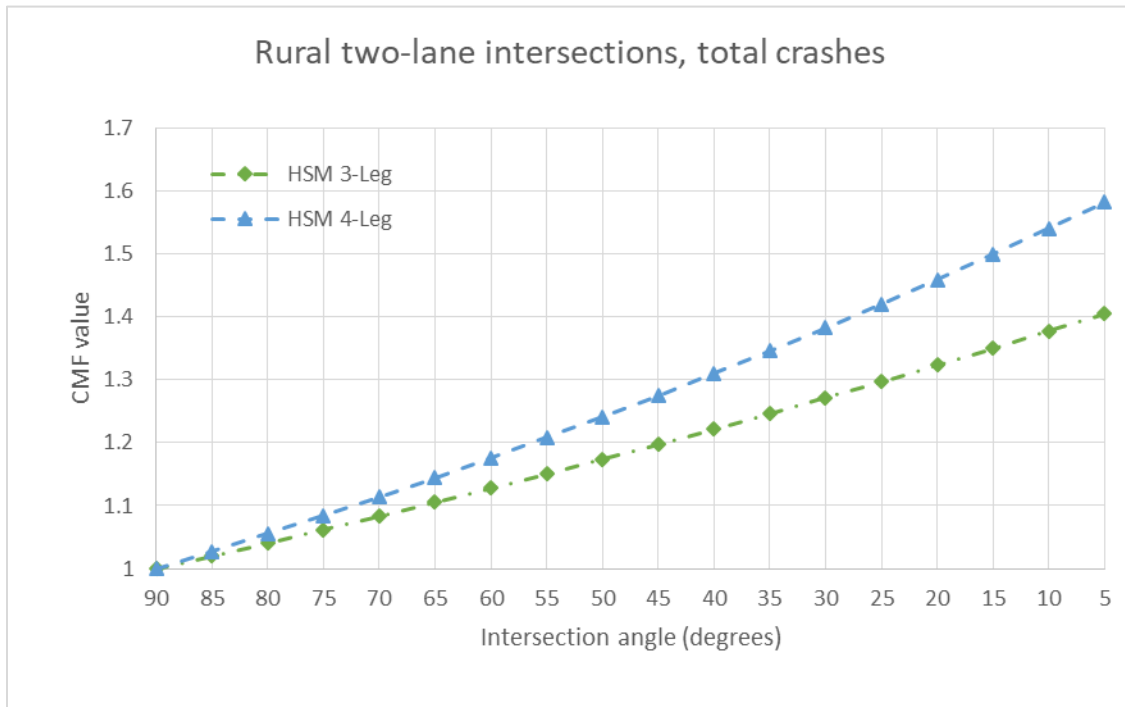
The fact that the largest angle at which the CMFunction values peak is 65 degrees warrants consideration of a critical minimum angle greater than 65 degrees if the goal is to select an angle at which safety is not substantially compromised in a right-angle intersection. Predictive models and CMFunctions indicate that any angle between 90 degrees and the current design policy value of 60 degrees will have a negative impact on safety; therefore, the policy of right-angle intersections being preferred still holds for both two-lane and multilane intersections.⁽¹⁾

For this study, the research team examined the intersection angle that should be established as a minimum for instances in which a right-angle intersection cannot be achieved. Selection of this angle was subjective and based on the level of diminished safety considered acceptable. For example, for rural four-leg intersections on two-lane roads, an intersection angle of 65 degrees resulted in a CMF no greater than 1.2. However, for the same intersection type, an intersection angle of at least 80 degrees was needed if the CMF was no greater than about 1.1. The research team suggests that the decision regarding the acceptable level of diminished safety should be made by a specific agency or a combination of AASHTO and FHWA. The practitioner can use the CMFunctions to determine the expected safety benefit of changing the intersection angle.

COMPARISON OF RESULTS TO PRIOR CMFs

Previously developed CMFs for intersection angle are few. As discussed in chapter 2, there are CMFs present in the HSM for total crashes at stop-controlled intersections on rural two-lane roads. These CMFs were derived from cross-sectional regression models in a manner similar to

the approach used in this research.⁽²⁵⁾ These CMFs were for use in chapter 10 of the HSM to develop safety predictions for rural two-lane roads. Separate CMFs were available for four-leg and three-leg intersections as shown in figure 45. Values were provided in the HSM for intersection angles between 5 degrees and 90 degrees. The predicted impact of intersection angle on safety was greater for four-leg intersections compared to three-leg intersections. Both CMFs were derived from exponential models and assume a log-linear relationship between crashes and intersection angle.



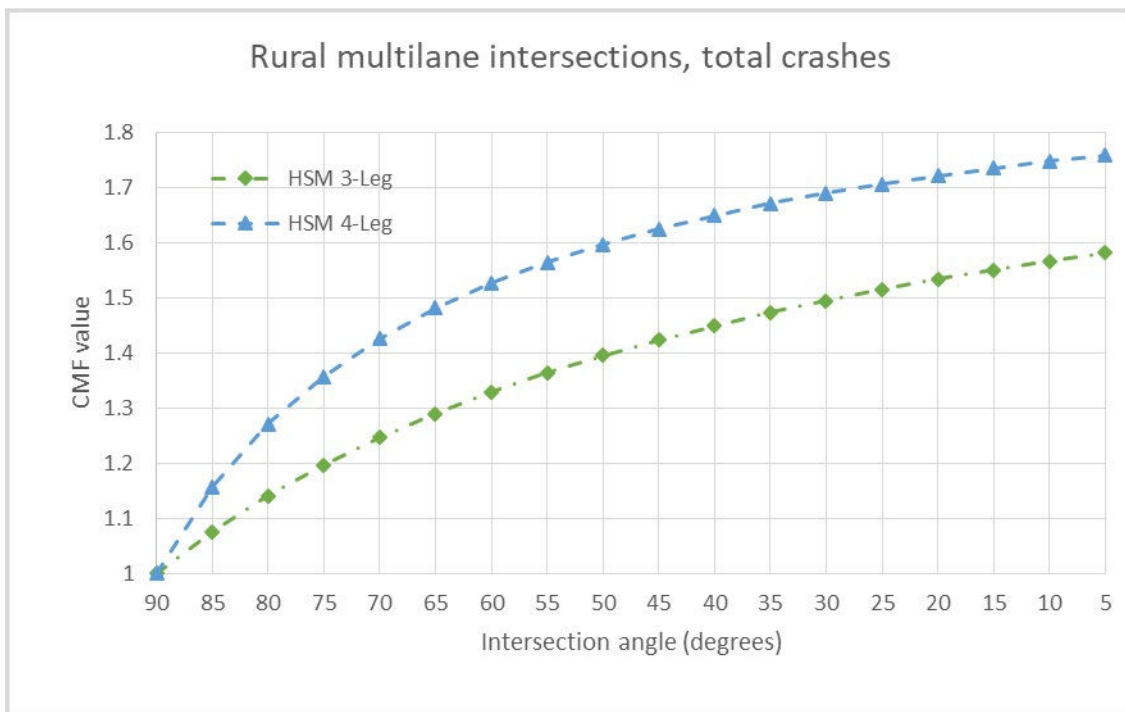
Source: FHWA.

Figure 45. Graph. CMFs from the HSM for total crashes at rural two-lane roadway intersections.⁽²⁴⁾

The HSM also includes CMFs to calculate the effects of intersection angle at rural multilane intersections. As noted in chapter 2, these CMFs were developed as part of an FHWA study to validate and calibrate the crash prediction statistical models for rural intersections within IHSDM.⁽²⁶⁾ Separate CMFs are available for four-leg and three-leg intersections. The range of intersection angles for which values are provided extend from 15 to 90 degrees. As shown in figure 45, the predicted effect of intersection angle on safety is greater for four-leg intersections compared to three-leg intersections.

Another model discussed in chapter 2 included a component for intersection angles.⁽²⁸⁾ After further review of the study, the research team determined it was not appropriate for comparison to the models of the current study. The model developed had a small sample size (29 skewed and 39 nonskewed intersections) and a limited range of traffic volumes on the major roadway (up to 5,200 vpd). The model was also for three- and four-leg intersections combined.

The first comparison made was for the CMFunctions developed for rural two-lane intersections. Figure 46 shows the HSM four-leg CMF and the recommended CMFunction from the current study. The CMFunction was developed by taking an average of the values predicted for the MN and OH datasets for total crashes at rural two-lane intersections. The recommended CMFunctions for both States were those developed from the flexible form model. The recommended study CMFunction produced values greater than the HSM function for angles between 60 and 90 degrees but lower values for angles less than 60 degrees. As previously noted, the HSM CMF also extended to a range that included a skew angle as small as five degrees and assumed a monotonic relationship between the CMF and intersection angle. However, the range of data available by angle of intersection at the study sites was not documented in the relevant research. As discussed in the remaining text of this section, data used for the CMFunction derived from the current study do not have this same range and there are specific recommendations for the lower end of the intersection-angle spectrum.



Source: FHWA.

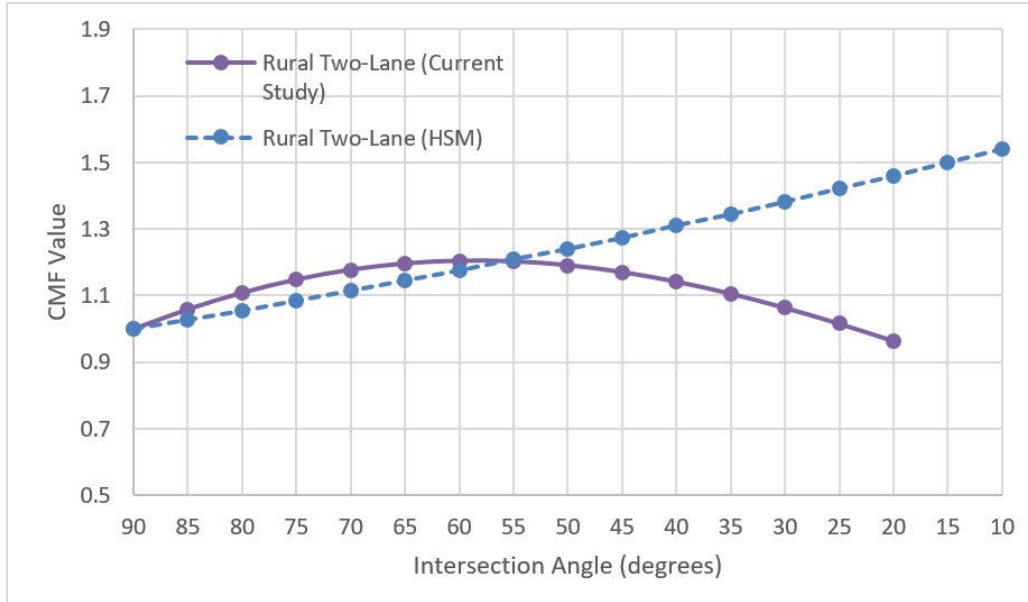
Figure 46. Graph. CMFs from the HSM for total crashes at rural multilane roadway intersections.⁽²⁴⁾

While both the current study CMFunction and the HSM CMF were derived from an NB regression model, there were differences in the methodology. The variables included in the model that produced the HSM CMF were required to be statistically significant at a significance level of 0.15 or less. Skew angle in that model had a *p*-value of 0.108. The comparative model from this study required all variables to be statistically significant at a significance level of 0.05 or less. Intersection angle in this model had a *p*-value less than 0.0001 for both MN and OH data. This difference in the statistically significant requirements can obviously affect the parameters included in the NB models and the regression coefficients of the derived CMFunctions. Regardless of the reasons, the base CMFunction from the current study produces comparable

values of the effect of intersection angle on safety for angles greater than 60 degrees and more conservative values for angles less than 60 degrees.

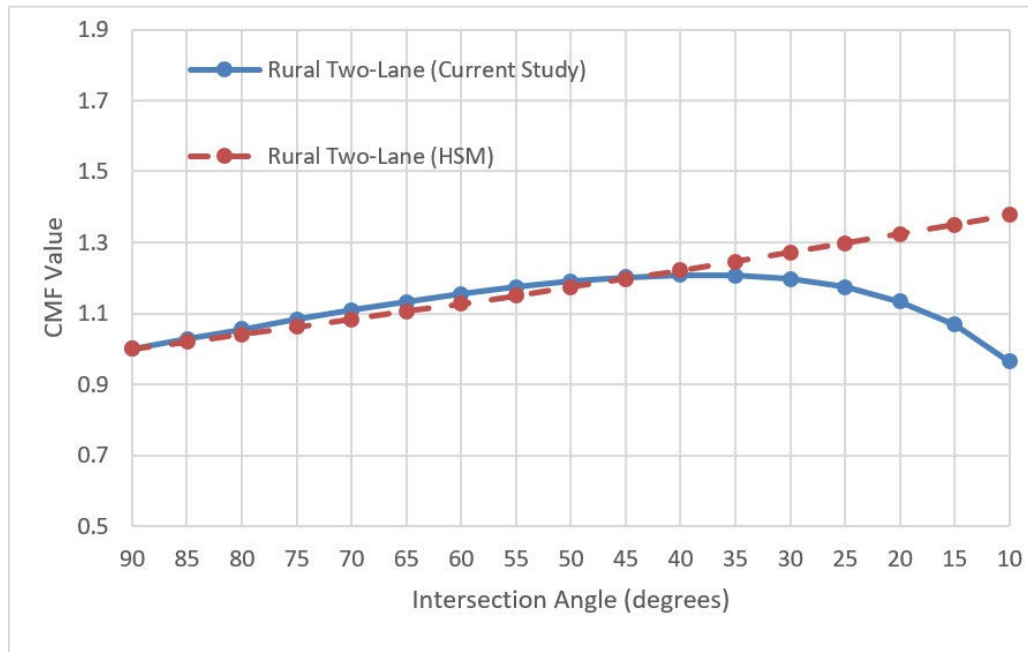
The CMFunction developed using OH data for the rural three-leg two-lane intersections also deviated from that prescribed in the HSM, as seen in figure 47 and figure 48. Between 90 degrees and 45 degrees, the two curves ran parallel and predicted nearly identical values. However, for an intersection angle less than 45 degrees, the HSM CMF estimated a much larger CMF value. The CMFunction developed using OH data followed an upward convex-curved shape while the HSM curve follows a monotonic relationship. Differences in statistical significance existed for the intersection-angle variable between the study used to develop the HSM curve and the study used to develop the OH curve. The p -value for the minimum-angle variable in the OH study was 0.0023. As with the rural four-leg two-lane intersections, the study curve was more conservative in predicted values at small intersection-angle measures.

The second comparison was for the CMFunctions developed for rural multilane intersections. Figure 49 shows the HSM four-leg CMF and the recommended average CMFunction from the current study for total crashes at rural multilane intersections. The recommended CMFunction was the average of the two curves developed using the flexible form model 1 for OH and the Hoerl Curve model for MN. There were obvious differences in the shape of these two functions. The CMFunction recommended by this study produced values much greater than the HSM function for angles between 60 and 90 degrees. At a peak of 65 degrees, CMFunction values from the current study began to decline. For intersection angles below approximately 62 degrees, the current study CMFunction produced values less than the values produced by the HSM CMF. The HSM CMF also extended to a range that included a skew angle as small as 15 degrees with an exponential relationship across all intersection angles. However, the range of data available by angle of intersection at the study sites was not documented in the relevant research. The data used for the CMFunction derived from the current study do not have this same range in MN and OH. There are specific recommendations for the lower end of the intersection angle spectrum, which are examined in the next section of this report.



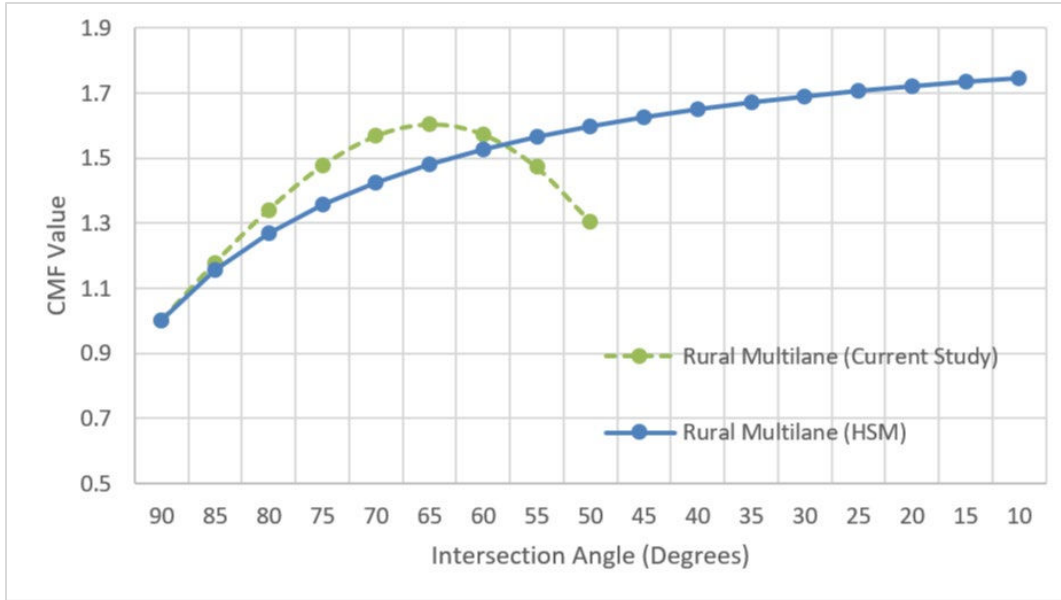
Source: FHWA.

Figure 47. Graph. CMFs from the current study and the HSM for total crashes at rural four-leg two-lane intersections.



Source: FHWA.

Figure 48. Graph. CMFs from the current study and the HSM for total crashes at rural three-leg two-lane intersections.

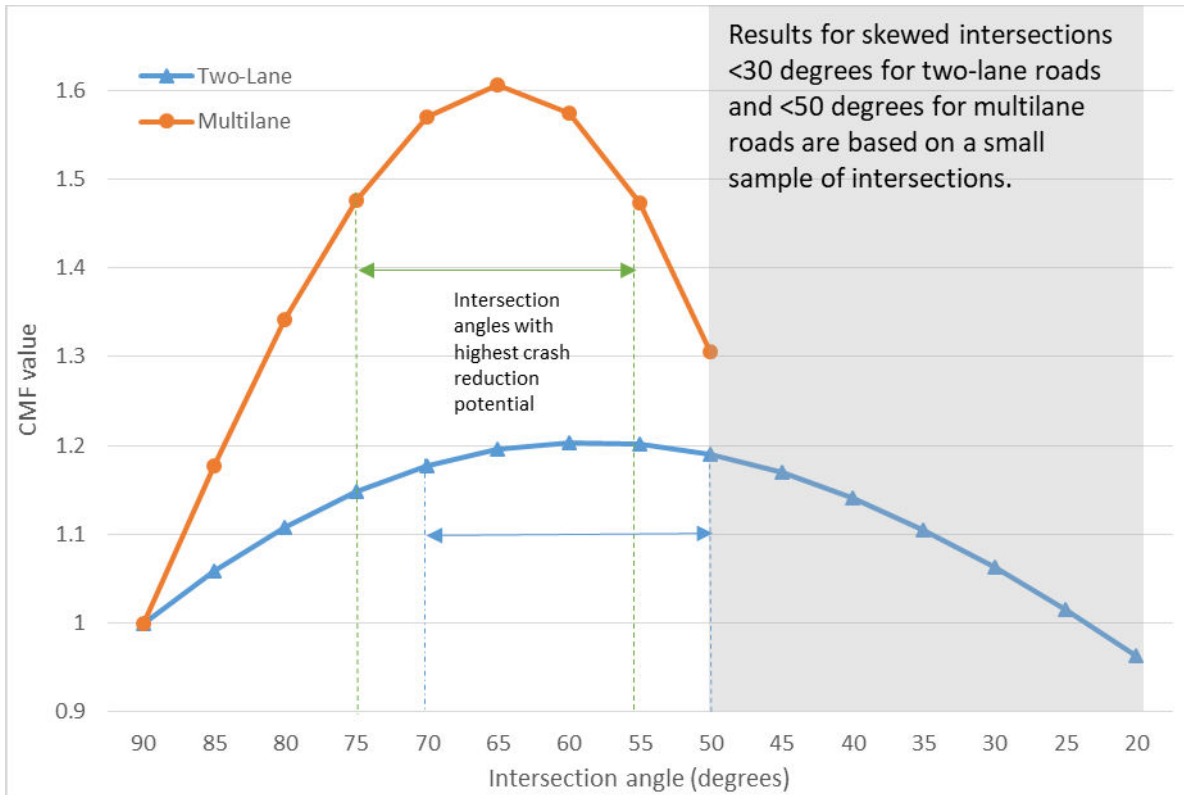


Source: FHWA.

Figure 49. Graph. CMFs from the current study and the HSM for total crashes at rural four-leg multilane intersections.

In summary, the CMFunctions for intersection angles derived from the models developed in the current study and those included in the current edition of the HSM have some differences regarding the range of intersection angles. The current study and HSM CMFs for rural four-leg two-lane intersections produced similar values for the range of angles between 90 and 60 degrees. The HSM CMF, however, continued to show a decrease in safety for intersections with angles below 60 degrees. Current research does not support this finding as indicated by the lower CMFunction values below 60 degrees. A similar finding was observed for rural three-leg two-lane roads, although the intersection angle at which findings of this research and the HSM CMF diverge is 45 degrees and lower. The rural multilane CMFunctions from the current study, compared to HSM CMFs, showed a more-pronounced effect of intersection angle on safety at locations with angles as small as five degrees. However, unlike HSM CMFs, the current study results did not show a continuing degradation in safety as a function of intersection angle as the angle continued to decrease.

The final point on the assessment of the critical angle focuses on the shape of the derived CMFunction and its meaning for practical applications. Prior to this study, the limited research attempting to relate crashes to intersection angles produced relationships that showed a continuous increase in crashes as the angle of the intersection decreased below 90 degrees. The CMFs currently included in the HSM indicate that this relationship existed from 90 degrees to an intersection angle of 5 degrees for rural two-lane intersections and 15 degrees for rural multilane intersections (figure 45 and figure 46). The results of this research produced a curvilinear relationship between crashes and intersection angle (figure 50).



Source: FHWA.

Figure 50. Graph. Crash-reduction potential based on CMFs for rural two-lane and multilane intersections.

One result of the shape of the CMF(flex) curve and CMF Hoerl Curve is the curve peaks for most intersection types between 50 and 65 degrees (table 45). Figure 50 shows the greatest potential for achieving crash reductions based on this CMF-angle relationship is to have intersections with intersecting angles on either side of this peak. For rural two-lane roads, the highest crash-reduction potential is between intersection angles of approximately 50 and 70 degrees. The two-lane CMFunction values in this range are at or greater than 1.15. For rural multilane roads, the highest crash-reduction potential falls between angles of approximately 55 and 75 degrees. The multilane CMFunction values in this range are at or greater than 1.45.

Acute angle intersections (less than 40 degrees) show reductions in crashes are much less than the high potential ranges previously addressed. The sample of intersections in this lower-angle range was limited in this study to the OH dataset. Certain subsets of the MN data also had low-angle truncations. Subsequently, the recommendations in the next chapter reflect this restriction in the data. Nonetheless, there were enough sites in the remainder of the angle spectrum for both States to have confidence in the shape of this relationship and the fact that there is a peak in crash reductions between 50 and 65 degrees followed by a lesser effect at more severe angles. The shape of the function is similar to the shape discovered in the raw crash data.

The reason for this shape is not fully understood. One possible explanation may be human behavior and an understanding by drivers that these locations with more acute angles require one to exercise additional caution. Another reason could be that many intersections in the lower

intersection-angle categories that had poor safety records had been improved over time. Thus, the safety performance for intersections that remain in these low-angle categories is better than the safety performance in the high-angle categories where systemically fewer improvements may have occurred over time. Finally, the results might also be an artifact of current policy. With 60 degrees as the current threshold for the minimum critical angle in many States, the focus of past interventions related to intersection-angle issues was on locations that fall below this threshold. The result of the last two possibilities may be a migration in high crash locations from locations with acute angles (less than 40 degrees) to locations in the new high potential range (50–75 degrees). Regardless of the reason, the results of this research indicate that there may be a greater benefit in addressing intersections with angles greater than 60 degrees as opposed to those with angles less than 60 degrees.

CHAPTER 6. SUMMARY AND CONCLUSIONS

SUMMARY

The preferred design for intersections includes adjacent legs that intersect at 90 degrees. However, there are occasions where physical constraints result in intersection angles less than 90 degrees, producing skewed intersections. These intersections create potential safety and operational problems for both motorists and nonmotorists. To date, the crash-based safety research on this issue has been limited.

A review of geometric design policies confirmed that there is consensus within the highway-design field that intersecting roadways should be aligned to meet at 90 degrees. There was also a common recognition of the safety and operational problems introduced for different modes of travel once an intersection becomes skewed. However, there are differences among these policies regarding the critical minimum angle: the angle at which consideration should be given to realigning the intersection or implementing additional traffic control measures. That angle currently ranges from 60 to 75 degrees, depending on the reference.

A review of the research literature revealed that there have been very few studies that attempted to define the safety relationship of intersection angle to crashes. One study that derived CMFs for intersection angle did so for rural two-lane roads only and assumes a monotonic relationship between crashes and intersection angle.⁽²⁵⁾ A second study derived intersection angle CMFs for rural multilane roads, assuming a similar relationship between crashes and the angle of the intersection.⁽²⁶⁾ The CMFs from both of these studies are included in the HSM.⁽²⁴⁾

Additional noncrash-based research has produced evidence that intersection angle can impact drivers and pedestrians whose physical capabilities have diminished. Older persons who have reduced flexibility may have difficulty turning their heads and necks to judge gaps in traffic at skewed intersections. Older or disabled pedestrians who walk at slower speeds will be exposed to traffic for a longer period of time at crossings that are lengthened as a result of the intersection angle. These research findings led to the critical minimum angle recommendation of 75 degrees in FHWA's *Highway Design Handbook for Older Drivers and Pedestrians* as a practice to accommodate age-related performance deficits.⁽⁶⁾

The objective of this study was to derive quantitative relationships between intersection angle and safety, where intersection crashes define safety. The relationships were used to determine appropriate CMFs for reducing or eliminating the skew angle of an intersection, determine if there is a critical minimum angle at which safety is substantially diminished, and assess the need for revising current geometric design policies and practices.

The data for this research were acquired from the FHWA HSIS, MNDOT, and ODOT. HSIS included intersection files from MN that allow the crash data, intersection geometric data, and traffic volumes to be linked by location. MNDOT provided the GIS base map and the GIS point file that allowed for the collection of supplemental data elements, including the measured angle of each intersection. The scope of the MN analysis was limited to minor leg stop-controlled intersections. The final MN database included 1,669 four-leg intersections and 1,109 three-leg intersections. The numbers of crashes included in the analysis over a 7-yr period was 8,482 for

four-leg intersections and 4,746 for three-leg intersections. ODOT provided data in road and intersection files that were linked in GIS to a crash dataset also provided by ODOT. The final OH database included 3,766 four-leg intersections and 6,122 three-leg intersections. The analysis period for the OH data was 5 yr and included 16,051 crashes at four-leg intersections and 22,895 crashes at three-leg intersections.

The approach for this evaluation was to develop a series of cross-sectional models using NB regression. Prior to the development of the MN models, researchers conducted data-mining efforts to determine the most important predictor variables from the many independent variables in the final database and the interactions among the important predictor variables. The results of the conditional RF and regression tree data-mining analyses were then used to develop safety-prediction models. The OH data were not analyzed through a data-mining process, but the data's significantly larger sample size allowed for greater diversity of developed models.

NB regression models were separately developed for total crashes for four-leg and three-leg intersections. When sample sizes permitted, additional models were developed for rural intersections and two-lane and multilane locations. MN data afforded different severity models including fatal-and-injury and PDO crashes, and the OH data allowed select urban models to be developed for total three- and four-leg intersections as well as urban two-lane intersections. Several combinations of variables related to intersection angle were explored to determine which models resulted in the best fit of the data. The model form that was most often the best fit for four-leg intersections was one that incorporated two angle variables: minimum intersection angle and $1 + \cos(\text{minimum intersection angle})$, although some models followed a function form referred to as the Hoerl Curve, which included a logarithmic term for the minimum angle.

The regression coefficients or estimates from the models were used to derive CMFunctions for four-leg intersections. Four-leg intersection CMFunctions included total, fatal-and-injury, and PDO collision categories for the following intersection types:

- All intersections.
- Rural intersections.
- Rural two-lane intersections.
- Rural multilane intersections.
- Urban intersections (total crashes only).
- Urban two-lane intersections (total crashes only).

The regression coefficients or estimates from the models were also used to derive CMFunctions for three-leg intersections but only for total crashes. This CMFunction for three-leg intersections applied to the following intersection types:

- All intersections.
- Rural intersections.
- Rural two-lane intersections.
- Urban intersections.
- Urban two-lane intersections.

RESEARCH CONCLUSIONS

The first objective of this research was to determine the relationship between intersection angle and safety. The previously developed NB regression models and the subsequently derived CMFunctions established the relationship for minor leg stop-controlled four-leg and three-leg intersections for the combinations of intersection types and collision categories in the previous section of this report. The CMFunctions for each of these scenarios are provided in figure 51 through figure 67. The sample of skewed four-leg intersections on two-lane roads with intersection angles less than 30 degrees was limited; therefore, the research team could not make specific recommendations regarding the safety aspects of intersection angles less than 30 degrees. The number of severely skewed intersections was even more limited for the multilane intersections. For intersections on multilane roads, the research team was unable to make specific recommendations regarding the safety aspects of intersection angles less than 50 degrees. Beyond the angles less than 50 degrees, the research team could not predict the CMFunction values because of small sample size. Moreover, intersections with extremely small angles are rare in practice. Therefore, State DOTs should use their discretion and engineering judgment in trying to address changes at intersections with extremely small angles. Due to the OH data, three-leg intersections were not as restricted at smaller angle measurements.

Results of this study showed that a 90-degree intersection angle is associated with the lowest expected number of crashes. Practitioners can use the CMFunctions estimated in this study to determine the safety effect of changing minimum intersection angle for a specific type of intersection. For example, if the practitioner is considering changing the minimum intersection angle at rural four-leg intersections on two-lane roads from 55 to 80 degrees (if 90 degrees is not possible), then the expected CMF associated with this change would be the ratio of the CMF for 80 degrees to the CMF for 55 degrees, which is $1.11/1.20 = 0.93$ and represents a seven-percent reduction in crashes. If, however, the intersection angle can be changed to 90 degrees from 55 degrees, the CMF for that change would be $1.00/1.20 = 0.83$ and represents a 17-percent reduction in crashes. The other objectives of the research were to determine if there was a critical minimum angle at which safety is substantially diminished and assess the need for revision of current geometric design policies and practices. The results of the analysis indicated that the largest CMFunction values for total, injury, or PDO crashes, regardless of the intersection types included (all, rural, rural two-lane, and rural multilane), most often occur at an angle of 65 degrees, with nearly all CMFunction peaks from both datasets falling between 50 and 65 degrees.

Researchers wanted to address the issue of what intersection angle should be established as a minimum for those exceptions where a right-angle intersection cannot be achieved. Selection of this angle is subjective and based on the level of diminished safety that is considered acceptable. For example, for rural four-leg intersections on two-lane roads, an intersection angle of 65 degrees will result in a CMF no greater than 1.2. However, for the same intersection, an intersection angle of at least 80 degrees is needed if the CMF is no greater than 1.1. The research team feels that the decision regarding the acceptable level of diminished safety should be made by a specific agency or a combination of AASHTO and FHWA.

$$CMF = \text{EXP}[0.0137(\alpha - 90)] \times [1 + \cos(\alpha)]^{1.2423}$$

Figure 51. Equation. Recommended CMFunction for all four-leg intersections, fatal-and-injury crashes.

$$CMF = \text{EXP}[0.0119(\alpha - 90)] \times [1 + \cos(\alpha)]^{1.1609}$$

Figure 52. Equation. Recommended CMFunction for all four-leg intersections, PDO crashes.

$$\begin{aligned} CMF_1 &= \text{EXP}[0.0298(\alpha - 90)] \times [1 + \cos(\alpha)]^{2.7022} \\ CMF_2 &= \text{EXP}[0.0432(\alpha - 90)] \times [1 + \cos(\alpha)]^{4.03055} \\ CMF &= (CMF_1 + CMF_2)/2 \end{aligned}$$

Figure 53. Equation. Recommended CMFunction for rural four-leg intersections, total crashes.

$$CMF = \text{EXP}[0.0119(\alpha - 90)] \times [1 + \cos(\alpha)]^{1.2432}$$

Figure 54. Equation. Recommended CMFunction for rural four-leg intersections, injury-and-fatal crashes.

$$CMF = \text{EXP}[0.0112(\alpha - 90)] \times [1 + \cos(\alpha)]^{1.1523}$$

Figure 55. Equation. Recommended CMFunction for rural four-leg intersections, PDO crashes.

$$\begin{aligned} CMF_1 &= \text{EXP}[0.0123(\alpha - 90)] \times [1 + \cos(\alpha)]^{1.2017} \\ CMF_2 &= \text{EXP}[0.0198(\alpha - 90)] \times [1 + \cos(\alpha)]^{2.0774} \\ CMF &= (CMF_1 + CMF_2)/2 \end{aligned}$$

Figure 56. Equation. Recommended CMFunction for rural four-leg two-lane intersections, total crashes.

$$CMF = \text{EXP}[0.0118(\alpha - 90)] \times [1 + \cos(\alpha)]^{1.2037}$$

Figure 57. Equation. Recommended CMFunction for rural four-leg two-lane intersections, fatal-and-injury crashes.

$$CMF = \text{EXP}[0.0113(\alpha - 90)] \times [1 + \cos(\alpha)]^{1.1473}$$

Figure 58. Equation. Recommended CMFunction for rural four-leg two-lane intersections, PDO crashes.

$$\begin{aligned}
CMF_1 &= \text{EXP}[(-0.1381 \times \alpha) + (8.6579 \times \ln(\alpha))]/332498818865.70 \\
CMF_2 &= \text{EXP}[0.0691(\alpha - 90)] \times [1 + \cos(\alpha)]^{5.6961} \\
CMF &= (CMF_1 + CMF_2)/2
\end{aligned}$$

Figure 59. Equation. Recommended CMFunction for rural four-leg multilane intersections, total crashes.

$$CMF = \text{EXP}[0.1661(\alpha - 90)] \times [1 + \cos(\alpha)]^{13.6599}$$

Figure 60. Equation. Recommended CMFunction for rural four-leg multilane intersections, fatal-and-injury crashes.

$$CMF = [1 + \cos(\alpha)]^{0.9039}$$

Figure 61. Equation. Recommended CMFunction for rural four-leg multilane intersections, PDO crashes.

$$CMF = \text{EXP}[0.0133(\alpha - 90)] \times [1 + \cos(\alpha)]^{1.3249}$$

Figure 62. Equation. Recommended CMFunction for urban four-leg intersections total crashes.

$$CMF = \text{EXP}[0.0108(\alpha - 90)] \times [1 + \cos(\alpha)]^{1.2948}$$

Figure 63. Equation. Recommended CMFunction for urban four-leg two-lane intersections, total crashes.

$$\begin{aligned}
CMF_1 &= \text{EXP}[0.0113(\alpha - 90)] \times [1 + \cos(\alpha)]^{1.0349} \\
CMF_2 &= \text{EXP}[0.0139(\alpha - 90)] \times [1 + \cos(\alpha)]^{1.6013} \\
CMF &= (CMF_1 + CMF_2)/2
\end{aligned}$$

Figure 64. Equation. Recommended CMFunction for rural three-leg intersections, total crashes.

$$CMF = \text{EXP}[(-0.0099 \times \alpha) + (0.3771 \times \ln(\alpha))]/2.2387$$

Figure 65. Equation. Recommended CMFunction for rural three-leg two-lane intersections, total crashes.

$$CMF = \text{EXP}[0.0059(\alpha - 90)] \times [1 + \cos(\alpha)]^{1.0339}$$

Figure 66. Equation. Recommended CMFunction for urban three-leg intersections, total crashes.

$$CMF = \text{EXP}[0.0046(\alpha - 90)] \times [1 + \cos(\alpha)]^{0.9766}$$

Figure 67. Equation. Recommended CMFunction for urban three-leg two-lane intersections, total crashes.

In figure 51 through figure 67, α is the intersection angle (in degrees) and defined as the smallest angle between any two adjacent legs at an intersection.

METHODOLOGY CONCLUSIONS

In addition to the research results in the previous section, there were two elements of this research project that should be noted for future efforts. First, the supplemental data-collection effort for MN made use of GIS files combined with traditional intersection-inventory data to locate the intersections of interest for the study. Once located, the COGO tool within ArcGIS was used to acquire all angles at each intersection. The tool was accurate and easy to use. The GIS data were also used with online aerial imagery from Google Maps to confirm the accuracy of the information and to collect supplemental data. The use of the aerial images identified errors in the GIS data for a few locations. The aerial images were used to acquire several supplemental data elements. The collection of these data was efficient unless the image resolution was low enough that the street-level view was required. In the latter cases, the collection time required for an intersection can be increased several times depending on the number of elements to be collected.

The other unique component of this research was the use of data-mining tools for determination of variables from the MN dataset to be included in the development of the safety-prediction models. Classification and regression trees are not unique to the field of road safety. Several references were cited in chapter 3 that used these methods in road safety. However, the use of conditional RF methods and conditional regression trees for assessing variable importance and interaction effects is unique. The approach used in this study allowed the list of predictor variables for consideration in the MN NB models to be trimmed from 34 to 39 to a manageable range of 10 to 16 depending on the intersection scenario being modeled. There is a learning curve for using these tools efficiently, including understanding the limitations of computer memory on setting certain analysis parameters. Once mastered, the tools are effective for allowing researchers to create a short list of the most important predictors and visually ascertain some of the interaction effects that may warrant further consideration during the development of cross-sectional regression models.

CHAPTER 7. FUTURE RESEARCH

This research study developed new CMFunctions for intersection angles and recommended a change in policy regarding the critical minimum angle currently used in the Green Book and other resources.⁽¹⁾ Several recommendations follow that build on the work of this study.

First, the data acquired and used for the study were limited to the State road network in MN and OH. There are always concerns with crash-based research about the transferability of results from a single State to the other States or the Nation. The research team recommends the methodology applied in this study be replicated in additional States to determine if similar results can be obtained and if those results support the recommendations of this effort. Although this study verified the results using datasets from two different States, further validation will lend strength to the predictive models.

Second, the intersections in the study were predominately rural because the sites were part of the two States' road networks. The results were therefore less comprehensive for urban intersections. The research team recommends additional urban data be acquired to supplement urban data collected for MN and OH or that a separate study be conducted using sites from an urban area only. The city of Charlotte, NC, which is now part of HSIS and whose data include GIS information, could be a candidate for a supplemental study.

Third, the research team noted in the methodology chapter that the desired sample of intersections would range in terms of skew severity. This was true for both States. The data in this study included almost all stop-controlled intersections in the roadway inventory files of MNDOT and ODOT. While comprehensive in terms of geographic coverage of these States, the number of intersections with angles less than 40 degrees was limited, particularly for four-leg intersections. Further research is recommended to better define the safety implications for intersections with more severe (acute) angles.

Fourth, cutting edge safety evaluation research indicates that propensity scores may provide the most comprehensive analysis of CMFs by comparing the general properties, including traffic volume and speed limit, of treated sites to untreated sites by using relative, weighted scores. A propensity score analysis could be conducted by considering right-angle intersections as treated sites and skewed intersections as untreated sites. This type of analysis may better capture differences in traffic volumes across different angle categories.

Fifth, this report focused solely on intersections with angle measurements of 90 degrees or less. The OH dataset had several three-leg intersections with one angle greater than 90 degrees; these intersections were excluded from the analysis, but some exploratory analysis not reported in this document identified questionable crash performance for angles greater than 90 degrees. Future research should be conducted to develop an appropriate CMF functional form that can capture the safety effects when intersection angles exceed 90 degrees.

Finally, the analysis conducted in this study focused on intersections. The dependent variable in the study was crash frequencies for the intersection, which was defined as any crash on any approach within 250 ft of the intersection. This was done because it was difficult to assign crashes to a specific approach using only the information available in the HSIS database.

The research team recommends a feasibility study be conducted to determine if an approach-level analysis is possible and if the analysis might result in more refined results regarding the intersection angle's effect on safety. For example, it might be possible to determine specific collision types and vehicle maneuvers most susceptible to problems at skewed intersections. Other data that would be beneficial to such an analysis are intersection-turning movement counts. As a first step in this feasibility study, a sample of police crash reports from both skewed and nonskewed intersections should be reviewed to determine if there are any collision patterns that are related to the angle of the intersection.

APPENDIX A. HSIS DATA VARIABLES

The FHWA HSIS was one source of data for this project. As discussed in chapter 4, a preliminary assessment of the HSIS guidebooks showed that MN is the only HSIS State that included an intersection file with a geometric variable to indicate if an intersection is skewed.⁽⁵⁶⁾ Requested data for this study included variables from the crash, roadlog, and intersection files for MN. This appendix includes variables available from HSIS in each of these files. The variables required for linkages between files or deemed most appropriate for this analysis are noted by an asterisk (*) in these tables and were acquired from HSIS.

Table 46. List of variables available from the HSIS MN crash file.

Variable Name	Description
<i>acc_date*</i>	Date accident occurred
<i>accdigm*</i>	Diagram of accident code (collision type)
<i>acctype*</i>	Type of accident
<i>accyr*</i>	Year accident occurred
<i>ambl_nbr</i>	Ambulance number
<i>caseno*</i>	Accident number
<i>county*</i>	County
<i>div_code*</i>	Road design
<i>hazmat</i>	Hazardous material carried
<i>hit_run*</i>	Hit and run
<i>hour*</i>	Hour accident occurred
<i>interch</i>	Interchange element code
<i>light*</i>	Light conditions
<i>loc_bike</i>	Location of pedestrian/bike accident
<i>loc_harm*</i>	Location of first harmful event
<i>loc_narr*</i>	Location description
<i>loc_type*</i>	Relation to intersection
<i>loc_wrk_zne*</i>	Location of acc in workzone
<i>locn_rel*</i>	Location reliability
<i>milepost*</i>	Modified reference point
<i>numvehs*</i>	Number of vehicles involved
<i>object1</i>	Fixed object struck
<i>off_type</i>	Type of investigating officer
<i>on_brdg</i>	Accident occurred on bridge
<i>pop_grp*</i>	Urban/rural population codes
<i>pubdmg</i>	Public property damage
<i>rd_char1*</i>	Road characteristics
<i>rdsurf*</i>	Road surface conditions
<i>rdwork</i>	Road work being performed
<i>rodwycls*</i>	Roadway classification
<i>rte_nbr*</i>	Route number
<i>rte_sys*</i>	Route system
<i>rtsysnbr</i>	Combined route system/route number
<i>schlbus</i>	School bus involved accident
<i>severity*</i>	Accident severity
<i>speed*</i>	Posted speed limit
<i>tot_inj</i>	Number of persons injured
<i>tot_kill</i>	Number of persons killed
<i>trf_cntl*</i>	Traffic control devices

Variable Name	Description
<i>trfcntlw*</i>	Traffic control working
<i>trvl dir*</i>	Travel direction
<i>twship</i>	Township number
<i>veh mov1</i>	Vehicle movement
<i>wast mat</i>	Waste material carried
<i>weather*</i>	Weather conditions
<i>weather1*</i>	Weather conditions
<i>weather2*</i>	Weather conditions
<i>weekday*</i>	Day of week accident occurred
<i>work zone*</i>	Workzone marked
<i>wrks presnt*</i>	Worker present

*Variables acquired from HSIS and required for linkages between files or deemed most appropriate for this analysis.

Table 47. List of variables available from the HSIS MN roadlog file.

Variable Name	Description
<i>aadt*</i>	Calculated average AADT
<i>access</i>	Control of access
<i>adln rd1</i>	Additional lanes—road 1
<i>adln rd2</i>	Additional lanes—road 2
<i>bas thr1</i>	Base thickness—road 1
<i>begmp*</i>	Calculated begin milepost
<i>brk cd</i>	Break code
<i>comm adi*</i>	Calculated average commercial AADT
<i>county</i>	County
<i>curb1*</i>	Curbs—road 1
<i>curb2*</i>	Curbs—road 2
<i>dir cde*</i>	Direction code
<i>endmp</i>	Calculated ending milepost
<i>fed aid</i>	Federal aid system
<i>fed sysd</i>	Federal aid system—designated
<i>fed sysr</i>	Federal aid system—regular
<i>func cls*</i>	Functional class
<i>h count</i>	Number of count stations per section
<i>inte cat</i>	Intersection category
<i>inv dte</i>	Inventory date
<i>lanewid*</i>	Lane width
<i>lshl ty2*</i>	Left-shoulder type—road 2
<i>lshl typ*</i>	Left-shoulder type—road 1
<i>lshl wd2*</i>	Left-shoulder width—road 2
<i>lshldwid*</i>	Left-shoulder width—road 1
<i>med type*</i>	Median type
<i>medwid*</i>	Median width (in feet)
<i>mvmt</i>	Million vehicle miles traveled
<i>nbrvolb</i>	Number of blank traffic volume counts
<i>nbrvol</i>	Total Number of traffic volume counts
<i>nbrvolf</i>	Number of full traffic volume counts
<i>no lane1</i>	Number through lanes toward increasing milepoints
<i>no lane2</i>	Number through lanes toward decreasing milepoints
<i>no lanes</i>	Total number of lanes
<i>oneway</i>	Divided and one-way code
<i>parking1</i>	Parking on road 1
<i>parking2</i>	Parking on road 2

Variable Name	Description
<i>ref pst</i>	Reference post
<i>remark</i>	Remarks—type of record
<i>rodwycls*</i>	Roadway classification
<i>row</i>	Right-of-way width
<i>rshl ty2*</i>	Right-shoulder type—road 2
<i>rshl typ*</i>	Right-shoulder type—road 1
<i>rshl wd2*</i>	Right-shoulder width—road 2
<i>rshldwid*</i>	Right-shoulder width—road 1
<i>rte nbr*</i>	Route number
<i>rte sys*</i>	Route system
<i>rtsysnbr*</i>	Combined route system/route number
<i>seg lng</i>	Calculated section length
<i>side wlk</i>	Sidewalks
<i>stm sew</i>	Storm sewers
<i>suf typ1</i>	Surface specification number—road 1
<i>suf typ2</i>	Surface specification number—road 2
<i>sur tkr1</i>	Surface thickness—road 1
<i>sur tkr2</i>	Surface thickness—road 2
<i>surf ty2</i>	Surface type—road 2
<i>surf typ</i>	Surface type—road 1
<i>surf wd2*</i>	Surface width—road 2 (in ft)
<i>surf wid*</i>	Surface Width—road 1 (in ft)
<i>turn ln</i>	Turning lanes toward increasing mileposts
<i>turn ln2</i>	Turning lanes toward decreasing mileposts
<i>update</i>	Date of update
<i>urb mnc*</i>	Urban/municipal code
<i>volgrp</i>	Traffic volume group
<i>voltyp</i>	Traffic volume type
<i>year*</i>	Year of traffic

*Variables acquired from HSIS and required for linkages between files or deemed most appropriate for this analysis.

Table 48. List of variables available from the HSIS MN intersection file.

Variable Type	Variable Name	Description
N/A	<i>rte sys*</i>	Route system
	<i>rte nbr*</i>	Route number
	<i>int synb*</i>	Combined <i>rte sys</i> / <i>rte nbr</i>
	<i>milepost*</i>	Modified reference point location
	<i>ref pnt*</i>	Reference point
	<i>elem nbr</i>	Interchange element code
	<i>endmp*</i>	Calculated ending milepost
	<i>int type*</i>	Intersection type
	<i>desc</i>	Intersection description
	<i>typedesc*</i>	Intersection description—revised
	<i>rail nbr</i>	Railroad crossing number
	<i>traf dev*</i>	Traffic control devices
	<i>trf cntl*</i>	Traffic control devices—revised
	<i>sign pro</i>	Traffic signals progression
	<i>sign tim</i>	Traffic signals timing
	<i>sign con</i>	Traffic signals construction
	<i>sign pla</i>	Signal head placement
	<i>sign ped</i>	Traffic signals pedestrian signals
	<i>traf tmo</i>	Flashing signal time on

Variable Type	Variable Name	Description
	<i>traf tmf</i>	Flashing signal time off
	<i>traf phs</i>	Traffic signals number of phases
	<i>traf pre</i>	Traffic signals preemption
	<i>rdwy lgh*</i>	Roadway lighting
	<i>gen env*</i>	General environment
	<i>spec env*</i>	Specific environment
	<i>dist cat</i>	Category assigned by district
	<i>cntl cat</i>	Central office category
	<i>sfty imy*</i>	Safety improvement year
	<i>sfty ind*</i>	Safety improvement district
	<i>sfty prj*</i>	Safety improvement project number
	<i>sfty cls*</i>	Safety improvement classification
	<i>efec dte</i>	Date of accident geocoding
	<i>nbr rtes</i>	Number of routes into intersection
	<i>nbr legs</i>	Number of legs into intersection
	<i>trafctl*</i>	Traffic-control devices
Segment (route)-specific	<i>rtesyl1*</i>	Route system—route 1
	<i>rtenbr1*</i>	Route number—route 1
	<i>refpnt1*</i>	Reference point—route 1
	<i>rdesc1</i>	Road description
	<i>lolimt1</i>	Segment 1 lower limit
	<i>uplimt1</i>	Segment 1 upper limit
	<i>nbr leg1</i>	Number of legs on segment 1
	<i>rtesyl1*</i>	Route system—route 1
	<i>rtenbr1*</i>	Route number—route 1
	<i>refpnt1*</i>	Reference point—route 1
	<i>rdesc1</i>	Road description
	<i>lolimt1</i>	Segment 1 lower limit
	<i>uplimt1</i>	Segment 1 upper limit
	Leg (approach)-specific	<i>legnbr11*</i>
<i>direct11*</i>		Segment 1, leg 1 direction
<i>aadt111*</i>		Segment 1, leg 1, year 1 AADT
<i>adtyr111*</i>		Segment 1, leg 1, year 1
<i>aadt112*</i>		Segment 1, leg 1, year 2 AADT
<i>adtyr112*</i>		Segment 1, leg 1, year 2
<i>aadt113*</i>		Segment 1, leg 1, year 3 AADT
<i>adtyr113*</i>		Segment 1, leg 1, year 3
<i>aadt114*</i>		Segment 1, leg 1, year 4 AADT
<i>adtyr114*</i>		Segment 1, leg 1, year 4
<i>aadt115*</i>		Segment 1, leg 1, year 5 AADT
<i>adtyr115*</i>		Segment 1, leg 1, year 5
<i>ap spd11*</i>		Segment 1, leg 1, approach speed limit
<i>apcntl11*</i>		Segment 1, leg 1, approach traffic control
<i>nbr rtes</i>		Number of routes into intersection
<i>nbr legs</i>		Number of legs into intersection
<i>trafctl*</i>		Traffic-control devices
<i>legnbr11*</i>		Segment 1, leg number 1
<i>direct11*</i>		Segment 1, leg 1 direction
<i>aadt111*</i>		Segment 1, leg 1, year 1 AADT
<i>adtyr111*</i>		Segment 1, leg 1, year 1
<i>aadt112*</i>		Segment 1, leg 1, year 2 AADT
<i>adtyr112*</i>		Segment 1, leg 1, year 2

Variable Type	Variable Name	Description
	<i>aadt113*</i>	Segment 1, leg 1, year 3 AADT
	<i>adtyr113*</i>	Segment 1, leg 1, year 3
	<i>aadt114*</i>	Segment 1, leg 1, year 4 AADT
	<i>adtyr114*</i>	Segment 1, leg 1, year 4
	<i>aadt115*</i>	Segment 1, leg 1, year 5 AADT
	<i>adtyr115*</i>	Segment 1, leg 1, year 5
	<i>ap_spd11*</i>	Segment 1, leg 1, Approach speed limit
	<i>apcnt111*</i>	Segment 1, leg 1, Approach traffic control

*Variables acquired from HSIS and required for linkages between files or deemed most appropriate for this analysis.

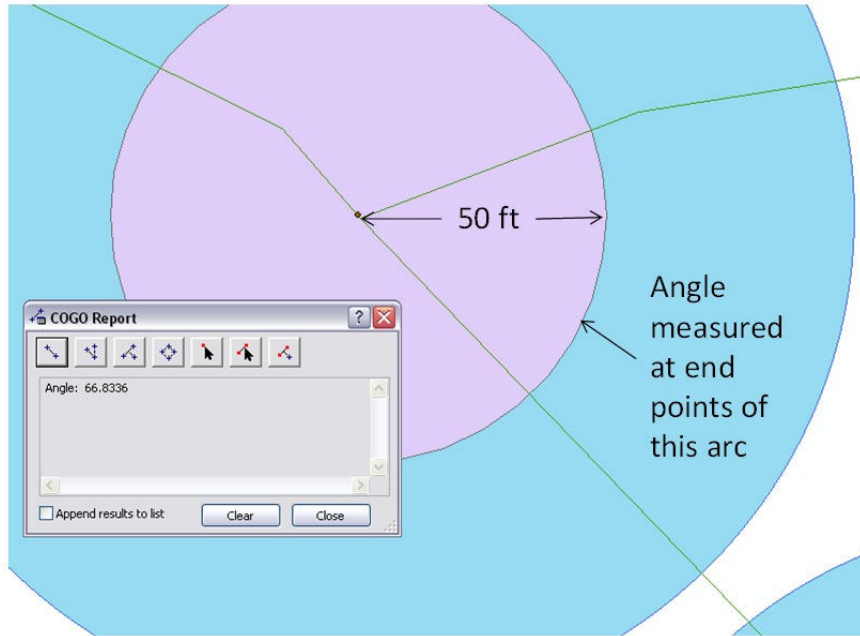
APPENDIX B. SUPPLEMENTAL DATA-COLLECTION PROCEDURE AND ISSUES

MN DATA-COLLECTION PROCEDURE

The protocol followed for nonskewed intersections for determining if the intersection was indeed not skewed was the same as the protocol used to collect intersection data with one additional step. Between steps 4 and 5 in chapter 4, researchers used the COGO tool to measure the most acute angle between all intersecting legs (as determined by visual inspection). If that angle was 85 degrees or greater, the intersection was deemed nonskewed, and the data collector proceeded to step 6. If the angle was less than 85 degrees, the data collector proceeded to step 5 and collected angle measurements for all legs of the intersection. This decision expedited the data-collection process and allowed more data to be collected for intersections with lesser angles. In part, this value was chosen because it is likely that an angle of 85 to 89 degrees was not discernible from a 90-degree angle to a driver, pedestrian, or bicyclist and thus not likely to impact their behaviors at such intersections.

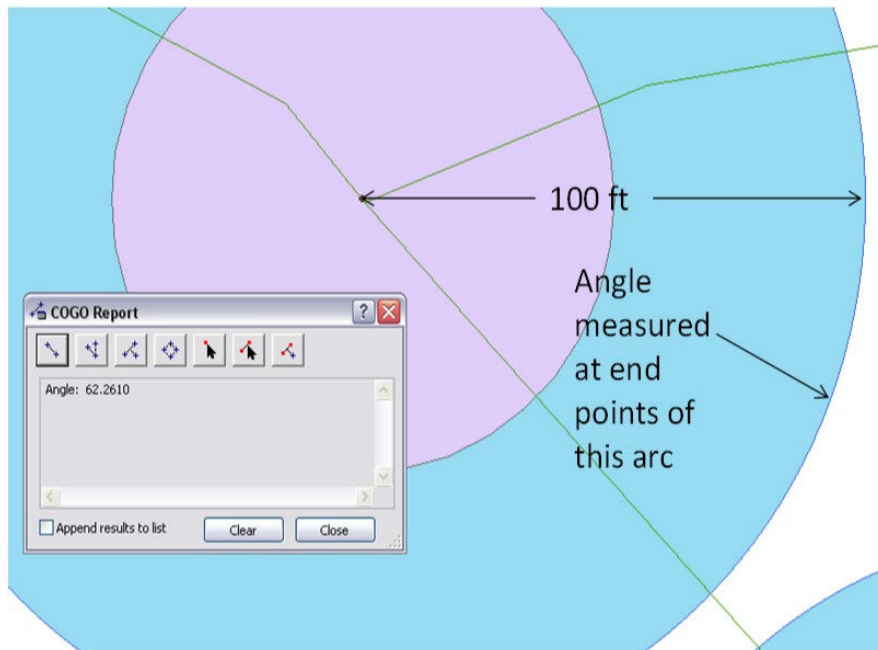
ArcGIS includes COGO that allows a user to measure angles between lines. This tool was used to obtain the angle between all legs at each intersection. During the test phase of experimenting with this tool, researchers discovered that the measured angle between adjacent legs could range widely depending on the points chosen on each leg to represent the end points of the arc. For two legs that continue in straight lines from the intersection, the distance matters little. However, for a leg with a curve starting close to the intersection, the angle measurement could vary depending on how far along the leg the data collector chooses to select the arc points. Figure 68 and figure 69 illustrate this issue with ArcGIS screenshots for one of the study intersections. Figure 68 shows a 50-foot buffer drawn around the intersection and used as a guide to locate the endpoints of the arc for measuring the angle. Figure 69 shows a 100-foot buffer for the same intersection. One of the legs of the intersection included a curve near the junction point. The angle measured at the 100-foot radius was 62 degrees, while the angle measured at the 50-foot radius was 67 degrees. Based on these initial tests, researchers employed a 50-foot distance from the point of intersection for all angle measurements. This distance ensured that angle measurements did not include nearby curves (or only a portion of the curve), matched the angle experienced by the first two drivers in the queue and provided a consistent method for all intersections.

Per step 7 in the data-collection protocol outlined in chapter 4, many supplemental data elements were collected using a combination of aerial (satellite) view and street-level images (StreetView) within Google Maps. The quality of the image available at a given intersection determined whether the data could be acquired from the aerial view only or if the street-level view was required. For some locations, the street-level view was necessary to record any sight obstructions, check for turning lanes, crosswalks, sidewalks and other features, and confirm the type of driveways that are present.



Portions of this document include intellectual property of Esri and its licensors and are used under license. © 2020 Esri and its licensors. All rights reserved.
 Modifications: FHWA.

Figure 68. Illustration. Measured intersection angle with the ArcGIS COGO tool and a 50-foot radius (67 degrees).⁽⁵⁹⁾



Portions of this document include intellectual property of Esri and its licensors and are used under license. © 2020 Esri and its licensors. All rights reserved.
 Modifications: FHWA.

Figure 69. Illustration. Measured intersection angle with the ArcGIS™ COGO tool and a 100-foot radius (62 degrees).⁽⁵⁹⁾

One of the lessons learned in this supplemental data-collection effort was the amount of time it takes to acquire information from this source of aerial imagery. At the start of this supplemental data-collection effort, researchers estimated that the additional data elements could be acquired and entered into the Excel workbook at a pace of 5 min per intersection. The effort required approximately 400 hr for the 4,780 intersections in the sample set. Within the first month of data acquisition, researchers learned that the initial estimate was not accurate. The number of low-resolution satellite images and the need to use street-level views to acquire many of the elements kept the pace closer to 12 min per intersection. Consequently, the number of intersections with all supplemental data for this study was reduced to meet budget and time constraints. Using the 12-min pace, researchers established a goal to spend no more than 600 hr, resulting in collection of supplemental data for 3,000 intersections.

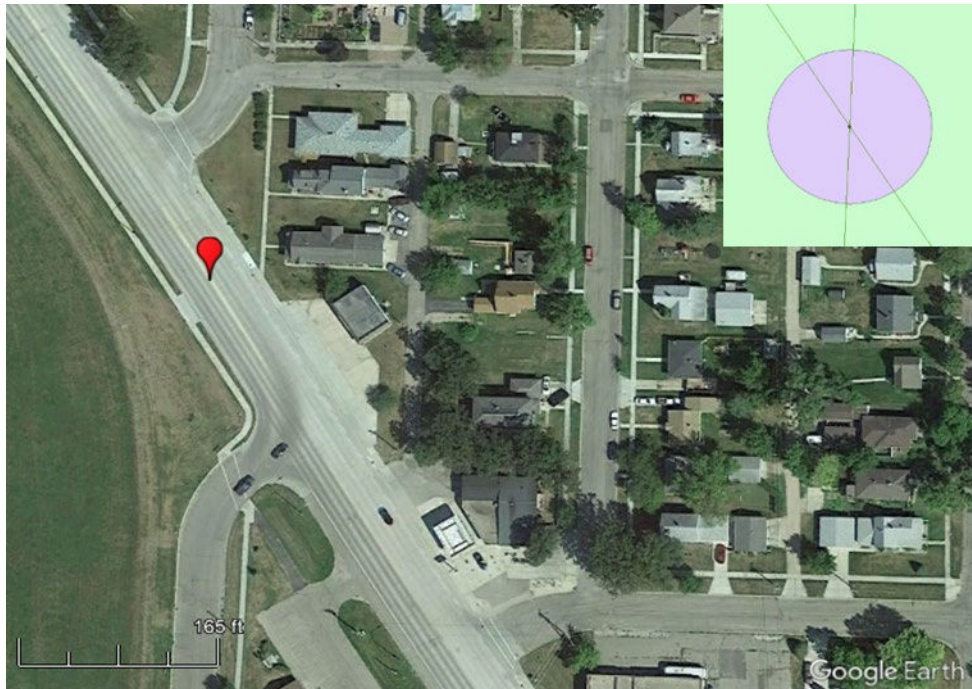
Researchers discovered additional issues in the course of the data-collection effort related to the accuracy and completeness of the spatial data. The issues ranged from intersections misclassified as skewed locations to intersections that were separated by grade.

During the supplemental data collection, the research team discovered several issues that warrant discussion and may benefit future researchers using spatial data and aerial imagery. These issues were discovered because the GIS shapefiles and the aerial images did not match. Researchers learned about the importance of using two sources of information to verify the data collected. Whenever these issues were discovered in this study, the intersection in question was flagged and a comment was added in the Excel workbook describing the problem. No further data were collected for the flagged intersections because they were eliminated from the final dataset. Approximately eight percent of intersections viewed were flagged for various reasons.

The remainder of this appendix includes five specific issues discovered during the supplemental data-collection effort. For each issue, an illustration shows both the roadway network lines from ArcGIS and the aerial image from Google Earth Maps.

Issue 1—Corrected Skewed Intersection

Figure 70 shows a typical skewed intersection from the GIS data. The roadway-network files show a four-leg intersection with two roadways crossing at an intersecting angle approximately 30 degrees. The aerial image, however, shows two three-leg intersections. The intersection appears to have been converted from a skewed four-leg intersection to two three-leg intersections with right-angle approaches.



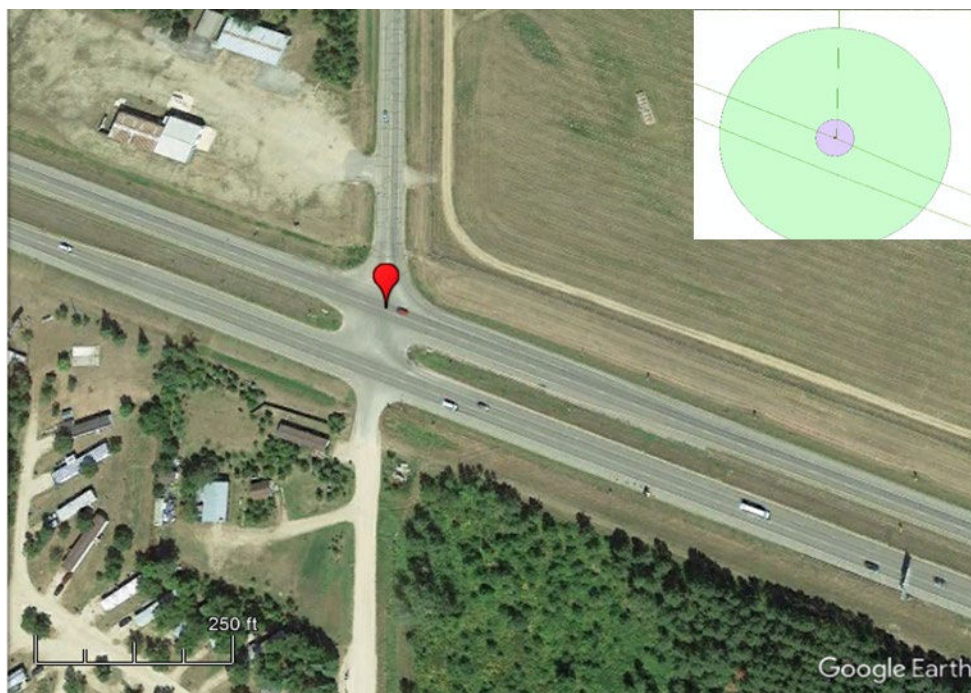
© 2015 Google Earth. Modified by FHWA.

Note: The GIS image was inserted by the research team to demonstrate that the intersection was incorrectly depicted in the GIS data as a four-leg intersection with two roadways crossing.

Figure 70. Illustration. Intersection shown as skewed four-leg location in the GIS roadway network and as two three-leg intersections in the aerial image.⁽⁷⁵⁾

Issue 2—Missing Approach Legs

In some cases, one or more of the approach legs was missing from the GIS roadway network. The example in figure 71 illustrates an intersection for which the GIS file shows a divided roadway with a three-leg intersection on one side of the roadway. The aerial image, however, shows a four-leg intersection including a paved connector in the median that allows turning movements in all directions.



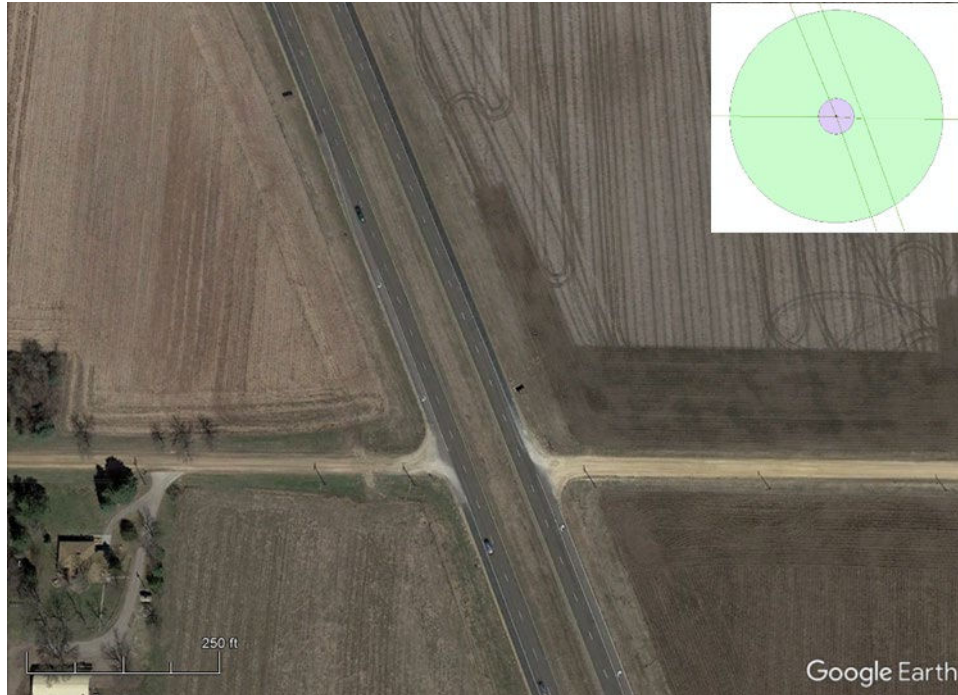
© 2015 Google Earth. Modified by FHWA.

Note: The GIS image was inserted by the research team to demonstrate that the intersection was incorrectly depicted in the GIS data as a divided roadway with one three-leg intersection.

Figure 71. Illustration. Intersection shown with a single minor leg approach in the GIS roadway network but with two minor leg approaches and a median connector in the aerial image.⁽⁷⁶⁾

Issue 3—Misclassification

On divided roadways, there were several cases showing that the spatial data incorrectly indicated that the intersection had full access to all turning movements. In figure 72, the GIS roadway network includes a four-leg intersection at a divided roadway, complete with a paved connector in the median to allow crossing and left turns from the minor road in each direction. However, no such connector exists in the aerial image, which shows two three-leg intersections on either side of the divided roadway. The approaches were aligned with each other.



© 2017 Google Earth. Modified by FHWA.

Note: The GIS image was inserted by the research team to demonstrate that the intersection was incorrectly depicted in the GIS data as a divided roadway with a paved connector.

Figure 72. Illustration. Intersection shown as a full access four-leg location in the GIS roadway network but as two three-leg intersections (no median connector) in the aerial image.⁽⁷⁷⁾

Issue 4—Grade Separation

The original HSIS data acquired for this study were filtered based on minor leg stop-control; therefore, a grade-separated intersection should not have been included in the original dataset. Figure 73, however, shows exactly that type of intersection. The GIS roadway network correctly shows the two roads crossing. However, the aerial image shows that this is not an at-grade crossing. Figure 73 illustrates the value of aerial images for confirming the accuracy of traditional digital data sources.



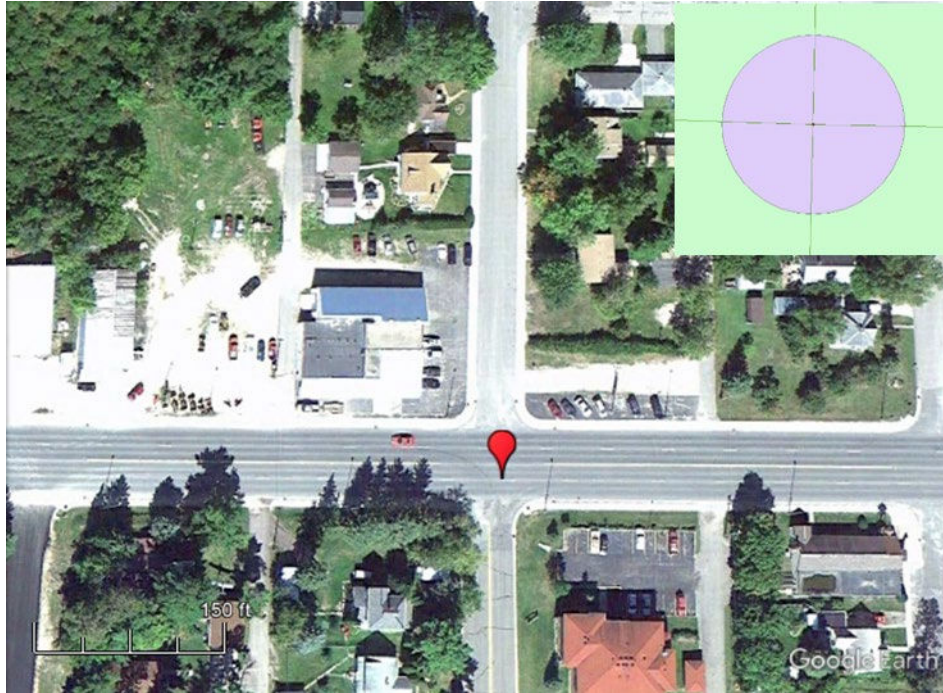
© 2015 Google Earth. Modified by FHWA.

Note: The GIS image was inserted by the research team to demonstrate that the intersection was incorrectly depicted in the GIS data as an at-grade crossing.

Figure 73. Illustration. Grade-separated intersection that should not have been included in the original HSIS data received.⁽⁷⁸⁾

Issue 5—Incorrect Classification

The MN HSIS data includes an intersection descriptor to indicate whether the intersection is skewed or not. This variable was used in this study to preliminarily determine the number of sites available in each of these categories for three- and four-leg intersections. Figure 74 shows an example of an intersection categorized as a skewed four-leg intersection within the HSIS data. Both the GIS roadway network and the aerial image show that the intersection is at a right-angle location. The supplemental data-collection effort was used to correct these misclassifications in both directions: skewed to right angle and right angle to skewed.



© 2011 Google Earth. Modified by FHWA.

Note: The GIS image was inserted by the research team to demonstrate that the intersection is a right-angle intersection that was incorrectly classified in the HSIS database as a skewed intersection.

Figure 74. Illustration. Intersection that was classified as skewed in the HSIS database but is a right-angle intersection in both the GIS roadway network and the aerial imagery.⁽⁷⁹⁾

APPENDIX C. DATA TABLES

Table 47 through table 72 were developed from the final database used in this research study. The tables provide descriptive statistics for many of the key variables used in the analysis. In the following tables, a right angle is defined as having an intersecting angle greater than or equal to 85 degrees.

Table 49. Four-leg intersections by angle classification and area type in MN.

Angle Classification	Number of Rural Intersections	Rural (%)	Number of Urban Intersections	Urban (%)	Total
Right angle	892	60.6	123	62.4	1,015
Skewed	580	39.4	74	37.6	654
Total	1,472	100.0	197	100.0	1,669

Table 50. Total crashes (2003–2009) at four-leg intersections by angle classification and area type in MN.

Angle Classification	Number of Rural Intersections	Rural (%)	Number of Urban Intersections	Urban (%)	Total
Right angle	4,349	74.1	2,124	81.3	6,473
Skewed	1,519	25.9	490	18.7	2,009
Total	5,868	100.0	2,614	100.0	8,482

Table 51. Four-leg intersections by intersection angle and area type in MN.

Intersection Angle (Degrees)	Number of Rural Intersections	Rural (%)	Number of Urban Intersections	Urban (%)	Total
<40	42	2.9	2	1.0	44
40–49	67	4.6	10	5.1	77
50–54	50	3.4	6	3.0	56
55–59	67	4.6	5	2.5	72
60–64	63	4.3	6	3.0	69
65–69	75	5.1	10	5.1	85
70–74	79	5.4	13	6.6	92
75–79	70	4.8	12	6.1	82
80–84	67	4.6	10	5.1	77
≥85	892	60.6	123	62.4	1,015
Total	1,472	100.0	197	100.0	1,669

Table 52. Total crashes (2003–2009) at four-leg intersections by intersection angle and area type in MN.

Intersection Angle (Degrees)	Number of Rural Intersections	Rural (%)	Number of Urban Intersections	Urban (%)	Total
<40	114	1.9	35	1.3	149
40–49	259	4.4	93	3.6	352
50–54	328	5.6	82	3.1	410
55–59	250	4.3	79	3.0	329
60–64	330	5.6	57	2.2	387
65–69	582	9.9	122	4.7	704
70–74	378	6.4	186	7.1	564
75–79	404	6.9	123	4.7	527
80–84	295	5.0	129	4.9	424
≥85	2,928	49.9	1,708	65.3	4,636
Total	5,868	100.0	2,614	100.0	8,482

Table 53. Fatal-and-injury crashes (2003–2009) at four-leg intersections by intersection angle and area type in MN.

Intersection Angle (Degrees)	Number of Rural Intersections	Rural (%)	Number of Urban Intersections	Urban (%)	Total
<40	48	2.1	11	1.3	59
40–49	96	4.1	29	3.3	125
50–54	117	5.0	25	2.9	142
55–59	108	4.6	31	3.6	139
60–64	141	6.0	20	2.3	161
65–69	267	11.4	42	4.8	309
70–74	157	6.7	68	7.8	225
75–79	167	7.2	44	5.1	211
80–84	110	4.7	44	5.1	154
≥85	1,124	48.1	553	63.8	1,677
Total	2,335	100.0	867	100.0	3,202

Table 54. PDO crashes (2003–2009) at four-leg intersections by intersection angle and area type in MN.

Intersection Angle (Degrees)	Number of Rural Intersections	Rural (%)	Number of Urban Intersections	Urban (%)	Total
<40	66	1.9	23	1.3	89
40–49	160	4.6	63	3.7	223
50–54	205	5.9	55	3.2	260
55–59	141	4.0	47	2.7	188
60–64	188	5.4	37	2.2	225
65–69	310	8.9	79	4.6	389
70–74	218	6.3	117	6.8	335
75–79	232	6.7	79	4.6	311
80–84	183	5.3	85	4.9	268
≥85	1,781	51.1	1,135	66.0	2,916
Total	3,484	100.0	1,720	100.0	5,204

Table 55. Intersection AADT for four-leg intersections by intersection angle and area type in MN.

Intersection Angle (Degrees)	Rural Min	Rural Avg	Rural Max	Urban Min	Urban Avg	Urban Max
<40	622	3,876	26,514	18,772	22,943	27,114
40–49	163	4,912	25,985	5,113	9,395	19,839
50–54	640	5,678	26,462	4,586	13,737	36,710
55–59	805	4,258	25,467	6,369	11,370	21,563
60–64	787	4,675	22,204	4,642	13,904	37,000
65–69	643	6,222	30,172	5,821	13,226	29,631
70–74	995	4,985	28,146	10,632	21,786	52,827
75–79	527	4,988	19,683	5,491	11,753	32,625
80–84	767	4,812	17,869	2,474	18,215	36,781
≥85	178	3,847	31,056	3,440	15,023	53,108
Average	613	4,825	25,356	6,734	15,135	34,720

Min = minimum; Avg = average; Max = maximum.

Table 56. Minor road AADT for four-leg intersections by intersection angle and area type in MN.

Intersection Angle (Degrees)	Rural Min	Rural Avg	Rural Max	Urban Min	Urban Avg	Urban Max
<40	13	318	1,951	650	1,011	1,372
40–49	5	443	2,418	650	1,480	2,543
50–54	33	627	4,035	129	860	1,603
55–59	14	684	11,195	539	1,079	1,495
60–64	20	562	5,632	128	608	824
65–69	23	630	2,657	456	748	1,881
70–74	23	549	2,677	377	1,296	3,225
75–79	22	617	3,183	552	1,114	2,375
80–84	42	542	3,168	56	651	1,348
≥85	4	505	3,421	34	1,057	2,953
Average	20	548	4,034	357	990	1,962

Min = minimum; Avg = average; Max = maximum.

Table 57. Major road AADT for four-leg intersections by intersection angle and area type in MN.

Intersection Angle (Degrees)	Rural Min	Rural Avg	Rural Max	Urban Min	Urban Avg	Urban Max
<40	588	3,558	25,662	17,400	21,932	26,464
40–49	125	4,469	25,662	2,821	7,915	17,300
50–54	492	5,051	25,662	3,788	12,878	35,107
55–59	529	3,574	20,161	5,245	10,291	20,069
60–64	601	4,113	19,525	4,116	13,295	36,286
65–69	600	5,592	29,893	5,171	12,478	27,750
70–74	835	4,436	27,043	9,275	20,490	50,429
75–79	498	4,371	18,996	4,937	10,639	30,250
80–84	685	4,270	17,596	1,917	17,564	35,433
≥85	124	3,343	30,118	2,515	13,966	52,071
Average	508	4,278	24,032	5,719	14,145	33,116

Min = minimum; Avg = average; Max = maximum.

Table 58. Total crash rates (per 100 M entering vehicles) for four-leg intersections by intersection angle and area type in MN.

Intersection Angle (Degrees)	Rural Min	Rural Avg	Rural Max	Urban Min	Urban Avg	Urban Max
<40	0.00	29.13	200.25	24.54	31.03	37.53
40–49	0.00	32.65	211.67	0.00	36.17	74.93
50–54	0.00	48.24	299.69	12.07	54.68	140.39
55–59	0.00	34.47	161.56	11.09	52.71	106.82
60–64	0.00	37.62	177.05	5.33	34.46	59.02
65–69	0.00	49.09	237.99	0.00	29.54	68.69
70–74	0.00	43.01	285.27	0.00	32.66	120.84
75–79	0.00	37.55	178.93	0.00	34.00	74.86
80–84	0.00	33.10	165.44	9.58	34.03	116.03
≥85	0.00	34.17	216.64	0.00	39.34	160.73
Average	0.00	37.90	213.45	6.26	37.86	95.98

Min = minimum; Avg = average; Max = maximum.

Table 59. Fatal-and-Injury crash rates (per 100 M entering vehicles) for four-leg intersections by intersection angle and area type in MN.

Intersection Angle (Degrees)	Rural Min	Rural Avg	Rural Max	Urban Min	Urban Avg	Urban Max
<40	0.00	11.31	72.82	7.22	9.86	12.51
40–49	0.00	14.60	125.08	0.00	12.39	32.11
50–54	0.00	14.60	61.15	0.00	20.25	54.94
55–59	0.00	14.12	80.78	5.54	20.00	41.09
60–64	0.00	15.32	68.85	0.00	10.85	23.87
65–69	0.00	24.21	216.36	0.00	10.94	23.36
70–74	0.00	18.80	120.80	0.00	12.68	65.32
75–79	0.00	14.70	107.36	0.00	11.75	27.25
80–84	0.00	13.75	118.17	3.19	12.55	42.19
≥85	0.00	13.24	119.14	0.00	12.98	49.33
Average	0.00	15.47	109.05	1.60	13.43	37.20

Min = minimum; Avg = average; Max = maximum.

Table 60. PDO crash rates (per 100 M entering vehicles) for four-leg intersections by intersection angle and area type in MN.

Intersection Angle (Degrees)	Rural Min	Rural Avg	Rural Max	Urban Min	Urban Avg	Urban Max
<40	0.00	17.82	127.43	17.32	20.13	22.93
40–49	0.00	17.81	87.59	0.00	23.13	55.05
50–54	0.00	32.77	239.75	8.53	33.23	79.35
55–59	0.00	20.28	80.78	3.17	32.35	65.74
60–64	0.00	22.11	108.20	5.29	23.61	50.59
65–69	0.00	24.75	100.82	0.00	18.39	47.55
70–74	0.00	23.89	213.95	0.00	19.82	55.52
75–79	0.00	22.39	89.58	0.00	22.25	54.44
80–84	0.00	19.17	85.83	0.00	21.47	73.84
≥85	0.00	20.61	144.42	0.00	25.86	118.98
Average	0.00	22.16	127.84	3.43	24.02	62.40

Min = minimum; Avg = average; Max = maximum.

Table 61. Three-leg intersections by angle classification and area type in MN.

Angle Classification	Number of Rural Intersections	Rural (%)	Number of Urban Intersections	Urban (%)	Total
Right angle	538	60.6	101	45.7	639
Skewed	350	39.4	120	54.3	470
Total	888	100.0	221	100.0	1,109

Table 62. Total crashes (2003–2009) at three-leg intersections by angle classification and area type in MN.

Angle Classification	Number of Rural Intersections	Rural (%)	Number of Urban Intersections	Urban (%)	Total
Right angle	2,236	79.0	1,341	70.5	3,577
Skewed	593	21.0	560	29.5	1,153
Total	2,829	100.0	1,901	100.0	4,730

Table 63. Three-leg intersections by intersection angle and area type in MN.

Intersection Angle (Degrees)	Number of Rural Intersections	Rural (%)	Number of Urban Intersections	Urban (%)	Total
<40	53	6.0	17	7.7	70
40–49	24	2.7	9	4.1	33
50–54	30	3.4	10	4.5	40
55–59	32	3.6	5	2.3	37
60–64	30	3.4	9	4.1	39
65–69	39	4.4	17	7.7	56
70–74	41	4.6	16	7.2	57
75–79	48	5.4	20	9.0	68
80–84	53	6.0	17	7.7	70
≥85	538	60.6	101	45.7	639
Total	888	100.0	221	100.0	1,109

Table 64. Total crashes (2003–2009) at three-leg intersections by intersection angle and area type in MN.

Intersection Angle (Degrees)	Number of Rural Intersections	Rural (%)	Number of Urban Intersections	Urban (%)	Total
<40	191	6.8	129	6.8	320
40–49	51	1.8	108	5.7	159
50–54	81	2.9	24	1.3	105
55–59	90	3.2	53	2.8	143
60–64	62	2.2	63	3.3	125
65–69	123	4.3	95	5.0	218
70–74	153	5.4	113	5.9	266
75–79	156	5.5	158	8.3	314
80–84	180	6.4	141	7.4	321
≥85	1,742	61.6	1,017	53.5	2,759
Total	2,829	100.0	1,901	100.0	4,730

Table 65. Fatal-and-injury crashes (2003–2009) at three-leg intersections by intersection angle and area type in MN.

Intersection Angle (Degrees)	Number of Rural Intersections	Rural (%)	Number of Urban Intersections	Urban (%)	Total
<40	82	8.0	49	7.5	131
40–49	20	1.9	36	5.5	56
50–54	26	2.5	10	1.5	36
55–59	30	2.9	15	2.3	45
60–64	21	2.0	22	3.4	43
65–69	37	3.6	34	5.2	71
70–74	55	5.3	35	5.4	90
75–79	57	5.5	59	9.0	116
80–84	70	6.8	49	7.5	119
≥85	631	61.3	344	52.7	975
Total	1,029	100.0	653	100.0	1,682

Table 66. PDO crashes (2003–2009) at three-leg intersections by intersection angle and area type in MN.

Intersection Angle (Degrees)	Number of Rural Intersections	Rural (%)	Number of Urban Intersections	Urban (%)	Total
<40	109	6.1	77	6.3	186
40–49	31	1.7	71	5.8	102
50–54	55	3.1	14	1.1	69
55–59	58	3.3	38	3.1	96
60–64	41	2.3	40	3.3	81
65–69	85	4.8	59	4.8	144
70–74	97	5.4	75	6.1	172
75–79	98	5.5	98	8.0	196
80–84	108	6.1	90	7.4	198
≥85	1,102	61.8	661	54.0	1,763
Total	1,784	100.0	1,223	100.0	3,007

Table 67. Intersection AADT for three-leg intersections by intersection angle and area type in MN.

Intersection Angle (Degrees)	Rural Min	Rural Avg	Rural Max	Urban Min	Urban Avg	Urban Max
<40	531	4,606	22,026	1,735	12,903	27,057
40–49	658	5,000	25,755	4,817	14,773	40,475
50–54	549	5,193	25,849	6,210	10,855	20,770
55–59	1,055	4,043	20,593	8,179	19,053	35,955
60–64	710	4,400	19,196	5,689	10,736	27,724
65–69	674	3,938	17,110	5,821	15,232	36,971
70–74	380	6,200	24,998	4,066	14,268	43,288
75–79	400	6,548	31,433	4,836	17,418	40,718
80–84	1,005	5,592	25,643	6,228	16,352	36,857
≥85	322	5,393	31,520	3,480	20,256	57,975
Average	628	5,091	24,412	5,106	15,185	36,779

Min = minimum; Avg = average; Max = maximum.

Table 68. Minor road AADT for three-leg intersections by intersection angle and area type in MN.

Intersection Angle (Degrees)	Rural Min	Rural Avg	Rural Max	Urban Min	Urban Avg	Urban Max
<40	11	850	4,579	36	1,006	8,437
40–49	20	595	2,759	349	2,996	19,021
50–54	31	720	4,055	6	881	3,686
55–59	55	564	3,362	747	2,626	4,605
60–64	79	568	2,261	397	950	2,823
65–69	24	523	2,182	36	714	2,701
70–74	4	726	4,391	95	1,647	12,184
75–79	8	638	2,793	73	842	2,370
80–84	6	865	7,061	73	1,101	7,358
≥85	3	640	7,013	81	1,191	7,443
Average	24	669	4,046	189	1,395	7,063

Min = minimum; Avg = average; Max = maximum.

Table 69. Major road AADT for three-leg intersections by intersection angle and area type in MN.

Intersection Angle (Degrees)	Rural Min	Rural Avg	Rural Max	Urban Min	Urban Avg	Urban Max
<40	318	3,756	21,936	1,498	11,898	26,407
40-49	287	4,405	25,662	4,186	11,777	24,139
50-54	519	4,473	25,662	3,437	9,974	20,764
55-59	779	3,479	20,179	7,432	16,426	33,393
60-64	365	3,832	18,729	5,057	9,786	24,901
65-69	624	3,415	17,056	5,171	14,518	36,321
70-74	370	5,474	24,850	3,319	12,621	42,643
75-79	318	5,910	31,343	4,186	16,576	39,286
80-84	644	4,727	20,161	5,485	15,251	36,143
≥85	318	4,753	31,464	3,121	19,065	55,786
Average	454	4,423	23,704	4,289	13,789	33,978

Min = minimum; Avg = average; Max = maximum.

Table 70. Total crash rates (per 100 M entering vehicles) for three-leg intersections by intersection angle and area type in MN.

Intersection Angle (Degrees)	Rural Min	Rural Avg	Rural Max	Urban Min	Urban Avg	Urban Max
<40	0.00	30.26	107.13	0.00	19.67	52.08
40-49	0.00	21.22	66.83	3.19	31.72	62.04
50-54	0.00	26.75	190.74	0.00	8.67	21.78
55-59	0.00	32.21	159.32	0.00	16.29	34.83
60-64	0.00	24.48	76.00	0.00	17.36	59.29
65-69	0.00	29.81	129.62	0.00	15.55	68.36
70-74	0.00	23.56	168.40	4.60	22.70	86.23
75-79	0.00	24.29	175.51	0.00	19.35	66.25
80-84	0.00	20.69	92.49	2.57	20.76	63.43
≥85	0.00	25.79	443.80	0.00	20.10	116.16
Average	0.00	25.91	160.98	1.04	19.22	63.05

Min = minimum; Avg = average; Max = maximum.

Table 71. Fatal-and-injury crash rates (per 100 M entering vehicles) for three-leg intersections by intersection angle and area type in MN.

Intersection Angle (Degrees)	Rural Min	Rural Avg	Rural Max	Urban Min	Urban Avg	Urban Max
<40	0.00	14.84	73.71	0.00	7.07	26.04
40-49	0.00	7.47	54.59	0.00	10.77	21.73
50-54	0.00	9.90	114.44	0.00	4.02	10.99
55-59	0.00	10.09	51.50	0.00	4.52	10.47
60-64	0.00	7.66	29.81	0.00	5.54	22.59
65-69	0.00	9.05	44.82	0.00	5.46	19.14
70-74	0.00	8.78	79.77	0.00	6.53	40.24
75-79	0.00	11.17	175.51	0.00	7.02	27.10
80-84	0.00	7.42	38.94	0.00	8.59	25.14
≥85	0.00	9.31	169.07	0.00	7.09	38.72
Average	0.00	9.57	83.21	0.00	6.66	24.22

Min = minimum; Avg = average; Max = maximum.

Table 72. PDO crash rates (per 100 M entering vehicles) for three-leg intersections by intersection angle and area type in MN.

Intersection Angle (Degrees)	Rural Min	Rural Avg	Rural Max	Urban Min	Urban Avg	Urban Max
<40	0.00	15.42	67.89	0.00	11.80	37.75
40-49	0.00	13.75	59.48	1.60	20.84	53.18
50-54	0.00	16.86	95.60	0.00	4.65	13.07
55-59	0.00	21.58	132.76	0.00	11.77	25.04
60-64	0.00	16.82	57.00	0.00	11.66	35.29
65-69	0.00	20.25	109.67	0.00	9.79	49.22
70-74	0.00	14.56	98.27	3.62	15.76	45.99
75-79	0.00	13.03	76.00	0.00	12.27	39.14
80-84	0.00	13.16	64.37	0.00	11.96	44.57
≥85	0.00	16.25	274.73	0.00	12.81	73.14
Average	0.00	16.17	103.58	0.52	12.33	41.64

Min = minimum; Avg = average; Max = maximum.

APPENDIX D. DATA DESCRIPTORS AND DATA-MINING RESULTS

DATA MINING: BACKGROUND AND APPLICATION

RF regression was used to determine the variables most likely to be the best predictors of crashes. Breiman and Cutler developed the RF algorithm for the framework of classification and regression trees.⁽⁴⁶⁾ Instead of having one tree, multiple trees are produced using a resampling method (500 regression trees are included by default in RF package in R), and the aggregate results are then combined. Breiman and Cutler believed that a single decision tree may not reveal all the important variables that contribute to the dependent variable (e.g., crashes) because some important variables can be masked by other important variables at a specific splitting node. In this case, RFs can help identify important predictors that may not appear in the output of a single classification or regression tree but are nevertheless highly predictive of the target variable.

There are very few studies in road-safety literature that have applied RF methods. Harb et al. employed RF to explore precrash maneuvers associated with rear-end, angle, and head-on crashes.⁽⁸⁰⁾ Rossi et al. concluded that the RF variable importance rankings are more stable than those produced by stepwise logistic regression.⁽⁸¹⁾ Strobl, Malley, and Tutz also note that high-ranked variables on a list detailing the importance of RFs as a result of a complex interaction that cannot be captured in a regression model.⁽⁴⁹⁾

The research team used the regression tree analysis as the data-mining method for this study to explore interactions among independent variables. Regression tree analysis is a robust data-mining and data-analysis tool that automatically searches for important patterns and relationships and quickly uncovers hidden structure even in highly complex data. It has been an active analytical technique in many scientific areas for many years. The analysis method does not require any predefined underlying relationship between targets (dependent variables) and predictors (independent variables) and has been shown to be a powerful tool to find the more important factors that contribute to the target variable. It also provides the ability to determine the level and type of interaction between independent variables as opposed to having to predefine such interactions when developing regression models.

There are two types of tree analysis. One type is a classification tree in which the dependent variable is binary, and the other type is a regression tree in which the dependent variable can be continuous or count data. The output is a tree that shows the most important predictor variables at the top of the tree in addition to combinations of variables that best predict the outcome variable. The analysis can also identify and explain the complex patterns associated with crash risk; it can effectively handle multicollinearity problems and observations with missing values.

It should be noted that Breiman's RF requires that the continuous dependent variables be normally distributed. Crash data are not normally distributed; therefore, more advanced techniques, known as conditional tree and conditional RF, were selected for this research effort.

There have been limited applications of tree analysis and other similar classification techniques in transportation. Council et al. employed classification trees to develop a speed-related crash typology to identify the crash, vehicle, and driver characteristics associated with speeding-related crashes.⁽⁸²⁾ In this effort, the target variable was a binary variable crash that was either speeding

related or not speeding related. Classification trees were also used in a more extensive study for NHTSA on this same topic in which the goal was the development of a speed-related crash taxonomy for different types of crashes.⁽⁸³⁾

A few studies have used regression trees to examine the safety of different roadway features. For example, Abdel-Aty et al. used regression trees to identify factors associated with different types of crashes at signalized intersections.⁽⁸⁴⁾ Park and Saccomanno used a tree-based partitioning method to classify intersections and then applied generalized linear regression techniques to identify contributing factors associated with crashes at railroad grade crossings.⁽⁸⁵⁾

Kuhnert, Dob, and McClure employed logistic regression, classification, and regression trees (CART) and multivariate adaptive regression splines (MARS) to analyze motor-vehicle injury data.⁽⁸⁶⁾ The aim of the study was to determine if taking risks was a significant contributor to crashes resulting in serious injury or death. By comparing the analysis results from logistic regression, the research team demonstrated that CART and MARS, which are capable of graphically displaying the analysis results and identifying the groups of people with potential high-crash risk, are informative and attractive models for motor-vehicle crash analysis. The research team also suggested that CART and MARS can be used as a precursor to a more-detailed logistic regression. However, the research team did not combine these methods for their study.

Other studies have used classification and regression trees for relating injury levels or specific types of crashes to drivers, vehicles, and environmental variables.⁽⁸⁷⁻⁹³⁾ These studies used the classification tree method in which the dependent variable was a binary variable.

DATA MINING: PROCEDURE AND ANALYSIS

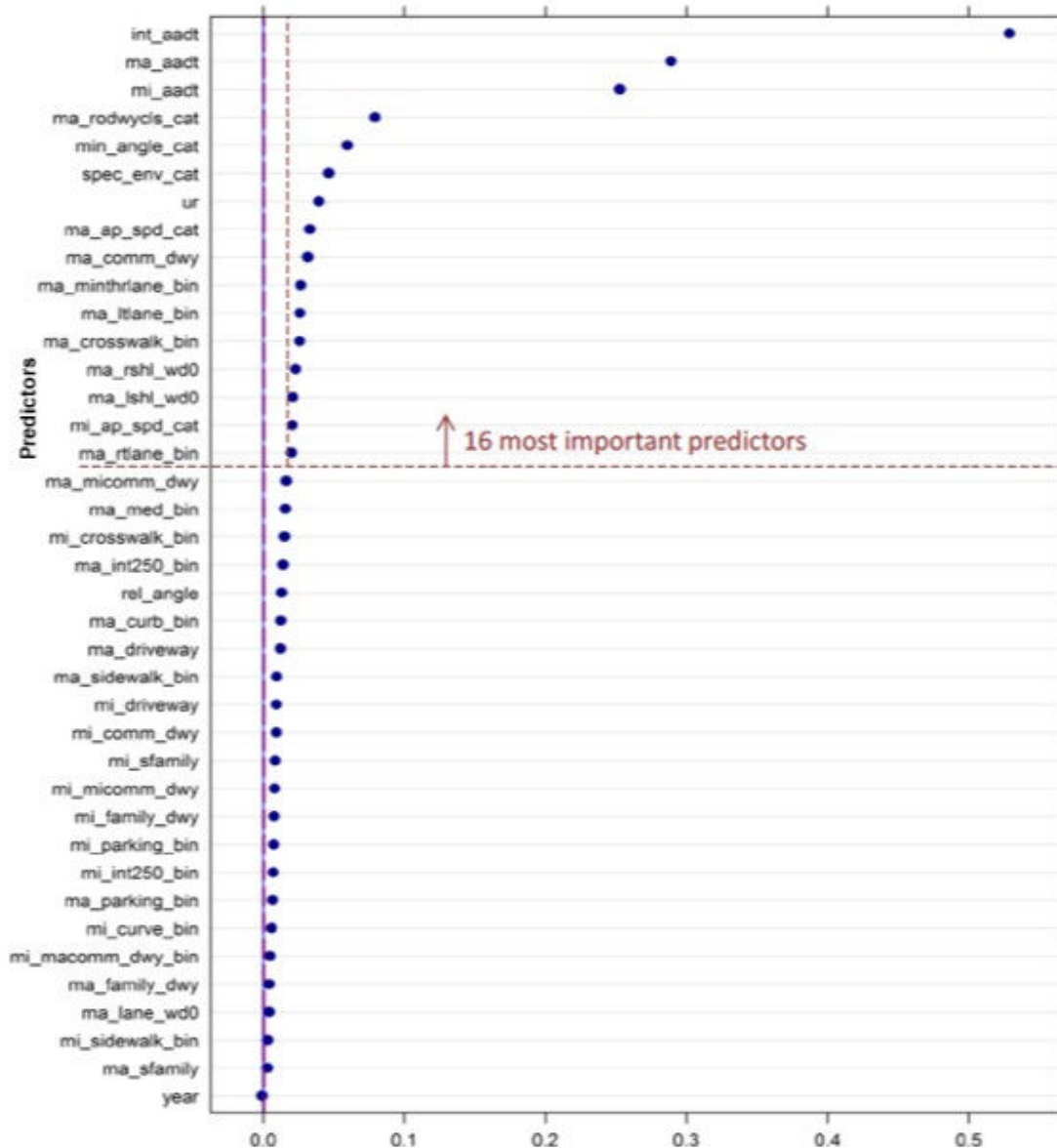
The parameter settings within the cforest algorithm were set to fit the type of predictor variables in the data and to develop the most robust results within the limits of the available computational power. For datasets that include different types (e.g., continuous versus categorical) of predictor variables, the recommendation is to use the default options *controls = cforest_unbiased* and permutation importance *varimp(obj)*.⁽⁴⁹⁾ For predictor variables that might be highly correlated, it is also recommended that the permutation importance setting be changed to conditional—*varimp(obj, conditional = TRUE)*. The computational power necessary for this latter condition is much greater than the default option. The computer on which the analysis was initially conducted included 16 gigabytes (GB) of random access memory (RAM) and was unable to produce results with the conditional permutation importance option because of the size of the database. A second attempt was made using a computer with 600 GB of RAM on the University of North Carolina campus; this attempt also failed to produce results. The program developer, Dr. Torsten Hothorn, confirmed through correspondence with another user that the application may not scale well. Thus, this option was not selected in the final analysis. Other options selected for the development of CRF results were generation of 1,500 trees, use of 15 randomly selected variables for each tree, and a splitting criterion based on a 5-percent significance level. In other words, 1,500 trees were produced for each RF analysis. The collective output from those 1,500 trees produced the final importance ranking of the predictor variables. For each of those 1,500 trees, 15 variables were randomly selected from the 39 and

34 variables available as candidates at each node. The permutation test statistic of 95 percent was exceeded to include a split in the computation of the importance value.

In addition to the parameter settings, the method of sampling also had to be established. The two options are bootstrap sampling with replacement and subsampling without replacement. Bootstrap sampling with replacement is the traditional method used in RF analysis, but it has recently been shown to artificially introduce associations between variables and produce bias toward the selection of predictor variables with more categories.⁽⁶⁸⁾ Thus, subsampling without replacement was selected as the chosen method. Specifically, the suggested default setting in function *cforest_unbiased ()* was adopted; 63.2 percent of the data were randomly sampled without replacement and were used as a training dataset while 36.8 percent were used as a test dataset.

The output from the CRF analysis for four-leg intersections with total crashes as the dependent or response variable is shown in figure 75. Variables can be considered informative and important if their variable importance value is greater than the absolute value of the lowest negative-scoring variable. The rationale for this is that the importance of irrelevant variables varies randomly around zero. The most important variables or strongest predictors are shown at the top of the plot. All variables to the right of the dashed line that extends the length of the chart are considered important. However, the farther a variable is from the top of the plot, the less predictive it is regarding the response variable (i.e., total crashes).

The goal of this analysis was to reduce the number of variables to a reasonable number for further consideration in the next phase of the analysis—development of NB models. Two criteria were established to produce this reduced list of variables. First, the number of variables selected had to be less than 50 percent of the starting number. For four-leg intersections, this meant the number of variables chosen could not exceed 19. For three-leg intersections, the maximum number of variables was 17. Second, the change in significance at the cutoff point between selected and nonselected variables was visually apparent on the plot. The goal of this criterion was to ensure that the breakpoint was not being chosen within a subset of variables with near identical importance values.



Source: FHWA.

Figure 75. Plot. Results of conditional RF (cforest) analysis for total crashes at four-leg intersections.

As shown in figure 75, the cutoff point was selected below the 16th most important predictor variable. There is an obvious change in the importance value between variables 16 and 17 in this list and the final number of variables selected is less than 19. Thus, both selection criteria are met. All the cforest plots for the six scenarios (three-leg and four-leg; total, fatal-and-injury, and PDO crashes) are provided in this appendix. Each plot shows the chosen cutoff point. A total of 16, 15, and 15 predictor variables, as shown in table 73, were selected for total, fatal-and-injury, and PDO crashes, respectively, for four-leg intersections. For three-leg intersections, a total of 10, 12, and 10 predictor variables were selected for total, fatal-and-injury, and PDO crashes, respectively.

With the most important predictor variables were identified through the CRF analysis, the next step in the data-mining process was the development and review of regression trees to either support or counter the CRF relative-importance findings and to identify interactions among these variables. Researchers used the ctree algorithm within Package party in R to develop the conditional inference trees within cforest. Thus, the same variable sets of 39 and 34 variables for four-leg and three-leg intersections, respectively, were used in the ctree analysis. In ctree, the permutation test was used to test the association between any of the input variables and the response. This association is measured by a p -value.

Three stopping criteria were established to define when the tree should no longer add branches. First, any split in the tree must be significant at a five-percent significance level ($p \leq 0.05$). Second, there must be a minimum number of data points in a node (N_{node}) to allow splitting to be considered. Third, there must be a minimum number of data points in a terminal node ($N_{terminal}$) to allow for a meaningful, but not overly complicated, tree to be generated. The starting number of data points for four-leg intersections was 11,683 (1,669 intersections multiplied by 7 yr). The starting number of data points for three-leg intersections was 7,763. For four-leg intersections, N_{node} and $N_{terminal}$ were set at 500 and 210, respectively. For three-leg intersections, N_{node} and $N_{terminal}$ were set at 300 and 140, respectively.

DATA DESCRIPTORS FOR MINNESOTA

Table 73 includes the variable names, data descriptors, and definitions or attributes for the data elements used in the analysis. The variable names are included in the tabular and graphical results from the data-mining analysis and the NB regression models. Graphical results from the data-mining analysis are included in this appendix. Figure 76 through figure 82 are the graphical results from the conditional RF analysis. Researchers used the cforest within Package party in R, version 1.0-6, statistical package. The four-leg intersections included 39 predictors in the dataset, while 34 predictors were included in the three-leg analysis. The most important predictors considered for inclusion in the NB models are shown in each figure. Figure 82 through figure 87 are the regression trees from the ctree analysis. Figures are provided for the following intersection configurations and crash severity classifications:

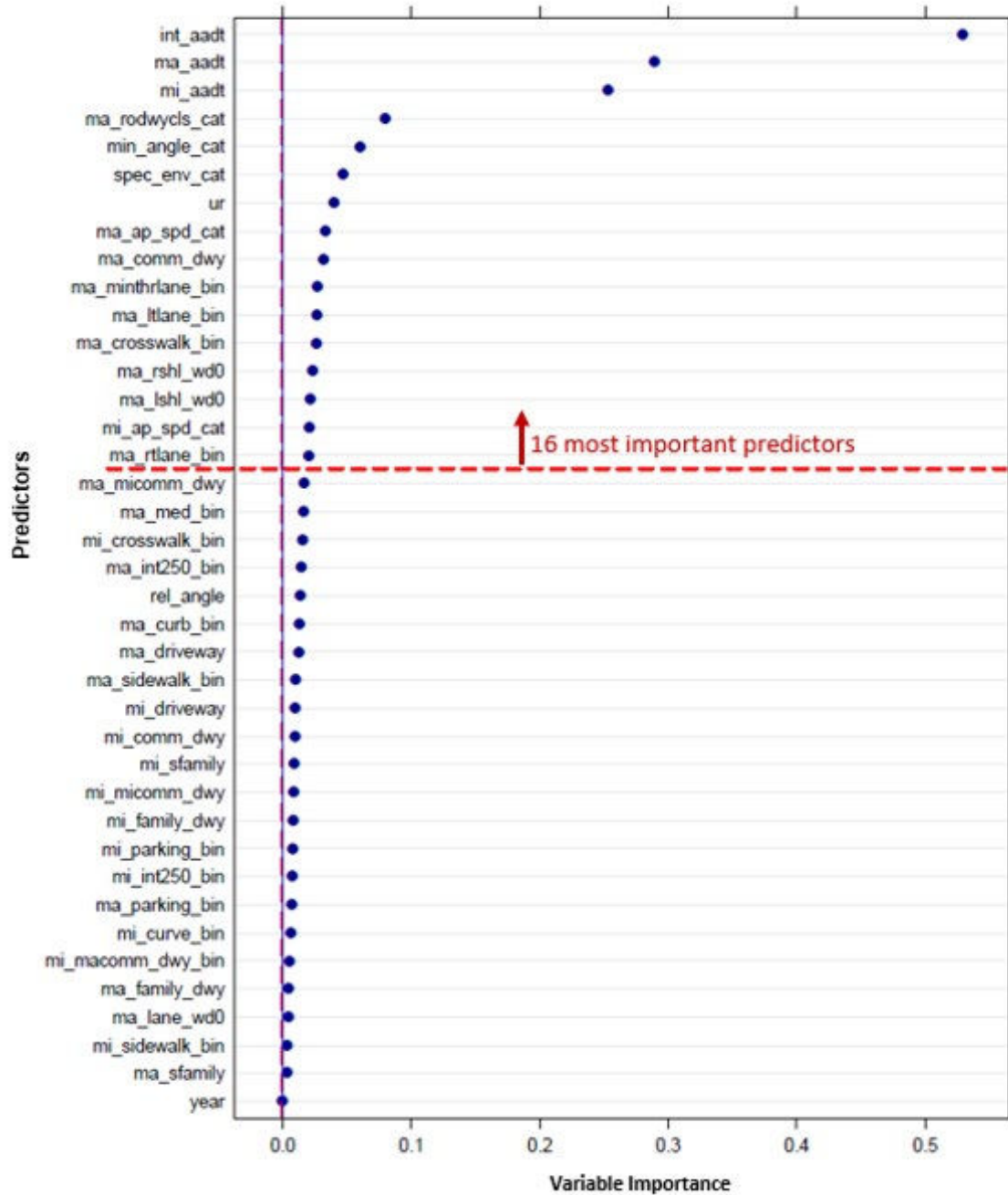
- Four-leg total crashes.
- Four-leg fatal-and-injury crashes.
- Four-leg PDO crashes.
- Three-leg total crashes.
- Three-leg fatal-and-injury crashes.
- Three-leg PDO crashes.

Table 73. Variable names, descriptors, definitions, and attributes for MN.

Variable Name	Descriptor	Definition and Attributes
<i>tot</i>	Total crashes—yearly	Total number of crashes occurring yearly across the 7-year study period (2003–2009)
<i>pdo</i>	Property-damage-only crashes—yearly	Total number of PDO crashes occurring yearly across the 7-year study period (2003–2009)
<i>inj</i>	Injury crashes—yearly	Total number of injury crashes occurring yearly across the 7-year study period (2003–2009)
<i>year</i>	Observation year—categorical variable	Crash and AADT observation year
<i>rel_angle</i>	Intersection angle complexity—categorical variable	Relative pattern of intersection angles (intersection complexity): 0 = no acute angle, 1 = 1 acute angle, 20 = 2 acute angles opposing, 21 = 2 acute angles adjacent
<i>min_angle</i>	Minimum angle	Minimum angle of intersection—smallest measured angle at the intersection (defined as intersection angle)
<i>min_angle_cat</i>	Minimum angle—category variable	10 categories: 1 = 1–39, 2 = 40–49, 3 = 50–54, 4 = 55–59, 5 = 60–64, 6 = 65–69, 7 = 70–74, 8 = 75–79, 9 = 80–84, 10 = 85+
<i>ma_int250_bin</i>	Intersection presence in 250 ft (minor road)—binary variable	0 = no, 1 = yes
<i>mi_int250_bin</i>	Intersection presence in 250 ft (major road)—binary variable	0 = no, 1 = yes
<i>mi_curve_bin</i>	Curve presence within 250 ft of intersection (minor road)—binary variable	0 = no curve, 1 = slight curve or sharp curve
<i>ma_minthrlane_bin</i>	Minimum number of through lanes (major road)—binary variable	0 = minimum number of through lanes on major approach is less than 3; 1 = otherwise
<i>ma_ltlane_bin</i>	Left-turn lane presence (major road)—binary variable	0 = no, 1 = yes
<i>ma_rtlane_bin</i>	Right-turn lane presence (major road)—binary variable	0 = no, 1 = yes
<i>ma_med_bin</i>	Median presence (major road)—binary variable	0 = no, 1 = yes
<i>ma_crosswalk_bin</i>	Crosswalk presence (major road)—binary variable	0 = no, 1 = yes
<i>mi_crosswalk_bin</i>	Crosswalk presence (minor road)—binary variable	0 = no, 1 = yes
<i>ma_sidewalk_bin</i>	Sidewalk presence (major road)—binary variable	0 = no, 1 = yes
<i>mi_sidewalk_bin</i>	Sidewalk presence (minor road)—binary variable	0 = no, 1 = yes
<i>ma_parking_bin</i>	Parking presence on major street (painted spaces visible or parked cars)—binary variable	0 = no, 1 = yes
<i>mi_parking_bin</i>	Parking presence on minor street (painted spaces visible or parked cars)—binary variable	0 = no, 1 = yes

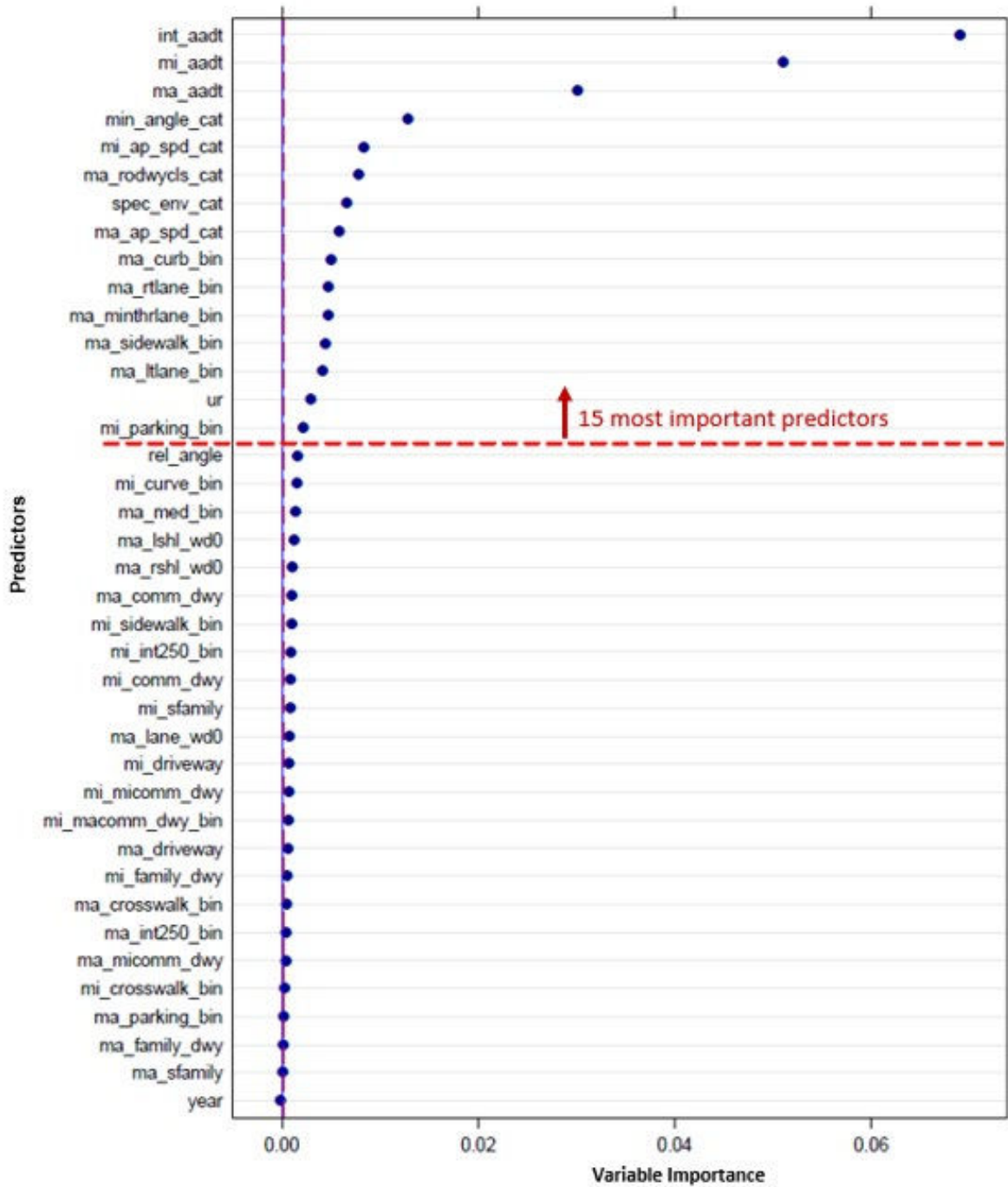
Variable Name	Descriptor	Definition and Attributes
<i>ma_curb_bin</i>	Curb presence (major road)—binary variable	0 = no, 1 = yes
<i>ur</i>	Urban or rural—binary variable	U = urban, R = rural
<i>ma_rodwycls_cat</i>	Roadway classification (major road)—categorical variable	1 = urban two-lane roads, 2 = urban multilane divided or nondivided nonfreeway, 3 = rural two-lane roads, 4 = rural multilane divided or nondivided nonfreeway
<i>spec_env_cat</i>	Specific environment—categorical variable	1 = strip commercial area or shopping center, 2 = residential area, 3 = agriculture, agriculture and isolated business/school, 0 = commercial business development or other
<i>mi_macomm_dwy_bin</i>	Major commercial driveway presence (minor road)—binary variable	0 = no, 1 = yes
<i>ma_micomm_dwy</i>	Number of minor commercial driveways—major road	Total number of minor commercial/industrial driveways on the major-road approaches within 250 ft of intersection.
<i>mi_micomm_dwy</i>	Number of minor commercial driveways—minor road	Total number of minor commercial/industrial driveways on the minor-road approaches within 250 ft of intersection
<i>ma_comm_dwy</i>	Number of commercial driveways—major road	Total number of commercial/industrial driveways on the major-road approaches within 250 ft of intersection
<i>mi_comm_dwy</i>	Number of commercial driveways—minor road	Total number of commercial/industrial driveways on the minor-road approaches within 250 ft of intersection
<i>ma_sfamily</i>	Number of single family residential driveways—major road	Total number of single family residential driveways on the major-road approaches within 250 ft of intersection
<i>mi_sfamily</i>	Number of single family residential driveways—minor road	Total number of single family residential driveways on the minor-road approaches within 250 ft of intersection
<i>ma_family_dwy</i>	Number of family residential driveways—major road	Total number of family residential driveways including single and multifamily driveways on the major-road approaches within 250 ft of intersection
<i>mi_family_dwy</i>	Number of family residential driveways—minor road	Total number of family residential driveways including single and multifamily driveways on the minor-road approaches within 250 ft of intersection
<i>ma_driveway</i>	Number of driveways—major road	Total number of all driveways on the major-road legs including major commercial/industrial driveways, minor commercial/industrial driveways, single family residential driveways, and multifamily residential driveways

Variable Name	Descriptor	Definition and Attributes
<i>mi_driveway</i>	Number of driveways—minor road	Total number of all driveways on the minor-road legs including major commercial/industrial driveways, minor commercial/industrial driveways, single family residential driveways, and multifamily residential driveways
<i>ma_aadt</i>	Total entering AADT—major road	Average of AADT on the two major-road legs
<i>mi_aadt</i>	Total entering AADT—minor road	Average of AADT on the two minor-road legs
<i>int_aadt</i>	Total entering AADT—intersection	$int\ AADT = ma\ AADT + mi\ AADT$
<i>ma_ap_spd_cat</i>	Speed limit (major road)—categorical variable	1 = average speed limit on major road = 0–31, 2 = average speed limit = 31–54, 3 = average speed limit > = 55
<i>mi_ap_spd_cat</i>	Speed limit (minor road)—categorical variable	1 = average speed limit on minor road = 0–31, 2 = average speed limit = 31–54, 3 = average speed limit > = 55
<i>ma_lshl_wd0</i>	Major road left-shoulder width	Average left-shoulder width in ft on the major road
<i>ma_rshl_wd0</i>	Major road right-shoulder width	Average right-shoulder width in ft on the major road
<i>ma_lane_wd0</i>	Major road lane width	Average lane width in ft on the major road
<i>mi_int</i>	Minor road AADT Ratio	Ratio of minor road AADT to intersection AADT: $mi_int = mi_aadt/int_aadt$
<i>lgmi_aadt</i>	Log value of minor road AADT	$lgmi_aadt = \ln(mi_aadt)$
<i>lgint_aadt</i>	Log value of intersection AADT	$lgint_aadt = \ln(int_aadt)$
<i>lgcos_int</i>	Derived variable-cos(min_angle) and intersection AADT	Derived variable that incorporates intersection AADT and cosine of the intersection angle: $lgcos_int = \ln[(int_aadt) \times (1 + \cos(min_angle))]$
<i>lgcos_mi</i>	Derived variable-cos(min_angle) and minor road AADT	Derived variable that incorporates minor road AADT and cosine of the intersection angle: $lgcos_mi = \ln[(mi_aadt) \times (1 + \cos(min_angle))]$
<i>lgcos_l</i>	Derived variable	$lgcos_l = 1 + \ln[1 + \cos(angle)]$
<i>cosl_lgint</i>	Interaction term of intersection AADT and cosine of the intersection angle	$cosl_lgint = [1 + \cos(angle)] \times \ln(intersection_aadt)$
<i>cosl_mmiint</i>	Interaction term of minor road to intersection AADT ratio and cosine of the intersection angle	$cosl_mmiint = [1 + \cos(angle)] \times (minor\ road\ aadt/intersection\ aadt)$
<i>angRl_mint</i>	Interaction term of intersection AADT and skew angle expressed in radians	$angRl_mint = [1 + (90-angle)\pi/180] \times \ln(intersection\ aadt)$



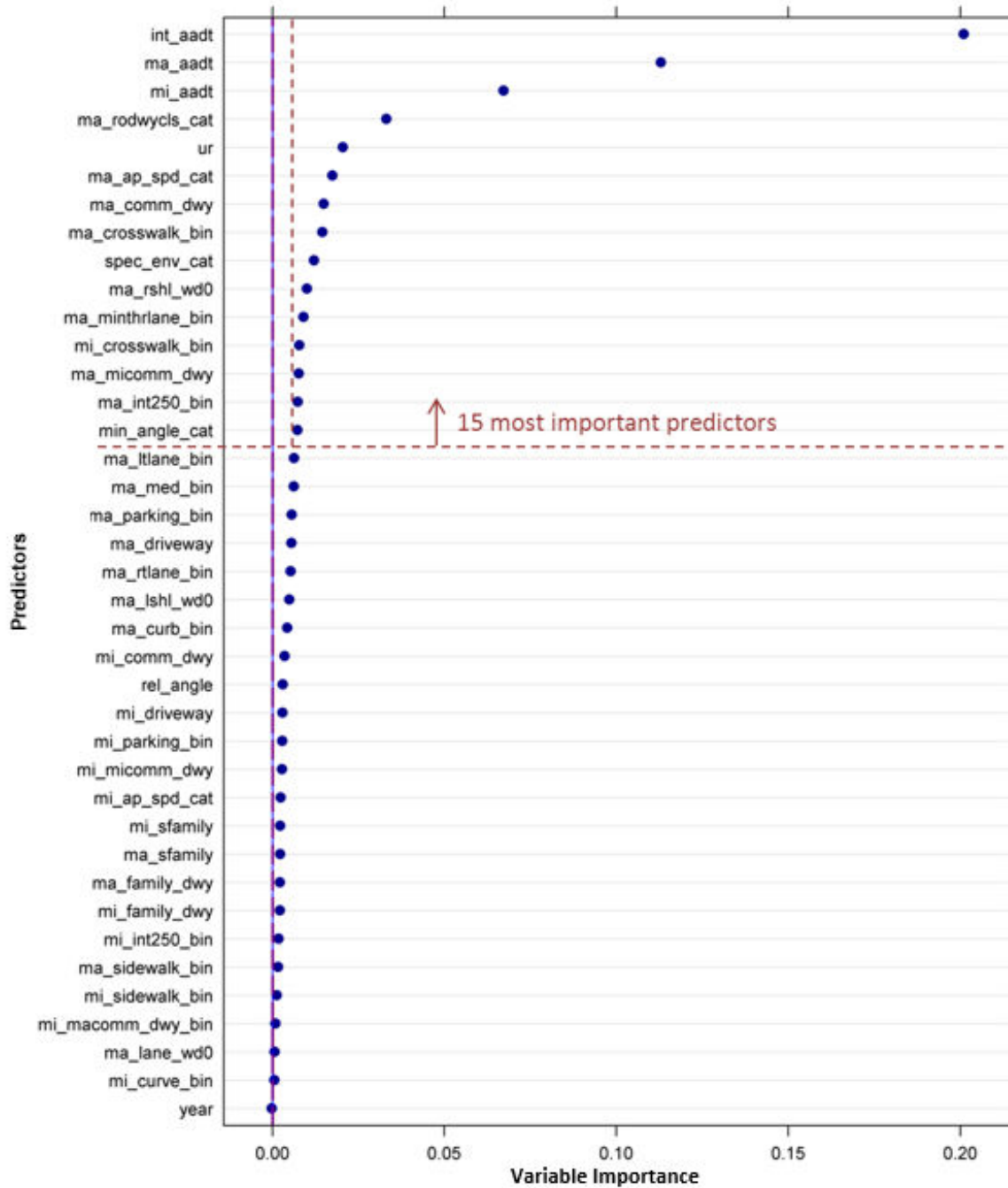
Source: FHWA.

Figure 76. Plot. Conditional RF (cforest) results for total crashes at four-leg intersections.



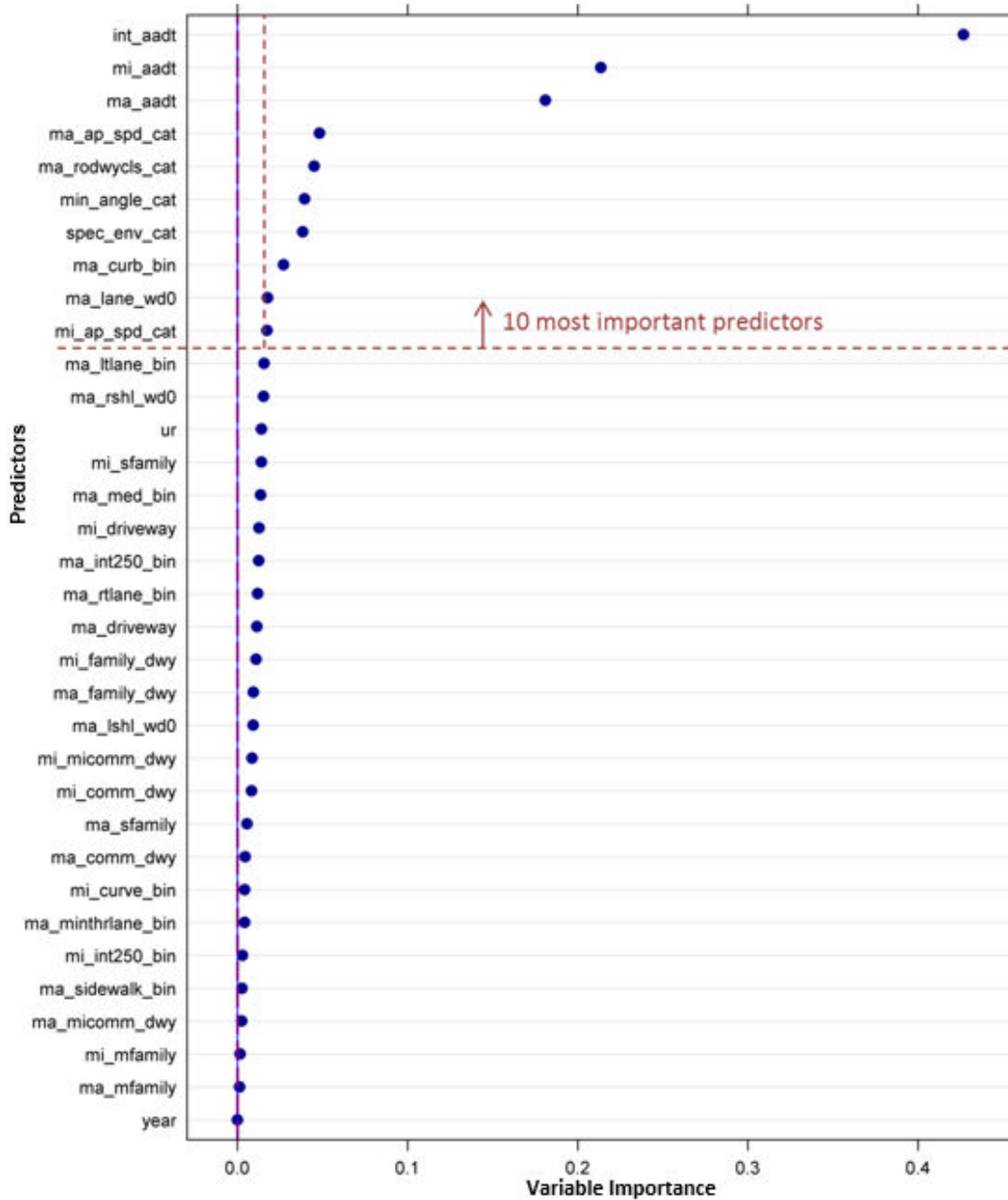
Source: FHWA.

Figure 77. Plot. Conditional RF (cforest) results for fatal-and-injury crashes at four-leg intersections.



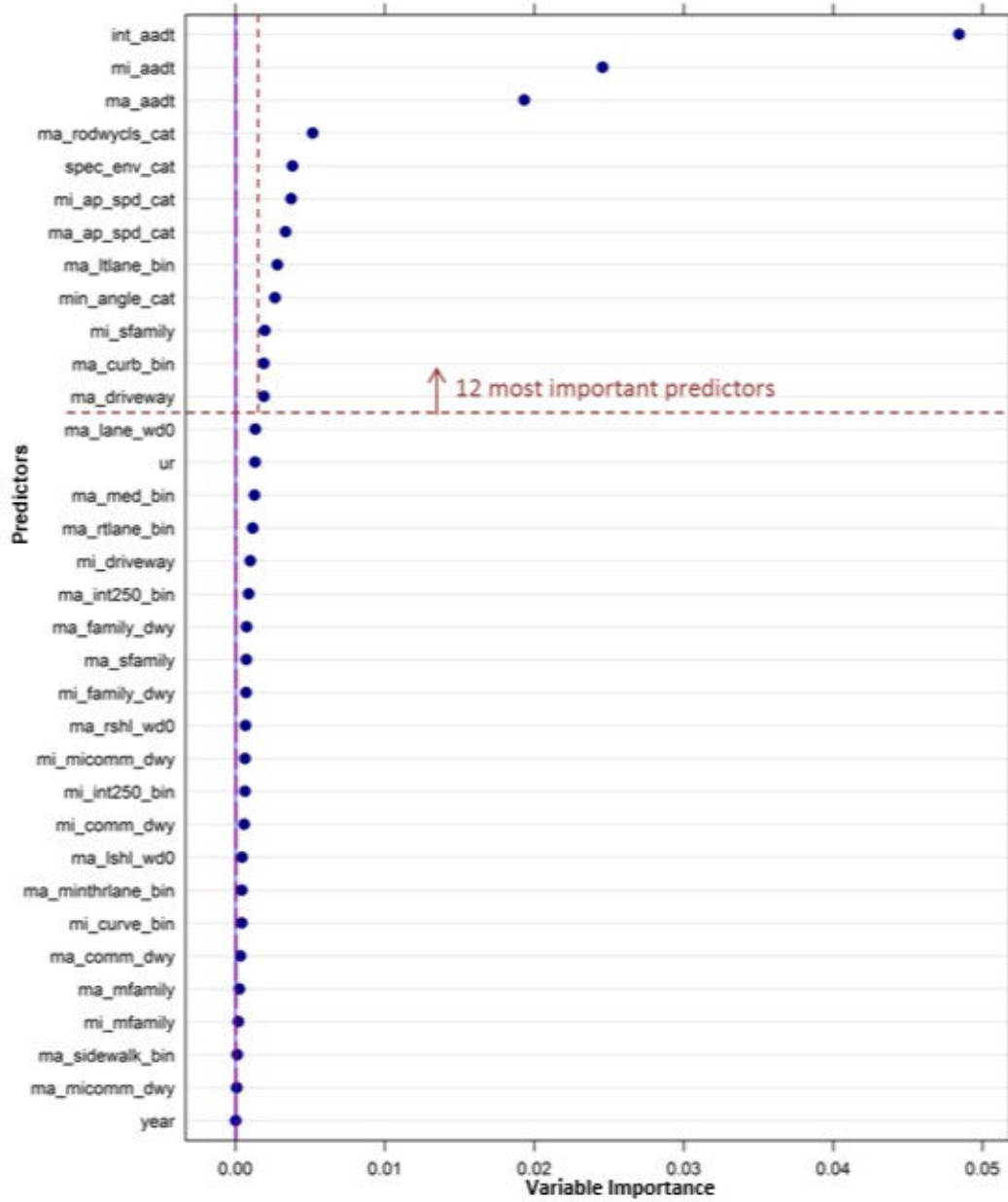
Source: FHWA.

Figure 78. Plot. Conditional RF (cforest) results for PDO crashes at four-leg intersections.



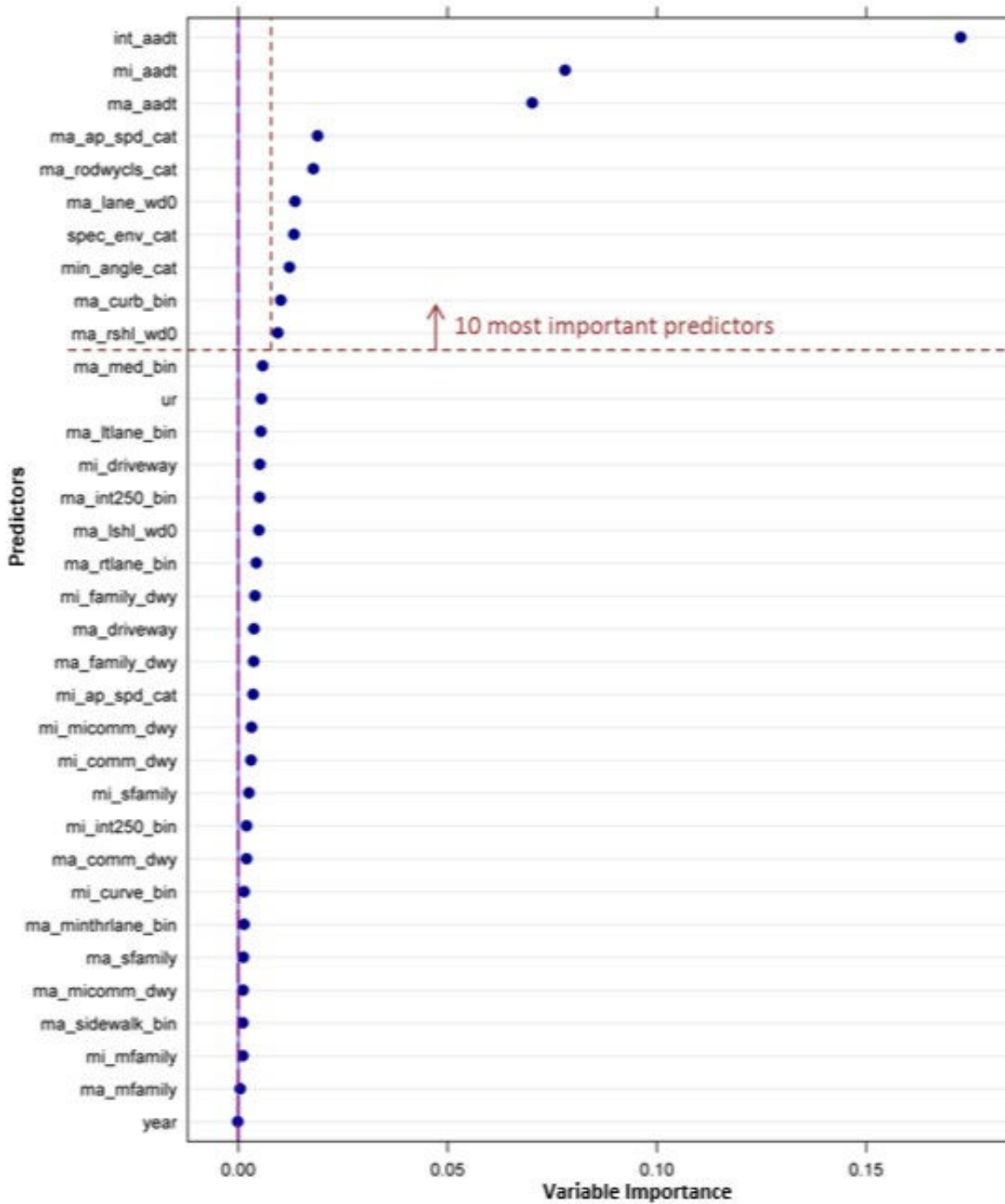
Source: FHWA.

Figure 79. Plot. Conditional RF (cforest) results for total crashes at three-leg intersections.



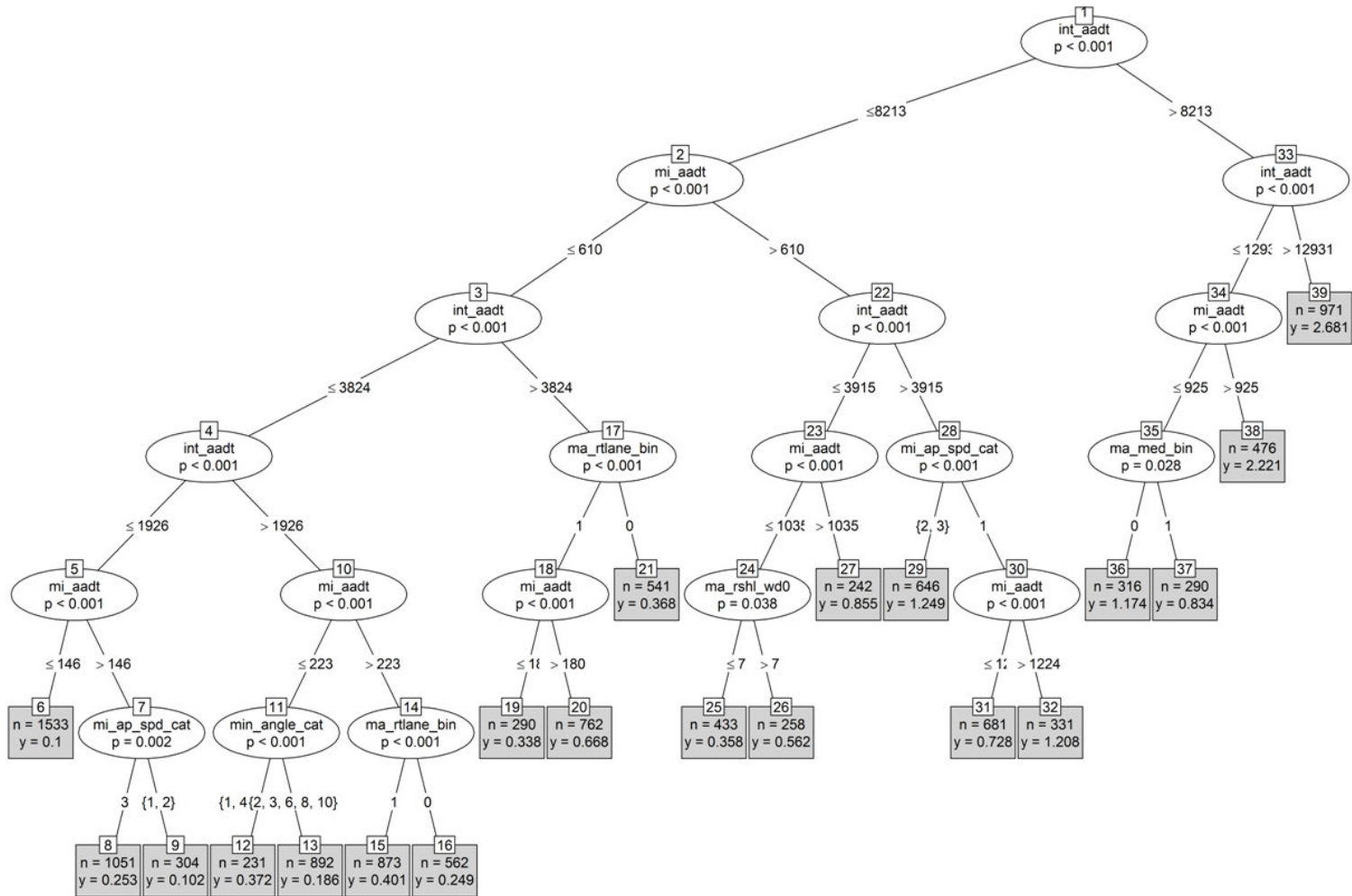
Source: FHWA.

Figure 80. Plot. Conditional RF (cforest) results for fatal-and-injury crashes at three-leg intersections.



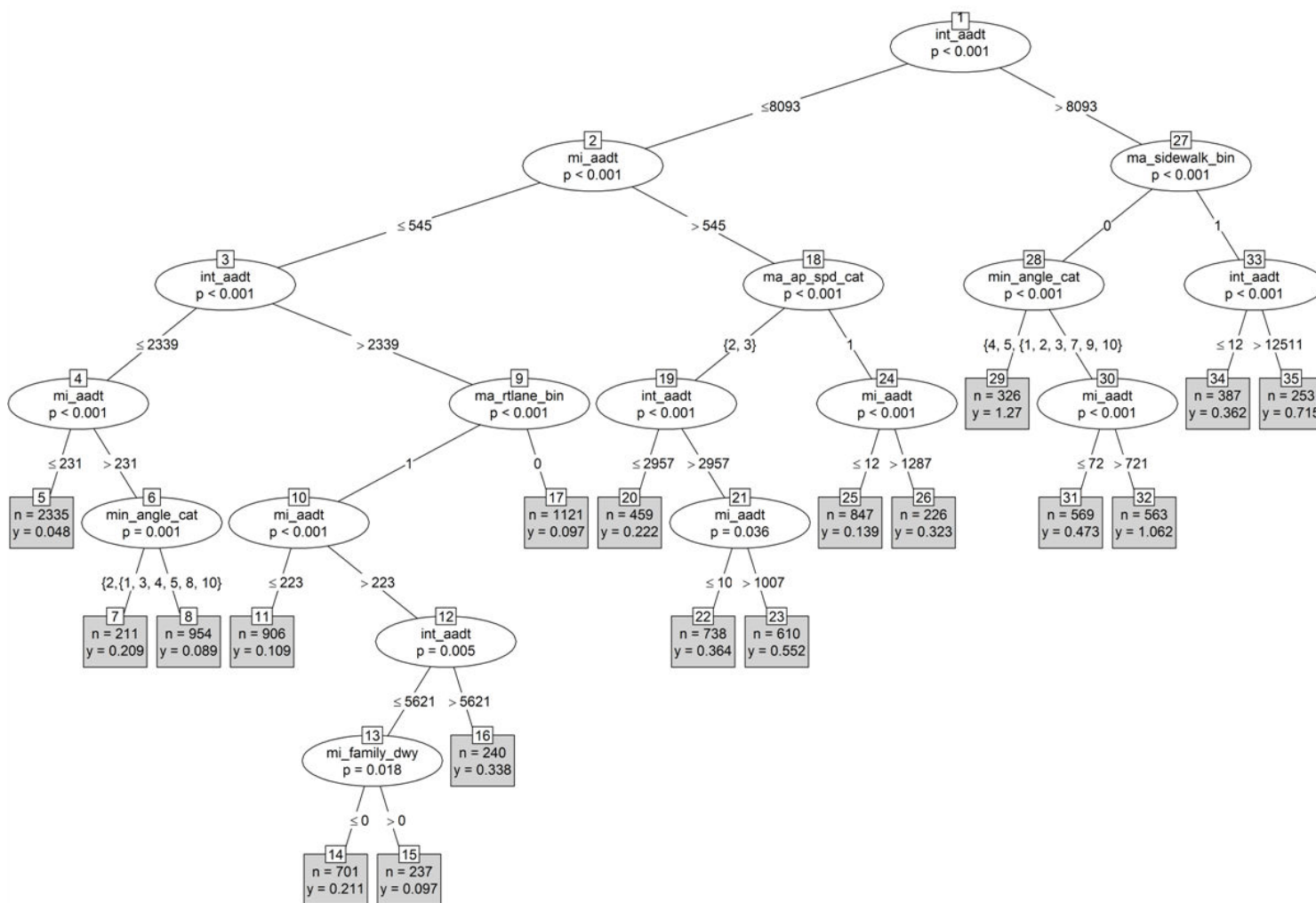
Source: FHWA.

Figure 81. Plot. Conditional RF (cforest) results for PDO crashes at three-leg intersections.



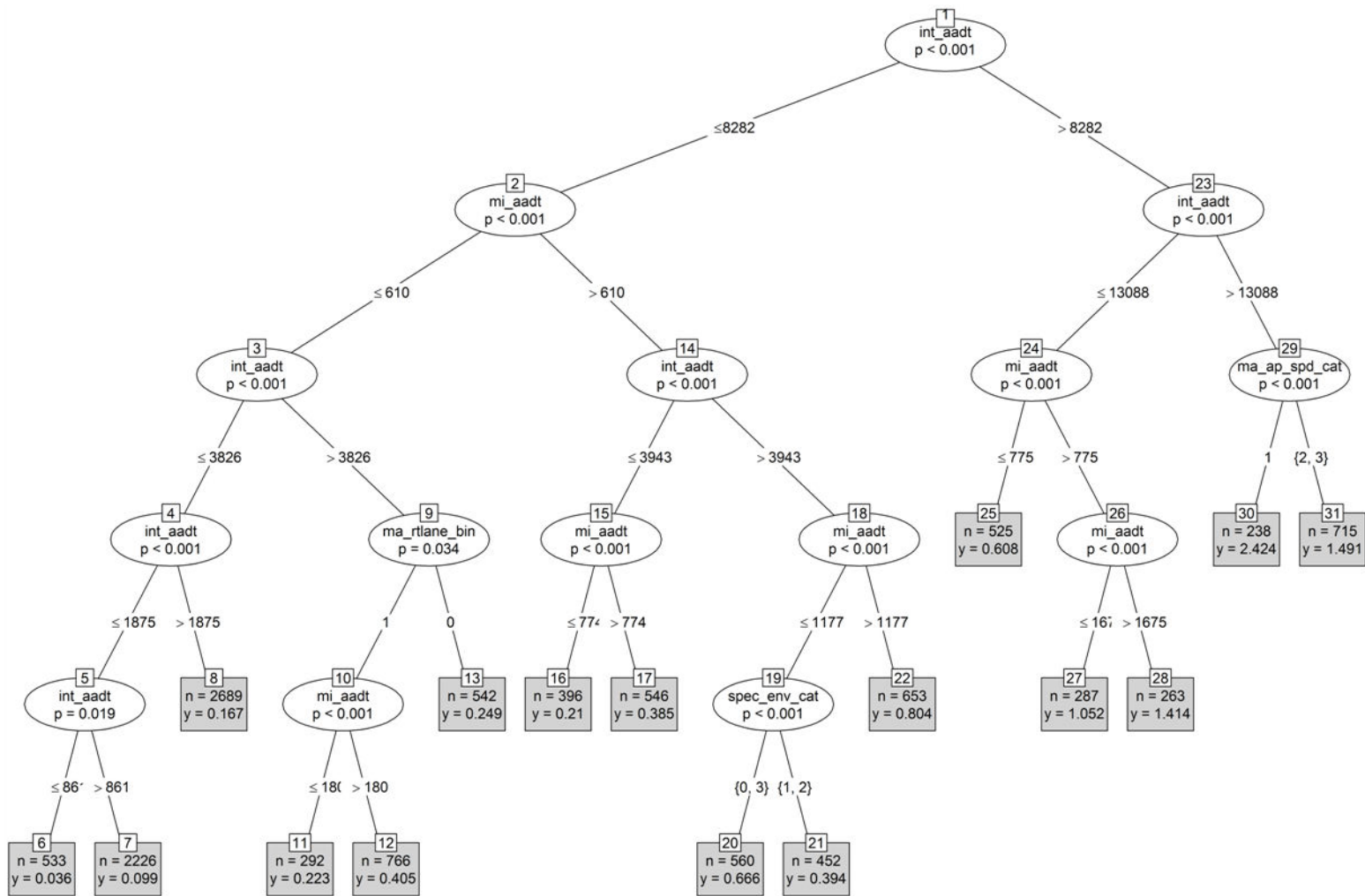
Source: FHWA.

Figure 82. Plot. Regression tree for total crashes at four-leg intersections (results from ctree analysis).



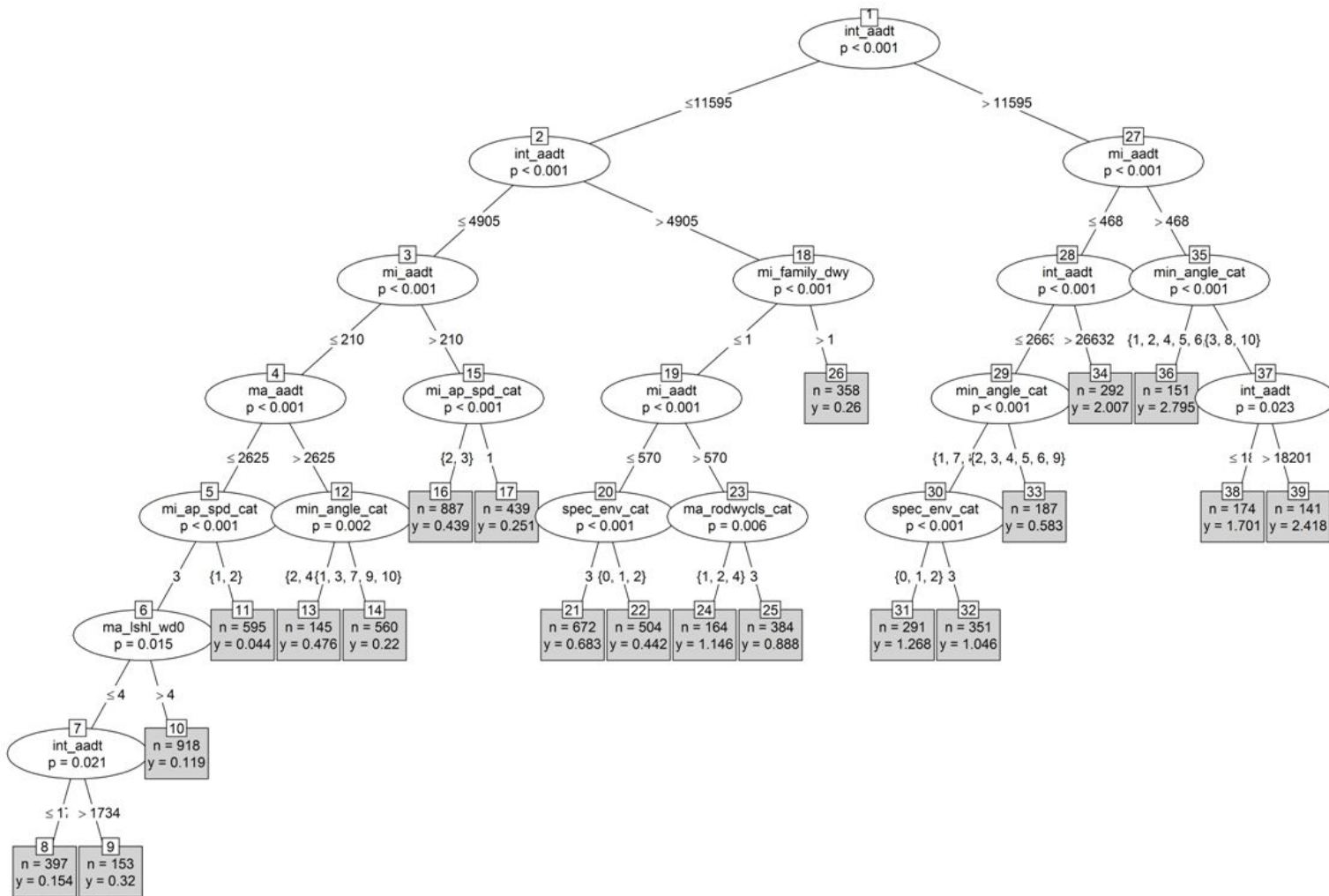
Source: FHWA.

Figure 83. Plot. Regression tree for fatal-and-injury crashes at four-leg intersections (results from ctree analysis).



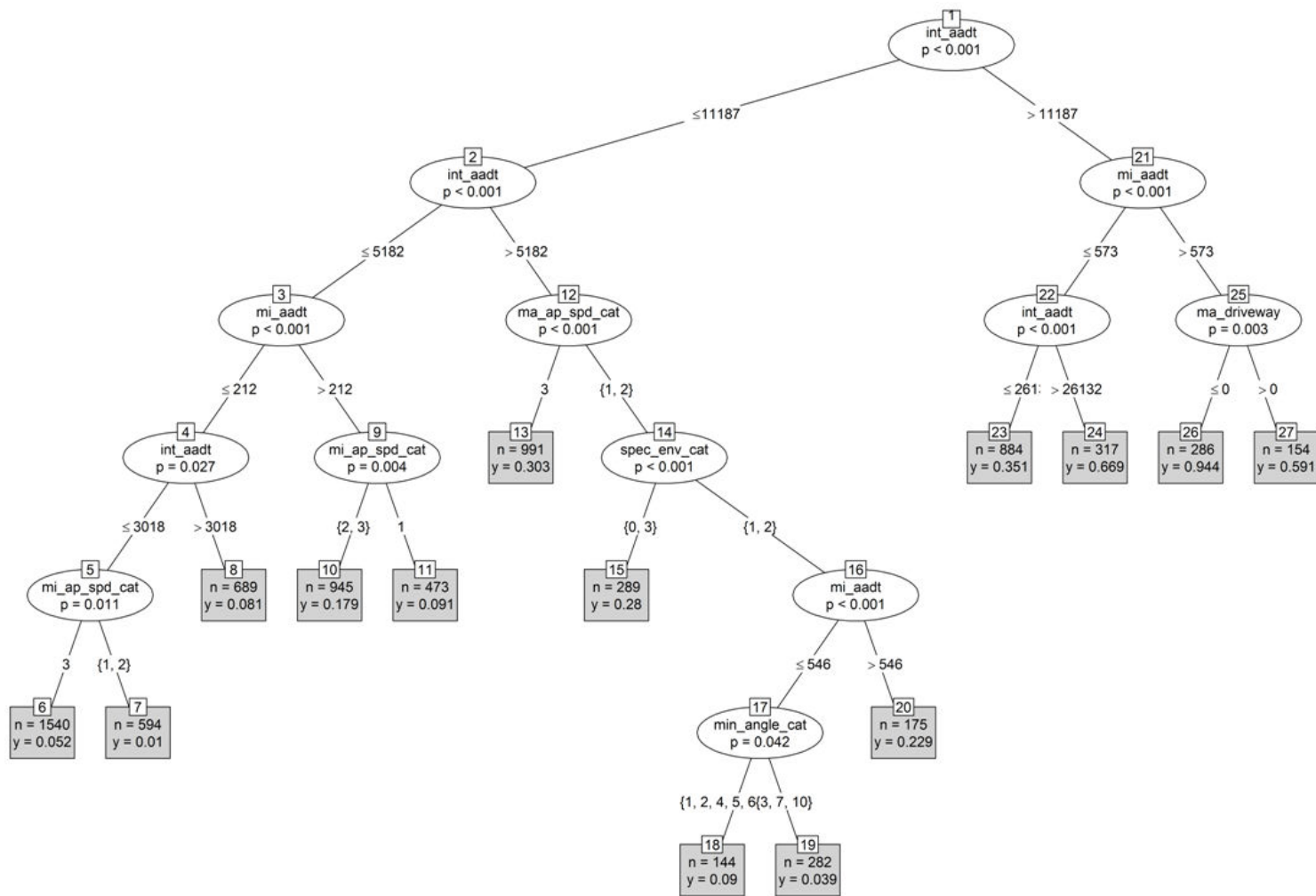
Source: FHWA.

Figure 84. Plot. Regression tree for PDO crashes at four-leg intersections (results from ctree analysis).



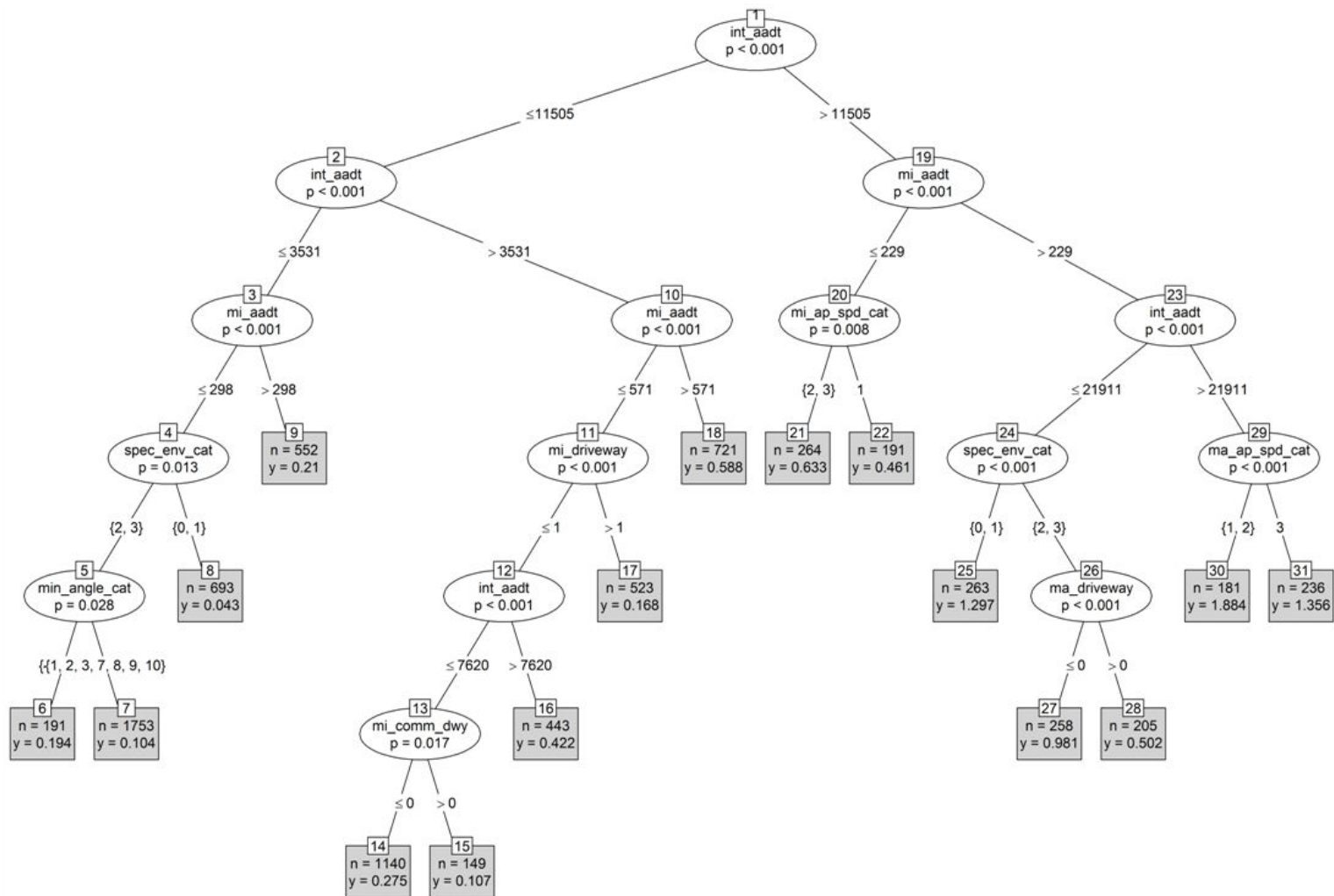
Source: FHWA.

Figure 85. Plot. Regression tree for total crashes at three-leg intersections (results from ctree analysis).



Source: FHWA.

Figure 86. Plot. Regression tree for injury crashes at three-leg intersections (results from ctree analysis).



Source: FHWA.

Figure 87. Plot. Regression tree for PDO crashes at three-leg intersections (results from ctree analysis).

DATA DESCRIPTORS FOR OHIO

Table 74. Variable names, descriptors, definitions, and attributes for OH.

Variable Name	Descriptor	Definition and Attributes
<i>min_angle</i>	Minimum angle	Minimum angle of intersection—smallest measured angle at the intersection (defined as intersection angle).
<i>lighting</i>	Lighting	A binary categorical variable capturing whether lighting is present at the intersection.
<i>ma_division</i>	Roadway division of major approach	A binary categorical variable capturing the division status of the major roadway at the intersection (D = divided; U = undivided).
<i>ma_rodwycls_cat</i>	Functional classification of major approach	A categorical variable capturing the functional classification of the roadway (e.g., local, minor collector, major collector, minor arterial, principal arterial).
<i>ma_aadt</i>	AADT of major approach	Average of AADT on the two major-road legs.
<i>mi_aadt</i>	AADT of minor approach	Average of AADT on the two minor-road legs.
<i>int_aadt</i>	Total intersection AADT	$int_aadt = ma_aadt + mi_aadt$
<i>mi_int</i>	Minor road/intersection AADT ratio	Ratio of minor road AADT to intersection AADT: $mi_int = mi_aadt/int_aadt$
<i>lgma_aadt</i>	Natural log of major approach AADT	$lgma_aadt = ln(mi_aadt)$
<i>lgmi_aadt</i>	Natural log of minor approach AADT	$lgmi_aadt = ln(mi_aadt)$
<i>lgint_aadt</i>	Natural log of total intersection AADT	$lgint_aadt = ln(int_aadt)$
<i>lgmi_int</i>	Natural log of minor road/intersection AADT ratio	$lgmi_int = ln(mi_int)$
<i>lgcos_int</i>	Cosine term of the intersection AADT term	Derived variable that incorporates intersection AADT and cosine of the intersection angle: $lgcos_int = ln[(int_aadt) \times (1 + \cos(min_angle))]$
<i>lgcos_mi</i>	Cosine term of the minor approach AADT term	Derived variable that incorporates minor road AADT and cosine of the intersection angle: $lgcos_mi = ln[(mi_aadt) \times (1 + \cos(min_angle))]$
<i>lgmin_angle</i>	Natural log of minimum angle	$lgmin_angle = ln(min_angle)$

Table 75. Number of sites in each angle bin for all rural, four-leg intersections in OH.

Minimum Angle Bin	Frequency	Percent
11–20	—	—
21–30	19	0.57
31–40	72	2.16
41–50	164	4.92
51–60	284	8.52
61–70	402	12.05
71–80	540	16.19
80+	1,854	55.59

—No data available.

Table 76. Number of sites in each angle bin for rural four-leg two-lane intersections in OH.

Minimum Angle Bin	Frequency	Percent
11-20	—	—
21-30	19	0.59
31-40	71	2.20
41-50	160	4.96
51-60	279	8.65
61-70	372	11.53
71-80	523	16.21
80+	1,803	55.87

—No data available.

Table 77. Number of sites in each angle bin for rural four-leg multilane intersections in OH.

Minimum Angle Bin	Frequency	Percent
11-20	—	—
21-30	—	—
31-40	—	—
41-50	—	—
51-60	5	4.85
61-70	30	29.13
71-80	17	16.50
80+	51	49.51

—No data available.

Table 78. Number of sites in each angle bin for rural three-leg total intersections in OH.

Minimum Angle Bin	Frequency	Percent
11-20	76	1.09
21-30	214	3.08
31-40	250	3.60
41-50	409	5.88
51-60	549	7.90
61-70	881	12.67
71-80	1,409	20.27
80+	3,163	45.50

Table 79. Number of sites in each angle bin for rural three-leg two-lane intersections in OH.

Minimum Angle Bin	Frequency	Percent
11-20	76	1.11
21-30	214	3.12
31-40	249	3.63
41-50	406	5.91
51-60	549	7.99
61-70	867	12.62
71-80	1,394	20.30
80+	3,113	45.33

Table 80. Number of sites in each angle bin for urban four-leg total intersections in OH.

Minimum Angle Bin	Frequency	Percent
11-20	—	—
21-30	—	—
31-40	11	2.59
41-50	23	5.42
51-60	41	9.67
61-70	55	12.97
71-80	94	22.17
80+	200	47.17

—No data available.

Table 81. Number of sites in each angle bin for urban four-leg two-lane intersections in OH.

Minimum Angle Bin	Frequency	Percent
11-20	—	—
21-30	—	—
31-40	11	2.95
41-50	23	6.17
51-60	36	9.65
61-70	47	12.60
71-80	81	21.72
80+	175	46.92

—No data available.

Table 82. Number of sites in each angle bin for urban three-leg total intersections in OH.

Minimum Angle Bin	Frequency	Percent
11-20	12	0.71
21-30	29	1.73
31-40	38	2.26
41-50	36	2.14
51-60	99	5.89
61-70	201	11.96
71-80	310	18.44
80+	956	56.87

Table 83. Number of sites in each angle bin for urban three-leg two-lane intersections in OH.

Minimum Angle Bin	Frequency	Percent
11-20	11	0.75
21-30	28	1.91
31-40	34	2.32
41-50	35	2.38
51-60	93	6.34
61-70	181	12.33
71-80	273	18.60
80+	813	55.38

APPENDIX E. SUPPLEMENTAL SAFETY-PREDICTION MODELS

The NB regression models developed for total crashes for four-leg and three-leg intersections were presented and discussed in chapter 5. Included in this appendix are the results for the remaining models developed as part of the analysis and used for the derivation of intersection angle CMFs. Models are only included if the intersection-angle parameters were significant and the models converged. Table 84 summarizes the additional severity models for MN and OH. All models were independently derived; therefore, the results from models for PDO crashes cannot be combined with results from models for fatal-and-injury models to produce an estimate equivalent to the estimate produced from the model for total crashes. Only total crash (all severities) models were developed for OH data.

Table 84. Summary of severity models included in appendix E.

State	Intersection Category	Collision Category	Model Type	Corresponding Table
MN	Four-leg—all sites, rural and urban	Total	Base	Table 85
MN	Four-leg—all sites, rural and urban	Total	Interaction	Table 86
MN	Four-leg—all sites, rural and urban	Total	Alternative base	Table 87
MN	Four-leg—all sites, rural and urban	Fatal and injury	Flexible form model 1	Table 92
MN	Four-leg—all sites, rural and urban	PDO	Alternative base	Table 93
MN	Four-leg—all sites, rural and urban	PDO	Flexible form model 1	Table 94
MN	Four-leg—all rural sites	Total	Alternative base	Table 95
MN	Four-leg—all rural sites	Total	Flexible form model 1	Table 96
MN	Four-leg—all rural sites	Fatal and injury	Alternative base	Table 97
MN	Four-leg—all rural sites	Fatal and injury	Flexible form model 1	Table 98
MN	Four-leg—all rural sites	PDO	Alternative base	Table 99
MN	Four-leg—all rural sites	PDO	Flexible form model 1	Table 100
MN	Four-leg—rural two-lane sites	Total	Alternative base	Table 101
MN	Four-leg—rural two-lane sites	Total	Flexible form model 1	Table 102
MN	Four-leg—rural two-lane sites	Fatal and injury	Flexible form model 1	Table 103
MN	Four-leg—rural two-lane sites	PDO	Alternative base	Table 104
MN	Four-leg—rural two-lane sites	PDO	Flexible form model 1	Table 104
MN	Four-leg—multilane rural sites	Total	Alternative base	Table 105
MN	Four-leg—multilane rural sites	Total	Flexible form model 1	Table 107
MN	Four-leg—multilane rural sites	Fatal and injury	Flexible form model 2	Table 108
MN	Four-leg—multilane rural sites	PDO	Alternative base	Table 109
MN	Four-leg—multilane rural sites	PDO	Flexible form model 2	Table 110
MN	Three-leg—all sites, rural and urban	Total	Base	Table 88
MN	Three-leg—all sites, rural and urban	Total	Alternative base	Table 89
MN	Three-leg—all sites, rural and urban	Total	Flexible form model 2	Table 90
MN	Three-leg—all sites, rural and urban	Total	Interaction model	Table 91
OH	Four-leg—rural two-lane sites	Total	Flexible form model 1	Table 111
OH	Four-leg—multilane rural sites	Total	Flexible form model 1	Table 112
OH	Four-leg—two-lane urban sites	Total	Flexible form model 1	Table 114
OH	Three-leg—rural two-lane sites	Total	Hoerl curve	Table 113
OH	Three-leg—two-lane urban sites	Total	Flexible form model 1	Table 115

MN SUPPLEMENTAL SAFETY-PREDICTION MODELS

All Four-Leg Intersections—Base Models for Total Crashes

The first set of models developed for four-leg intersections was for total crashes, including all rural and urban sites. The database included 8,482 crashes distributed across 1,669 intersections over a 7-year period. Intersection AADT, major road AADT, and minor road AADT were among the 16 most important predictors from the conditional RF analysis. Scatterplots of these variables are shown in figure 88 and figure 89. Major road AADT and intersection AADT are highly correlated; they each have a Pearson Correlation Coefficient (r) equal to 0.995. Minor road AADT and intersection AADT do not share the same level of correlation ($r = 0.380$). Intersection AADT and minor road AADT were also the two AADT variables that most frequently appeared in the regression tree results. Thus, intersection AADT and minor road AADT were selected for inclusion in the models. Major road AADT was not selected because of its strong correlation with intersection AADT.

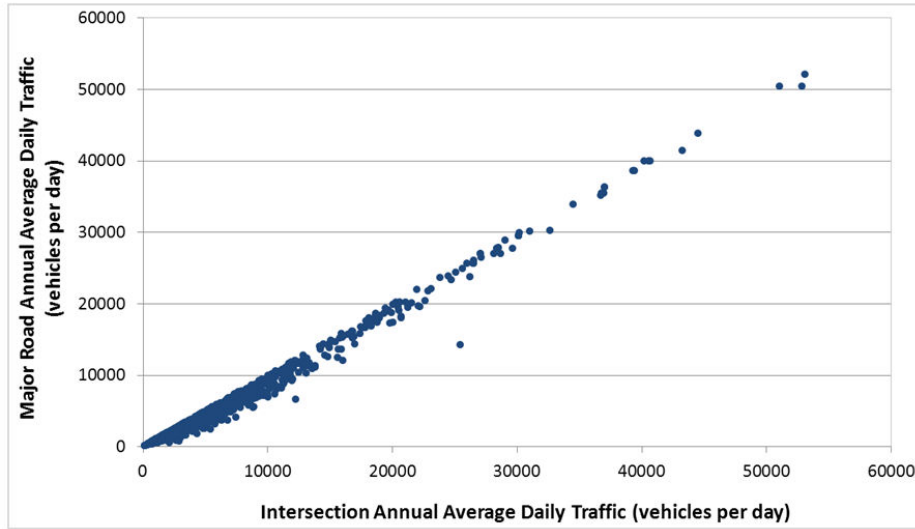
Additionally, each developed model was examined by substituting intersection AADT with major road AADT. The researchers confirmed that the model including intersection AADT better fits the data compared to the model with major road AADT in terms of lower value of AIC and BIC.

The initial base model, with only the significant variables ($p \leq 0.05$) retained, is shown in table 85. Both intersection AADT and minor road AADT are significant, predicting an increase in crashes as either value increases. Intersection angle (*min_angle*) is significant with a p -value of 0.0203. For each one degree increase in angle (i.e., moving toward a right angle), total crashes are estimated to decrease by 0.0021.

Major roadway class (*ma_rodwycls_cat*) is also significant for the category of rural two-lane roads compared to rural multilane roads. However, urban multilane roads and two-lane roads are not significantly different from rural multilane roads. Adjacent land use (*spec_env_cat*) is another significant variable, indicating significant differences between the rural agricultural land use and the other categories of central business district, commercial/strip development, and other. The speed limit on the major roadway (*ma_ap_spd_cat*) is significant, indicating a difference between intersections with a major road speed limit of 30 mph or less and those greater than 50 mph. Finally, the right-shoulder width on the major road is also significant, indicating a decrease in crashes as the shoulder width increases.

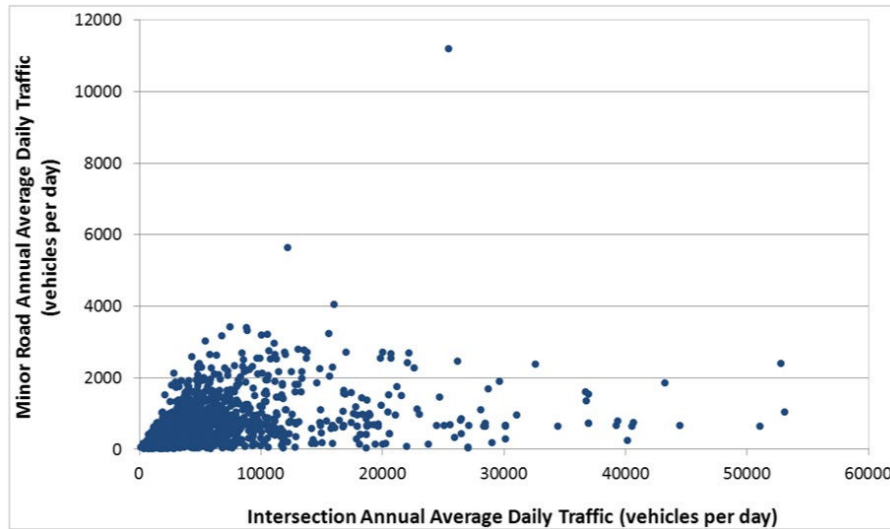
The next model developed was an alternative base model that included an additional variable for the ratio of minor road AADT to intersection AADT (*mi_int*). All other variables from the initial base model were retained. The model parameters are shown in table 86. The added variable is significant with a p -value of 0.0014. As the proportion of traffic on the minor road increases relative to total intersection AADT, total crashes are predicted to increase using this model. All variables that were significant in the initial base model are also significant in this alternative model. The parameter estimate for intersection angle is the same (-0.0021) in both models. There was very little change in the BIC for the two models, from 23,088 for the initial model to 23,087 for the alternative model. However, the improvement in the AIC was substantial, from

22,985 for the initial model to 22,977. Thus, the alternative model is considered an improved model.



Source: FHWA.

Figure 88. Graph. Scatterplot of intersection AADT versus major road AADT for all four-leg intersections in MN.



Source: FHWA.

Figure 89. Graph. Scatterplot of intersection AADT versus minor road AADT for all four-leg intersections in MN.

Table 85. Initial base model results for total crashes at all four-leg intersections in MN.

Parameter Description	Estimate	Standard Error	Lower 95% CL	Upper 95% CL	Chi-Square	Statistical Significance
Intercept	-9.1045	0.2269	-9.5493	-8.6597	1,609.38	<0.0001
lgint aadt	0.7757	0.024	0.7287	0.8228	1,042.83	<0.0001
lgmi aadt	0.4127	0.0161	0.3811	0.4443	655.73	<0.0001
ma rodwycls cat (1)	0.2081	0.0575	0.0954	0.3209	13.09	0.0003
ma rodwycls cat (2)	0.0957	0.0618	-0.0255	0.2168	2.39	0.1218
ma rodwycls cat (3)	-0.0402	0.0476	-0.1335	0.053	0.71	0.3979
ma rodwycls cat (4)	0	0	0	0	—	—
spec env cat (0)	-0.1283	0.0549	-0.2359	-0.0208	5.47	0.0194
spec env cat (1)	-0.1251	0.0539	-0.2308	-0.0194	5.38	0.0203
spec env cat (2)	-0.4892	0.0575	-0.6018	-0.3765	72.44	<0.0001
spec env cat (3)	0	0	0	0	—	—
min angle	-0.0021	0.0009	-0.0039	-0.0003	5.38	0.0203
ma ap spd cat (1)	-0.2434	0.0584	-0.3579	-0.1289	17.36	<0.0001
ma ap spd cat (2)	-0.0814	0.0526	-0.1845	0.0218	2.39	0.1221
ma ap spd cat (3)	0	0	0	0	—	—
ma rshl wd0	-0.021	0.0049	-0.0305	-0.0115	18.79	<0.0001
Dispersion	0.4323	0.0247	0.3866	0.4834	—	—
Goodness-of-fit parameter: AIC (smaller is better)	22,985	—	—	—	—	—
Goodness-of-fit parameter: BIC (smaller is better)	23,088	—	—	—	—	—

—No data available.

Table 86. Alternative base model results for total crashes at all four-leg intersections in MN.

Parameter Description	Estimate	Standard Error	Lower 95% CL	Upper 95% CL	Chi-Square	Statistical Significance
Intercept	-9.3507	0.2401	-9.8213	-8.88	1,516.36	<0.0001
lgint aadt	0.8458	0.0325	0.7821	0.9096	676.14	<0.0001
lgmi aadt	0.3383	0.0282	0.283	0.3936	143.63	<0.0001
mi int	0.7304	0.2288	0.282	1.1788	10.19	0.0014
ma rodwycls cat (1)	0.2213	0.0576	0.1083	0.3343	14.74	0.0001
ma rodwycls cat (2)	0.1003	0.0618	-0.0209	0.2215	2.63	0.1048
ma rodwycls cat (3)	-0.044	0.0476	-0.1373	0.0494	0.85	0.3558
ma rodwycls cat (4)	0	0	0	0	—	—
spec env cat (0)	-0.1166	0.055	-0.2243	-0.0088	4.49	0.034
spec env cat (1)	-0.1194	0.054	-0.2251	-0.0136	4.89	0.0269
spec env cat (2)	-0.4781	0.0576	-0.5909	-0.3652	68.98	<0.0001
spec env cat (3)	0	0	0	0	—	—
min angle	-0.0021	0.0009	-0.0039	-0.0003	5.39	0.0202
ma ap spd cat (1)	-0.241	0.0584	-0.3555	-0.1265	17.02	<0.0001
ma ap spd cat (2)	-0.0894	0.0527	-0.1927	0.0139	2.88	0.0898
ma ap spd cat (3)	0	0	0	0	—	—
ma rshl wd0	-0.0206	0.0049	-0.0302	-0.0111	18.12	<0.0001
Dispersion	0.4326	0.0246	0.3869	0.4836	—	—
Goodness-of-fit parameter: AIC (smaller is better)	22,977	—	—	—	—	—
Goodness-of-fit parameter: BIC (smaller is better)	23,087	—	—	—	—	—

—No data available.

All Four-Leg Intersections—Interaction Model for Total Crashes

The final model developed was built on the results found in the flexible form models. The objective was to develop a model with an improved fit, but with parameters that accounted for the interaction between angle and traffic volume, knowing that traffic volume is commonly known to be the strongest predictor of crashes. These parameters could then be used to develop a more robust crash modification function (CMFunction) for intersection angle that accounts for changes in traffic volumes.

Through a series of trial and error experiments with varying interaction forms, the final set of interaction terms used in the model are shown in figure 90, figure 91, and figure 92.

$$cos1_lgint = [1 + \cos(\text{angle})] \times \ln(\text{intersection aadt})$$

Figure 90. Equation. Interaction term of intersection AADT and cosine of the intersection angle.

$$\text{cos1_mimiint} = [1 + \cos(\text{angle})] \times (\text{minor road aadt}/\text{intersection aadt})$$

Figure 91. Equation. Interaction term of minor road to intersection AADT ratio and cosine of the intersection angle.

$$\text{angR1_mint} = [1 + (90 - \text{angle})\pi/180] \times \ln(\text{intersection aadt})$$

Figure 92. Equation. Interaction term of intersection AADT and skew angle expressed in radians.

In all three of these variables in figure 90, figure 91, and figure 92, the angle term becomes 1.0 when the intersection angle is 90 degrees. Thus, the predicted effect on crashes for right-angle intersections is a function of the intersection and minor road AADT terms in the three variables.

The interaction model is provided in table 87. The same set of significant variables for roadway classification, land use, speed limit, and right-shoulder width exist in this model with the same directional effects as previously included in the flexible form models. The variable *min_angle* was not significant in the final model. Instead, the effects of intersection angle are being accounted for within the three interaction terms, all of which are significant (*p*-values of <0.0001).

The BIC and AIC for this interaction model are 23,072 and 22,954, respectively. The flexible form model 1 values for BIC and AIC were 23,073 and 22,954, respectively. The lack of a difference in these two criteria indicates a negligible improvement in the model fit.

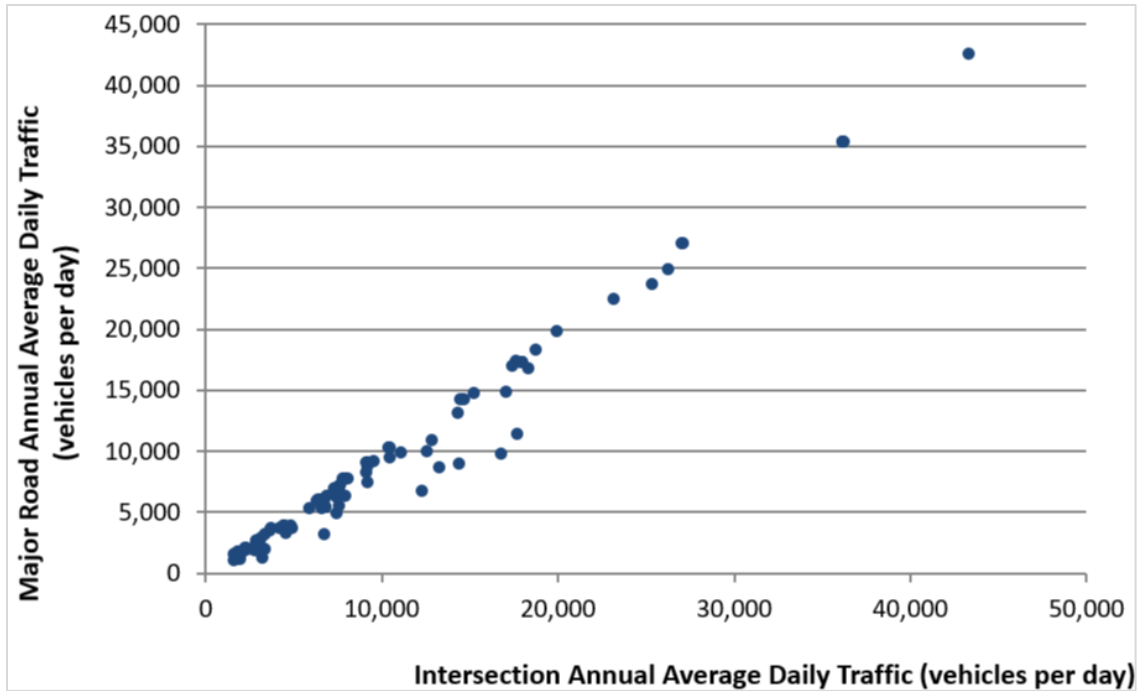
Table 87. Interaction model results for total crashes at all four-leg intersections in MN.

Parameter Description	Estimate	Standard Error	Lower 95% CL	Upper 95% CL	Chi-Square	Statistical Significance
Intercept	-9.4339	0.2234	-9.8719	-8.996	1,782.7	<0.0001
cos1 lgint	0.4688	0.0965	0.2797	0.6579	23.61	<0.0001
lgmi aadt	0.3438	0.0263	0.2923	0.3954	170.86	<0.0001
lgint aadt	0.7836	0.0361	0.7129	0.8543	471.96	<0.0001
angR1 mint	-0.4219	0.0882	-0.5947	-0.249	22.87	<0.0001
cos1 mmiint	0.5369	0.1712	0.2014	0.8725	9.84	0.0017
ma_rodwycls_cat (1)	0.2299	0.0575	0.1173	0.3426	16	<0.0001
ma_rodwycls_cat (2)	0.1145	0.0619	-0.0069	0.2358	3.42	0.0645
ma_rodwycls_cat (3)	-0.0354	0.0475	-0.1286	0.0578	0.55	0.4566
ma_rodwycls_cat (4)	0	0	0	0	—	—
spec env cat (0)	-0.1286	0.0549	-0.2363	-0.0209	5.48	0.0192
spec env cat (1)	-0.1273	0.0539	-0.2329	-0.0217	5.58	0.0182
spec env cat (2)	-0.48	0.0576	-0.5928	-0.3672	69.55	<0.0001
spec env cat (3)	0	0	0	0	—	—
ma ap spd cat (1)	-0.229	0.0583	-0.3432	-0.1147	15.42	<0.0001
ma ap spd cat (2)	-0.0898	0.0527	-0.1931	0.0135	2.9	0.0884
ma ap spd cat (3)	0	0	0	0	—	—
ma rshl wd0	-0.0221	0.0049	-0.0317	-0.0126	20.8	<0.0001
Dispersion	0.4259	0.0244	0.3806	0.4766	—	—
Goodness-of-fit parameter: AIC (smaller is better)	22,954	—	—	—	—	—
Goodness-of-fit parameter: BIC (smaller is better)	23,072	—	—	—	—	—

—No data available.

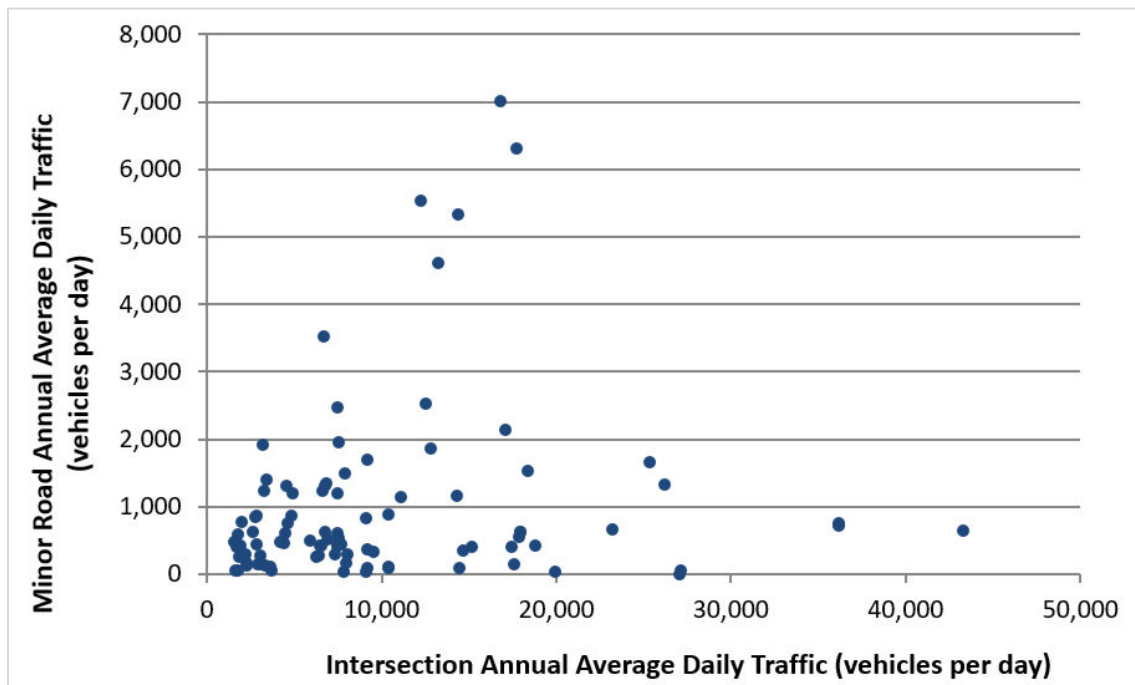
Three-Leg Intersections—Base Models for Total Crashes

The first set of models developed for three-leg intersections was for total crashes, which included all rural and urban sites. The database included 4,730 crashes distributed across 1,109 intersections over 7 yr. Intersection AADT, major road AADT, and minor road AADT were among the 10 most important predictors from the CRF analysis. Scatterplots of these variables are shown in figure 93 and figure 94. Major road AADT and intersection AADT were highly correlated and had a Pearson Correlation Coefficient (r) equal to 0.990. Minor road AADT and intersection AADT did not share the same level of correlation ($r = 0.296$). Intersection AADT and minor road AADT were also the two AADT variables that most frequently appeared in the regression tree results. Thus, intersection AADT and minor road AADT were selected for inclusion in the models. Major road AADT was not selected because of its strong correlation with intersection AADT.



Source: FHWA.

Figure 93. Graph. Scatterplot of intersection AADT versus major road AADT for all three-leg intersections in MN.



Source: FHWA.

Figure 94. Graph. Scatterplot of intersection AADT versus minor road AADT for all three-leg intersections in MN.

The initial base model, with only the significant variables ($p \leq 0.05$) retained, is shown in table 88. Both intersection AADT and minor road AADT were significant and predicted an increase in crashes as either value increased. Lane width on the major road was significant with a p -value < 0.0001 and indicated an increase in crashes as the lane width increased. Adjacent land use (*spec_env_cat*) was another significant variable, which indicated significant differences between the rural agricultural land use and the other categories of central business district, commercial/strip development, and other.

The next model developed was an alternative base model that included an additional variable for the ratio of minor road AADT to intersection AADT (*mi_int*). All other variables from the initial base model were retained. Table 89 shows the results. The added variable was significant at a p -value of 0.0169. As the proportion of traffic on the minor road increased relative to intersection AADT, total crashes were predicted to increase using this model. All variables that were significant in the initial base model are also significant in this alternative model. The goodness-of-fit metrics moved in opposing directions for the two models. The BIC for the initial model is 14,329 compared to 14,332 for the alternative model, indicating that the initial model was a positive improvement over the alternative model. However, the AIC changed from 14,274 for the initial model to 14,270 for the alternative model. The magnitude of the change in the AIC was substantial. Thus, the alternative model was an improved model.

Table 88. Initial base model results for total crashes at all three-leg intersections in MN.

Parameter Description	Estimate	Standard Error	Lower 95% CL	Upper 95% CL	Chi-Square	Statistical Significance
Intercept	-9.1882	0.1962	-9.5726	-8.8037	2,194.21	<0.0001
lgint aadt	0.8246	0.0217	0.782	0.8672	1,438.19	<0.0001
lgmi aadt	0.2527	0.0162	0.2209	0.2845	242.04	<0.0001
ma lane wd0	0.0087	0.0019	0.005	0.0124	21.34	<0.0001
spec env cat (0)	-0.2407	0.0599	-0.3581	-0.1233	16.14	<0.0001
spec env cat (1)	-0.3289	0.0512	-0.4293	-0.2284	41.2	<0.0001
spec env cat (2)	-0.5306	0.0537	-0.6359	-0.4254	97.65	<0.0001
spec env cat (3)	0	0	0	0	—	—
Dispersion	0.5938	0.0407	0.5191	0.6792	—	—
Goodness-of-fit parameter: AIC (smaller is better)	14,274	—	—	—	—	—
Goodness-of-fit parameter: BIC (smaller is better)	14,329	—	—	—	—	—

—No data available.

The results from flexible form model 2 are shown in table 90. Again, the same variables significant in the base models remained significant in this model. Intersection angle (*min_angle*) was included in the model as before and is significant with a p -value of < 0.0001 . The estimate for this variable was 0.0269. The additional variable $1 + \cos(\text{angle})$ was significant with a p -value of < 0.0001 and an estimate of 2.3765.

Table 89. Alternative base model results for total crashes at all three-leg intersections in MN.

Parameter Description	Estimate	Standard Error	Lower 95% CL	Upper 95% CL	Chi-Square	Statistical Significance
Intercept	-9.4144	0.2185	-9.8426	-8.9862	1,856.81	<0.0001
lgint aadt	0.8726	0.0296	0.8146	0.9306	868.93	<0.0001
lgmi aadt	0.2024	0.0265	0.1505	0.2542	58.49	<0.0001
mi int	1.1477	0.4803	0.2063	2.0891	5.71	0.0169
ma lane wd0	0.0087	0.0019	0.005	0.0124	21.13	<0.0001
spec env cat (0)	-0.2341	0.06	-0.3517	-0.1164	15.21	<0.0001
spec env cat (1)	-0.3296	0.0513	-0.43	-0.2291	41.34	<0.0001
spec env cat (2)	-0.5161	0.054	-0.622	-0.4102	91.23	<0.0001
spec env cat (3)	0	0	0	0	—	—
Dispersion	0.5939	0.0407	0.5193	0.6793	—	—
Goodness-of-fit parameter: AIC (smaller is better)	14,270	—	—	—	—	—
Goodness-of-fit parameter: BIC (smaller is better)	14,332	—	—	—	—	—

—No data available.

The variable that was not significant, and therefore not included in either model, was intersection angle (*min_angle*). When this variable was added to the initial model, its *p*-value was 0.4149. When added to the alternative model, its *p*-value was 0.4957.

Table 90. Flexible form model 2 results for total crashes at all three-leg intersections in MN.

Parameter Description	Estimate	Standard Error	Lower 95% CL	Upper 95% CL	Chi-Square	Statistical Significance
Intercept	-8.2597	0.5037	-9.2469	-7.2726	268.94	<0.0001
lgint aadt	0.8707	0.0296	0.8127	0.9286	866.96	<0.0001
lgmi aadt	0.2036	0.0265	0.1517	0.2554	59.23	<0.0001
lgcos 1	-1.0909	0.4454	-1.9639	-0.2179	6	0.0143
mi int	1.0752	0.4812	0.1322	2.0183	4.99	0.0254
ma lane wd0	0.0087	0.0019	0.005	0.0124	21.17	<0.0001
spec env cat (0)	-0.2301	0.06	-0.3478	-0.1124	14.69	0.0001
spec env cat (1)	-0.3224	0.0513	-0.4228	-0.2219	39.55	<0.0001
spec env cat (2)	-0.5144	0.0541	-0.6204	-0.4085	90.56	<0.0001
spec env cat (3)	0	0	0	0	—	—
min angle	-0.0125	0.0049	-0.0222	-0.0029	6.47	0.011
Dispersion	0.5884	0.0406	0.5141	0.6736	—	—
Goodness-of-fit parameter: AIC (smaller is better)	14,267	—	—	—	—	—
Goodness-of-fit parameter: BIC (smaller is better)	14,344	—	—	—	—	—

—No data available.

Three-Leg Intersections—Interaction Model for Total Crashes

While the flexible form model did not result in an improvement over the base model, an interactive model was developed to see if the addition of the interaction terms resulted in significant intersection angle terms within an improved model. The same three terms previously used for the four-leg models were used for the three-leg model. In all three of these variables, the angle term became 1.0 when the intersection angle was 90 degrees. Thus, the predicted effect on crashes for right-angle intersections was a function of the intersection and minor road AADT terms in the three variables.

The interaction model is provided in table 91. The same significant variables for land use and major road lane width existed in this model with the same directional effects previously found in the flexible form models. The variable *min_angle* was not significant in the final model. Instead, the effects of angle were accounted for within the two significant interaction terms.

The BIC and AIC for this interaction model were 14,338 and 14,268, respectively. The alternative base values for BIC and AIC were 14,332 and 14,270, respectively. The difference in the BIC values indicated a positive improvement in model fit for the base model over the interaction model. The AIC difference indicated an indistinguishable difference in the two models. Thus, the alternative base model without a variable for intersection angle is still considered to be the best predictive model.

Table 91. Interaction model results for total crashes at all three-leg intersections in MN.

Parameter Description	Estimate	Standard Error	Lower 95% CL	Upper 95% CL	Chi-Square	Statistical Significance
Intercept	-9.1818	0.1959	-9.5657	-8.7979	2,197.31	<0.0001
lgint aadt	0.847	0.0245	0.799	0.895	1,194.87	<0.0001
lgmi aadt	0.2497	0.0163	0.2178	0.2816	235.68	<0.0001
cos1 lgint	-0.1685	0.0579	-0.282	-0.055	8.46	0.0036
angR1 mint	0.1476	0.0491	0.0513	0.2439	9.03	0.0027
ma lane wd0	0.0086	0.0019	0.0049	0.0123	20.85	<0.0001
spec env cat (0)	-0.2396	0.0599	-0.357	-0.1221	15.99	<0.0001
spec env cat (1)	-0.318	0.0512	-0.4184	-0.2176	38.52	<0.0001
spec env cat (2)	-0.528	0.0537	-0.6333	-0.4227	96.65	<0.0001
spec env cat (3)	0	0	0	0	—	—
Dispersion	0.5865	0.0405	0.5122	0.6716	—	—
Goodness-of-fit parameter: AIC (smaller is better)	14,268	—	—	—	—	—
Goodness-of-fit parameter: BIC (smaller is better)	14,338	—	—	—	—	—

—No data available.

Four-Leg Intersections—Additional Models

Additional four-leg intersection models were developed for the following subsets of data:

- All Intersections—Fatal-and-Injury Crashes.
- All Intersections—PDO Crashes.
- Rural Intersections—Total Crashes.
- Rural Intersections—PDO Crashes.
- Rural Two-Lane Intersections—Total Crashes.
- Rural Two-Lane Intersections—Fatal-and-Injury Crashes.
- Rural Two-Lane Intersections—PDO Crashes.
- Rural Multilane Intersections—Total Crashes.
- Rural Multilane Intersections—Fatal-and-Injury Crashes.
- Rural Multilane Intersections—PDO Crashes.

The rural two-lane intersection models include locations where there are two lanes on all four approach legs. The rural multilane intersection models include locations where the major road includes four lanes on each approach leg and the minor road includes two lanes on each approach. An attempt was made to also develop urban models for total crashes. The sample of urban intersections, especially the number of skewed intersections, in the database was not large enough to produce separate models for urban crashes.

Table 92. Flexible form model 1 results for fatal-and-injury crashes at all four-leg intersections in MN.

Parameter Description	Estimate	Standard Error	Lower 95% CL	Upper 95% CL	Chi-Square	Statistical Significance
Intercept	-12.0101	0.2959	-12.5902	-11.4301	1,646.89	<0.0001
lgcos int	0.745	0.0266	0.693	0.7971	786.8	<0.0001
lgcos mi	0.4973	0.0238	0.4507	0.5439	438.09	<0.0001
spec env cat (0)	-0.2561	0.0831	-0.419	-0.0933	9.5	0.0021
spec env cat (1)	-0.1544	0.0769	-0.3051	-0.0036	4.03	0.0448
spec env cat (2)	-0.5595	0.0856	-0.7272	-0.3918	42.75	<0.0001
spec env cat (3)	0	0	0	0	—	—
ma ap spd cat (1)	-0.3427	0.0835	-0.5064	-0.179	16.83	<0.0001
ma ap spd cat (2)	-0.1955	0.0753	-0.343	-0.048	6.75	0.0094
ma ap spd cat (3)	0	0	0	0	—	—
mi parking bin (0)	0.1975	0.0808	0.0391	0.3559	5.97	0.0145
mi parking bin (1)	0	0	0	0	—	—
Min angle	0.0137	0.0014	0.0109	0.0165	93.88	<0.0001
Dispersion	0.5681	0.0542	0.4712	0.6849	—	—
Goodness-of-fit parameter: AIC (smaller is better)	13,233	—	—	—	—	—
Goodness-of-fit parameter: BIC (smaller is better)	13,314	—	—	—	—	—

—No data available.

Table 93. Alternative base model results for PDO crashes at all four-leg intersections in MN.

Parameter Description	Estimate	Standard Error	Lower 95% CL	Upper 95% CL	Chi-Square	Statistical Significance
Intercept	-10.0577	0.294	-10.634	-9.4815	1,170.36	<0.0001
lgint aadt	0.9153	0.0392	0.8385	0.9921	545.65	<0.0001
lgmi aadt	0.2484	0.0338	0.1822	0.3145	54.13	<0.0001
mi int	0.9698	0.2775	0.426	1.5137	12.22	0.0005
ma rodwycls cat (1)	0.2451	0.0673	0.1132	0.3769	13.27	0.0003
ma rodwycls cat (2)	0.1648	0.0718	0.0241	0.3054	5.27	0.0217
ma rodwycls cat (3)	0.0358	0.0581	-0.0782	0.1497	0.38	0.5384
ma rodwycls cat (4)	0	0	0	0	—	—
spec env cat (0)	-0.0371	0.054	-0.143	0.0688	0.47	0.4923
spec env cat (1)	-0.1134	0.0498	-0.211	-0.0159	5.19	0.0227
spec env cat (2)	-0.4237	0.0562	-0.5337	-0.3136	56.92	<0.0001
spec env cat (3)	0	0	0	0	—	—
ma rshl wd0	-0.0205	0.0049	-0.0302	-0.0108	17.18	<0.0001
min angle	-0.0023	0.0011	-0.0045	-0.0002	4.56	0.0327
Dispersion	0.4751	0.0361	0.4094	0.5514	—	—
Goodness-of-fit parameter: AIC (smaller is better)	17,633	—	—	—	—	—
Goodness-of-fit parameter: BIC (smaller is better)	17,729	—	—	—	—	—

—No data available.

Table 94. Flexible form model 1 results for PDO crashes at all four-leg intersections in MN.

Parameter Description	Estimate	Standard Error	Lower 95% CL	Upper 95% CL	Chi-Square	Statistical Significance
Intercept	-11.3261	0.3203	-11.9539	-10.6984	1,250.5	<0.0001
lgcos_int	0.9144	0.0391	0.8377	0.9911	546.39	<0.0001
lgcos_mi	0.2465	0.0337	0.1805	0.3126	53.51	<0.0001
mi_int	0.9805	0.2771	0.4373	1.5237	12.52	0.0004
ma rodwycls cat (1)	0.2481	0.0672	0.1164	0.3798	13.63	0.0002
ma rodwycls cat (2)	0.1698	0.0717	0.0293	0.3103	5.61	0.0179
ma rodwycls cat (3)	0.0376	0.0581	-0.0762	0.1515	0.42	0.5171
ma rodwycls cat (4)	0	0	0	0	—	—
spec env cat (0)	-0.04	0.054	-0.1458	0.0659	0.55	0.4591
spec env cat (1)	-0.1153	0.0497	-0.2128	-0.0179	5.38	0.0204
spec env cat (2)	-0.4243	0.0561	-0.5344	-0.3143	57.12	<0.0001
spec env cat (3)	0	0	0	0	—	—
ma_rshl_wd0	-0.0219	0.0049	-0.0316	-0.0122	19.58	<0.0001
Min_angle	0.0119	0.0012	0.0096	0.0142	102.05	<0.0001
Dispersion	0.4728	0.036	0.4073	0.5489	—	—
Goodness-of-fit parameter: AIC (smaller is better)	17,625	—	—	—	—	—
Goodness-of-fit parameter: BIC (smaller is better)	17,721	—	—	—	—	—

—No data available.

Table 95. Alternative base model results for total crashes at all rural four-leg intersections in MN.

Parameter Description	Estimate	Standard Error	Lower 95% CL	Upper 95% CL	Chi-Square	Statistical Significance
Intercept	-8.8488	0.2495	-9.3379	-8.3598	1,257.51	<0.0001
lgint aadt	0.7231	0.027	0.6703	0.7759	719.79	<0.0001
lgmi aadt	0.4638	0.0178	0.4289	0.4987	677.22	<0.0001
ma ap spd cat (1)	-0.5262	0.0497	-0.6237	-0.4287	111.97	<0.0001
ma ap spd cat (2)	-0.2434	0.0541	-0.3494	-0.1374	20.26	<0.0001
ma ap spd cat (3)	0	0	0	0	—	—
ma minthrlane bin (0)	-0.1282	0.0516	-0.2293	-0.0271	6.18	0.0129
ma minthrlane bin (1)	0	0	0	0	—	—
ma rshl wd0	-0.0158	0.0057	-0.0269	-0.0047	7.73	0.0054
Min angle	-0.0032	0.001	-0.0052	-0.0013	10.35	0.0013
Dispersion	0.4083	0.0306	0.3525	0.4731	—	—
Goodness-of-fit parameter: AIC (smaller is better)	18,122	—	—	—	—	—
Goodness-of-fit parameter: BIC (smaller is better)	18,187	—	—	—	—	—

—No data available.

Table 96. Flexible form model 1 results for total crashes at all rural four-leg intersections in MN.

Parameter Description	Estimate	Standard Error	Lower 95% CL	Upper 95% CL	Chi-Square	Statistical Significance
Intercept	-10.1291	0.2729	-10.664	-9.5941	1,377.26	<0.0001
lgcos int	0.7205	0.0268	0.6679	0.7731	721.34	<0.0001
lgcos mi	0.4626	0.0178	0.4278	0.4975	676.26	<0.0001
ma ap spd cat (1)	-0.5231	0.0496	-0.6204	-0.4258	111.05	<0.0001
ma ap spd cat (2)	-0.2452	0.054	-0.351	-0.1394	20.62	<0.0001
ma ap spd cat (3)	0	0	0	0	—	—
ma minthrlane bin (0)	-0.1254	0.0515	-0.2262	-0.0245	5.93	0.0149
ma minthrlane bin (1)	0	0	0	0	—	—
ma rshl wd0	-0.0168	0.0057	-0.0279	-0.0057	8.77	0.0031
Min angle	0.0112	0.0011	0.0091	0.0133	106.32	<0.0001
Dispersion	0.4031	0.0305	0.3475	0.4675	—	—
Goodness-of-fit parameter: AIC (smaller is better)	18,107	—	—	—	—	—
Goodness-of-fit parameter: BIC (smaller is better)	18,172	—	—	—	—	—

—No data available.

Table 97. Alternative base model results for fatal-and-injury crashes at all rural four-leg intersections in MN.

Parameter Description	Estimate	Standard Error	Lower 95% CL	Upper 95% CL	Chi-Square	Statistical Significance
Intercept	-10.2182	0.3049	-10.8158	-9.6206	1,123.26	<0.0001
lgint aadt	0.6929	0.0341	0.626	0.7597	412.07	<0.0001
lgmi aadt	0.556	0.0267	0.5036	0.6083	433.33	<0.0001
ma ap spd cat (1)	-0.9992	0.0696	-1.1355	-0.8629	206.32	<0.0001
ma ap spd cat (2)	-0.4946	0.0827	-0.6567	-0.3325	35.77	<0.0001
ma ap spd cat (3)	0	0	0	0	—	—
Min angle	-0.0033	0.0015	-0.0062	-0.0004	4.9	0.0269
Dispersion	0.5711	0.0668	0.4542	0.7183	—	—
Goodness-of-fit parameter: AIC (smaller is better)	10,334	—	—	—	—	—
Goodness-of-fit parameter: BIC (smaller is better)	10,385	—	—	—	—	—

—No data available.

Table 98. Flexible form model 1 results for fatal-and-injury crashes at all rural four-leg intersections in MN.

Parameter Description	Estimate	Standard Error	Lower 95% CL	Upper 95% CL	Chi-Square	Statistical Significance
Intercept	-11.5581	0.337	-12.2187	-10.8975	1,175.99	<0.0001
lgcos int	0.6885	0.034	0.6219	0.7551	410.31	<0.0001
lgcos mi	0.5547	0.0267	0.5024	0.607	432.55	<0.0001
ma ap spd cat (1)	-0.9909	0.0695	-1.1271	-0.8547	203.19	<0.0001
ma ap spd cat (2)	-0.4961	0.0826	-0.6581	-0.3341	36.03	<0.0001
ma ap spd cat (3)	0	0	0	0	—	—
Min angle	0.0119	0.0016	0.0087	0.015	54.67	<0.0001
Dispersion	0.5644	0.0665	0.4481	0.7109	—	—
Goodness-of-fit parameter: AIC (smaller is better)	10,325	—	—	—	—	—
Goodness-of-fit parameter: BIC (smaller is better)	10,376	—	—	—	—	—

—No data available.

Table 99. Alternative base model results for PDO crashes at all rural four-leg intersections in MN.

Parameter Description	Estimate	Standard Error	Lower 95% CL	Upper 95% CL	Chi-Square	Statistical Significance
Intercept	-9.9049	0.2786	-10.4509	-9.359	1,264.38	<0.0001
<i>lgint aadt</i>	0.8482	0.0421	0.7657	0.9307	405.7	<0.0001
<i>lgmi aadt</i>	0.3096	0.0386	0.2339	0.3853	64.28	<0.0001
<i>mi int</i>	0.7183	0.301	0.1283	1.3083	5.69	0.017
<i>ma ap spd cat (1)</i>	-0.1573	0.0486	-0.2526	-0.0621	10.48	0.0012
<i>ma ap spd cat (2)</i>	-0.1105	0.0667	-0.2412	0.0201	2.75	0.0972
<i>ma ap spd cat (3)</i>	0	0	0	0	—	—
<i>min angle</i>	-0.0029	0.0012	-0.0053	-0.0004	5.23	0.0222
Dispersion	0.4841	0.0486	0.3977	0.5893	—	—
Goodness-of-fit parameter: AIC (smaller is better)	13,641	—	—	—	—	—
Goodness-of-fit parameter: BIC (smaller is better)	13,699	—	—	—	—	—

—No data available.

Table 100. Flexible form 1 model results for PDO crashes at all rural four-leg intersections in MN.

Parameter Description	Estimate	Standard Error	Lower 95% CL	Upper 95% CL	Chi-Square	Statistical Significance
Intercept	-11.1462	0.3031	-11.7402	-10.5523	1,352.77	<0.0001
<i>lgcos int</i>	0.8452	0.042	0.7628	0.9276	404.53	<0.0001
<i>lgcos mi</i>	0.3071	0.0385	0.2316	0.3826	63.52	<0.0001
<i>mi int</i>	0.7293	0.3006	0.1402	1.3185	5.89	0.0153
<i>ma ap spd cat (1)</i>	-0.1489	0.0486	-0.2441	-0.0538	9.41	0.0022
<i>ma ap spd cat (2)</i>	-0.1124	0.0666	-0.243	0.0182	2.85	0.0915
<i>ma ap spd cat (3)</i>	0	0	0	0	—	—
<i>min angle</i>	0.0112	0.0013	0.0086	0.0138	70.08	<0.0001
Dispersion	0.4795	0.0484	0.3935	0.5844	—	—
Goodness-of-fit parameter: AIC (smaller is better)	13,634	—	—	—	—	—
Goodness-of-fit parameter: BIC (smaller is better)	13,692	—	—	—	—	—

—No data available.

Table 101. Alternative base model results for total crashes at rural two-lane, four-leg intersections in MN.

Parameter Description	Estimate	Standard Error	Lower 95% CL	Upper 95% CL	Chi-Square	Statistical Significance
Intercept	-9.518	0.2815	-10.0696	-8.9663	1,143.57	<0.0001
<i>lgint aadt</i>	0.8455	0.049	0.7495	0.9416	297.81	<0.0001
<i>lgmi aadt</i>	0.3543	0.0423	0.2714	0.4372	70.17	<0.0001
<i>mi int</i>	0.8111	0.2901	0.2425	1.3796	7.82	0.0052
<i>ma ap spd cat (1)</i>	-0.5648	0.053	-0.6687	-0.4609	113.49	<0.0001
<i>ma ap spd cat (2)</i>	-0.3057	0.0595	-0.4223	-0.1891	26.4	<0.0001
<i>ma ap spd cat (3)</i>	0	0	0	0	—	—
<i>ma rshl wd0</i>	-0.0136	0.006	-0.0254	-0.0019	5.17	0.023
<i>min angle</i>	-0.0025	0.0011	-0.0046	-0.0003	5.01	0.0252
Dispersion	0.4158	0.0372	0.3488	0.4956	—	—
Goodness-of-fit parameters: AIC (smaller is better)	15,445	—	—	—	—	—
Goodness-of-fit parameters: BIC (smaller is better)	15,509	—	—	—	—	—

—No data available.

Table 102. Flexible form model 1 results for total crashes at rural two-lane, four-leg intersections in MN.

Parameter Description	Estimate	Standard Error	Lower 95% CL	Upper 95% CL	Chi-Square	Statistical Significance
Intercept	-10.8054	0.3052	-11.4035	-10.2072	1,253.57	<0.0001
<i>lgcos int</i>	0.8445	0.049	0.7486	0.9405	297.48	<0.0001
<i>lgcos mi</i>	0.3513	0.0423	0.2684	0.4341	69.07	<0.0001
<i>mi int</i>	0.8229	0.2899	0.2548	1.391	8.06	0.0045
<i>ma ap spd cat (1)</i>	-0.5602	0.053	-0.664	-0.4565	111.94	<0.0001
<i>ma ap spd cat (2)</i>	-0.3104	0.0595	-0.4269	-0.1938	27.23	<0.0001
<i>ma ap spd cat (3)</i>	0	0	0	0	—	—
<i>ma rshl wd0</i>	-0.0147	0.006	-0.0265	-0.0029	6.01	0.0142
<i>min angle</i>	0.012	0.0012	0.0097	0.0144	102.71	<0.0001
Dispersion	0.4137	0.0371	0.347	0.4932	—	—
Goodness-of-fit parameter: AIC (smaller is better)	15,437	—	—	—	—	—
Goodness-of-fit parameter: BIC (smaller is better)	15,502	—	—	—	—	—

—No data available.

Table 103. Flexible form model 1 results for fatal-and-injury crashes at rural two-lane, four-leg intersections in MN.

Parameter Description	Estimate	Standard Error	Lower 95% CL	Upper 95% CL	Chi-Square	Statistical Significance
Intercept	-11.2025	0.4135	-12.013	-10.392	733.83	<0.0001
<i>lgcos int</i>	0.6425	0.0476	0.5493	0.7358	182.35	<0.0001
<i>lgcos mi</i>	0.5612	0.0318	0.4988	0.6236	310.63	<0.0001
<i>mi ap spd cat (1)</i>	-0.4156	0.1119	-0.6348	-0.1963	13.8	0.0002
<i>mi ap spd cat (2)</i>	0.0529	0.1418	-0.2251	0.3309	0.14	0.7091
<i>mi ap spd cat (3)</i>	0	0	0	0	—	—
<i>ma ap spd cat (1)</i>	-0.6677	0.1275	-0.9177	-0.4178	27.41	<0.0001
<i>ma ap spd cat (2)</i>	-0.334	0.1142	-0.5577	-0.1102	8.56	0.0034
<i>ma ap spd cat (3)</i>	0	0	0	0	—	—
<i>min angle</i>	0.0118	0.0018	0.0083	0.0153	43.37	<0.0001
Dispersion	0.555	0.0826	0.4145	0.743	—	—
Goodness-of-fit parameter: AIC (smaller is better)	8,559	—	—	—	—	—
Goodness-of-fit parameter: BIC (smaller is better)	8,624	—	—	—	—	—

—No data available.

Table 104. Alternative base model results for PDO crashes at rural two-lane, four-leg intersections in MN.

Parameter Description	Estimate	Standard Error	Lower 95% CL	Upper 95% CL	Chi-Square	Statistical Significance
Intercept	-10.2505	0.3515	-10.9393	-9.5616	850.61	<0.0001
<i>lgint aadt</i>	0.9521	0.0603	0.8338	1.0703	249	<0.0001
<i>lgmi aadt</i>	0.1984	0.0507	0.0991	0.2977	15.34	<0.0001
<i>mi int</i>	1.301	0.3565	0.6024	1.9996	13.32	0.0003
<i>min angle</i>	-0.0027	0.0013	-0.0053	0	3.92	0.0477
Dispersion	0.5487	0.0601	0.4428	0.6801	—	—
Goodness-of-fit parameter: AIC (smaller is better)	11,592	—	—	—	—	—
Goodness-of-fit parameter: BIC (smaller is better)	11,635	—	—	—	—	—

—No data available.

Table 105. Flexible form model 1 results for PDO crashes at rural two-lane, four-leg intersections in MN.

Parameter Description	Estimate	Standard Error	Lower 95% CL	Upper 95% CL	Chi-Square	Statistical Significance
Intercept	-11.4997	0.3818	-12.248	-10.7513	907.18	<0.0001
<i>lgcos int</i>	0.9508	0.0603	0.8326	1.069	248.66	<0.0001
<i>lgcos mi</i>	0.1965	0.0506	0.0972	0.2958	15.06	0.0001
<i>mi int</i>	1.3078	0.3563	0.6095	2.0062	13.47	0.0002
<i>min angle</i>	0.0113	0.0014	0.0085	0.0141	62.06	<0.0001
Dispersion	0.5461	0.0599	0.4405	0.677	—	—
Goodness-of-fit parameter: AIC (smaller is better)	11,587	—	—	—	—	—
Goodness-of-fit parameter: BIC (smaller is better)	11,630	—	—	—	—	—

—No data available.

Table 106. Alternative base model results for total crashes at rural multilane four-leg intersections in MN.

Parameter Description	Estimate	Standard Error	Lower 95% CL	Upper 95% CL	Chi-Square	Statistical Significance
Intercept	-7.068	0.7781	-8.5931	-5.5428	82.5	<.0001
<i>lgint aadt</i>	0.5307	0.07	0.3934	0.6679	57.41	<.0001
<i>lgmi aadt</i>	0.5073	0.0414	0.4262	0.5884	150.34	<.0001
<i>min angle</i>	-0.0095	0.0026	-0.0145	-0.0044	13.58	0.0002
Dispersion	0.346	0.055	0.2534	0.4726	—	—
Goodness-of-fit parameter: AIC (smaller is better)	2,206	—	—	—	—	—
Goodness-of-fit parameter: BIC (smaller is better)	2,229	—	—	—	—	—

—No data available.

Table 107. Flexible form model 1 results for total crashes at rural multilane four-leg intersections in MN.

Parameter Description	Estimate	Standard Error	Lower 95% CL	Upper 95% CL	Chi-Square	Statistical Significance
Intercept	-7.6378	0.6268	-8.8663	-6.4092	148.47	<0.0001
<i>lgcos int</i>	0.4979	0.0606	0.3791	0.6168	67.46	<0.0001
<i>lgcos mi</i>	0.5017	0.0406	0.4221	0.5814	152.42	<0.0001
Dispersion	0.3391	0.0545	0.2475	0.4646	—	—
Goodness-of-fit parameter: AIC (smaller is better)	2,200	—	—	—	—	—
Goodness-of-fit parameter: BIC (smaller is better)	2,218	—	—	—	—	—

—No data available.

Table 108. Flexible form model 2 results for fatal-and-injury crashes at rural multilane four-leg intersections in MN.

Parameter Description	Estimate	Standard Error	Lower 95% CL	Upper 95% CL	Chi-Square	Statistical Significance
Intercept	-24.2717	3.1456	-30.4369	-18.1065	59.54	<0.0001
<i>lgint aadt</i>	0.5125	0.1031	0.3104	0.7146	24.71	<0.0001
<i>lgmi aadt</i>	0.6025	0.063	0.4791	0.726	91.45	<0.0001
<i>ma ap spd cat</i> (1)	-0.6391	0.2052	-1.0412	-0.2369	9.7	0.0018
<i>ma ap spd cat</i> (2)	0.4578	0.2267	0.0136	0.9021	4.08	0.0434
<i>ma ap spd cat</i> (3)	0	0	0	0	—	—
<i>lgcos l</i>	13.6599	2.5214	8.7181	18.6017	29.35	<0.0001
<i>min angle</i>	0.1661	0.032	0.1034	0.2289	26.95	<0.0001
Dispersion	0.4461	0.1046	0.2817	0.7064	—	—
Goodness-of-fit parameter: AIC (smaller is better)	1,432	—	—	—	—	—
Goodness-of-fit parameter: BIC (smaller is better)	1,468	—	—	—	—	—

—No data available.

Table 109. Alternative base model results for PDO crashes at rural multilane four-leg intersections in MN.

Parameter Description	Estimate	Standard Error	Lower 95% CL	Upper 95% CL	Chi-Square	Statistical Significance
Intercept	-6.7533	0.9048	-8.5266	-4.9799	55.71	<0.0001
<i>lgint aadt</i>	0.5024	0.0818	0.342	0.6628	37.7	<0.0001
<i>lgmi aadt</i>	0.4155	0.0479	0.3216	0.5095	75.12	<0.0001
<i>min angle</i>	-0.01	0.0029	-0.0158	-0.0042	11.51	0.0007
Dispersion	0.2682	0.0793	0.1502	0.4789	—	—
Goodness-of-fit parameter: AIC (smaller is better)	1,693	—	—	—	—	—
Goodness-of-fit parameter: BIC (smaller is better)	1,715	—	—	—	—	—

—No data available.

Table 110. Flexible form model 2 results for PDO crashes at rural multilane four-leg intersections in MN.

Parameter Description	Estimate	Standard Error	Lower 95% CL	Upper 95% CL	Chi-Square	Statistical Significance
Intercept	-12.5641	2.3483	-17.1667	-7.9615	28.63	<0.0001
<i>lgint aadt</i>	0.5014	0.0812	0.3423	0.6605	38.16	<0.0001
<i>lgmi aadt</i>	0.4072	0.0474	0.3144	0.5001	73.93	<0.0001
<i>lgcos l</i>	5.2021	1.9258	1.4276	8.9767	7.3	0.0069
<i>min angle</i>	0.0544	0.0241	0.0072	0.1015	5.11	0.0239
Dispersion	0.2433	0.0771	0.1308	0.4528	—	—
Goodness-of-fit parameter: AIC (smaller is better)	1,687	—	—	—	—	—
Goodness-of-fit parameter: BIC (smaller is better)	1,715	—	—	—	—	—

—No data available.

OH SUPPLEMENTAL SAFETY-PREDICTION MODELS

SPFs were only developed for total crashes for OH; therefore, all supplemental OH SPFs are grouped and shown in table 111 through table 115.

Table 111. Model fit statistics for OH for rural four-leg two-lane intersections in OH.

Parameter Description	Category	Estimate	Standard Error	Statistical Significance
Intercept	N/A	-20.3179	2.0484	<0.0001
<i>lgcos int</i>	N/A	1.9211	0.2224	<0.0001
<i>lgcos mi</i>	N/A	0.1563	0.0396	<0.0001
<i>lgma aadt</i>	N/A	-1.0479	0.1887	<0.0001
<i>min angle</i>	N/A	0.0198	0.0025	<0.0001
<i>ma rodwycls cat</i>	Local	0.1798	0.1367	0.1883
<i>ma rodwycls cat</i>	Major collector	0.2105	0.0615	0.0006
<i>ma rodwycls cat</i>	Minor arterial	0.1390	0.0612	0.0232
<i>ma rodwycls cat</i>	Minor collector	0.3346	0.1013	0.0010
<i>ma rodwycls cat</i>	Principal arterial	Base category	—	—
Dispersion	N/A	0.4676	0.0210	—
Goodness-of-fit parameter: AIC (smaller is better)	14,243.2137	—	—	—
Goodness-of-fit parameter: BIC (smaller is better)	14,304.0068	—	—	—

—No data available.

N/A = not applicable.

Table 112. Model fit statistics for OH for rural four-leg multilane intersections in OH.

Parameter Description	Category	Estimate	Standard Error	Statistical Significance
Intercept	N/A	-59.1611	12.7590	<0.0001
<i>lgcos int</i>	N/A	5.6961	1.2066	<0.0001
<i>lgma aadt</i>	N/A	-4.6540	1.1136	<0.0001
<i>min Angle</i>	N/A	0.0691	0.0186	0.0002
Dispersion	N/A	0.3647	0.0797	—
Goodness-of-fit parameter: AIC (smaller is better)	549.7794	—	—	—
Goodness-of-fit parameter: BIC (smaller is better)	562.9530	—	—	—

—No data available.

N/A = not applicable.

Table 113. Model fit statistics for OH for rural three-leg two-lane intersections in OH.

Parameter Description	Category	Estimate	Standard Error	Statistical Significance
Intercept	N/A	-1.1299	0.5186	0.0293
<i>lgint aadt</i>	N/A	0.9586	0.228	<0.0001
<i>mi int</i>	N/A	1.4695	0.1195	<0.0001
<i>min Angle</i>	N/A	-0.0099	0.0032	0.0023
<i>lgmin angle</i>	N/A	0.3771	0.1754	0.0315
<i>ma rodwycls cat</i>	Local	-1.537	0.1224	0.2092
<i>ma rodwycls cat</i>	Major collector	0.1560	0.0471	0.0009
<i>ma rodwycls cat</i>	Minor arterial	0.0639	0.0472	0.1759
<i>ma rodwycls cat</i>	Minor collector	0.0796	0.0813	0.3280
<i>ma rodwycls cat</i>	Principal arterial	Base category	—	—
Dispersion	N/A	0.4427	0.0191	—
Goodness-of-fit parameter: AIC (smaller is better)	23,124.2373	—	—	—
Goodness-of-fit parameter: BIC (smaller is better)	23,192.5836	—	—	—

—No data available.

Table 114. Model fit statistics for OH for urban four-leg two-lane intersections in OH.

Parameter Description	Category	Estimate	Standard Error	Statistical Significance
Intercept	N/A	-12.5185	2.7113	<0.0001
<i>lgcos int</i>	N/A	1.2948	0.2573	<0.0001
<i>lgma aadt</i>	N/A	-0.6912	0.2331	0.0030
<i>min angle</i>	N/A	0.0108	0.0043	0.0111
Dispersion	N/A	0.5187	0.0497	—
Goodness-of-fit parameter: AIC (smaller is better)	2,260.8867	—	—	—
Goodness-of-fit parameter: BIC (smaller is better)	2,280.4945	—	—	—

—No data available.

Table 115. Model fit statistics for OH for urban three-leg two-lane intersections in OH.

Parameter Description	Category	Estimate	Standard Error	Statistical Significance
Intercept	N/A	-9.4208	0.4562	<0.0001
<i>lgcos int</i>	N/A	0.9766	0.0458	<0.0001
<i>lin angle</i>	N/A	0.0046	0.0015	0.0028
Dispersion	N/A	0.5722	0.0319	—
Goodness-of-fit parameter: AIC (smaller is better)	7,251.6243	—	—	—
Goodness-of-fit parameter: BIC (smaller is better)	7,272.7909	—	—	—

—No data available.

APPENDIX F. CMFUNCTION DEVELOPMENT AND ADDITIONAL MODELS

MN CMFUNCTIONS

Four-Leg Intersections—Total Crashes at All Intersections

The first CMF developed for total crashes across all four-leg intersections (both rural and urban) is from the alternative base model and takes the form shown in figure 95.

$$CMF(\text{base}) = \frac{\text{EXP}(\beta\alpha)}{\text{EXP}(\beta 90)} = \text{EXP}[\beta(\alpha - 90)]$$

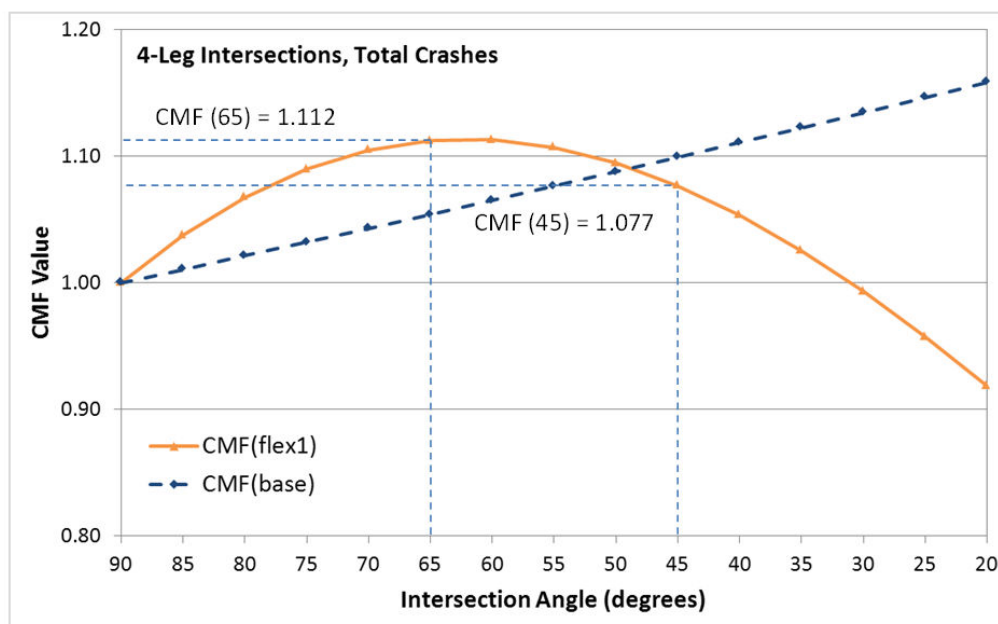
Figure 95. Equation. CMF base model calculation for total crashes at all four-leg intersections.

Where:

α = intersection angle in degrees.

β = -0.0021 for four-leg total crashes.

The log-linear relationship between the derived $CMF(\text{base})$ values and intersection angle is shown in figure 96. As the angle of the intersection decreased from 90 to 20 degrees, the CMF increased, as shown in figure 96. At an angle of 65 degrees, total intersection crashes were predicted to increase by 5.4 percent over what would be expected at a right-angle intersection. At 45 degrees, the predicted increase is 9.9 percent. The largest CMF value is 1.158 at 20 degrees, which is the smallest angle in the database for four-leg intersections.



Source: FHWA.

Figure 96. Graph. CMFs derived from the flexible form model 1 and alternative base model for total crashes at all four-leg intersections in MN.

The CMF derived for total crashes at all four-leg intersections is from the flexible form model 2, which takes the form shown in figure 97.

$$CMF(\text{flex2}) = \frac{\{EXP(\beta_1 \alpha) \times [1 + \cos(\alpha)]^{\beta_2}\}}{\{EXP(\beta_1 90) \times [1 + \cos(90)]^{\beta_2}\}}$$

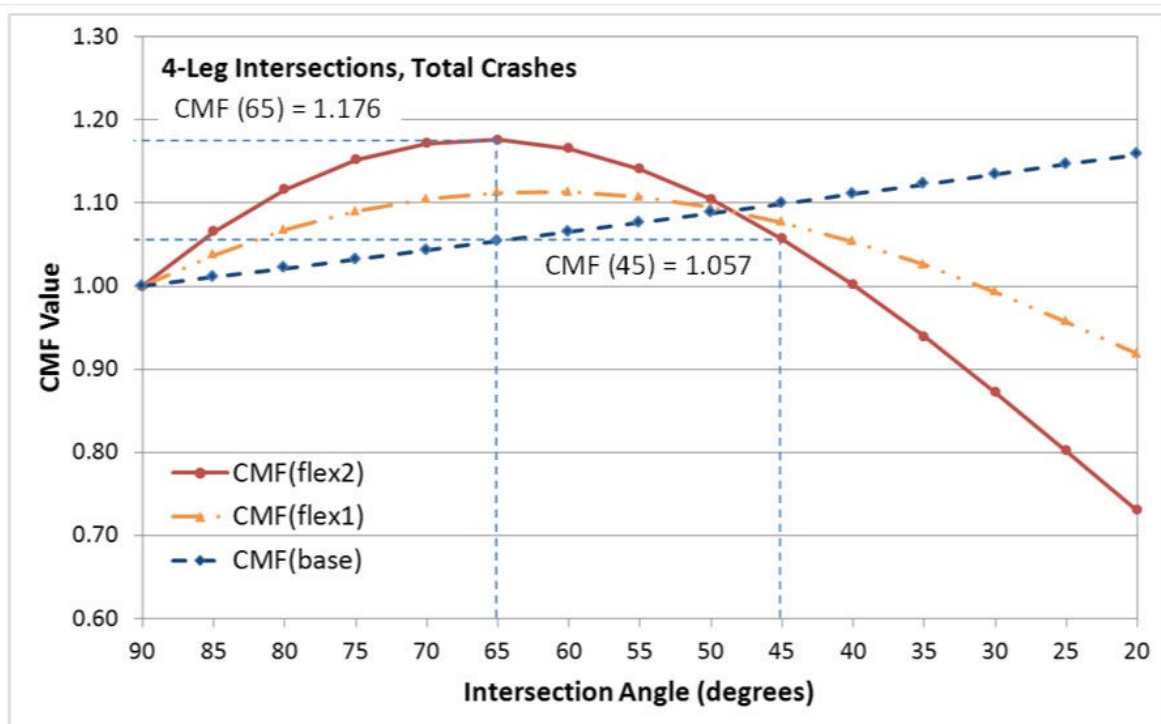
$$= EXP[(\beta_1(\alpha - 90))] \times [1 + \cos(\alpha)]^{\beta_2}$$

Figure 97. Equation. CMF flexible form model 2 calculation for total crashes at all four-leg intersections.

Where:

- α = intersection angle, expressed in degrees.
- β_1 = 0.0269 for total crashes at all four-leg intersections.
- β_2 = 2.3675 for total crashes at all four-leg intersections.

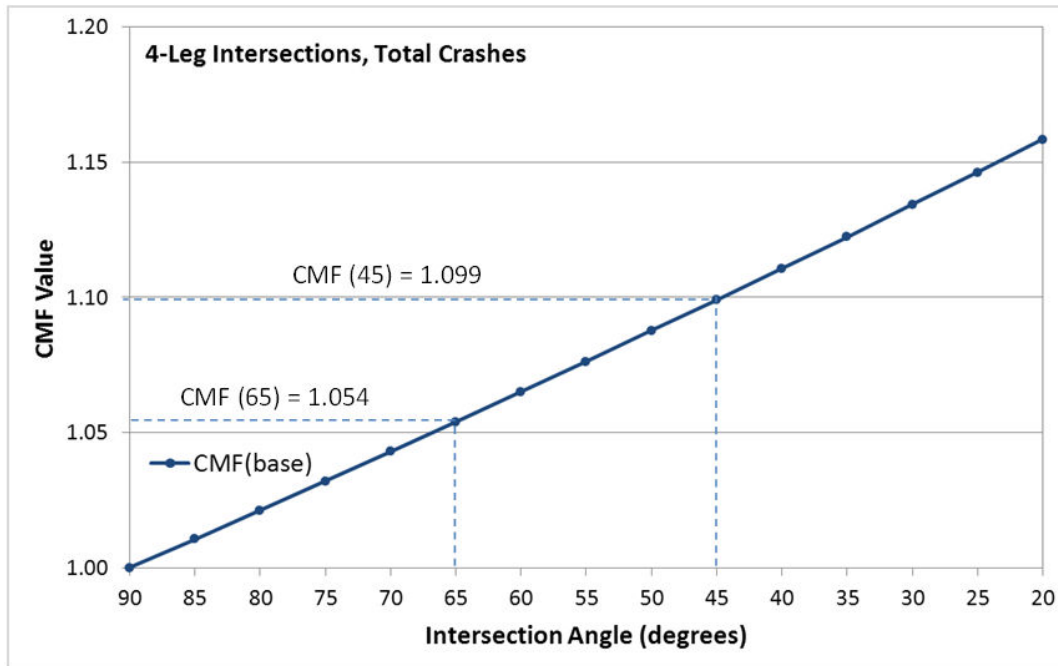
The CMF as distributed across the range of intersection angles is shown in figure 98. The shape of the function is similar to the shape produced for CMF(flex1). As the angle of the intersection decreased from 90 to approximately 65 degrees, total crashes increased. The rate of increase for CMF(flex2) was greater than the rate of increase for CMF(flex1). The result was higher CMF values for the CMF(flex2) function compared to the flex1 function in this upper range of angles. For example, total intersection crashes are predicted to increase by 17.6 percent at an intersection with an angle of 65 degrees over what would be expected at a right-angle intersection using the flex2 function. This value compares to 11.2 percent when using the flex1 function.



Source: FHWA.

Figure 98. Graph. CMFs derived from the flexible form models 1 and 2 and alternative base model for total crashes at all four-leg intersections in MN.

At approximately 65 degrees, the direction of the curve turned downward and crashes continued to decrease as the intersection angle decreases. The rate of decrease for the CMF(flex2) function was greater than the rate for the flex1 function. This resulted in lower predicted CMF values for the flex2 function when compared to the CMF(flex1) function in this lower range of intersection angles. At 45 degrees, the predicted increase over a right-angle intersection was 5.7 percent from CMF(flex2) compared to 7.7 percent from CMF(flex1). Finally, this escalating rate of decrease for CMF(flex2) resulted in CMF values of less than 1.0 for intersections with angles approaching 40 degrees or less. By comparison, CMF(flex1) did not result in values of less than 1.0 until the angles reach 30 degrees or less.



Source: FHWA.

Figure 99. Graph. CMF derived from the alternative base model for total crashes at all four-leg intersections in MN.

Four-Leg Intersections—Total Crashes at Rural Intersections

The first CMF developed for total crashes at four-leg rural intersections is from the alternative base model with the form shown in figure 100.

$$CMF(\text{base}) = \text{EXP}[\beta(\alpha - 90)]$$

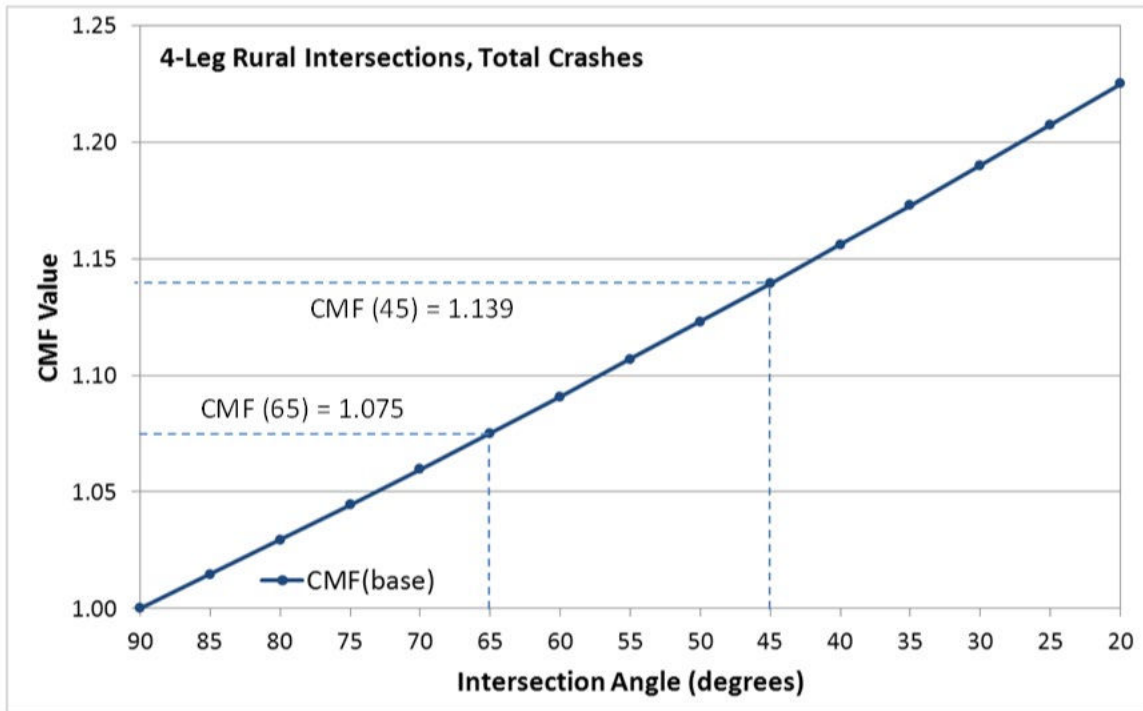
Figure 100. Equation. CMF base model calculation for total crashes at rural four-leg intersections.

Where:

α = intersection angle, expressed in degrees.

β = -0.0029 for total crashes at rural four-leg intersections.

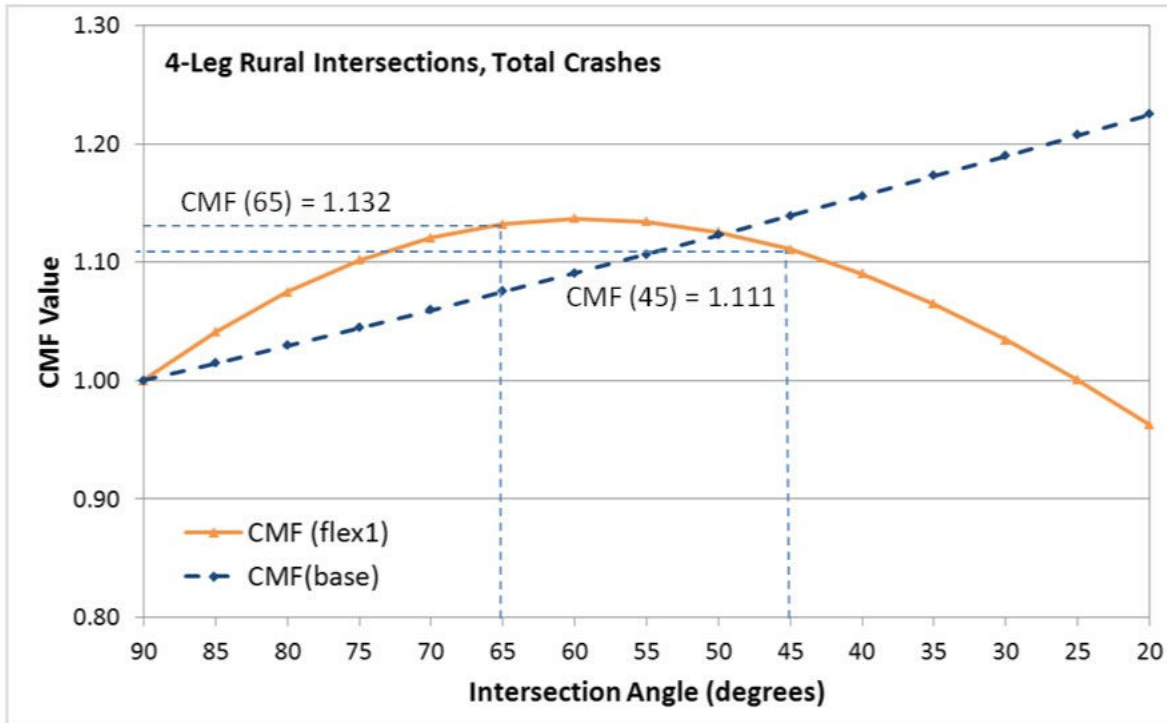
The log-linear relationship between the derived CMF and intersection angles is shown in figure 101. As the angle of the intersection decreased from 90 to 20 degrees, total crashes increased (figure 101). At an angle of 65 degrees, total intersection crashes were predicted to increase by 7.5 percent over what would be expected at a right-angle intersection. At 45 degrees, the predicted increase was 13.9 percent. The largest CMF value was 1.225 at 20 degrees, which was the smallest angle in the database. The rate of increase for rural intersections was greater than what was previously shown for all intersections; hence, the CMF value for any given intersection angle less than 90 degrees is larger for rural intersections compared to all intersections.



Source: FHWA.

Figure 101. Graph. CMF derived from the alternative base model for total crashes at rural four-leg intersections in MN.

The CMF as distributed across the range of intersection angles is shown in figure 102. The results were nonlinear and in the shape of an upward convex parabola. As the angle of the intersection decreased from 90 to approximately 60 degrees, total crashes increased. At that point, the direction of the curve turned downward, and crashes continued to decrease as the intersection angle decreased. At an angle of 65 degrees, total intersection crashes were predicted to increase by 13.2 percent over what would be expected at a right-angle intersection. At 45 degrees, the predicted increase was 11.1 percent. The CMF was less than 1.0 for intersections with angles reaching 25 degrees or less. The CMF(flex1) function for rural intersections produced CMF values greater than those produced by the same function for all intersections.



Source: FHWA.

Figure 102. Graph. CMFs derived from the flexible form model 1 and alternative base model for total crashes at rural four-leg intersections in MN.

Four-Leg Intersections—Total Crashes at Two-Lane Rural Intersections

The next set of CMFs developed for four-leg intersections was for rural two-lane intersections. These locations had two lanes on major-road approach legs. (All intersections had two lanes on the minor-road approach legs.) The first CMF developed for total crashes was from the alternative base model and took the form shown in figure 103.

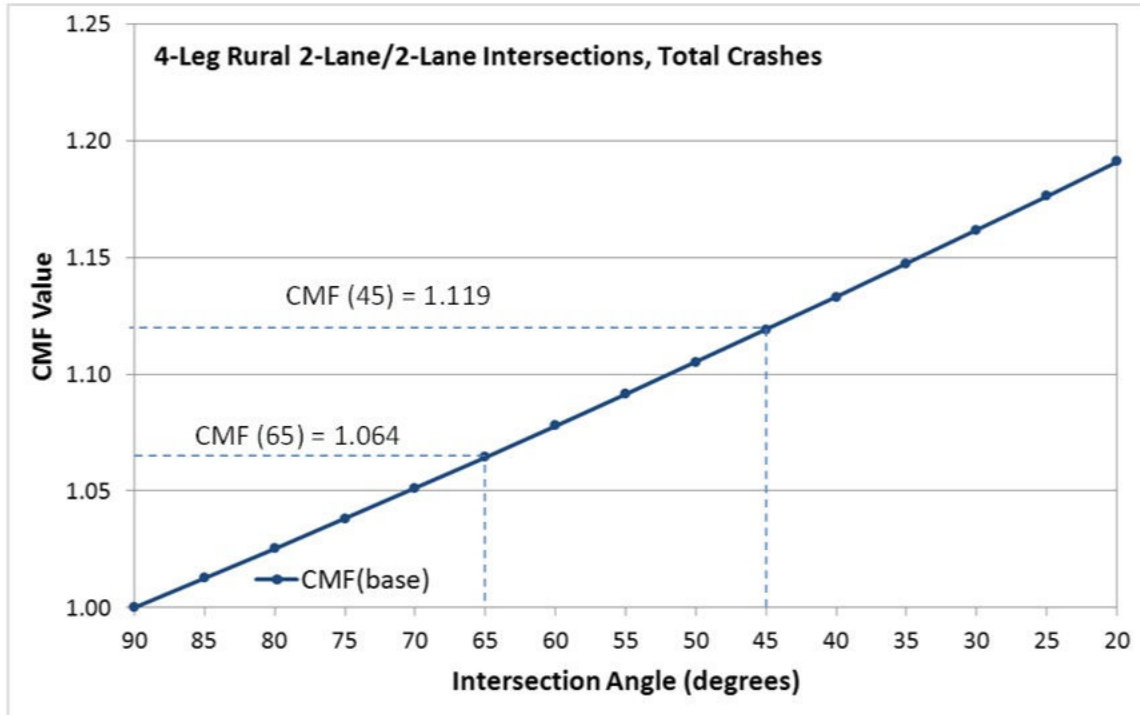
$$CMF(\text{base}) = \text{EXP}[\beta(\alpha - 90)]$$

Figure 103. Equation. CMF base-model calculation for total crashes at rural four-leg two-lane intersections.

Where:

α = intersection angle in degrees.

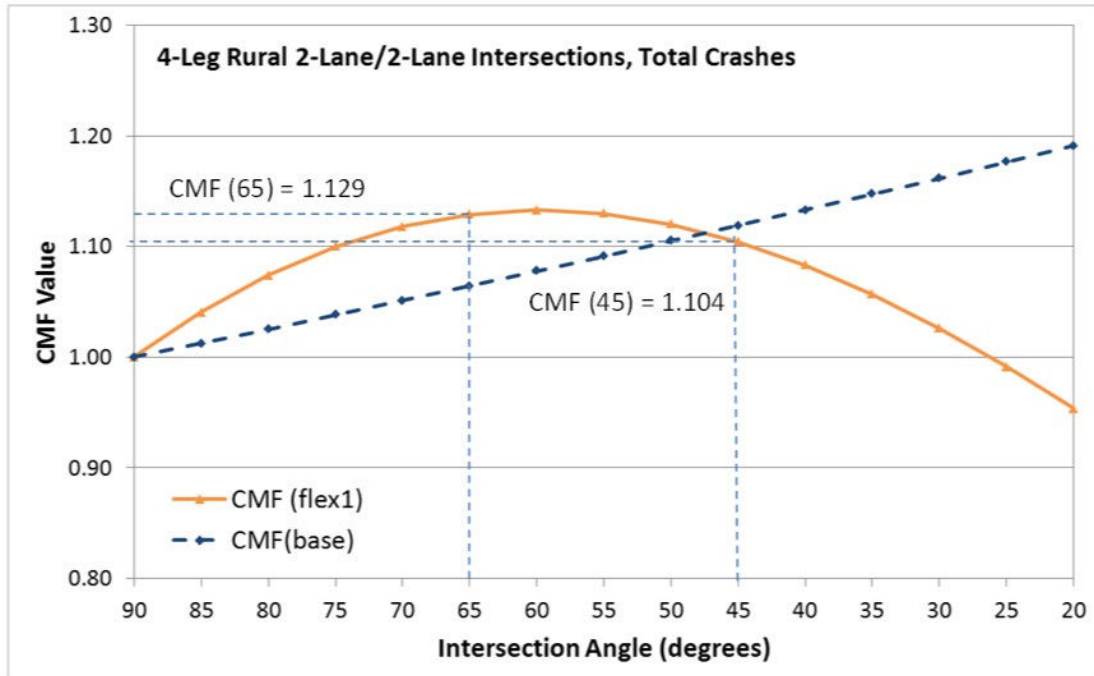
β = -0.0025 for rural four-leg two-lane total crashes.



Source: FHWA.

Figure 104. Graph. CMF derived from the alternative base model for total crashes at rural four-leg two-lane intersections in MN.

The log-linear relationship between the derived CMF and intersection angles is shown in figure 104. As the angle of the intersection decreased from 90 to 20 degrees, total crashes increased, as shown in figure 104. At an angle of 65 degrees, total intersection crashes were predicted to increase by 6.4 percent over what would be expected at a right-angle intersection. At 45 degrees, the predicted increase was 11.9 percent. The largest CMF value was 1.191 at 20 degrees, which is the smallest angle in the database.



Source: FHWA.

Figure 105. Graph. CMFs derived from the flexible form model 1 and alternative base model for total crashes at rural four-leg two-lane intersections in MN.

The CMF as distributed across the range of intersection angles is shown in figure 105. The results are nonlinear and in the shape of an upward convex parabola. As the angle of the intersection decreased from 90 to approximately 60 degrees, total crashes increased. At that point, the direction of the curve turned downward, and crashes continued to decrease as the intersection angle decreases. At an angle of 65 degrees, total intersection crashes were predicted to increase by 12.9 percent over what would be expected at a right-angle intersection. At 45 degrees, the predicted increase was 10.4 percent. The CMF was less than 1.0 for intersections with angles approaching 25 degrees or less.

Four-Leg Intersections—Total Crashes at Multilane Rural Intersections

The final set of CMFs developed was for four-leg rural intersections with four lanes on the major-road approach legs and two lanes on the minor-road approach legs. The first CMF developed for total crashes was from the alternative base model and took the form shown in figure 106.

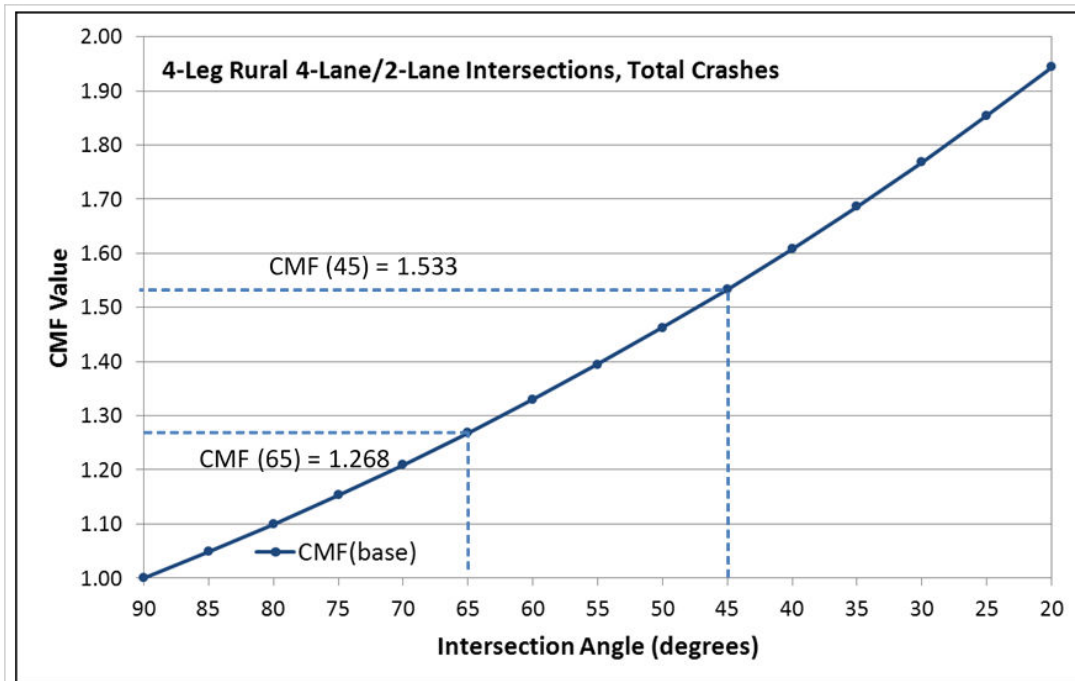
$$CMF(\text{base}) = \text{EXP}[\beta(\alpha - 90)]$$

Figure 106. Equation. CMF base model calculation for total crashes at rural four-leg multilane intersections.

Where:

α = intersection angle in degrees.

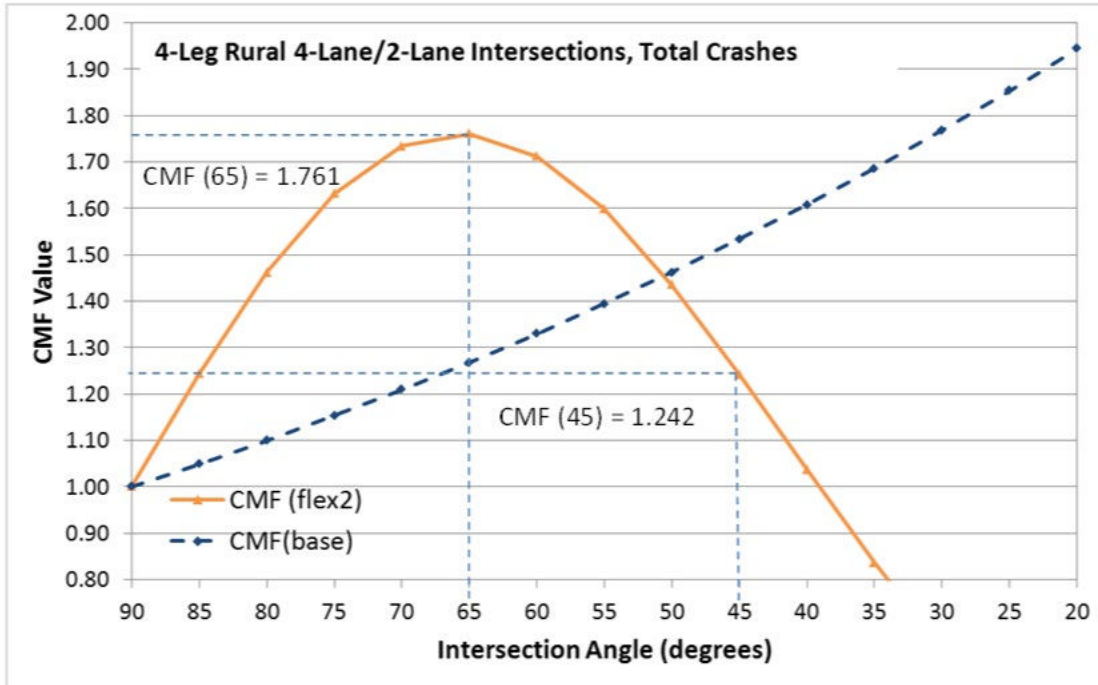
β = -0.0095 for rural four-leg multilane total crashes.



Source: FHWA.

Figure 107. Graph. CMFs derived from the alternative base model for total crashes at rural four-leg multilane intersections in MN.

The log between the derived CMF and intersection angles is shown in figure 107. As the angle of the intersection decreased from 90 to 20 degrees, total crashes increased, as shown in figure 107. At an angle of 65 degrees, total intersection crashes were predicted to increase by 26.8 percent over what would be expected at a right-angle intersection. At 45 degrees, the predicted increase was 53.3 percent. The expected increases in crashes were much greater at the multilane intersections compared to the two-lane intersections.



Source: FHWA.

Figure 108. Graph. CMFs derived from the flexible form model 1 and alternative base model for total crashes at rural four-leg multilane intersections.

Initial CMFunction results based on just the MN data are shown in table 116. Table 117 shows CMF results with shaded peak angles for the different injury severities based on the MN data.

Table 116. CMFunctions derived by NB model form for MN.

Intersection and Collision Category	Alternative Base	Flexible Form 1	Flexible Form 2
Four-leg all sites, total crashes	X	X	X
Four-leg all sites, fatal-and-injury crashes	—	X	—
Four-leg all sites, PDO crashes	X	X	—
Four-leg rural sites, total crashes	X	X	—
Four-leg rural sites, fatal-and-injury crashes	X	X	—
Four-leg rural sites, PDO crashes	X	X	—
Four-leg rural two-lane sites, total crashes	X	X	—
Four-leg rural two-lane sites, fatal-and-injury crashes	—	X	—
Four-leg rural two-lane sites, PDO crashes	X	X	—
Four-leg rural multilane sites, total crashes	X	—	X
Four-leg rural multilane sites, fatal-and-injury crashes	—	—	X
Four-leg rural multilane sites, PDO crashes	X	—	X
Three-leg all sites, total crashes	X	—	—
Three-leg rural sites, total crashes	X	—	—

— Sufficient data not present.

X = sufficient data present.

Table 117. CMF values derived from the flexible form models for four-leg rural intersections.

Intersection Scenario and Collision Category	80 Degrees	75 Degrees	70 Degrees	65 Degrees	60 Degrees	55 Degrees
All sites, total	—	1.09	1.1*	1.11*	1.11*	1.11*
All sites, injury	—	1.08	1.1*	1.1*	1.1*	1.09
All sites, PDO	—	1.09	1.11	1.12*	1.12*	1.12*
Rural sites, total	1.08	1.11	1.13	1.15	1.15	1.16*
Rural sites, injury	1.08	1.11	1.14	1.15	1.16*	1.16*
Rural sites, PDO	1.08	1.1	1.12	1.13	1.14*	1.14*
Rural two-lane sites, total	—	1.1	1.12	1.13*	1.13*	1.13*
Rural two-lane sites, injury	1.08	1.11	1.13	1.14*	1.14*	1.14*
Rural two-lane sites, PDO	—	1.1	1.12	1.13*	1.13*	1.13*
Rural multilane sites, total	1.46	1.63	1.73	1.76*	1.71	1.6
Rural multilane sites, injury	1.69	1.92	2.01	1.94*	1.74	1.46
Rural multilane sites, PDO	1.34	1.46	1.56	1.61*	1.61*	1.58

— Data not available.

*Intersection angles in each intersection scenario/collision category with the highest CMF values.

ACKNOWLEDGMENTS

The research team would like to express appreciation to the following State departments of transportation for granting permission to share information and data used in this report:

- Ohio.
- Minnesota.
- North Carolina.

This project used data from the HSIS.

Some of the map figures in this document were modified by the authors. The original maps are the copyright property of Google Earth and can be accessed from <https://www.google.com/earth>.⁽⁷⁵⁻⁷⁹⁾ GIS images were inserted by the research team to demonstrate that the intersection was incorrectly depicted in the GIS data as an at-grade crossing.

REFERENCES

1. American Association of State Highway and Transportation Officials. (2011). *A Policy on Geometric Design of Highways and Streets*, Sixth Edition, AASHTO, Washington, DC.
2. Institute of Transportation Engineers. (2009). *Traffic Engineering Handbook*, Sixth Edition, ITE, Washington, DC.
3. Institute of Transportation Engineers. (2003). *Neighborhood Street Design Guidelines*, ITE, Washington, DC.
4. Institute of Transportation Engineers. (1999). *Traffic Engineering Handbook*, Fifth Edition, ITE, Washington, DC.
5. Institute of Transportation Engineers. (1984). *Recommended Guidelines for Subdivision Streets*, ITE, Washington, DC.
6. Staplin, L., Lococo, K., Byington, S., and Harkey, D. (2001). *Highway Design Handbook for Older Drivers and Pedestrians*, Report No. FHWA-RD-01-103, Federal Highway Administration, Washington, DC.
7. National Highway Traffic Safety Administration. (2009). *Traffic Safety Facts 2009: A Compilation of Motor Vehicle Crash Data from the Fatality Analysis Reporting System and the General Estimates System*, Report No. DOT HS 811 402, United States Department of Transportation, Washington, DC.
8. Kuciemba, S.R. and Cirillo, J.A. (1992). *Safety Effectiveness of Highway Design Features, Volume V: Intersections*, Report No. FHWA-RD-91-048, Federal Highway Administration, Washington, DC.
9. Bauer, K.M. and Harwood, D.W. (1996). *Statistical Models of At-Grade Intersection Accidents*, Report No. FHWA-RD-96-125, Federal Highway Administration, Washington, DC.
10. Council, F. and Nujjetty, A.P. (2015). "Highway Safety Information System Guidebook for the Minnesota State Data Files." (website) Available online: <https://www.hsisinfo.org/guidebooks/minnesota.cfm>, last accessed April 15, 2020.
11. The University of North Carolina Highway Safety Research Center. (2010). Focus State Analysis Tables (Technical Memorandum), Chapel Hill, NC.
12. National Highway Traffic Safety Administration. (2017). "NCSA Data Resource Website: Fatality Analysis Reporting System (FARS) Encyclopedia." (website) Available online: <https://www-fars.nhtsa.dot.gov/Main/index.aspx>, last accessed March 13, 2020.

13. Antonucci, N.D., Hardy, K.K., Slack, K.L., Pfefer, R., and Neuman, T.R. (2004). *Guidance for Implementation of the AASHTO Strategic Highway Safety Plan, Volume 12: A Guide for Reducing Collisions at Signalized Intersections*, NCHRP Report 500 Series, The National Academies of Science, Engineering, and Medicine. National Academies Press, Washington, DC.
14. Harkey, D.L., Carter, D.L., Barlow, J.M., and Bentzen, B.L. (2007). *Accessible Pedestrian Signals: A Guide to Best Practice*, NCHRP Web-only Document 117A. (website) Available online: http://onlinepubs.trb.org/onlinepubs/nchrp/nchrp_w117a.pdf, last accessed March 13, 2020.
15. Neuman, T.R., Pfefer, R., Slack, K.L., Hardy, K.K., Harwood, D.W., Potts, I.B., Torbic, D.J., and Kohlman Rabbani, E.R. (2003). *Guidance for Implementation of the AASHTO Strategic Highway Safety Plan, Volume 5: A Guide for Reducing Collisions at Unsignalized Intersections*, NCHRP Report 500 Series, The National Academies of Science, Engineering, and Medicine, National Academies Press, Washington, DC.
16. Neuman, T. (1985). *Intersection Channelization Design Guide*, NCHRP Report 27, The National Academies of Science, Engineering, and Medicine, National Academies Press, Washington, DC.
17. American Association of State Highway and Transportation Officials. (1966). *A Policy on Geometric Design of Rural Highways*, AASHTO, Washington, DC.
18. Iowa Department of Transportation. (2012). “Design Manual.” (website) Available online: <https://iowadot.gov/design/design-manual>, last accessed March 13, 2020.
19. Montana Department of Transportation. (2004). “Road Design Manual.” (website) Available online: <http://www.mdt.mt.gov/publications/manuals.shtml>, last accessed March 13, 2020.
20. Illinois Department of Transportation Bureau of Local Roads and Streets. (2005). *Bureau of Local Roads and Streets Manual*, Illinois Department of Transportation, Springfield, IL. Available online: <http://www.idot.illinois.gov/Assets/uploads/files/Doing-Business/Manuals-Guides-&-Handbooks/Highways/Local-Roads-and-Streets/Local%20Roads%20and%20Streets%20Manual.pdf>, last accessed March 13, 2020.
21. California Department of Transportation. (2009). *Highway Design Manual*. Available online: <https://dot.ca.gov/-/media/dot-media/programs/design/documents/hdm-complete-14dec2018.pdf#page=807>, last accessed March 13, 2020.
22. Chandler, B., Myers, M., Atkinson, J., Bryer, T., Retting, R., Smithline, J., Peter, W., Thomas, G., Venglar, S., Sunkari, S., Malone, B., and Izadpanah, P. (2013). *Signalized intersections: Informational Guide*, Second Edition, Report No. FHWA-SA-13-027, Federal Highway Administration, Washington, DC.
23. American Association of State Highway and Transportation Officials. (2004). *Guide for the Planning, Design, and Operation of Pedestrian Facilities*. AASHTO, Washington, DC.

24. American Association of State Highway and Transportation Officials. (2010). *Highway Safety Manual*, First Edition, AASHTO, Washington, DC.
25. Harwood, D.W., Council, F.M., Hauer, E., Hughes, W.E., and Vogt, A. (2000). *Prediction of the Expected Safety Performance of Rural Two-Lane Highways*, Report No, FHWA-RD-99-207, Federal Highway Administration, Washington, DC.
26. Washington, S., Persaud, B., Lyon, C., and Oh, J. (2005). *Validation of Accidents Models for Intersections*, Report No, FHWA-RD-03-037, Federal Highway Administration, Washington, DC.
27. Vogt, A. (1999). *Crash Models for Rural Intersections: Four-Lane by Two-Lane Stop-Controlled and Two-Lane by Two-Lane Signalized*, Report No. FHWA-RD-99-128, Federal Highway Administration, Washington, DC.
28. McCoy, P.T., Tripi, E.J., and Bonneson, J.A. (1994). *Guidelines for Realignment of Skewed Intersections*, Research Project Number RES1 (0099) P471, Nebraska Department of Roads, Lincoln, NE.
29. Hanna, J.T., Flynn, T.E., and Webb, L.T. (1976). "Characteristics of intersection accidents in rural municipalities." *Transportation Research Record: Journal of the Transportation Research Board*, No. 601, pp. 79–82, The National Academies of Science, Engineering, and Medicine. National Academies Press, Washington, DC.
30. Kulmala, R. (1995). *Safety at Rural Three- and Four-Arm Junctions. Development and Application of Accident Prediction Models*, VTT Publications 233. VTT Technical Research Centre of Finland, Espoo, Finland.
31. Gattis, J.L. and Low, S.T. (1998). "Intersection angle geometry and the driver's field of view." *Transportation Research Record: Journal of the Transportation Research Board*, No. 1612, pp. 10–16, The National Academies of Science, Engineering, and Medicine, National Academies Press, Washington, DC.
32. Gattis, J.L. and Low, S.T. (1997). *Intersection Angles and the Driver's Field of View*, Report No. MBTC 97.73, Arkansas State Highway and Transportation Department, Little Rock, AR.
33. Son, Y., Kim, S., and Lee, J. (2002). "Methodology to calculate sight distance available to drivers at skewed intersections." *Transportation Research Record: Journal of the Transportation Research Board*, 1796(1): pp. 41–47, The National Academies of Science, Engineering, and Medicine, National Academies Press, Washington, DC.
34. Garcia, A. (2005). "Lateral vision angles and skewed intersections design." *Proceedings, 3rd International Symposium on Highway Geometric Design*, Chicago, IL.
35. García, A. and Libreros, L. (2007). "Safety effect of the skew angle in right turn maneuvers." *Proceedings, 3rd International Symposium on Highway Geometric Design*, Seattle, WA.

36. Harkey, D., Staplin, L., Lococo, K., Srinivasan, R., Baek, J., Daul, M. McGee, H., et al. (2011). *2011 Handbook for Designing Roadways for the Older Population* (Draft Publication), Federal Highway Administration, Washington, DC.
37. Smith, B.H. and Sethi, P.K. (1975). "Aging and the nervous system." *Geriatrics*, 30, pp. 109–115, Magnus Med Club, Westerville, OH.
38. Isler, R.B., Parsonson, B.S., and Hansson, G.J. (1997). "Age related effects of restricted head movements on the useful field of view of drivers." *Accident Analysis & Prevention*, 29(6), pp. 793–801, Elsevier, Amsterdam, Netherlands.
39. Ostrow, A.C., Shaffron, P., and McPherson, K. (1992). "The effects of a joint range-of-motion physical fitness training program on the automobile driving skills of older adults." *Journal of Safety Research*, 23, pp. 207–219, Elsevier, Amsterdam, Netherlands.
40. Yee, D. (1985). "A survey of the traffic safety needs and problems of drivers age 55 and over." In *Needs and Problems of Older Drivers: Survey Results and Recommendations*. American Automobile Association Foundation for Traffic Safety, Washington, DC.
41. Staplin, L., Harkey, D., Lococo, K., and Tarawneh, M. (1997). *Intersection Geometric Design and Operational Guidelines for Older Drivers and Pedestrians, Volume I, Final Report*, Report No. FHWA-RD-96-132, Federal Highway Administration, Washington, DC.
42. Classen, S., Shechtman, O., Stephens, B., Davis, E., Justiss, M., Bendixen, R., Belchior, P., et al. (2007). "The impact of roadway intersection design on driving performance of young and senior adults." *Traffic Injury Prevention*, 8, pp. 69–77, Taylor & Francis Online, London.
43. Wilson, D.G. and Grayson, G.B. (1980). *Age-Related Differences in the Road Crossing Behavior of Adult Pedestrians*, Report No. TRRL-L-933, Transport and Road Research Laboratory, Crowthorne, England.
44. Stolof, E.R., McGee, H., and Eccles, K. (2007). *Pedestrian Signal Safety for Older Persons*. American Automobile Association Foundation for Traffic Safety, Washington, DC.
45. Federal Highway Administration (2009). *Manual on Uniform Traffic Control Devices, 2009 Edition*. FHWA, Washington, DC.
46. Breiman, L. and Cutler, A. (2013). *Random Forests*. (website) Available online: <http://www.stat.berkeley.edu/~breiman/RandomForests>, last accessed March 13, 2020.
47. Breiman, L., Friedman, J.H., Olshen, R.A., and Stone, C.J. (1984). *Classification and Regression Trees*, Wadsworth, Belmont, CA.
48. Loh, W. (2011). "Classification and regression trees." *WIREs Data Mining and Knowledge Discovery*, 1, pp. 14–23, Wiley Periodicals, Hoboken, NJ.
49. Strobl, C., Malley, J., and Tutz, G. (2009). *An Introduction to Recursive Partitioning*, Technical Report No. 55, Department of Statistics, University of Munich, Munich, Germany.

50. Hauer, E. (2004). "Statistical road safety modeling." *Transportation Research Record: Journal of the Transportation Research Board*, No. 1897, pp. 81–87, The National Academies of Science, Engineering, and Medicine, National Academies Press, Washington, DC.
51. Bauer, K.M. and Harwood, D.W. (2013). *Safety Effects of Horizontal Curve and Grade Combinations*. Available online: <https://www.fhwa.dot.gov/publications/research/safety/13077/index.cfm>, last accessed April 15, 2020.
52. Lord, D. and Mannering, F. (2010). "The statistical analysis of crash-frequency data: a review and assessment of methodological alternatives." *Transportation Research Part A: Policy and Practice*, 44, pp. 291–305, Elsevier, Amsterdam, Netherlands.
53. Federal Highway Administration. (2013). Available online: www.cmfclearinghouse.org, last accessed March 13, 2020.
54. Gross, F., Persaud, B., and Lyon, C. (2010). *A Guide to Developing Quality Crash Modification Factors*, Report No. FHWA-SA-10-032, Federal Highway Administration, Washington, DC.
55. Highway Safety Information System. (website) Available online: www.hsisinfo.org, last accessed April 15, 2020.
56. Council, F.M. and Mohamedshah, Y. (2007). *Highway Safety Information System Guidebook for the Minnesota State Data Files*. Federal Highway Administration, Washington, DC.
57. Minnesota Department of Transportation. (2013). "GIS BaseMap." (website) Available online: <https://www.dot.state.mn.us/maps/gdma/index.html>, last accessed March 13, 2020.
58. Google Maps. (2012). Available online: <https://www.google.com/maps>, last accessed March 13, 2020.
59. ESRI. (2102). ArcGIS, Version 10. Redlands, CA.
60. Federal Highway Administration. (2016). *Summary of State SPF Calibration and Development Efforts*. Available online: http://www.cmfclearinghouse.org/resources_spf.cfm, last accessed April 15, 2020.
61. Minnesota Department of Public Safety (2016). *Minnesota Motor Vehicle Crash Facts 2015*. Available online: <https://dps.mn.gov/divisions/ots/reports-statistics/Documents/2015-crash-facts.pdf>, last accessed April 15, 2020.
62. Minnesota Department of Transportation. (2017). "Transportation Fact Cards." (website) Available online: www.dot.state.mn.us/trafficeng/publ/triviocard, last accessed March 13, 2020.

63. Ohio Department of Transportation. (2017). “Highway Safety Improvement Program: Crash Data Analysis & Tools.” (website) Available online: www.dot.state.oh.us/Divisions/Planning/ProgramManagement/HighwaySafety/HSIP/Pages/Crash-Data-Analysis-Tools.aspx, last accessed March 13, 2020.
64. Liaw, A. and Wiener, M. (2002). “Classification and regression by randomforest.” *R News* 2(3), pp. 18–22.
65. Hothorn, T., Hornik, K., Strobl, C., and Zeileis, A. (2020). *party: A laboratory for recursive partytioning*. (website) Available online: <http://cran.r-project.org/web/packages/party/index.html>, last accessed March 13, 2020.
66. Hothorn, T., Buehlmann, P., Dudoit, S., Molinaro, A. and Van Der Laan, M. (2006). “Survival ensembles.” *Biostatistics*, 7(3), pp. 355–373.
67. Strobl, C., Boulesteix, A., Zeileis, A., and Hothorn, T. (2007). (website) “Bias in random forest variable importance measures: Illustrations, sources and a solution.” *BMC Bioinformatics*, 8(25). Available online: <http://www.biomedcentral.com/1471-2105/8/25>, last accessed March 13, 2020.
68. Strobl, C., Boulesteix, A., Kneib, T., Augustin, T., and Zeileis, A. (2008). “Conditional variable importance for random forests.” *BMC Bioinformatics*, 9(307). Available online: <http://www.biomedcentral.com/1471-2105/9/307>, last accessed March 13, 2020.
69. SAS (2011). *SAS/STAT® 9.3 User’s Guide*. SAS Institute Inc., Cary, NC.
70. Akaike, H. (1973). “Information theory and an extension of the maximum likelihood principle,” In Petrov, B.N. and F. Csaki (Eds.), *Second International Symposium on Information Theory*, pp. 267–281. Akademiai Kiado, Budapest, Hungary.
71. Schwarz, G.E. (1978). “Estimating the dimension of a model.” *Annals of Statistics*, Vol 6(2), pp. 461–464, Institute of Mathematical Statistics, Cleveland, OH.
72. Burnham, K.P. and Anderson, D.R. (2002). *Model selection and multi-model inference: A practical information-theoretic approach*, Second Edition, Springer-Verlag, New York, NY.
73. Raftery, A.E. (1999). “Bayes factors and BIC.” *Sociological Methods & Research*, 2(3), 411–427, SAGE Journals, Thousand Oaks, CA.
74. Hauer, E. (2015). *The Art of Regression Modeling in Road Safety*. Springer International, Switzerland.
75. “3-leg Intersection.” Map. Google Earth. Maxar Technologies, USDA Farm Service Agency. Fremont, CA. Accessed April 15, 2020. <https://www.google.com/maps/place/47%C2%B046'05.7%22N+96%C2%B035'59.9%22W/@47.7682221,96.601233,627m/data=!3m1!1e3!4m5!3m4!1s0x0:0x0!8m2!3d47.7682528!4d-96.5999831>. Scale 165 ft.

76. “Divided Roadway with Connector.” Map. Maxar Technologies, USDA Farm Service Agency. Fremont, CA. Accessed April 15, 2018.
<https://www.google.com/maps/place/47%C2%B030'20.5%22N+94%C2%B056'56.3%22W/@47.5056944,94.9511609,630m/data=!3m2!1e3!4b1!4m5!3m4!1s0x0:0x0!8m2!3d47.5056875!4d-94.9489622>. Scale 250 ft.
77. “Divided Roadway.” Map. Maxar Technologies, U.S. Geological Survey, USDA Farm Service Agency. Google Maps. Fremont, CA. Accessed April 15, 2020.
<https://www.google.com/maps/place/44%C2%B042'09.7%22N+93%C2%B001'40.4%22W/@44.7026944,93.0300776,663m/data=!3m2!1e3!4b1!4m5!3m4!1s0x0:0x0!8m2!3d44.7026903!4d-93.0278875>. Scale 250 ft.
78. “Grade-separated Intersection.” Map. Google Earth. Fremont, CA. Accessed May 31, 2018.
<https://www.google.com/maps/place/44%C2%B007'21.7%22N+92%C2%B031'15.5%22W/@44.1226944,92.5231609,670m/data=!3m2!1e3!4b1!4m5!3m4!1s0x0:0x0!8m2!3d44.1226933!4d-92.5209758>.
79. Google. “Right-angle Intersection.” Map. Maxar Technologies, USDA Farm Service Agency. Google Earth. Fremont, CA. Accessed April 15, 2020.
<https://www.google.com/maps/place/47%C2%B031'18.4%22N+95%C2%B024'16.8%22W/@47.5217778,95.4068554,630m/data=!3m2!1e3!4b1!4m5!3m4!1s0x0:0x0!8m2!3d47.521775!4d-95.4046533>. Scale 150 ft.
80. Harb, R., Yan, X., Radwan, E., and Su, X. (2009). “Exploring precrash maneuvers using classification trees and random forests.” *Accident Analysis and Prevention*, 41, pp. 98–107, Elsevier, Amsterdam, Netherlands.
81. Rossi, A., Amaddeo, F., Sandri, M., and Tansella, M. (2005). “Determinants of once-only contact in a community-based psychiatric service.” *Social Psychiatry and Psychiatric Epidemiology*, 40(1), pp. 50–56, Springer, Switzerland.
82. Council, F.M., Reurings, M., Srinivasan, R., Masten, S., and Carter, D. (2010). *Development of a Speeding-Related Crash Typology*, Report No. FHWA-HRT-10-024, Federal Highway Administration, Washington, DC.
83. Thomas, L.J., Srinivasan, R., Lan, B., and Council, F.M. (2012). *Speeding Related Crash Taxonomy: Crash Types and Factors Associated with Driving Too Fast for Conditions, Volume I*, Draft Report submitted to National Highway Traffic Safety Administration, Washington, DC.
84. Abdel-Aty, M., Keller, J., and Brady, P.A. (2005). “Analysis of types of crashes at signalized intersections by using complete crash data and tree-based regression.” *Transportation Research Record: Journal of the Transportation Research Board*, No. 1908, pp. 37–45, The National Academies of Science, Engineering, and Medicine, National Academies Press, Washington, DC.

85. Park, Y. and Saccomanno, F. (2005). "Collision frequency analysis using tree-based stratification," *Transportation Research Record: Journal of the Transportation Research Board*, No. 1908, 121–129, The National Academies of Science, Engineering, and Medicine, National Academies Press, Washington, DC.
86. Kuhnert, P.M., Do, K., and McClure, R. (2000). "Combining non-parametric models with logistic regression: an application to motor vehicle injury data." *Computational Statistics & Data Analysis*, 34, pp. 371–386, Elsevier, Amsterdam, Netherlands.
87. Miller, J.S., Garber, N. J., and Korukonda, S. K. (2010). *Causal Factors for Intersection Crashes in Northern Virginia*, Report No. FHWA/VTRC 10-R22, Virginia Transportation Research Council, Charlottesville, VA.
88. Chang, L.Y. and Wang, H.W. (2006). "Analysis of traffic injury severity: An application of non-parametric classification tree techniques." *Accident Analysis and Prevention*, 38, pp. 1019–1027, Elsevier, Amsterdam, Netherlands.
89. Chang, L.Y. and Chen, W.C. (2005). "Data mining of tree-based models to analyze freeway accident frequency." *Journal of Safety Research*, 36, pp. 365–375, Elsevier, Amsterdam, Netherlands.
90. Karlaftis, M. G. and Golias, I. (2002). "Effects of road geometry and traffic volumes on rural roadway accident rates." *Accident Analysis and Prevention*, 34, pp. 357–365, Elsevier, Amsterdam, Netherlands.
91. Mohaymany, A.S., Kashani, A.T., and Ranjbari, A. (2010). "Identifying driver characteristics influencing overtaking crashes." *Traffic Injury Prevention*, 11, pp. 411–416, Taylor & Francis Online, London.
92. Yan, X. and Radwan, E. (2006). "Analyses of rear-end crashes based on classification tree models." *Traffic Injury Prevention*, 7(3), pp. 276–282, Taylor & Francis Online, London.
93. Stewart, J.R. (1996). "Applications of classification and regression tree methods in roadway safety studies." *Transportation Research Record: Journal of the Transportation Research Board*, No. 1542, 1–5, The National Academies of Science, Engineering, and Medicine, National Academies Press, Washington, DC.

